

# UC Irvine

## UC Irvine Electronic Theses and Dissertations

### Title

Breaking C—N Bonds: From Designing Cross-Coupling Reactions to Facilitating CO<sub>2</sub> Conversion with Transition Metal Catalysts

### Permalink

<https://escholarship.org/uc/item/921655tc>

### Author

Matus, Alissa Christina

### Publication Date

2023

### Copyright Information

This work is made available under the terms of a Creative Commons Attribution-NonCommercial-ShareAlike License, available at <https://creativecommons.org/licenses/by-nc-sa/4.0/>

Peer reviewed|Thesis/dissertation

UNIVERSITY OF CALIFORNIA,  
IRVINE

Breaking C–N Bonds: From Designing Cross-Coupling Reactions to Facilitating CO<sub>2</sub>  
Conversion with Transition Metal Catalysts

DISSERTATION

submitted in partial satisfaction of the requirements for the degree of

DOCTOR OF PHILOSOPHY

in Chemistry

by

Alissa Christina Matus

Dissertation Committee:  
Professor Jenny Y. Yang, Chair  
Professor Vy M. Dong  
Professor A. S. Borovik  
Assistant Professor Tayloria N. G. Adams

2023

Chapter 1 © 2020 MDPI  
Chapter 2 © 2021 American Chemical Society  
All other materials © 2023 Alissa Christina Matus

## DEDICATION

To God First. It has been an honor to study and make sense of your Creation.  
Thank you for allowing me to make it through this season of life.  
Truly the Lord is my Shepard, I shall not want.

My mother and father. Your love and support of me is inspiring.  
I see your sacrifices and I am filled with gratitude.  
I hope now I can give some of that love and support back to you.  
Thank you for this life I have. Thank you.

My grandparents. I hope I've made you proud.  
I wish you could have been here to celebrate with me.

The rest of my family, my cheerleaders.  
I have followed in your footsteps to achieve my own kind of greatness.  
The love and joy you've shared with me has filled my cup.

Apple Pie, my soul feels shiny and new when I am with you.  
Thanks for helping me re-learn how to love unconditionally.  
And Susie, you laid a foundation for me to rescue and love Apple Pie. You are missed.

My sweet amazing brilliant angel friends, I think the world of each of you.  
I am humbled by your friendships and thankful to have you all.

Lastly – to those who we have lost to suicide.  
I understand you so deeply, I will keep living for you.  
You deserved much better than these spaces gave you.  
This whole thesis is for you.

## TABLE OF CONTENTS

LIST OF FIGURES.....	vi
LIST OF TABLES.....	ix
LIST OF SCHEMES.....	x
ACKNOWLEDGEMENTS.....	xi
VITA.....	xiii
ABSTRACT OF THE DISSERTATION.....	xix
INTRODUCTION.....	1
<b>CHAPTER 1: Kumada Cross-Coupling Reaction of Acyclic Sulfonamides.....</b>	<b>15</b>
1.1 Introduction.....	16
1.2 Results and Discussion.....	17
1.2.1 Synthesis of Sulfonamide Substrates for Cross-Coupling.....	17
1.2.2 Effect of Temperature on Kumada Cross-Coupling Reaction.....	19
1.3 Conclusion .....	20
1.4 Experimental.....	21
1.4.1 General Procedures for Substrate Synthesis.....	21
1.4.1.1 <u>Method A</u> : Imine Condensation of <i>p</i> -Toluenesulfonamide with Aldehydes.....	22
1.4.1.2 <u>Method B</u> : Preparation of Grignard Reagents.....	22
1.4.1.3 <u>Method C</u> : Grignard Addition to Imines.....	23
1.4.1.4 <u>Method D</u> : Methylation of Sulfonamides.....	23
1.4.2 <u>Method E</u> : General Kumada Cross-Coupling Reaction Procedures.....	24
1.4.3 Preparation of Methylmagnesium Iodide.....	24
1.4.4 Preparation of (( <i>R</i> )-BINAP)NiCl <sub>2</sub> .....	25
1.4.5 Characterization Data of Kumada Cross-Coupling Products.....	25
1.4.6 Characterization Data of Starting Materials.....	28
1.5 References.....	33
1.6 <sup>1</sup> H and <sup>13</sup> C NMR Spectra.....	37
<b>CHAPTER 2: Domino Cross-Electrophile Coupling of Propargylic Tosylpiperidines.....</b>	<b>60</b>
2.1 Introduction.....	61
2.2 Results and Discussion.....	62
2.2.1 Synthesis of Piperidine Substrates.....	62
2.2.2 Cross-Electrophile Coupling Methods and Dicarbofunctionalization Scope.....	63
2.2.3 Mechanistic Investigation .....	65
2.3 Conclusion .....	69
2.4 Experimental Details.....	70
2.4.1 Preparation of (( <i>R</i> )-BINAP)NiCl <sub>2</sub> .....	71
2.4.2 Preparation of MeMgI.....	71

2.4.2.1 <u>Method A</u> : Domino Cross-Electrophile Coupling Reaction of Propargylic Tosylpiperidines .....	72
2.4.2.2 Cross-Electrophile Coupling Reaction without MgI <sub>2</sub> .....	72
2.4.2.2.1 Cross-Electrophile Coupling Reaction with MgI <sub>2</sub> .....	72
2.4.3 General Procedures for Substrate Synthesis.....	73
2.4.3.1 <u>Method B</u> : Sonogashira Cross-Coupling Reaction of Aryl Halides with Propargyl Alcohol.....	73
2.4.3.1.1 Sonogashira Cross-Coupling with Aryl Bromides.....	73
2.4.3.1.2 Sonogashira Cross-Coupling with Aryl Iodides.....	73
2.4.3.2 <u>Method C</u> : Synthesis of Homoallylic Tosylamine.....	74
2.4.3.3 <u>Method D</u> : Swern Oxidation of Propargylic Alcohols to Aldehydes.....	74
2.4.3.4 <u>Method E</u> : Iron (III) Chloride/BmimPF <sub>6</sub> -Promoted Aza-Prins Reaction.....	75
2.4.4 Characterization Data of Cyclopropane Products.....	75
2.4.5 Characterization Data of Starting Materials.....	78
2.5 References.....	87
2.6 <sup>1</sup> H, <sup>13</sup> C, <sup>19</sup> F, and COSY NMR Spectra.....	91

**CHAPTER 3: Examining Structure and Reactivity of Isolated Ru-MACHO® Dihydrides for Reduction of CO<sub>2</sub> and Carbamates.....** 112

3.1 Introduction.....	113
3.2 Results and Discussion.....	114
3.2.1 Synthesis and Characterization of H <sub>2</sub> Ru-MACHO Dihydrides.....	114
3.2.1.1 Comparing NMR Data Across Methods.....	116
3.2.1.2 Crystal Structures.....	117
3.2.2 Reactivity of Isolated H <sub>2</sub> Ru-MACHO.....	121
3.2.2.1 Stoichiometric Reactivity of Isolated H <sub>2</sub> Ru-MACHO and CO <sub>2</sub> .....	121
3.2.2.2 Stoichiometric Reactivity of H <sub>2</sub> Ru-MACHO with Dimethylammonium Dimethyl Carbamate.....	122
3.3 Conclusion .....	123
3.4 Experimental Details.....	124
3.4.1.1 <u>Method A</u> : Superhydride® Reduction.....	125
3.4.1.2 <u>Method B</u> : NaH Reduction.....	125
3.4.1.3 <u>Method C</u> : Stoichiometric CO <sub>2</sub> Reduction.....	126
3.4.1.4 <u>Method D</u> : Stoichiometric Carbamate Reduction.....	126
3.4.2 Characterization Data for Ru-MACHO Dihydride.....	126
3.5 References.....	129
3.6 <sup>1</sup> H, <sup>31</sup> P, and <sup>31</sup> P{ <sup>1</sup> H} NMR and IR Spectra.....	132

**APPENDIX A: Electrochemical Activity of Ru-MACHO® for CO<sub>2</sub> Reduction.....** 139

A.1 Introduction.....	140
A.2 Results and Discussion.....	140
A.2.1 Cyclic Voltammetry of Ru-MACHO® upon addition of Water as an Acid Source and 1 atm of CO <sub>2</sub> .....	140
A.2.2 Cyclic Voltammetry of H <sub>2</sub> Ru-MACHO.....	142
A.3 Conclusion.....	144
A.4 Experimental Details.....	144

A.5 References.....	145
---------------------	-----

**APPENDIX B: Stoichiometric Reduction of Carbamates with Known CO<sub>2</sub> Reduction Catalysts.....147**

B.1 Introduction .....	148
B.2 Results and Discussion .....	149
B.2.1 [HPt(DMPE) <sub>2</sub> ] and Ammonium Carbamate.....	150
B.2.2 HRh(DPPBz) <sub>2</sub> and Ammonium Carbamate.....	151
B.3 Conclusion.....	153
B.4 Experimental Details .....	154
B.5 References .....	154

## LIST OF FIGURES

<b>Figure 0.1:</b> General process of CO <sub>2</sub> reduction using light-derived electrochemistry to produce C1+ products. Figure adapted from Hidden Analytical.....	4
<b>Figure 0.2:</b> Cycle of proposed electrochemical RCC of CO <sub>2</sub> with amines.....	5
<b>Figure 0.3:</b> Overview of the transformation described in this thesis. <b>A:</b> Chapter 1. <b>B:</b> Chapter 2. <b>C:</b> Chapter 3.....	6
<b>Figure 2.1:</b> Scope of Difunctionalized Cyclopropane Products.....	64
<b>Figure 2.2:</b> Other Piperidines Synthesized for XEC.....	64
<b>Figure 3.1:</b> NMR spectra of product isolated from Super-Hydride® reduction of Ru-MACHO® in THF- <i>d</i> <sub>8</sub> . <b>A:</b> <sup>1</sup> H NMR spectrum <b>B:</b> <sup>31</sup> P NMR spectrum.....	115
<b>Figure 3.2:</b> NMR spectra of product isolated from NaH reduction of Ru-MACHO® in THF- <i>d</i> <sub>8</sub> . <b>A:</b> <sup>1</sup> H NMR spectrum <b>B:</b> <sup>31</sup> P NMR spectrum.....	115
<b>Figure 3.3:</b> NMR spectra of product isolated from NaH reduction of Ru-MACHO® in THF- <i>d</i> <sub>8</sub> at 50 °C. <b>A:</b> <sup>1</sup> H NMR spectrum <b>B:</b> <sup>31</sup> P NMR spectrum.....	116
<b>Figure 3.4:</b> <b>A:</b> Crystal structure of <b>3.3</b> . Thermal ellipsoids are drawn at 50% probability. Non-hydride hydrogen atoms and non-coordinating solvent molecules are omitted for clarity. <b>B:</b> ChemDraw showing 3D structure.....	118
<b>Figure 3.5:</b> <b>A:</b> Crystal structure of <b>3.4</b> . Thermal ellipsoids are drawn at 50% probability. Non-hydride and N–H hydrogen atoms and solvent molecules are omitted for clarity. <b>B:</b> ChemDraw showing 3D structure.....	119
<b>Figure 3.6:</b> <b>A:</b> <sup>1</sup> H NMR of hydride region (–14 ppm to –18 ppm) after exposing Super-Hydride®-reduced Ru-MACHO® to 1 atm of CO <sub>2</sub> in THF- <i>d</i> <sub>8</sub> . <b>B:</b> Products formed after CO <sub>2</sub> reduction.....	121



<b>Figure 3.7:</b> HSQC ( <i>x</i> -axis: $^1\text{H}$ ; <i>y</i> -axis: $^{13}\text{C}$ ) of NMR-scale experiment with reduced Ru-MACHO® under 1 atm of $\text{CO}_2$ in THF- <i>d</i> <sub>8</sub> .....	122
<b>Figure 3.8:</b> NMR spectra after adding excess dimethylammonium dimethyl carbamate to <b>3.4</b> in THF- <i>d</i> <sub>8</sub> . <b>A:</b> $^1\text{H}$ NMR spectrum, formyl proton and $\text{H}_2$ peaks are labeled. <b>B:</b> $^{31}\text{P}$ NMR spectrum..	123
<b>Figure 3.9.</b> $^1\text{H}$ NMR Spectra of Ru-MACHO® from STREM Chemicals in THF- <i>d</i> <sub>8</sub> . Impurities are labeled and were present following opening of the purchased bottle in a glovebox.....	125
<b>Figure A.1:</b> Ru-MACHO®-type hydrogenation catalysts with turnover numbers for MeOH production .....	140
<b>Figure A.2:</b> Ru-MACHO® (1mM), CoCp* (3mM, not pictured), TBAPF <sub>6</sub> (100mM), H <sub>2</sub> O (1.7 mM) under 1 atm $\text{CO}_2$ THF. Before scanning, iR compensation was performed.....	141
<b>Figure A.3:</b> Ru-MACHO® (1mM), TBAPF <sub>6</sub> (100mM), in PhCN. Not iR compensated.....	142
<b>Figure A.4:</b> CV of 3mM $\text{H}_2\text{RuMACHO}$ , 100 mM TBAPF <sub>6</sub> , <b>3 mM CoCp*</b> in THF, under 1 atm of $\text{N}_2$ (red trace), and under and 1 atm $\text{CO}_2$ in THF (blue trace). Not iR compensated.....	143
<b>Figure A.5:</b> $\text{H}_2\text{-Ru-MACHO}$ , TBAPF <sub>6</sub> , <b>CoCp*</b> and $\text{CO}_2$ in THF. Not iR compensated.....	143
<b>Figure B.1:</b> Metal hydride complexes of interest in RCC with amine capture agents. <b>A:</b> Metal hydrides known to generate formate and methanol using amine-captured $\text{CO}_2$ . <b>B:</b> Metal hydrides with known $\text{CO}_2$ reduction activity.....	149
<b>Figure B.2:</b> NMR spectra of <b>B.1</b> and ammonium carbamate. <b>A:</b> $^1\text{H}$ NMR spectrum taken in MeCN- <i>d</i> <sub>3</sub> . <b>B:</b> $^{31}\text{P}$ NMR spectrum taken in MeCN- <i>d</i> <sub>3</sub> . <b>C:</b> $^1\text{H}$ NMR spectrum taken in DMSO- <i>d</i> <sub>6</sub> . .....	151
<b>Figure B.3:</b> NMR Spectra of <b>B.2</b> in DMSO- <i>d</i> <sub>6</sub> . <b>A:</b> $^1\text{H}$ NMR spectra at 5 minutes (red) and 15 minutes (blue). <b>B:</b> $^{31}\text{P}$ NMR spectra at 5 minutes (red) and 15 minutes (blue).....	152

**Figure B.4:** NMR Spectra of **B.2** and ammonium carbamate in MeCN-*d*<sub>3</sub>. **A:** <sup>1</sup>H NMR spectrum.  
**B:** <sup>31</sup>P NMR spectrum.....153

## LIST OF TABLES

<b>Table 1.1:</b> Examination of the Effect of Temperature on Kumada Cross-Coupling.....	20
<b>Table 3.1:</b> Summary of NMR data collected from Ru-MACHO® reductions in THF-d <sub>8</sub> . <b>A:</b> Reduction run at 50 °C.....	117
<b>Table 3.2:</b> Selected Recrystallization Trials. <sup>a</sup> Recrystallization trials were setup in 20 mL scintillation vials with internal glass wells of varying sizes: Large well = 1 dram shell vial, flat bottom; medium well = 0.5 dram shell vial, flat bottom; small well = 5 mm glass tube.....	117
<b>Table 3.3:</b> Metal–hydride bond lengths determined experimentally via X-ray crystallography. <sup>a</sup> Structural information from <b>3.3</b> . <sup>b</sup> Structural information from <b>3.4</b> .....	119
<b>Table B.1:</b> Formate Quantification in DMSO- <i>d</i> <sub>6</sub> .....	151

## LIST OF SCHEMES

<b>Scheme 0.1:</b> Cross-Coupling and Cross-Electrophile Coupling Reactions.....	2
<b>Scheme 0.2:</b> Selected Examples of $Csp^3-N$ Bonds in Cross-Coupling Reactions.....	3
<b>Scheme 0.3:</b> Selected Examples of C–N Bonds Utilized in XEC Reactions .....	3
<b>Scheme 1.1:</b> Kumada Cross-Coupling of Acyclic, Uncharged Sulfonamides .....	16
<b>Scheme 1.2:</b> Synthesis of Kumada Cross-Coupling Substrates .....	18
<b>Scheme 1.3:</b> Kumada Cross-Coupling of Sulfonamide <b>1.9</b> .....	18
<b>Scheme 1.4:</b> Scope of Kumada Cross-Coupling of Acyclic Sulfonamides.....	19
<b>Scheme 2.1:</b> Cross-Electrophile Coupling (XEC) of Chlorotosylpiperidines.....	61
<b>Scheme 2.2:</b> Selected Examples of Domino Reactions involving XEC .....	62
<b>Scheme 2.3:</b> Substrate Synthesis from Aryl Iodides.....	63
<b>Scheme 2.4:</b> Substrate Synthesis from Aryl Bromides.....	63
<b>Scheme 2.5:</b> Original Mechanism Proposed for Domino XEC Reaction.....	66
<b>Scheme 2.6:</b> Mechanistic Experiments.....	67
<b>Scheme 2.7:</b> Revised Domino XEC Mechanism.....	68
<b>Scheme 3.1:</b> Methods of Reducing of Ru-MACHO in this Chapter .....	114
<b>Scheme 3.2:</b> Mechanism of cis-trans isomerization (Heldebrant, 2016) .....	120
<b>Scheme B.1:</b> Reduction of Ammonium Carbamate with a Metal Hydride.....	149

## ACKNOWLEDGEMENTS

The National Science Foundation (NSF) Graduate Research Fellowship () from the NSF has provided me with the unparalleled privilege to focus my efforts in graduate school primarily on my research. I was granted this fellowship during a particularly challenging period of my career, and I have no doubts that I would not have continued pursuing my PhD without it. I am also grateful for the funding I have received from the U.S. Department of Energy.

I have had the opportunity to participate in many wonderful conferences and have received scholarships and grants from many funding sources. I would like to thank BlackinChem, the American Chemical Society (ACS), the National Organization for the Professional Advancement of Black Chemists and Chemical Engineers (NOBCCChE), UCI's Graduate Division, and the UCI Department of Chemistry for helping me explore the professional world of chemistry and expand my network. In addition to providing me with funding, these organizations, particularly NOBCCChE and ACS, have given me the opportunity to connect with Black and brown scholars from across the globe, which has helped fill me with the strength to endure the final years of graduate school. Thank you.

I acknowledge the ACS and MDPI for permission to include Chapters 1 and 2, which were originally published in *Molecules* and *ACS Catalysis*, respectively.

The first time I participated in academic research was in the lab of Professor Marcia Ewers at Cal Poly Pomona when I was sixteen. As a high school student, this work was unbelievably influential, and Professor Ewers took an enormous chance by allowing me into her research group. I am endlessly thankful for this experience and Professor Ewers' encouragement.

As an undergraduate student, I first attended Dominican University of California (DUoC). To date, this school provided me with the most diverse educational experience I have ever had outside of high school, and my time there not only encouraged me to develop a love for science, but also for research science. At DUoC, Professor Maria Graciela Carranza gave me my first glimpse into synthetic chemistry research. I was amazed! The idea of using chemicals as tools for building complex structures was so exciting to encounter for the first time. Also, having a woman of color as a PI in synthetic chemistry is a rare occurrence. Seeing her accomplishments as a scientist empowered me to feel capable of pursuing chemistry as a career.

Attending Azusa Pacific University (APU) was undoubtedly a blessing. At this school, I had access to brilliant, empathetic, truly kind professors, and I deeply wish that all of academia could be like the environment I was able to experience there. My research mentor, Professor Kevin S. Huang, was also my organic chemistry professor, and it was in that class that I finally fell in love with chemistry. The lessons were dynamic and exciting, and Dr. Huang encouraged me to explore deeper into the subject as his research student. I had so much reverence for these experiences, and the pedagogy my professors developed for us was truly excellent. Along with Dr. Huang, I would like to thank Dr. Jennifer Young, Dr. Carrie S. Miller, Dr. Louise Huang, Dr. Matthew Berezuk, and Dr. Eric Davis, Dr. "Peanut" McCoy, for their phenomenal classes and for making my experience as a chemistry major truly uplifting. Having the opportunity to develop my science and personal faith was unique and I am so grateful I was able to do this at APU. Thank you all for giving me excellent examples of what a professor can be. I also had the deep fortune to make wonderful friends and be surrounded by excellent women in chemistry. To my study group girlies, Cassidy Crandell, Laura Mejia, and Sydney Burkholder, thank you for holding my hand through physical chemistry and inspiring me to work my hardest.

My quest to obtain a PhD in Chemistry at UCI has been one of the most challenging experiences of my life. I have many people to acknowledge, starting with my PI, Professor Jenny Y. Yang. Thank you for pushing me to succeed and face my imposter syndrome head-on. I cannot tell you how much it meant to me to have your support and understanding, particular when I joined the group and during my candidacy preparations. My view of research is broad, appreciative, and well-rounded because of you. The mentorship you have provided has encouraged me so much. For my coworkers; I would like to thank the graduate students and postdoctoral fellows in both the Jarvo and Yang groups, for the encouragement, support, and camaraderie. In particular, I would like to thank Dr. Erika Lucas, Dr. Taylor Thane, Dr. Zachary Thammavongsy, Dr. Tyler Kerr, and Dr. Ana Chrsitina Garcia for providing me with mentorship in both official and unofficial capacities. As external mentors, I would also like to include special thanks for Dr. Megan Newcomb and Dr. Krista Fruehauf, who provided me with exceptional support during my 2<sup>nd</sup> year-report, candidacy exams, and more – both of these scholars have filled me with so much inspiration and courage to continue, and I will never forget their dedication to helping me. To my fellow student coworkers (and other soon-to-be-PhDs), particularly Claire Herbert, Nadia Hirbawi, Patricia Lin, Erin Joy Araneta, Jesus Galeana, Hien Nguyen, Clarabella Li, Andrew Cypcar, Colleen Miller, Elise Payong, Jared Stanley, Faith Flingkenschelt, Ciara Gillis, Ute Petri, and Claire Zimmerman, I believe so strongly in each of you, and am excited to see you finish your own degrees! Having you as coworkers has provided so much brightness throughout my time at UCI. To the other UCI professors who have acted as mentors to me, including Professor Tayloria Adams, Professor Doug Tobias, Professor Ann Marie Carlton, and Professor Renée Link, your mentorship has lifted me up to heights I never thought possible. Thank you for pouring into my cup and helping me believe in myself without changing who I am.

One of the biggest reasons I have survived graduate school is friendship. I have so many friends that I have made at UCI, and I would like to thank you each, namely (in alphabetical order by last name, hehe): Sarah Bredenkamp, Paul Carlson, Brooke Payne Carpenter, Lia Dam, Rakia Dhaoui, Ellie Frank, Madi Flesch, James Griffin, Dora Kadish, Maj Krumberger, Johnny Kozlowski, Bryant Lim, Khawla Mustafa, Mariana Navarro, Barry Rich, Aoon Rizvi, Moises Romero, Oanh Tran, Cynthia Wong, and Ali Younis – you are the future of chemistry. In the face of overwhelming white supremacy in higher education each of you stands confidently against this evil. From your beautiful hearts and minds to the love and support you've shared with me, I know confidently that the world is better because you all are in it. It is a tremendous honor to be your friend. I cannot wait to celebrate this milestone with you all, and many more.

I have faced so much darkness in graduate school. During the times when that darkness became almost unbearable, I owe my survival to my dear parents, Anthony Matus and Carla Baquet Matus. Your unwavering love, support, and belief in me has held me up in ways I can't fully communicate with words. Thank you for being there for me. Thank you for helping me survive this program. Thank you for your love. I love you so much, and I pray *constantly* that I will be able to take care of you as I go through my career. Your enormous sacrifices for me, throughout my entire life, are why I am able to complete this degree now. My family, alive and dead, is my greatest source of inspiration. I am who I am now because of the legacies I am following.

There are so many more people I want to thank, and I wish I could state plainly just how much love and support I have received from my support system – but I will try to let the rest of my thesis speak to the gratitude I hold in my heart.

## VITA

Alissa Christina Matus

### Education:

- 2018-2023      Ph.D., Chemistry, GPA: 3.89  
University of California, Irvine
- 2015-2018      B.S., Chemistry, GPA: 3.78, *Cum Laude*  
Azusa Pacific University

### Research Experience:

- 2018-2023      *Doctoral Research* (University of California, Irvine)  
Electrochemical Conversion of CO<sub>2</sub> to Methanol and other Fuel Sources  
using Transition Metal Hydrides.  
(Advisor: Professor Jenny Y. Yang)  
Development of Kumada Cross-Coupling of Sulfonamides. Nickel-  
Catalyzed Cascade Reaction of Propargyl Piperidines. (Advisor: Professor  
Elizabeth R. Jarvo)
- 2016-2017      *Undergraduate Research* (Azusa Pacific University)  
Investigation of Grubbs Catalyst-Mediated Olefin Isomerization  
(Advisor: Professor Kevin S. Huang)
- 2014-2015      *Undergraduate Research* (Dominican University of California)  
Total Synthesis and Biological Activity Screening of Eryvarin H.  
(Advisor: Professor Maria G. Carranza)

### Teaching Experience:

- Spring 2020      Laboratory Teaching Assistant (virtual), *General Chemistry, ILC*  
Led two virtual laboratory sections; graded assignments and exams through  
Canvas and Gradescope; answered student questions via Piazza; held  
weekly office hours via Zoom (virtual teaching administered due to  
COVID-19 restrictions)
- Spring 2019      Lecture Teaching Assistant, *Organic Chemistry, CHEM51C*  
Led three discussion sections; graded weekly quizzes and exams; held  
weekly office hours; distributed practice materials
- Winter 2019      Laboratory Teaching Assistant, *Organic Chemistry, CHEM51LB*  
Led two laboratory sections; graded assignments and exams through  
Canvas and Gradescope; answered student questions via Piazza; held  
weekly office hours

Fall 2018                      Laboratory Teaching Assistant, *General Chemistry, CHEM1LD*  
Led two laboratory sections; graded assignments and exams through  
Canvas; held weekly office hours

Students Formally Mentored while at UC Irvine:

Research Laboratory Mentorship

Colleen Miller: Graduate student, University of California, Irvine, 2021-  
present; Current 2<sup>nd</sup> year graduate student and NSF GRFP Honorable  
Mention

Erin Joy Araneta: Undergraduate student, University of California, Irvine,  
2020-2023; Current 1<sup>st</sup> year graduate student at the University of Southern  
California and NSF GRFP Fellow

ChemUNITY Mentorship, UC Irvine Department of Chemistry Peer Mentorship Program

Ciara Gillis: Graduate Student, University of California, Irvine, 2022-  
present; Current 1<sup>st</sup> year graduate student

Rakia Dhaoui: Graduate student, University of California, Irvine, 2019-  
2020; Current 4<sup>th</sup> year PhD candidate and NSF GRFP Fellow

Shannon Saluga: Graduate student, University of California, Irvine, 2019-  
2020); Current 4<sup>th</sup> year PhD candidate and NSF GRFP Fellow

Claire Herbert: Graduate student, University of California, Irvine, 2019-  
2020); Current 4<sup>th</sup> year PhD candidate and industrial intern

Science Champions 4 Change, California Community College Mentorship Program (virtual)

Moira Moore: Undergraduate Student, Las Positas College, 2021; Current  
full-time student at University of California, Davis

Selected Awards, Honors, and Titles:

2023                      CAS Future Leaders Top 100 (CAS Division of the American Chemical  
Society)

2023                      ACS Leadership Development Institute Fellow (American Chemical  
Society and NOBCCHE partnership)

2022                      Department of Chemistry Conference Fall Travel Grant (University of  
California, Irvine)



- 2022 Advancing Science Conference Grant, NOBCCChE National Conference (National Organization for the Professional Advancement of Black Chemists and Chemical Engineers)
- 2022 ACS Bridge Project Travel & Professional Development Award (American Chemical Society)
- 2022 Graduate Division Inclusive Excellence Fellow (University of California, Irvine)
- 2022 Black in Chem ACS San Diego Travel Grant (#BlackinChem non-profit)
- 2021 Department of Chemistry Diversity Fellow (University of California, Irvine)
- 2021 Lasting Encounters between Aspiring and Distinguished Scientists (LEADS) Scholar (American Chemical Society)
- 2020 National Science Foundation Graduate Research Fellow (University of California, Irvine)
- 2017 Woman of Excellence in Chemistry Award (Azusa Pacific University)
- 2017 Center for Research in Science STEM Fellow (Azusa Pacific University)
- 2017 Best Poster Presentation, Chemistry (Azusa Pacific University)

Publications:

Hewitt, K.A.; Herbert, C.A.; **Matus, A.C.**; Jarvo, E.R. Nickel-Catalyzed Kumada Cross-Coupling Reactions of Benzylic Sulfonamides. *Molecules* 2021, 26, 5947. <https://doi.org/10.3390/molecules26195947>.

Hewitt, K.A.; Xie, P.-P.; Thane, T.A.; Hirbawi, N.; Zhang, S.-Q., **Matus, A. C.**; Lucas, E. L.; Hong, X.; Jarvo, E. R. Nickel-Catalyzed Domino Cross-Electrophile Coupling Dicarbofunctionalization Reaction to Afford Vinylcyclopropanes. *ACS Catalysis* 2021, 23, 14369. <https://doi.org/10.1021/acscatal.1c04235>.

Presentations:

**Matus, A. C.**; Yang, J. Y. *Identifying Electrocatalysts for Reactive CO<sub>2</sub> Capture (RCC)*. Southeastern Regional Meeting of the ACS, Oral Presentation (in-person), October 2022.

**Matus, A. C.;** Yang, J. Y. *Identifying Electrocatalysts for Combined Capture and Conversion of Carbon Dioxide to Formate*. NOBCCHE National Conference, Oral Presentation (in-person), September 2022.

**Matus, A. C.;** Yang, J. Y. *Electrochemical CO<sub>2</sub> conversion to formate (HCOO<sup>-</sup>) from amine-captured CO<sub>2</sub>*. ACS Spring, Poster Presentation (in-person), March 2022

**Matus, A. C.** *Mentorship and Me: A workshop covering best practices for mentorship of students from historically excluded groups*. **Invited Symposium Organizer**, UC Chemical Symposium, Workshop Host (virtual), March 2022

**Matus, A. C.;** Yang, J. Y. *Addressing the future of science: Combining electrocatalytic CO<sub>2</sub> capture and conversion and mentorship at UC Irvine*. Invited Talk, ACS Rocky Mountain Regional Meeting, Oral Presentation (virtual), October 2021

**Matus, A. C.;** Yang, J. Y. *Combined electrocatalytic CO<sub>2</sub> capture and conversion*. ACS Fall National Meeting, Oral Presentation (virtual), August 2021

**Matus, A. C.;** Hewitt, K. A.; Jarvo, E. R. *Nickel-Catalyzed Kumada Cross-Coupling Reactions of Sulfonamides*. ACS Fall National Meeting, Poster Session (in-person), August 2019

**Matus, A. C.;** Huang, K. S. *Analysis of Transition Metal Catalyzed Isomerization of Terminal Alkenes*. Azusa Pacific University Fall Research Day, Poster Session (in-person), September 2017; Southern California Conference for Undergraduate Research, Poster Session (in-person), November 2017

Professional Societies, Organizations, and Outreach Initiatives:

2022-present *Diverse Educational Community and Doctoral Experience (DECADE)* (University of California, Irvine)  
School of Physical Sciences DECADE representative

- Provide advising to DECADE leadership (faculty and staff) and the Graduate Dean's Diversity Council
- Plan programs and events for the Chemistry Department and School of Physical Sciences
  - Graduate Student Clubs and Orgs Fair (Fall 2022) – Six school organizations in attendance
  - Movie viewing (Winter 2023) – *Stutz*, with emphasis on managing neurodivergence in daily life

2022-present *Cosmetic Chemistry Society Organization Advisor* (University of California, Irvine)  
Official advisor to undergraduate-led organization

- Oversee and provide advising to eight undergraduate students as they organize club events and cosmetic chemistry demonstrations

- 2020-present *End Racism Initiative* (University of California, Irvine)  
Working Group 2, Representation: Recruitment and Outreach to Black Students
- Correspondence with faculty, staff, and other students via Zoom and Slack focusing on Working Group topic, university-wide
  - Presentation of conclusions found within group to Working Group leaders (2021)
- 2020-present *National Organization for the Professional Advancement of Black Chemists and Chemical Engineers* (University of California, Irvine)  
Member at large, co-founder of UC Chapter
- Procurement of >\$2,500 of funding from Chemistry Department for participation in NOBCChE National Meeting (2021, virtual)
  - Organization of UC-system-wide participation of students for regional chapter creation
- 2020-2022 *Science Champions 4 Change: Championing young scientists through their academic journeys* (Mentorship initiative for STEM students at California Community Colleges)  
Founder and Mentor
- Designed leadership and mentorship training sessions for mentors, organized monthly “Champion Huddles”
  - Recruited students from community colleges throughout California to aid with career planning and school transferring
  - Matched over 60 students and mentors into mentorship pairs
  - Two successful cohorts of mentors/mentees (Spring 2021 and Fall 2021)
- 2019-present *ChemUNITY: Chemistry Peer Mentorship Program* (University of California, Irvine)  
Co-founder and Mentor, Leader
- Founded, designed, and executed mentorship program as a second-year graduate student
  - Performed mentorship training for each new cohort of mentees
  - Designed and held community building events for first-year students (quarterly)
    - “Grad School 101” panels with senior graduate student panelists
    - Pizza debriefs for successful completion of the first year of graduate school for mentees
  - Personal mentorship of four first-year students
  - Secured over \$2000 of departmental support for programming and mentorship support
  - Four successful cohorts of mentors/mentees (2019-2020, 2020-2021, 2021-2022, 2022-2023) with over 120 first-year graduate students mentored (average of 32 students per year)

2019-2021

*Iota Sigma Pi* (University of California, Irvine)

Professional Development Coordinator (2019-2020)

- Organized fellowship writing workshops for applicants to engage in peer reviewing of drafts
- Recruited woman-identifying faculty members to give seminars during monthly meetings
- Led a *curriculum vitae* writing workshop for all members

Triennial Convention Coordinator (2020-2021)

- Single-handedly converted in-person convention programming to online programming due to the COVID-19 pandemic
  - Design of merchandise for sale by national council, including a collaborative pin design made by D-Orbital games founder, Dr. Zachary Thammavongsy
  - Organization of giveaways, panels (featuring Dr. Paulette Vincent-Ruz and Dr. Devin Swiner), and keynote speech (Dr. Frances Arnold, Nobel Laureate)
  - Incorporation of community participation into convention programming, including invitation of high school students nationwide to keynote presentation
  - Distribution and collection of reports from all chapters, sponsorship details, organization
  - Identified willing sponsors and negotiated funding for online convention programming
- Introduced topics of intersectionality and importance of diversity, equity, and inclusion work to the board of directors during 2021 national convention

## ABSTRACT OF THE DISSERTATION

Breaking C–N Bonds: From Designing Cross-Coupling Reactions to Facilitating CO<sub>2</sub> Conversion with Transition Metal Catalysts

by

Alissa Christina Matus

Doctor of Philosophy in Chemistry

University of California, Irvine, 2023

Professor Jenny Y. Yang, Chair

The utility of transition metals as mediators of chemical transformations cannot be understated. Transition metal complexes are capable of catalyzing a vast variety of reactions, from cross-coupling and cross-electrophile coupling reactions that allow for the synthesis of structurally diverse molecules, to CO<sub>2</sub> valorization to generate fuel.

For catalysis that focuses on the construction of privileged motifs for the production of new drugs or bioactive materials, a major concern is chemoselectivity and variety of reagents available as coupling partners. One method in particular that seeks to address this is cross-electrophile coupling, which typically exploits Ni catalysts to differentiate between electrophilic coupling partners. The coupling partners can also contain non-traditional electrophiles, such as amines or sulfonamides.

Research efforts focused on decreasing the impact of CO<sub>2</sub> emissions must work to design processes that generate high-value products without requiring a high input of energy. One method that addresses this concern is combined CO<sub>2</sub> capture and CO<sub>2</sub> conversion, where electrochemistry

can be utilized to perform CO<sub>2</sub> conversion under mild conditions. Many complexes typically used in harsh hydrogenation reactions may be repurposed as electrocatalysts.

**Chapter 1** and **Chapter 2** describe the design of new Ni-catalyzed cross-coupling and cross-electrophile coupling reactions. These new methods exploit Ni's capacity to engage sluggish electrophiles and demonstrate the use of sulfonamide C–N bonds as reliable coupling partners. **Chapter 1** shows the scope of a new Kumada cross-coupling reaction that avoids  $\beta$ -hydride elimination with  $\beta$ -branching substrates. **Chapter 2** details the domino cross-electrophile dicarbofunctionalization of propargyl piperidines to afford highly functionalized vinyl cyclopropanes.

**Chapter 3** details the exploration of an isolated dihydride, formed by reducing the commercially available hydrogenation catalyst Ru-MACHO®, which demonstrates the ability to convert CO<sub>2</sub> and carbamate to formate.

# **INTRODUCTION**

## 0.1 Transition Metal-Catalyzed Transformations

The ubiquity of transition metals in chemical research cannot be understated.<sup>1-3</sup> Not only do transition metals allow for the synthetic mimicry of natural systems, but the design of novel reactions in complex natural product synthesis also relies heavily on transition metal catalysts.<sup>4, 5</sup> Cross coupling reactions are heavily relied upon to build structural complexity, particularly for synthetic access to natural products and their derivatives.<sup>6-8</sup> With the 2010 Nobel Prize in Chemistry, awarded for palladium-catalyzed cross-coupling reaction development, the transformative power of transition metal catalyzed cross-coupling reactions was acknowledged by the world.<sup>1</sup>

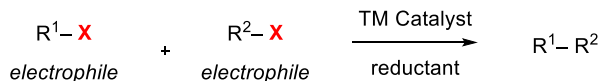
### 0.1.1 From Cross-Coupling to Cross-Electrophile Coupling

Scheme 0.1. Cross-Coupling and Cross-Electrophile Coupling Reactions

**A. Cross-Coupling**



**B. Cross-Electrophile Coupling**



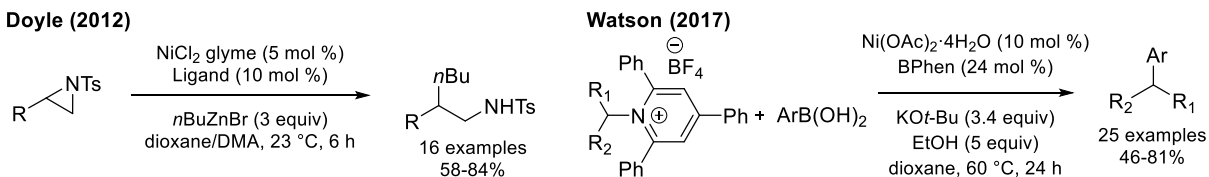
While traditional cross-coupling reactions are well-precedented and established, some clear caveats exist that limit scope. In a cross-coupling reaction, chemoselectivity is achieved by utilizing a nucleophilic reagent and an electrophilic coupling partner (Scheme 0.1A).<sup>9</sup> These nucleophilic reagents vary, and can include Grignard, organolithium, and other carbon-based nucleophiles. The increased reactivity associated with nucleophilic reagents can limit the scope of cross-coupling reactions, preventing the use of substrates containing more susceptible groups such as aldehydes. In contrast, cross-electrophile coupling (XEC) reactions, also referred to as reductive cross-coupling reactions, combine two electrophilic coupling partners to produce a product, along with a reducing agent to aid in catalyst turnover (Scheme 0.1B).<sup>10</sup> Ni-based catalysts are



particularly useful in XEC, because they can undergo multiple parallel pathways (ie.  $\text{Ni}^{\text{I/III}}$  or  $\text{Ni}^{0/\text{II}}$ ), allowing for easier differentiation between electrophiles.<sup>11-15</sup>

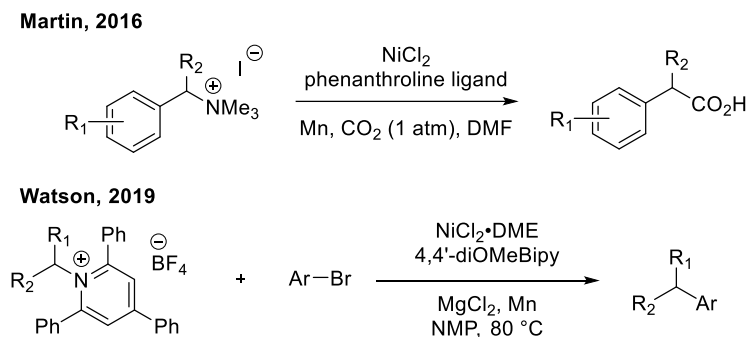
### 0.1.1.1 Engaging C–N Bonds in Catalysis

**Scheme 0.2: Selected Examples of  $\text{Csp}^3$ –N Bonds in Cross-Coupling Reactions**



The exploration of new carbon-based electrophiles for cross-coupling has mostly shifted from alkyl or aryl halides to electrophiles containing C–O bonds.<sup>14, 16-18</sup> However, utilizing C–N bonds in cross-coupling reactions can provide opportunities to build complexity from easy-to-install functionalities, such as aryl Katritzky salts (Scheme 0.2).<sup>15, 19</sup> In contrast to cross-coupling, homocoupling is a major drawback of XEC, extending from issues in differentiating between electrophilic reagents.<sup>10</sup>

**Scheme 0.3: Selected Examples of C–N Bonds Utilized in XEC Reactions**



While recent developments of XEC methods have incorporated organic reductants or electrochemical techniques to avoid the use of reactive nucleophiles as reducing agents (Scheme 0.3), much is still unknown about the mechanistic aspects of XEC reactions and how catalysts engage different types of electrophiles.<sup>20-23</sup> Future XEC reaction development efforts must focus on a combination of less detrimental reducing agents with advanced mechanistic investigations.

## 0.1.2 CO<sub>2</sub> Reduction and Electrochemistry

CO<sub>2</sub> remains the most abundant greenhouse gas, with atmospheric concentrations continuing to rise steadily.<sup>24</sup> While concerning, the ubiquity of CO<sub>2</sub> in the atmosphere provides a challenge to chemists interested in producing feedstock chemicals or chemical fuels.<sup>5, 25-27</sup> Research efforts dedicated to decreasing the impact of CO<sub>2</sub> emissions must work to design processes that generate high-value products without requiring a high input of energy.<sup>28</sup>

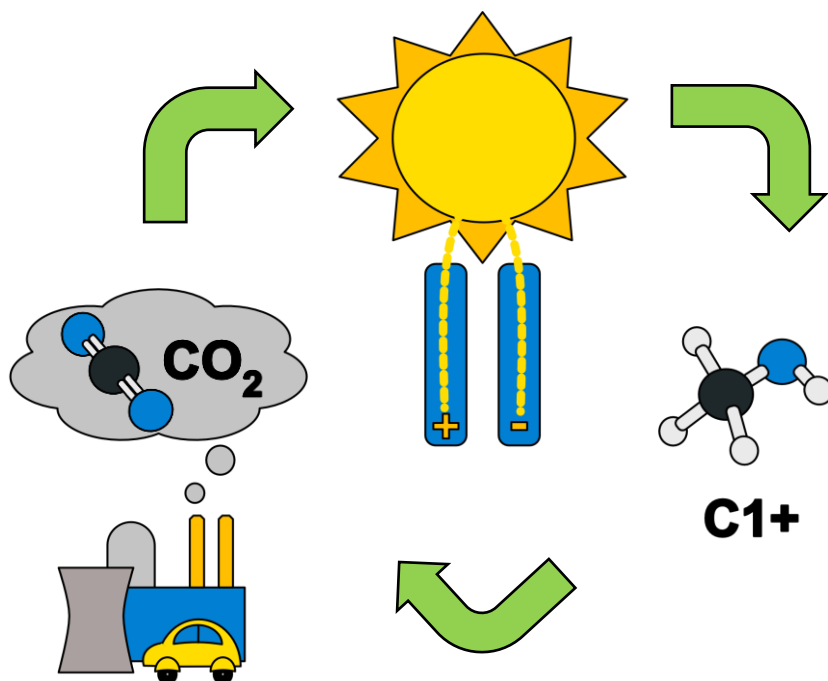


**Figure 0.1.** General process of CO<sub>2</sub> reduction using light-derived electrochemistry to produce C1+ products. Figure adapted from Hidden Analytical.<sup>29</sup>

Previous Yang group work has demonstrated selective reduction of CO<sub>2</sub> to formate using homogeneous electrocatalysis with metal hydride intermediates.<sup>30-34</sup> Metal hydrides are a powerful class of complexes, and display varying levels of reactivity depending on metal identity, ligand environment, and solvation effects.<sup>35-37</sup> As the Yang group and others have demonstrated, metal hydrides can be generated via electrochemical cycles for CO<sub>2</sub> reduction.<sup>30-34</sup> These approaches mimic biological process by aiming to use light-derived energy to drive electrochemical transformations (Figure 0.1).<sup>5, 38-40</sup> One method that addresses this concern is combined CO<sub>2</sub>

capture and CO<sub>2</sub> conversion, where electrochemistry can be utilized to reduce captured-CO<sub>2</sub> substrates.<sup>41-43</sup> This is in stark contrast to hydrogenation catalysis, which exploits extreme temperatures and pressures to regenerate the active catalyst and hydrogenate captured-CO<sub>2</sub> substrates.<sup>42, 44-47</sup>

### 0.1.2.1 Reactive CO<sub>2</sub> Capture

Reactive capture of CO<sub>2</sub> (RCC) involves the direct conversion of captured CO<sub>2</sub> following the reaction of gaseous CO<sub>2</sub> and a capture reagent.<sup>48</sup> Traditional carbon capture and utilization (CCU) methods rely on thermal energy to convert CO<sub>2</sub> to value-added products, whereas electrochemical RCC can provide a less energetically costly alternative.<sup>25, 42, 49</sup> Electrochemical conversion of CO<sub>2</sub> to products like formate and methanol has provided an excellent platform for RCC methods, as the conversion step can be performed under mild conditions.<sup>50</sup>

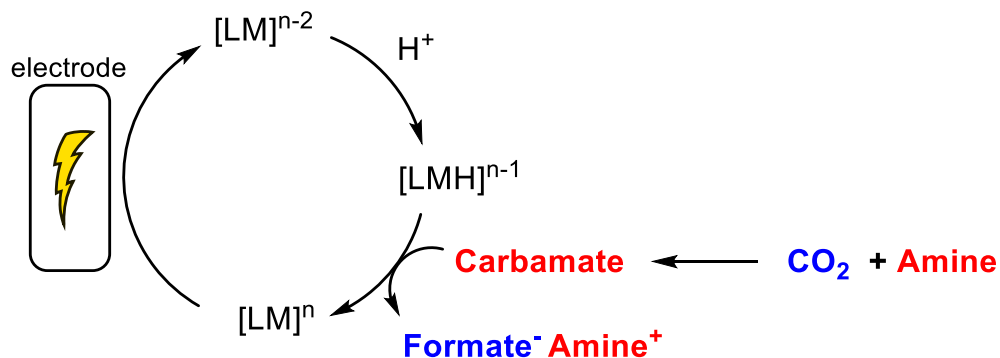


**Figure 0.2.** Cycle of proposed electrochemical RCC of CO<sub>2</sub> with amines.

In Figure 0.2, a catalytic cycle for RCC is proposed based on previous work reported by the Yang group.<sup>30</sup> In this cycle a carbamate (formed by reacting an amine with CO<sub>2</sub> gas) is reduced by a metal hydride that can be regenerated by electrochemical reduction followed by protonation with an acid. An example of this chemistry from the Kang group successfully utilizes an Fe–H to generate formate and methanol in a sequential reduction, starting from carbamates as the substrate.<sup>51</sup> Amines act as useful CO<sub>2</sub> sorbents and be regenerated for reuse under hydrogenative

and electrochemical conditions.<sup>52-55</sup> Carbamates, the substrates for reduction or hydrogenation that are formed by reacting amines with CO<sub>2</sub>, have great synthetic utility in C–C bond forming reactions, and can serve as useful substrates for the identification of RCC catalysts.<sup>56, 57</sup>

## 0.2 Research Goals

The work described herein describes the successful development of a new Kumada cross-coupling reaction using benzylic sulfonamides (Figure 0.3A), the expansion of a XEC reaction that results in the carbodifunctionalization of propargylic piperidines (Figure 0.3B), and the synthesis, isolation, and characterization of a Ru-MACHO® dihydride capable of reducing CO<sub>2</sub> and dimethylammonium dimethyl carbamate to formate (Figure 0.3C). These advances explore the use of Ni and Ru transition metal complexes and involve the engaging of a C–N bond to generate valuable products.

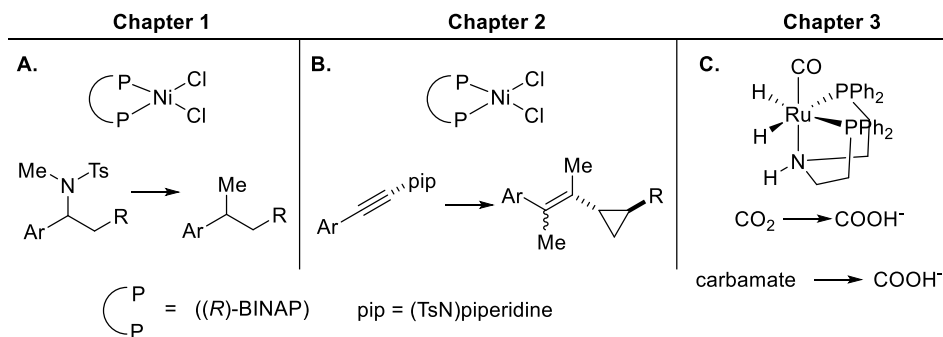


**Figure 0.3.** Overview of the transformations described in this thesis. **A:** Chapter 1. **B:** Chapter 2. **C:** Chapter 3.

### 0.3 References

- (1) Johansson Seechurn, C. C. C.; Kitching, M. O.; Colacot, T. J.; Snieckus, V. Palladium-Catalyzed Cross-Coupling: A Historical Contextual Perspective to the 2010 Nobel Prize. *Angewandte Chemie International Edition* **2012**, *51* (21), 5062-5085. DOI: <https://doi.org/10.1002/anie.201107017>.
- (2) Hills, I. D.; Fu, G. C. Elucidating Reactivity Differences in Palladium-Catalyzed Coupling Processes: The Chemistry of Palladium Hydrides. *Journal of the American Chemical Society* **2004**, *126* (41), 13178-13179. DOI: 10.1021/ja0471424.
- (3) Werner, H. At Least 60 Years of Ferrocene: The Discovery and Rediscovery of the Sandwich Complexes. *Angewandte Chemie International Edition* **2012**, *51* (25), 6052-6058. DOI: <https://doi.org/10.1002/anie.201201598>.
- (4) Breslow, R. Biomimetic Chemistry and Artificial Enzymes: Catalysis by Design. *Accounts of Chemical Research* **1995**, *28* (3), 146-153. DOI: 10.1021/ar00051a008.
- (5) Proppe, A. H.; Li, Y. C.; Aspuru-Guzik, A.; Berlinguette, C. P.; Chang, C. J.; Cogdell, R.; Doyle, A. G.; Flick, J.; Gabor, N. M.; van Grondelle, R.; et al. Bioinspiration in light harvesting and catalysis. *Nature Reviews Materials* **2020**, *5* (11), 828-846. DOI: 10.1038/s41578-020-0222-0.
- (6) Jana, R.; Pathak, T. P.; Sigman, M. S. Advances in Transition Metal (Pd,Ni,Fe)-Catalyzed Cross-Coupling Reactions Using Alkyl-organometallics as Reaction Partners. *Chemical Reviews* **2011**, *111* (3), 1417-1492. DOI: 10.1021/cr100327p.
- (7) Bolm, C. Cross-Coupling Reactions. *The Journal of Organic Chemistry* **2012**, (77), 5221–5223. DOI: 10.1021/jo301069c.

- (8) Tabassum, S.; Zahoor, A. F.; Ahmad, S.; Noreen, R.; Khan, S. G.; Ahmad, H. Cross-coupling reactions towards the synthesis of natural products. *Molecular Diversity* **2022**, *26* (1), 647-689. DOI: 10.1007/s11030-021-10195-6.
- (9) Seyferth, D. Alkyl and Aryl Derivatives of the Alkali Metals: Useful Synthetic Reagents as Strong Bases and Potent Nucleophiles. 1. Conversion of Organic Halides to Organoalkali-Metal Compounds. *Organometallics* **2006**, *25* (1), 2-24. DOI: 10.1021/om058054a.
- (10) Everson, D. A.; Weix, D. J. Cross-Electrophile Coupling: Principles of Reactivity and Selectivity. *The Journal of Organic Chemistry* **2014**, *79* (11), 4793-4798. DOI: 10.1021/jo500507s.
- (11) Diccianni, J. B.; Diao, T. Mechanisms of Nickel-Catalyzed Cross-Coupling Reactions. *Trends in Chemistry* **2019**, *1* (9), 830-844. DOI: <https://doi.org/10.1016/j.trechm.2019.08.004>.
- (12) *Modern Organonickel Chemistry*; Wiley-VCH, 2005.
- (13) Tasker, S. Z.; Standley, E. A.; Jamison, T. F. Recent advances in homogeneous nickel catalysis. *Nature* **2014**, *509* (7500), 299-309. DOI: 10.1038/nature13274.
- (14) Tollefson, E. J.; Hanna, L. E.; Jarvo, E. R. Stereospecific Nickel-Catalyzed Cross-Coupling Reactions of Benzylic Ethers and Esters. *Accounts of Chemical Research* **2015**, *48* (8), 2344-2353. DOI: 10.1021/acs.accounts.5b00223.
- (15) Dander, J. E.; Garg, N. K. Breaking Amides using Nickel Catalysis. *ACS Catalysis* **2017**, *7* (2), 1413-1423. DOI: 10.1021/acscatal.6b03277.
- (16) Yu, D.-G.; Li, B.-J.; Shi, Z.-J. Exploration of New C–O Electrophiles in Cross-Coupling Reactions. *Accounts of Chemical Research* **2010**, *43* (12), 1486-1495. DOI: 10.1021/ar100082d.

- (17) Mesganaw, T.; Garg, N. K. Ni- and Fe-Catalyzed Cross-Coupling Reactions of Phenol Derivatives. *Organic Process Research & Development* **2013**, *17* (1), 29-39. DOI: 10.1021/op300236f.
- (18) Weix, D. J. Methods and Mechanisms for Cross-Electrophile Coupling of Csp<sup>2</sup> Halides with Alkyl Electrophiles. *Accounts of Chemical Research* **2015**, *48* (6), 1767-1775. DOI: 10.1021/acs.accounts.5b00057.
- (19) Basch, C. H.; Liao, J.; Xu, J.; Piane, J. J.; Watson, M. P. Harnessing Alkyl Amines as Electrophiles for Nickel-Catalyzed Cross Couplings via C–N Bond Activation. *Journal of the American Chemical Society* **2017**, *139* (15), 5313-5316. DOI: 10.1021/jacs.7b02389.
- (20) Hu, X.; Cheng-Sánchez, I.; Cuesta-Galisteo, S.; Nevado, C. Nickel-Catalyzed Enantioselective Electrochemical Reductive Cross-Coupling of Aryl Aziridines with Alkenyl Bromides. *Journal of the American Chemical Society* **2023**, *145* (11), 6270-6279. DOI: 10.1021/jacs.2c12869.
- (21) DeLano, T. J.; Reisman, S. E. Enantioselective Electroreductive Coupling of Alkenyl and Benzyl Halides via Nickel Catalysis. *ACS Catalysis* **2019**, *9* (8), 6751-6754. DOI: 10.1021/acscatal.9b01785.
- (22) Franke, M. C.; Longley, V. R.; Rafiee, M.; Stahl, S. S.; Hansen, E. C.; Weix, D. J. Zinc-free, Scalable Reductive Cross-Electrophile Coupling Driven by Electrochemistry in an Undivided Cell. *ACS Catalysis* **2022**, *12* (20), 12617-12626. DOI: 10.1021/acscatal.2c03033.
- (23) Wang, J.; Eehalt, L. E.; Huang, Z.; Beleh, O. M.; Guzei, I. A.; Weix, D. J. Formation of C(sp<sup>2</sup>)–C(sp<sup>3</sup>) Bonds Instead of Amide C–N Bonds from Carboxylic Acid and Amine Substrate Pools by Decarbonylative Cross-Electrophile Coupling. *Journal of the American Chemical Society* **2023**, *145* (18), 9951-9958. DOI: 10.1021/jacs.2c11552.

- (24) Trends in Atmospheric Carbon Dioxide. NOAA/Global Monitoring Laboratory. 04/05/2023. <https://gml.noaa.gov/ccgg/trends/mlo.html> (accessed 04/04/2023).
- (25) Olah, G. A.; Prakash, G. K. S.; Goepfert, A. Anthropogenic Chemical Carbon Cycle for a Sustainable Future. *Journal of the American Chemical Society* **2011**, *133* (33), 12881-12898. DOI: 10.1021/ja202642y.
- (26) Hussain, I.; Alasiri, H.; Ullah Khan, W.; Alhooshani, K. Advanced electrocatalytic technologies for conversion of carbon dioxide into methanol by electrochemical reduction: Recent progress and future perspectives. *Coordination Chemistry Reviews* **2023**, *482*, 215081. DOI: <https://doi.org/10.1016/j.ccr.2023.215081>.
- (27) Kinzel, N. W.; Werlé, C.; Leitner, W. Transition Metal Complexes as Catalysts for the Electroconversion of CO<sub>2</sub>: An Organometallic Perspective. *Angewandte Chemie International Edition* **2021**, *60* (21), 11628-11686. DOI: <https://doi.org/10.1002/anie.202006988>.
- (28) Sifat, N. S.; Haseli, Y. A Critical Review of CO<sub>2</sub> Capture Technologies and Prospects for Clean Power Generation. *Energies* **2019**, *12* (21). DOI: <https://doi.org/10.3390/en12214143>  
Agricultural & Environmental Science Collection; Materials Science & Engineering Collection; Publicly Available Content Database.
- (29) Using Differential Electrochemical Mass Spectrometry (DEMS) for CO<sub>2</sub> Conversion. Hidden Analytical: 2022.
- (30) Ceballos, B. M.; Yang, J. Y. Directing the reactivity of metal hydrides for selective CO<sub>2</sub> reduction. *Proceedings of the National Academy of Sciences* **2018**, *115* (50), 12686-12691. DOI: doi:10.1073/pnas.1811396115.



- (31) Ceballos, B. M.; Yang, J. Y. Highly Selective Electrocatalytic CO<sub>2</sub> Reduction by [Pt(dmpe)<sub>2</sub>]<sup>2+</sup> through Kinetic and Thermodynamic Control. *Organometallics* **2020**, *39* (9), 1491-1496. DOI: 10.1021/acs.organomet.9b00720.
- (32) Cunningham, D. W.; Yang, J. Y. Kinetic and mechanistic analysis of a synthetic reversible CO<sub>2</sub>/HCO<sub>2</sub><sup>-</sup> electrocatalyst. *Chemical Communications* **2020**, *56* (85), 12965-12968, 10.1039/D0CC05556E. DOI: 10.1039/D0CC05556E.
- (33) Cunningham, D. W.; Barlow, J. M.; Velazquez, R. S.; Yang, J. Y. Reversible and Selective CO<sub>2</sub> to HCO<sub>2</sub><sup>-</sup> Electrocatalysis near the Thermodynamic Potential. *Angewandte Chemie International Edition* **2020**, *59* (11), 4443-4447. DOI: <https://doi.org/10.1002/anie.201913198>.
- (34) Wang, X. S.; Yang, J. Y. Translating aqueous CO<sub>2</sub> hydrogenation activity to electrocatalytic reduction with a homogeneous cobalt catalyst. *Chemical Communications* **2023**, *59* (3), 338-341, 10.1039/D2CC05473F. DOI: 10.1039/D2CC05473F.
- (35) Waldie, K. M.; Ostericher, A. L.; Reineke, M. H.; Sasayama, A. F.; Kubiak, C. P. Hydricity of Transition-Metal Hydrides: Thermodynamic Considerations for CO<sub>2</sub> Reduction. *ACS Catalysis* **2018**, *8* (2), 1313-1324. DOI: 10.1021/acscatal.7b03396.
- (36) Tsay, C.; Livesay, B. N.; Ruelas, S.; Yang, J. Y. Solvation Effects on Transition Metal Hydricity. *Journal of the American Chemical Society* **2015**, *137* (44), 14114-14121. DOI: 10.1021/jacs.5b07777.
- (37) Wiedner, E. S.; Chambers, M. B.; Pitman, C. L.; Bullock, R. M.; Miller, A. J. M.; Appel, A. M. Thermodynamic Hydricity of Transition Metal Hydrides. *Chemical Reviews* **2016**, *116* (15), 8655-8692. DOI: 10.1021/acs.chemrev.6b00168.
- (38) Shafaat, H. S.; Yang, J. Y. Uniting biological and chemical strategies for selective CO<sub>2</sub> reduction. *Nature Catalysis* **2021**, *4* (11), 928-933. DOI: 10.1038/s41929-021-00683-1.

- (39) Ilic, S.; Gesiorski, J. L.; Weerasooriya, R. B.; Glusac, K. D. Biomimetic Metal-Free Hydride Donor Catalysts for CO<sub>2</sub> Reduction. *Accounts of Chemical Research* **2022**, *55* (6), 844-856. DOI: 10.1021/acs.accounts.1c00708.
- (40) Appel, A. M.; Bercaw, J. E.; Bocarsly, A. B.; Dobbek, H.; DuBois, D. L.; Dupuis, M.; Ferry, J. G.; Fujita, E.; Hille, R.; Kenis, P. J. A.; et al. Frontiers, Opportunities, and Challenges in Biochemical and Chemical Catalysis of CO<sub>2</sub> Fixation. *Chemical Reviews* **2013**, *113* (8), 6621-6658. DOI: 10.1021/cr300463y.
- (41) Kothandaraman, J.; Lopez, J. S.; Jiang, Y.; Walter, E. D.; Burton, S. D.; Dagle, R. A.; Heldebrant, D. J. Integrated Capture and Conversion of CO<sub>2</sub> to Methanol in a Post-Combustion Capture Solvent: Heterogeneous Catalysts for Selective C-N Bond Cleavage. *Advanced Energy Materials* **2022**, *12* (46), 2202369, <https://doi.org/10.1002/aenm.202202369>. DOI: <https://doi.org/10.1002/aenm.202202369> (accessed 2023/04/11).
- (42) Kar, S.; Goeppert, A.; Prakash, G. K. S. Integrated CO<sub>2</sub> Capture and Conversion to Formate and Methanol: Connecting Two Threads. *Accounts of Chemical Research* **2019**, *52* (10), 2892-2903. DOI: 10.1021/acs.accounts.9b00324.
- (43) Sun, S.; Sun, H.; Williams, P. T.; Wu, C. Recent advances in integrated CO<sub>2</sub> capture and utilization: a review. *Sustainable Energy & Fuels* **2021**, *5* (18), 4546-4559, 10.1039/D1SE00797A. DOI: 10.1039/D1SE00797A.
- (44) Kar, S.; Kothandaraman, J.; Goeppert, A.; Prakash, G. K. S. Advances in catalytic homogeneous hydrogenation of carbon dioxide to methanol. *Journal of CO<sub>2</sub> Utilization* **2018**, *23*, 212-218. DOI: <https://doi.org/10.1016/j.jcou.2017.10.023>.

- (45) Erickson, J. D.; Preston, A. Z.; Linehan, J. C.; Wiedner, E. S. Enhanced Hydrogenation of Carbon Dioxide to Methanol by a Ruthenium Complex with a Charged Outer-Coordination Sphere. *ACS Catalysis* **2020**, *10* (13), 7419-7423. DOI: 10.1021/acscatal.0c02268.
- (46) Rezayee, N. M.; Huff, C. A.; Sanford, M. S. Tandem Amine and Ruthenium-Catalyzed Hydrogenation of CO<sub>2</sub> to Methanol. *Journal of the American Chemical Society* **2015**, *137* (3), 1028-1031. DOI: 10.1021/ja511329m.
- (47) Jeletic, M. S.; Hulley, E. B.; Helm, M. L.; Mock, M. T.; Appel, A. M.; Wiedner, E. S.; Linehan, J. C. Understanding the Relationship Between Kinetics and Thermodynamics in CO<sub>2</sub> Hydrogenation Catalysis. *ACS Catalysis* **2017**, *7* (9), 6008-6017. DOI: 10.1021/acscatal.7b01673.
- (48) Siegel, R. E.; Pattanayak, S.; Berben, L. A. Reactive Capture of CO<sub>2</sub>: Opportunities and Challenges. *ACS Catalysis* **2023**, *13* (1), 766-784. DOI: 10.1021/acscatal.2c05019.
- (49) Li, M.; Irtem, E.; Iglesias van Montfort, H.-P.; Abdinejad, M.; Burdyny, T. Energy comparison of sequential and integrated CO<sub>2</sub> capture and electrochemical conversion. *Nature Communications* **2022**, *13* (1), 5398. DOI: 10.1038/s41467-022-33145-8.
- (50) Sullivan, I.; Goryachev, A.; Digdaya, I. A.; Li, X.; Atwater, H. A.; Vermaas, D. A.; Xiang, C. Coupling electrochemical CO<sub>2</sub> conversion with CO<sub>2</sub> capture. *Nature Catalysis* **2021**, *4* (11), 952-958. DOI: 10.1038/s41929-021-00699-7.
- (51) Bi, J.; Hou, P.; Liu, F.-W.; Kang, P. Electrocatalytic Reduction of CO<sub>2</sub> to Methanol by Iron Tetradentate Phosphine Complex Through Amidation Strategy. *ChemSusChem* **2019**, *12* (10), 2195-2201. DOI: <https://doi.org/10.1002/cssc.201802929>.
- (52) Chai, S. Y. W.; Ngu, L. H.; How, B. S. Review of carbon capture absorbents for CO<sub>2</sub> utilization. *Greenhouse Gases: Science and Technology* **2022**, *12* (3), 394-427. DOI: <https://doi.org/10.1002/ghg.2151>.

- (53) Jakobsen, J. B.; Rønne, M. H.; Daasbjerg, K.; Skrydstrup, T. Are Amines the Holy Grail for Facilitating CO<sub>2</sub> Reduction? *Angewandte Chemie International Edition* **2021**, *60* (17), 9174-9179. DOI: <https://doi.org/10.1002/anie.202014255>.
- (54) Balaraman, E.; Gunanathan, C.; Zhang, J.; Shimon, L. J. W.; Milstein, D. Efficient hydrogenation of organic carbonates, carbamates and formates indicates alternative routes to methanol based on CO<sub>2</sub> and CO. *Nature Chemistry* **2011**, *3* (8), 609-614. DOI: 10.1038/nchem.1089.
- (55) Kar, S.; Sen, R.; Kothandaraman, J.; Goeppert, A.; Chowdhury, R.; Munoz, S. B.; Haiges, R.; Prakash, G. K. S. Mechanistic Insights into Ruthenium-Pincer-Catalyzed Amine-Assisted Homogeneous Hydrogenation of CO<sub>2</sub> to Methanol. *Journal of the American Chemical Society* **2019**, *141* (7), 3160-3170. DOI: 10.1021/jacs.8b12763.
- (56) Christian Malapit , M. T., Andrew Pendergast ,Sagar Udyavara ,Wesley Beck ,Ryan Smith ,Selma Kadic ,Tommy Primo ,Ding Wu ,Tanner Stone ,Henry White ,Matthew Neurock ,Matthew Sigman ,Shelley Minter. Electrochemical cobalt-catalyzed selective carboxylation of benzyl halides with CO<sub>2</sub> enabled by low-coordinate cobalt electrocatalysts. **2021**. DOI: 10.26434/chemrxiv-2021-thftp.
- (57) Luo, X.; Song, X.; Xiong, W.; Li, J.; Li, M.; Zhu, Z.; Wei, S.; Chan, A. S. C.; Zou, Y. Copper-Catalyzed C–H Carbamoyloxylation of Aryl Carboxamides with CO<sub>2</sub> and Amines at Ambient Conditions. *Organic Letters* **2019**, *21* (7), 2013-2018. DOI: 10.1021/acs.orglett.9b00122.

# Chapter 1: Kumada Cross-Coupling Reaction of Acyclic Sulfonamides

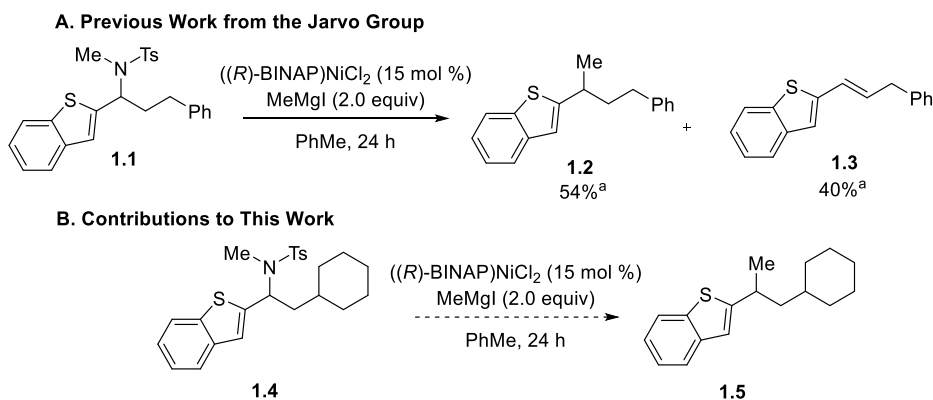
Portions of this chapter have been published:

Hewitt, K.A.; Herbert, C.A.; **Matus, A.C.**; Jarvo, E.R. *Molecules* 2021, 26, 5947.

## 1.1 Introduction

The development of cross-coupling reactions using transition metal catalysis has transformed synthetic organic chemistry, leading to new and effective ways to form carbon-carbon bonds.<sup>1-3</sup> The use of palladium catalysts is prevalent in cross-coupling reactions, however the role of nickel in transition metal-catalyzed cross-coupling reactions has grown rapidly over the past two decades.<sup>4</sup> Palladium catalyst reactivity is well understood, but nickel provides an inexpensive alternative. Because nickel is more electropositive in comparison to palladium, nickel catalysts can undergo more facile oxidative addition.<sup>4-9</sup> This reactivity has allowed for the development of cross-coupling reactions that involve the activation of bonds often considered challenging to engage, such as carbon-oxygen and carbon-nitrogen bonds.<sup>10-12</sup>

**Scheme 1.1: Kumada Cross-Coupling of Acyclic, Uncharged Sulfonamides**



<sup>a</sup>Yield determined by <sup>1</sup>H NMR based on the comparison to PhTMS as internal standard.

Typically, carbon-nitrogen bonds are difficult to engage in cross-coupling reactions and are activated by incorporating ring strain or charge in the cross-coupling substrates.<sup>13</sup> The Doyle and Watson groups have demonstrated this reactivity through the use of styrenyl aziridines and Katritzky pyridinium salts as electrophilic coupling partners.<sup>14-15</sup> The Jarvo group has gained particular interest in cross-coupling and cross-electrophile coupling reactions of less activated sulfonamides, and has previously demonstrated the Kumada cross-coupling reaction of benzylic

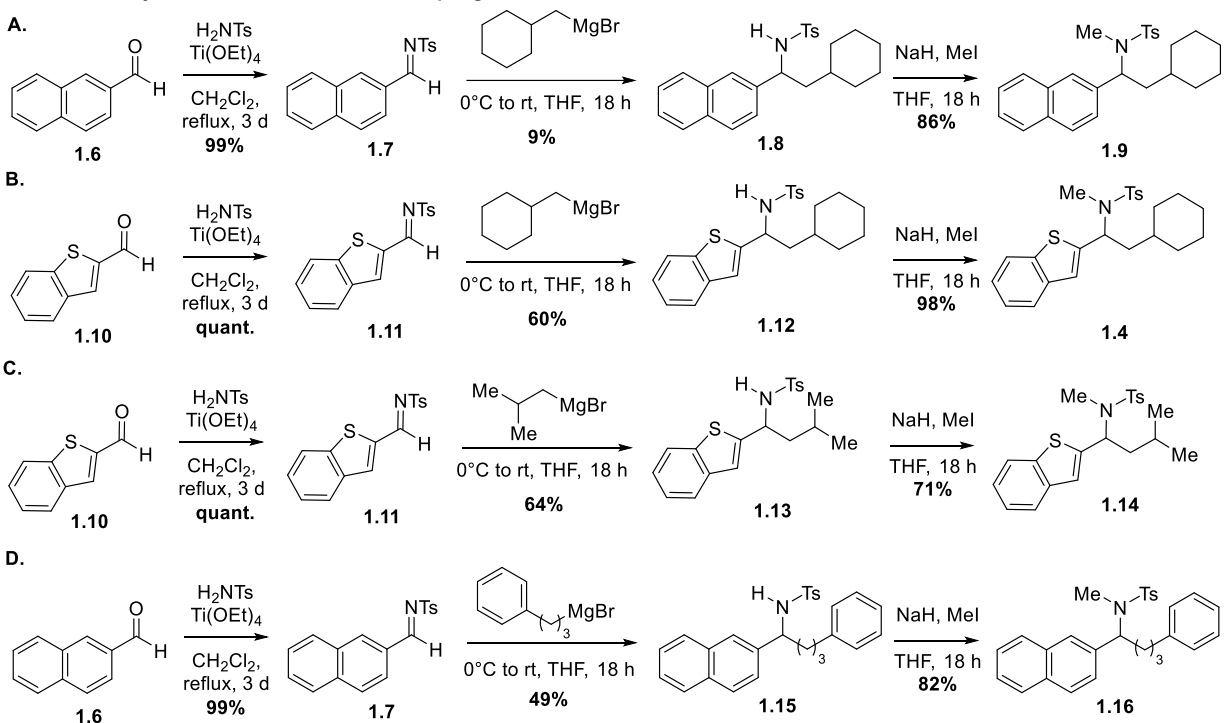
sulfonamides (Scheme 1.1A).<sup>16-17</sup> However, a significant amount of side product resulting from competitive  $\beta$ -hydride elimination was produced. The goal of this work was to develop a Kumada cross-coupling reaction that suppressed  $\beta$ -hydride elimination. To progress towards this goal, I synthesized four substrates containing various degrees of  $\beta$ -branching (Scheme 1.1B) to subject to the Kumada cross-coupling reaction conditions, and also examined the impacts of heat on product outcome.

## **1.2 Results and Discussion**

### **1.2.1 Synthesis of Sulfonamide Substrates for Cross-Coupling**

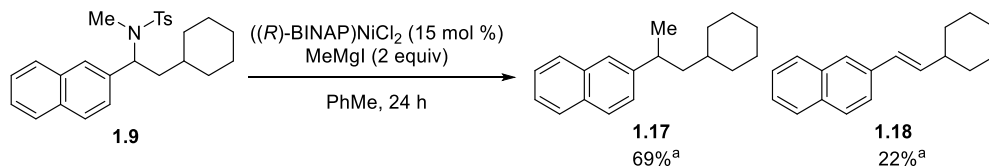
In order to further the development of the Kumada cross-coupling reaction of sulfonamides, I first investigated the effect that a cyclohexyl group would have on  $\beta$ -hydride elimination. The target substrates could be accessed in three steps from commercially available aldehydes as outlined in Scheme 1.2A. An imine condensation reaction with aldehyde **1.6** and *p*-toluenesulfonamide afforded imine **1.7**. Grignard addition with cyclohexylmethylmagnesium bromide then afforded **1.8**. Methylation using sodium hydride and iodomethane afforded the  $\beta$ -branched sulfonamide substrate **1.9**.

**Scheme 1.2: Synthesis of Kumada Cross-Coupling Substrates**



With  $\beta$ -branched substrate **1.9** in hand, I then investigated the Kumada cross-coupling reaction. When subjected to previously optimized Kumada cross-coupling conditions, substrate **1.9** produced a 69% yield of **1.17** with 22% production of **1.18** from  $\beta$ -hydride elimination (Scheme 1.3). No starting material was observed after the cross-coupling reaction, and I was unable to isolate products from other potential decomposition pathways. This increase in yield and decrease in  $\beta$ -hydride elimination in comparison to the previously demonstrated reaction (Scheme 1.1A) was encouraging. I then synthesized and examined substrates **1.4**, **1.14**, and **1.16** following the synthetic routes shown in Scheme 1.2 (B–D).

**Scheme 1.3. Kumada Cross-Coupling Reaction of Sulfonamide 1.9**

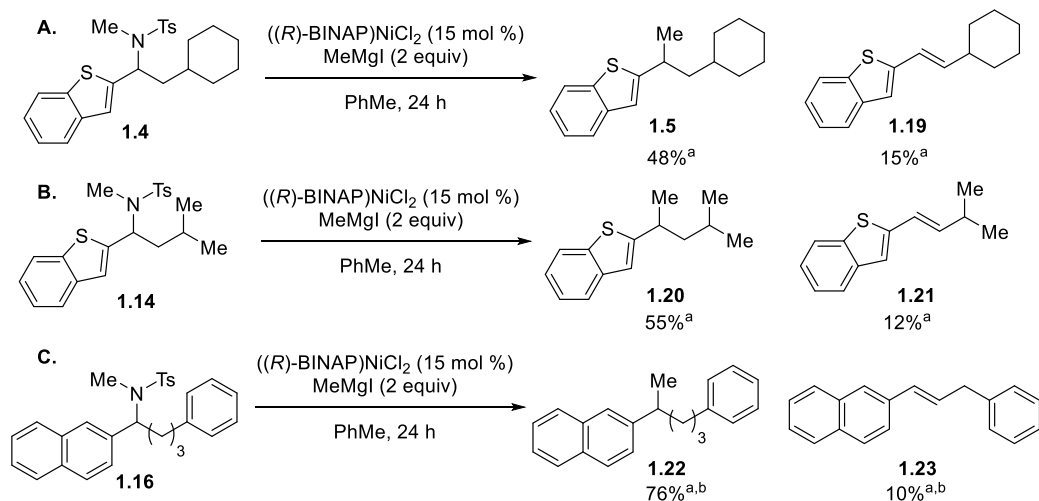


<sup>a</sup>Yield determined by <sup>1</sup>H NMR based on the comparison to PhTMS as an internal standard.



Substrates **1.4** and **1.14** provide direct comparisons to the previously examined benzothiophene-containing sulfonamide **1.1**, and both cyclohexyl and isopropyl functionalities suppressed  $\beta$ -hydride elimination to less than 15% (Scheme 1.4A, B). These results indicate that steric bulk near the reaction center influences the conversion of substrate to product. To further investigate  $\beta$ -hydride elimination, I synthesized sulfonamide **1.16**, which contains no  $\beta$ -branching. I expected to observe a significant amount of **1.23** production from the  $\beta$ -hydride elimination pathway. However, the yield of **1.22** was high in comparison to formation of **1.23** (Scheme 1.4C). To examine this reactivity further, I will investigate the outcome of Kumada cross-coupling reactions with substrates containing less steric bulk, and more extended alkyl substituents.

**Scheme 1.4. Scope of Kumada Cross-Coupling of Acyclic Sulfonamides**

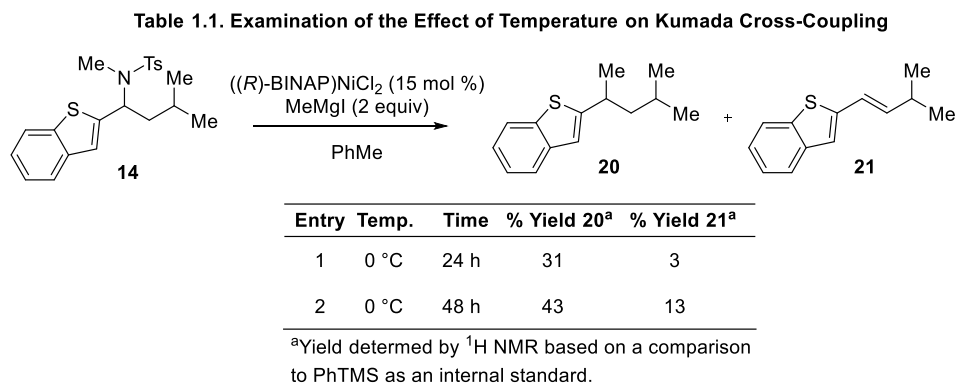


<sup>a</sup>Yield determined by <sup>1</sup>H NMR based on the comparison to PhTMS as an internal standard. <sup>b</sup>Isolated yield of **1.22** and **1.23**: 80%, 9%, respectively.

## 1.2.2 Effect of Temperature on Kumada Cross-Coupling Reaction

Low temperature was utilized in attempts to slow the rate of  $\beta$ -hydride elimination. After initial results at room temperature were obtained, I selected sulfonamide **1.14** as a model substrate, and performed the Kumada cross-coupling reaction at 0 °C (Table 1.1, entry 1). I observed a 31% yield of product **1.20**, 3% yield of **1.21** from the  $\beta$ -hydride elimination pathway, and 38% starting material still present. I hypothesized that the remaining starting material may be converted to

product if the reaction were to proceed at 0 °C over a longer period. To investigate this hypothesis, the reaction was allowed to stir for 48 h (Table 1.1, entry 2). However, I observed similar results to those of the standard reaction conditions (Scheme 1.4B) and saw that the yield of **1.20** only increased to 43%, while  $\beta$ -hydride elimination resulted in a 13% yield of **1.21**. These low-temperature Kumada cross-coupling data are consistent with the reduced rate of  $\beta$ -hydride elimination, but do not appear to promote greater conversion of substrate to product.



### 1.3 Conclusion

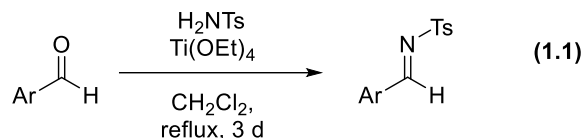
In conclusion, I expanded the scope of the Kumada cross-coupling reaction utilizing acyclic, benzylic sulfonamides with limited  $\beta$ -hydride elimination. While temperature had limited impact on product distribution,  $\beta$ -branching substrates were well-tolerated by the method and only produced 10% of the  $\beta$ -hydride elimination product at the lowest. The developed Kumada cross-coupling reaction was further expanded by my coworkers to incorporate enantioenriched cyclic sulfonamide substrates, affording acyclic products in good yields with high stereoselectivity.<sup>18</sup> This reaction was also applied to access an analog of a known ATPase inhibitor, displaying the broad synthetic utility of the method. The developed Kumada cross-coupling reaction detailed here displays the utility of nickel catalysis in engaging  $Csp^3-N$  bond-containing electrophiles.

## 1.4 Experimental

### 1.4.1 General Procedures for Substrate Synthesis

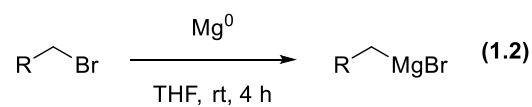
All reactions were carried out under a N<sub>2</sub> atmosphere, unless otherwise noted. All glassware was oven- or flame-dried prior to use. Tetrahydrofuran (THF), diethyl ether (Et<sub>2</sub>O), dichloromethane (CH<sub>2</sub>Cl<sub>2</sub>), and toluene (PhMe) were degassed with Ar and then passed through two 4 x 36 inch columns of anhydrous neutral A-2 alumina (8 x 14 mesh; LaRoche Chemicals; activated under a flow of argon at 350 °C for 12 h) to remove H<sub>2</sub>O.<sup>19</sup> Other solvents were purchased anhydrous commercially, or purified as described. <sup>1</sup>H NMR spectra were recorded on Bruker DRX-400 (400 MHz <sup>1</sup>H), GN-500 (500 MHz <sup>1</sup>H, 125.4 MHz <sup>13</sup>C), CRYO-500 (500 MHz <sup>1</sup>H, 125.8 MHz <sup>13</sup>C), or AVANCE-600 (600 MHz <sup>1</sup>H, 150.9 MHz <sup>13</sup>C, 564.7 MHz <sup>19</sup>F) spectrometers. Proton chemical shifts are reported in ppm (δ) relative to internal tetramethylsilane (TMS, δ 0.0). Data are reported as follows: chemical shift (multiplicity [singlet (s), broad singlet (br s), doublet (d), doublet of doublets (dd), triplet (t), doublet of triplets (dt), doublet of doublet of triplets (ddt), quartet (q) quintet (quin), sextet (sextet), apparent doublet (ad), multiplet (m), coupling constants [Hz], integration). Carbon chemical shifts are reported in ppm (δ) relative to TMS with the respective solvent resonance as the internal standard (CDCl<sub>3</sub>, δ 77.16 ppm). NMR data were collected at 25 °C. Analytical thin-layer chromatography (TLC) was performed using Silica Gel 60 F254 precoated plates (0.25 mm thickness). Visualization was accomplished by irradiation with a UV lamp and stains were used as needed. Flash chromatography was performed using SiliaFlash F60 (40-63 μm, 60 Å) from SiliCycle. Automated chromatography was carried out on a Teledyne Isco CombiFlash Rf Plus. Melting points (m.p.) were obtained using a MelTemp melting point apparatus and are uncorrected. High resolution mass spectrometry was performed by the University of California, Irvine Mass Spectrometry Center.

#### 1.4.1.1 Method A: Imine Condensation of *p*-Toluenesulfonamide with Aldehydes



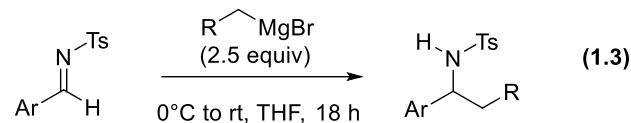
This procedure is adapted from a procedure reported by Zhang.<sup>20</sup> To a flame-dried round-bottom flask equipped with a stir bar was added aldehyde (1.0 equiv) and *p*-toluenesulfonamide (1.0 equiv). The flask was equipped with an oven-dried reflux condenser, evacuated, and backfilled with N<sub>2</sub>. CH<sub>2</sub>Cl<sub>2</sub> (70. mM in substrate) and Ti(OEt)<sub>4</sub> (2.0 equiv) were added to the flask, and the reaction mixture was allowed to stir at reflux for 3 d. After cooling to room temperature, the reaction mixture was quenched with H<sub>2</sub>O and filtered via vacuum filtration. The layers were separated and the aqueous layer was washed with CH<sub>2</sub>Cl<sub>2</sub> (x 3). The combined organic layers were washed with brine, dried over Na<sub>2</sub>SO<sub>4</sub>, filtered, and concentrated in vacuo. The imine product was typically carried into the next step without further purification.

#### 1.4.1.2 Method B: Preparation of Grignard Reagents



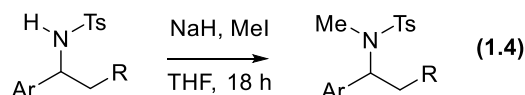
To a flame-dried two-neck flask equipped with a stir bar and reflux condenser was added magnesium turnings (5.0 equiv). The flask and magnesium turnings were flame-dried under vacuum, and the flask was then back-filled with N<sub>2</sub>. THF (5.0 M in alkyl bromide) and a crystal of iodine (ca. 2 mg) were added to the flask. Alkyl bromide (1.0 equiv) was added dropwise over 30 minutes to maintain a gentle reflux. The mixture was allowed to stir at room temperature for 3 h, and the resulting Grignard reagent was transferred to a flame-dried round bottom flask. The Grignard reagent was titrated to 0.3 M–0.7M by the Knochel method.<sup>21</sup>

### 1.4.1.3 Method C: Grignard Addition to Imines



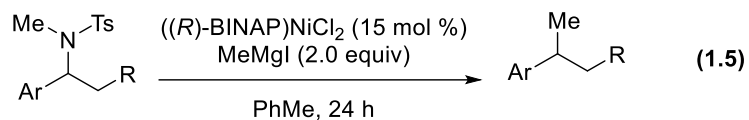
To a flame-dried flask equipped with a stir bar was added fresh Grignard reagent (2.5 equiv in THF). The reaction mixture was cooled to 0°C and imine (1.0 equiv) dissolved in THF was added dropwise to flask. The reaction mixture was warmed to room temperature and allowed to stir for 18 h. The reaction mixture was quenched with saturated aqueous NH<sub>4</sub>Cl and extracted with EtOAc (x 3). The combined organic layers were washed with brine, dried over Na<sub>2</sub>SO<sub>4</sub>, filtered, and concentrated in vacuo.

### 1.4.1.4 Method D: Methylation of Sulfonamides



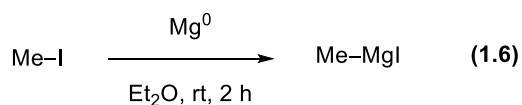
This procedure is adapted from a procedure reported by Jarvo.<sup>22</sup> To a suspension of NaH (1.3 equiv) in THF (50. mM in NaH) was added a solution of sulfonamide in THF (1.0 equiv, 0.50 M in substrate) dropwise. Reaction mixture was allowed to stir for 1 h at room temperature, then MeI (1.1 equiv) was added dropwise, and the reaction mixture continued to stir for 18 h. The reaction mixture was quenched with saturated aqueous NH<sub>4</sub>Cl and extracted with EtOAc (x 3). The combined organic layers were washed with brine, dried over Na<sub>2</sub>SO<sub>4</sub>, filtered, and concentrated in vacuo.

### 1.4.2 Method E: General Kumada Cross-Coupling Reaction Procedures



In a glovebox, an oven-dried 7 mL vial equipped with a stir bar was charged with ((*R*)-BINAP)NiCl<sub>2</sub> (15 mol %), acyclic sulfonamide (1.0 equiv) and PhMe (0.20 M in substrate). MeMgI in Et<sub>2</sub>O (2.0 equiv) was added dropwise and the reaction mixture was allowed to stir for 24 h at room temperature. The reaction was removed from the glovebox, quenched with MeOH, filtered through a plug of silica gel eluting with Et<sub>2</sub>O, and concentrated in vacuo. Phenyltrimethylsilane (PhTMS; 8.6 μL, 50. μmol) was added and the yield was determined by <sup>1</sup>H NMR based on comparison to PhTMS as internal standard before further purification.

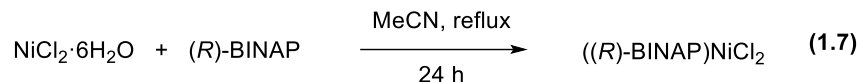
### 1.4.3 Preparation of Methylmagnesium Iodide



Under a N<sub>2</sub> atmosphere, a three-necked flask equipped with a stir bar, reflux condenser, and Schlenk filtration apparatus was charged with magnesium turnings (2.80 g, 115 mmol). The flask and magnesium turnings were then flame-dried under vacuum and the flask was backfilled with N<sub>2</sub>. Anhydrous Et<sub>2</sub>O (25 mL) and a crystal of iodine (ca. 2 mg) were added to the flask. The reaction mixture was brought to 0 °C and freshly distilled iodomethane (5.0 mL, 80. mmol) was slowly added over 30 min to maintain a gentle reflux. The reaction mixture was brought to room temperature and allowed to stir for 2 h, then filtered through the fritted Schlenk filter into a pear-shaped flask under N<sub>2</sub> atmosphere. The pear-shaped flask was capped with a septum, sealed with parafilm, and stored in the glovebox under a N<sub>2</sub> atmosphere for up to eight weeks without

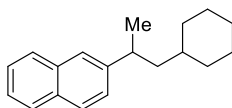
detrimental effects. The resulting Grignard reagent was titrated by Knochel's method to 2.4 M to 3.0 M.<sup>21</sup>

#### 1.4.4 Preparation of ((*R*)-BINAP)NiCl<sub>2</sub>



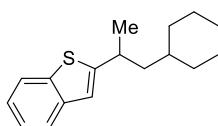
This method is based on a procedure reported by Jamison.<sup>23</sup> To a flame-dried flask equipped with a stir bar was added NiCl<sub>2</sub>·6H<sub>2</sub>O (1.0 equiv). The flask was placed under vacuum and flame-dried until most of the nickel compound had turned from emerald green to yellow-orange. Some of the green hydrate complex is necessary for the reaction to proceed. The flask was allowed to cool to room temperature, and the solid was dissolved in MeCN (50. mM). The chiral (*R*)-BINAP (1.0 equiv) was added to the reaction flask, which was then fitted with a reflux condenser. The reaction mixture was heated to reflux and allowed to stir for 24 h. The reaction was cooled to room temperature and the black crystalline product was vacuum filtered. The precipitate was washed with excess MeCN.

#### 1.4.5 Characterization Data of Kumada Cross-Coupling Products



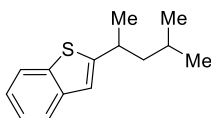
**2-(1-cyclohexylpropan-2-yl)naphthalene (1.17)** was prepared according to Method E. The following amounts of reagents were used: ((*R*)-BINAP)NiCl<sub>2</sub> (11 mg, 15 μmol, 15 mol %), **1.9** (44 mg, 0.10 mmol, 1.0 equiv), PhMe (0.50 mL, 0.20 M in substrate), and methymagnesium iodide (70. μL, 2.9 M, 0.20 mmol, 2.0 equiv). Before purification, a <sup>1</sup>H NMR yield of 69% was obtained based on comparison to PhTMS as an internal standard. The compound was purified by flash chromatography (0–20% EtOAc/hexanes) to afford the title compound as a clear, colorless oil (14

mg, 0.055 mmol, 55% isolated yield). **TLC**  $R_f$  = 0.74 (100% hexanes);  **$^1\text{H NMR}$**  (500 MHz,  $\text{CDCl}_3$ ),  $\delta$  7.78 (m, 2H), 7.60 (br s, 1H), 7.43 (m, 2H), 7.35 (dd,  $J$  = 8.6 Hz, 1.4 Hz, 1H), 7.25 (s, 1H), 2.99 (sext,  $J$  = 1H), 1.81 (d,  $J$  = 12.8 Hz, 1H), 1.62 (m, 5H), 1.46 (m, 1H), 1.28 (d,  $J$  = 6.9 Hz, 3H), 1.13 (m, 4H), 0.89 (q,  $J$  = 12.3 Hz, 2H);  **$^{13}\text{C NMR}$**  (125.8 MHz,  $\text{CDCl}_3$ )  $\delta$  145.8, 133.8, 132.3, 128.0, 127.72, 127.68, 126.0, 125.9, 125.2, 125.1, 46.3, 37.0, 35.3, 33.9, 33.5, 26.9, 26.4, 26.4, 23.1; **HRMS** (TOF MS  $\text{CI}^+$ )  $m/z$  calcd for  $\text{C}_{19}\text{H}_{24}$  ( $\text{M}$ ) $^+$  252.1878 found 252.1868.

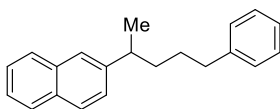


**2-(1-cyclohexylpropan-2-yl)benzo[b]thiophene (1.5)** was prepared according to Method E. The following amounts of reagents were used: ((*R*)-BINAP)NiCl<sub>2</sub> (11 mg, 15  $\mu\text{mol}$ , 15 mol %), **1.4** (43 mg, 0.10 mmol, 1.0 equiv), PhMe (0.50 mL, 0.20 M in substrate), and methymagnesium iodide (70.  $\mu\text{L}$ , 2.8 M, 0.20 mmol, 2.0 equiv). Before purification, a  $^1\text{H NMR}$  yield of 48% was obtained based on comparison to PhTMS as an internal standard. The compound was purified by flash chromatography (0–15% Et<sub>2</sub>O/pentanes) to afford the title compound as a clear, colorless oil (isolated yield was not determined due to the coelution of product formed through  $\beta$ -hydride elimination). **TLC**  $R_f$  = 0.74 (100% pentanes);  **$^1\text{H NMR}$** : (600 MHz,  $\text{CDCl}_3$ )  $\delta$  7.83 (d,  $J$  = 7.2 Hz, 1H), 7.72 (d,  $J$  = 7.8 Hz, 1H), 7.36 (m, 1H), 7.30 (m, 1H), 7.06 (s, 1H), 3.27 (sext,  $J$  = 12.6 Hz, 1H), (d,  $J$  = 12.8 Hz, 2H), 1.69 (m, 4H), 1.53 (m, 1H), 1.40 (d,  $J$  = 6.8 Hz, 3H), 1.33 (m, 2H), 1.22 (m, 2H), 0.95 (m, 2H);  **$^{13}\text{C NMR}$**  (150.9 MHz,  $\text{CDCl}_3$ )  $\delta$  153.6, 140.2, 138.9, 124.1, 123.4, 122.9, 122.4, 119.0, 66.0, 46.7, 35.2, 33.7, 33.3, 26.8, 26.4, 23.8, 15.4; **HRMS** (TOF MS  $\text{CI}^+$ )  $m/z$  calcd for  $\text{C}_{17}\text{H}_{22}\text{S}$  ( $\text{M}$ ) $^+$  258.1442, found 258.1453.





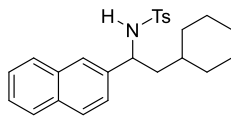
**2-(4-methylpentan-2-yl)benzo[*b*]thiophene (1.20)** was prepared according to Method E. The following amounts of reagents were used: ((*R*)-BINAP)NiCl<sub>2</sub> (11 mg, 15 μmol, 15 mol %), **1.14** (39 mg, 0.10 mmol, 1.0 equiv), PhMe (0.50 mL, 2.0 M in substrate), and methymagnesium iodide (70. μL, 2.8 M, 0.20 mmol, 2.0 equiv). Before purification, a <sup>1</sup>H NMR yield of 55% was obtained based on comparison to PhTMS as an internal standard. The compound was purified by flash chromatography (0–20% EtOAc/hexanes) to afford the title compound as a clear, colorless oil (isolated yield was not determined due to the coelution of product formed through β-hydride elimination). **TLC** R<sub>f</sub> = 0.71 (100% hexanes); **<sup>1</sup>H NMR** (600 MHz, CDCl<sub>3</sub>) δ 7.76 (d, *J* = 7.9 Hz, 1.9 Hz, 1H), 7.66 (d, *J* = 7.8 Hz, 1H), 7.32–7.21 (m, 1H), 7.12 (d, *J* = 8.7 Hz, 1H), 6.83 (d, *J* = 8.7 Hz, 1H), 3.17 (sext, *J* = 6.83, 1H), 1.90–1.82 (m, 1H), 1.68–1.53 (m, 1H), 1.50–1.44 (m, 1H), 1.35 (d, *J* = 6.8 Hz, 3H), 0.90 (d, *J* = 22.7 Hz, 6.5 Hz, 6H); **<sup>13</sup>C NMR** (150.9 MHz, CDCl<sub>3</sub>) δ 129.5, 124.1, 123.4, 122.9, 122.4, 119.1, 113.9, 48.4, 34.2, 29.9, 25.7, 23.6, 22.9, 22.4; **HRMS** (TOF MS CI<sup>+</sup>) *m/z* calcd for C<sub>14</sub>H<sub>18</sub>S (M)<sup>+</sup> 218.1129, found 218.1186.



**2-(5-phenylpentan-2-yl)naphthalene (1.22)** was prepared according to Method E. The following amounts of reagents were used: ((*R*)-BINAP)NiCl<sub>2</sub> (5.6 mg, 7.5 μmol, 15 mol %), **1.16** (22 mg, 50. μmol, 1.0 equiv), PhMe (0.25 mL, 0.20 M in substrate), and methymagnesium iodide (40. μL, 2.8 M, 0.10 mmol, 2.0 equiv). Before purification, a <sup>1</sup>H NMR yield of 76% was obtained based on

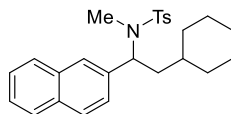
comparison to PhTMS as an internal standard. The compound was purified by flash chromatography (0–20% EtOAc/hexanes) to afford the title compound as a clear, colorless oil (11 mg, 40.  $\mu$ mol, 80%). **TLC**  $R_f$  = 0.74 (100% hexanes);  **$^1\text{H NMR}$**  (500 MHz,  $\text{CDCl}_3$ )  $\delta$  7.79 (d,  $J$  = 8.1 Hz, 1H), 7.77 (d,  $J$  = 8.2 Hz, 2H), 7.57 (s, 1H), 7.42 (td,  $J$  = 6.8 Hz, 1.2 Hz, 2H), 7.32 (dd,  $J$  = 8.4 Hz, 1.7 Hz, 1H), 7.23 (t,  $J$  = 7.5 Hz, 2H), 7.14 (t,  $J$  = 7.4 Hz, 1H), 7.11 (d,  $J$  = 7.0 Hz, 2H), 2.87 (sext,  $J$  = 5.5 Hz, 1H), 2.58 (m, 2H), 1.71 (m, 2H), 1.60 (m, 1H), 1.51 (m, 1H), 1.31 (d,  $J$  = 6.9 Hz, 3H);  **$^{13}\text{C NMR}$**  (125.8 MHz,  $\text{CDCl}_3$ )  $\delta$  145.2, 142.7, 133.7, 132.3, 128.5 (2C), 128.3 (2C), 128.0, 127.7, 127.6, 125.94, 125.91, 125.7, 125.3, 125.2, 40.1, 37.8, 36.1, 29.6, 22.4; **HRMS** (TOF MS  $\text{CI}^+$ )  $m/z$  calcd for  $\text{C}_{21}\text{H}_{22}$  ( $\text{M}$ ) $^+$  274.1721, found 274.1710.

#### 1.4.6 Characterization Data of Starting Materials

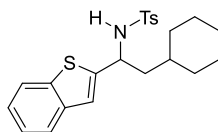


***N*-(2-cyclohexyl-1-(naphthalen-2-yl)ethyl)-4-methylbenzenesulfonamide (1.8)** was prepared according to Method C. The following amounts of reagents were used: 4-methyl-*N*-(naphthalen-2-ylmethylene)benzenesulfonamide **1.7** (789 mg, 2.50 mmol, 1.00 equiv), (cyclohexylmethyl)magnesium bromide (9.0 mL, 0.70 M in THF, 6.3 mmol, 2.5 equiv), THF (8.3 mL, 0.30 M in substrate). The compound was purified by flash column chromatography (0–20% EtOAc/hexanes) to afford the title compound as a yellow solid (98 mg, 0.24 mmol, 9%); **m.p.** 149–151°C; **TLC**  $R_f$  = 0.60 (20% EtOAc/hexanes);  **$^1\text{H NMR}$**  (500 MHz,  $\text{CDCl}_3$ )  $\delta$  7.73 (d,  $J$  = 9.1 Hz, 1H), 7.62 (d,  $J$  = 8.4 Hz, 2H), 7.48–7.37 (m, 4H), 7.36 (br s, 1H), 7.13 (d,  $J$  = 8.5 Hz, 1H), 6.90 (d,  $J$  = 8.2 Hz, 2H), 4.82 (br d,  $J$  = 7.3 Hz, 1H), 4.54 (q,  $J$  = 7.6 Hz, 1H), 2.15 (s, 3H), 1.77–1.56 (m, 7H), 1.24–1.15 (m, 1H), 1.14–1.00 (m, 3H), 0.98–0.79 (m, 2H);  **$^{13}\text{C NMR}$**  (125.8 MHz,  $\text{CDCl}_3$ )  $\delta$  142.9, 138.4, 137.6, 133.1, 132.7, 129.1 (2C), 128.4, 127.8, 127.5, 127.1 (2C), 126.1,

125.9, 125.8, 124.1, 56.0, 45.5, 33.9, 33.2, 33.0, 26.4, 26.1, 26.0, 21.3; **HRMS** (TOF MS ES+)  $m/z$  calcd for  $C_{25}H_{29}NO_2SNa$  ( $M + Na$ )<sup>+</sup> 430.1817, found 430.1819.

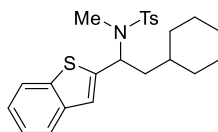


***N*-(2-cyclohexyl-1-(naphthalen-2-yl)ethyl)-*N*,4-dimethylbenzenesulfonamide (1.9)** was prepared according to Method D. The following amounts of reagents were used: **1.8** (186 mg, 0.456 mmol, 1.00 equiv), NaH (17 mg, 0.70 mmol, 1.5 equiv), MeI (40.  $\mu$ L, 0.60 mmol, 1.1 equiv), THF (11 mL, 50. mM in substrate). The compound was purified by flash chromatography (0–10% EtOAc/hexanes) to afford the title compound as a yellow oil (180 mg, 0.43 mmol, 86%). **TLC**  $R_f$  = 0.37 (10% EtOAc/hexanes); **<sup>1</sup>H NMR** (500 MHz,  $CDCl_3$ )  $\delta$  7.87 (d,  $J$  = 9.2 Hz, 1H), 7.82 (dd,  $J$  = 11.3 Hz, 7.5 Hz, 2H), 7.75 (d,  $J$  = 8.2 Hz, 2H), 7.65 (br s, 1H), 7.56–7.51 (m, 2H), 7.49 (dd,  $J$  = 8.5 Hz, 1.5 Hz, 1H), 7.30 (d,  $J$  = 8.0 Hz, 2H), 5.45 (br t,  $J$  = 7.7 Hz, 1H), 2.72 (s, 3H), 2.46 (s, 3H), 2.02–1.88 (m, 2H), 1.81 (d,  $J$  = 12.5 Hz, 1H), 1.78–1.72 (m, 2H), 1.72–1.60 (m, 2H), 1.26–1.12 (m, 4 H), 1.09–0.87 (m, 2H); **<sup>13</sup>C NMR** (125.8 MHz,  $CDCl_3$ )  $\delta$  143.1, 137.6, 136.3, 133.1, 132.9, 129.6 (2C), 128.2, 128.1, 127.6, 127.3 (2C), 126.8, 126.6, 126.2, 57.5 (2C), 38.2, 34.2, 33.5, 33.4, 28.9, 26.6, 26.22, 26.21, 21.6; **HRMS** (TOF MS ES+)  $m/z$  calcd for  $C_{26}H_{31}NO_2SNa$  ( $M + Na$ )<sup>+</sup> 444.1973, found 444.1968.



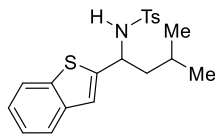
***N*-(1-(benzo[*b*]thiophen-2-yl)-2-cyclohexylethyl)-4-methylbenzenesulfonamide (1.12)** was prepared according to Method C. The following amounts of reagents were used: *N*-

(benzo[*b*]thiophen-2-ylmethylene)-4-methylbenzenesulfonamide (**1.11**) (326 mg, 1.03 mmol, 1.00 equiv), (3-phenylpropyl)magnesium bromide (6.45 mL, 0.400 M in THF, 2.58 mmol, 2.50 equiv), THF (3.5 mL, 0.30 M in substrate). The compound was purified via flash column chromatography (0–15% EtOAc/hexanes) to afford the title compound as a yellow solid (260 mg, 0.62 mmol, 60%). **TLC R<sub>f</sub>** = 0.46 (20% EtOAc/hexanes); **m.p.** 158–160°C; **<sup>1</sup>H NMR** (500 MHz, CDCl<sub>3</sub>) δ 7.67 (d, *J* = 7.9 Hz, 1H), 7.56 (d, *J* = 8.1 Hz, 2H), 7.34–7.21 (m, 3H), 7.00 (d, *J* = 8.0 Hz, 2H), 6.84 (s, 1H), 4.77 (q, *J* = 7.7 Hz, 1H), 4.64 (d, *J* = 7.8 Hz, 1H), 2.22 (s, 3H), 1.82–1.56 (m, 6H), 1.34–1.22 (m, 2H), 1.17–1.01 (m, 3H), 0.90–0.81 (m, 2H); **<sup>13</sup>C NMR** (125.8 MHz, CDCl<sub>3</sub>) δ 144.8, 142.3, 138.4, 138.2, 136.6, 128.3 (2C), 126.2 (2C), 123.4, 122.6, 121.4, 121.2, 51.3 (2C), 44.7, 33.1, 32.14, 32.10, 25.5, 25.1, 25.1, 20.4 **HRMS** (TOF MS ES<sup>+</sup>) *m/z* calcd for C<sub>23</sub>H<sub>27</sub>NO<sub>2</sub>S<sub>2</sub>Na (M + Na)<sup>+</sup> 436.1381, found 436.1376.

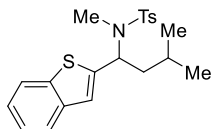


*N*-(1-benzo[*b*]thiophen-2-yl)-2-cyclohexylethyl-*N*,4-dimethylbenzenesulfonamide (**1.4**) was prepared according to Method D. The following amounts of reagents were used: **1.12** (170 mg, 0.41 mmol, 1.0 equiv), NaH (31 mg, 0.53 mmol, 1.3 equiv), MeI (30. μL, 0.45 mmol, 1.1 equiv), THF (8.2 mL, 50. mM in substrate). The compound was purified by flash column chromatography (20% EtOAc/hexanes) to afford the title compound as a clear, colorless oil (170 mg, 0.40 mmol, 98%). **TLC R<sub>f</sub>** = 0.40 (10% EtOAc/hexanes); **<sup>1</sup>H NMR** (500 MHz, CDCl<sub>3</sub>) δ 7.73 (d, *J* = 7.8 Hz, 1H), 7.70 (d, *J* = 8.3 Hz, 2H), 7.66 (d, *J* = 7.2 Hz, 1H), 7.30 (dtd, *J* = 16.4 Hz, 7.2 Hz, 1.3 Hz, 2H), 7.24 (d, *J* = 8.0 Hz, 2H), 7.05 (s, 1H), 5.50 (t, *J* = 7.6, 1H), 2.71 (s, 3H), 2.39 (s, 3H), 1.92–1.78 (m, 2H), 1.76–1.59 (m, 5H), 1.33–1.23 (m, 1H), 1.20–1.10 (m, 3H), 1.04–0.83 (m, 2H); **<sup>13</sup>C NMR**

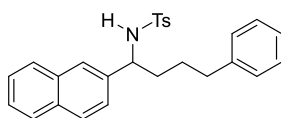
(125.8 MHz, CDCl<sub>3</sub>)  $\delta$  144.1, 143.0, 139.4, 139.1, 137.0, 129.4 (2C), 127.2 (2C), 124.2, 123.3, 122.3, 122.5, 122.1, 53.9, 40.3, 34.0, 33.4, 33.0, 28.7, 26.3, 26.0, 25.9, 21.4; **HRMS** (TOF MS ES+)  $m/z$  calcd for C<sub>24</sub>H<sub>29</sub>NO<sub>2</sub>S<sub>2</sub>Na (M + Na)<sup>+</sup> 450.1537, found 450.1530.



***N*-(1-benzo[*b*]thiophen-2-yl)-3-methylbutyl-4-methylbenzenesulfonamide (1.13)** was prepared according to Method C. The following amounts of reagents were used: *N*-(benzo[*b*]thiophen-2-ylmethylene)-4-methylbenzenesulfonamide (**1.11**) (389 mg, 1.23 mmol, 1.00 equiv), isobutylmagnesium bromide (7.7 mL, 0.40 M, 3.0 mmol, 2.5 equiv), THF (4.1 mL, 0.40 M in substrate). The compound was purified by flash column chromatography (0–20% EtOAc/hexanes) to afford the title compound as a white powder (290 mg, 0.79 mmol, 64%). **TLC**  $R_f$  = 0.58 (20% EtOAc/hexanes); **m.p.** 99–101 °C; **<sup>1</sup>H NMR** (400 MHz, CDCl<sub>3</sub>)  $\delta$  7.62 (d,  $J$  = 7.7 Hz, 1H),  $\delta$  7.57 (d,  $J$  = 8.3 Hz, 2H), 7.50 (d,  $J$  = 7.2 Hz, 1 Hz), 7.30–7.17 (m, 2H), 6.92 (d,  $J$  = 8.0 Hz, 2H), 6.82 (s, 1H), 5.55 (d,  $J$  = 8.1 Hz, 1H), 4.72 (q,  $J$  = 7.7 Hz, 1H), 2.14 (s, 3H), 1.79–1.54 (m, 3H), 0.85 (dd,  $J$  = 10.1 Hz, 6.4 Hz, 6H); **<sup>13</sup>C NMR** (125.7 MHz, CDCl<sub>3</sub>)  $\delta$  145.4, 142.8, 139.1, 139.0, 137.4, 128.8 (2C), 126.9 (2C), 124.03, 124.01, 123.2, 122.1, 121.9, 52.7, 46.5, 24.5, 22.1, 22.0, 20.9; **HRMS** (TOF MS ES+)  $m/z$  calcd for C<sub>20</sub>H<sub>23</sub>NO<sub>2</sub>S<sub>2</sub>Na (M + Na)<sup>+</sup> 396.1068, found 396.1078.

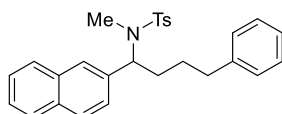


***N*-(1-benzo[*b*]thiophen-2-yl)-3-methylbutyl)-*N*,4-dimethylbenzenesulfonamide (1.14)** was prepared according to Method D. The following amounts of reagents were used: **1.13** (292 mg, 0.782 mmol, 1.00 equiv), NaH (24 mg, 1.0 mmol, 1.3 equiv), MeI (50.  $\mu$ L, 0.86 mmol, 1.1 equiv), THF (17 mL, 50. mM in substrate). The compound was purified by flash column chromatography (0–20% EtOAc/hexanes) to afford the title compound as a clear, colorless oil (210 mg, 0.55 mmol, 71%). **TLC**  $R_f$  = 0.44 (10% EtOAc/hexanes);  **$^1\text{H NMR}$**  (500 MHz)  $\delta$  7.70 (dd,  $J$  = 8.0 Hz, 6.1 Hz, 3H), 7.63 (d,  $J$  = 7.3 Hz, 1 H), 7.33–7.24 (m, 2H), 7.21 (d,  $J$  = 8.4 Hz, 2H), 7.03 (s, 1H), 5.47 (t,  $J$  = 7.5 Hz, 1H), 2.72 (s, 3H), 2.36 (s, 3H), 1.86–1.77 (m, 1H), 1.74–1.59 (m, 2H), 0.97 (dd,  $J$  = 15.9 Hz, 6.6 Hz, 6H);  **$^{13}\text{C NMR}$**  (125.8 MHz,  $\text{CDCl}_3$ )  $\delta$  143.9, 143.3, 139.5, 139.2, 137.0, 129.5 (2C), 127.4 (2C), 124.4, 124.4, 123.5, 122.7, 122.2, 54.9, 41.8, 28.9, 24.9, 22.8, 22.5, 21.5; **HRMS** (TOF MS ES+)  $m/z$  calcd for  $\text{C}_{21}\text{H}_{25}\text{NO}_2\text{S}_2\text{Na}$  ( $\text{M} + \text{Na}$ ) $^+$  410.1224, found 410.1227.



**4-methyl-*N*-(1-(naphthalen-2-yl)-4-phenylbutyl)benzenesulfonamide (1.15)** was prepared according to Method C. The following amounts of reagents were used: (4-methyl-*N*-(naphthalen-2-ylmethylene)benzenesulfonamide (**1.7**) (1.10 g, 2.36 mmol, 1.50 equiv), (3-phenylpropyl)magnesium bromide (4.6 mL, 0.50 M in THF, 3.5 mmol, 1.5 equiv), THF (18 mL, 0.20 M in substrate). The compound was purified by flash chromatography (0–20% EtOAc/hexanes) to yield the title compound as a yellow solid (0.498 g, 1.16 mmol, 49%); **m.p.** 144–146°C; **TLC**  $R_f$  = 0.53 (20% EtOAc/hexanes);  **$^1\text{H NMR}$**  (500 MHz,  $\text{CDCl}_3$ )  $\delta$  7.70–7.67 (m, 1H), 7.56 (d,  $J$  = 8.6 Hz, 2H), 7.44 (d,  $J$  = 8.3 Hz, 2H), 7.40–7.35 (m, 2H), 7.29 (s, 1H), 7.18 (t,  $J$  = 7.4 Hz, 2H), 7.15–7.08 (m, 2H), 7.01 (d,  $J$  = 7.0 Hz, 2H), 6.82 (d,  $J$  = 7.9 Hz, 2H), 5.50 (d,  $J$  =

7.9 Hz, 1H), 4.43 (q,  $J = 7.5$  Hz, 1H), 2.50 (t,  $J = 7.7$  Hz, 2H), 2.08 (s, 3H), 1.92–1.80 (m, 1H), 1.80–1.70 (m, 1H), 1.64–1.55 (m, 1H), 1.51–1.38 (m, 1H);  $^{13}\text{C}$  NMR (125.8 MHz,  $\text{CDCl}_3$ )  $\delta$  143.0, 141.8, 137.8, 137.7, 133.0, 132.7, 129.1 (2C), 128.53, 128.50 (2C), 128.4 (2C), 127.9, 127.6, 127.1 (2C), 126.1, 126.0, 125.9, 125.8, 124.1, 58.6, 36.9, 35.4, 27.7, 21.3; **HRMS** (TOF MS ES+)  $m/z$  calcd for  $\text{C}_{27}\text{H}_{27}\text{NO}_2\text{SNa}$  ( $\text{M} + \text{Na}$ ) $^+$  452.1660, found 452.1651.



***N*,4-dimethyl-*N*-(1-(naphthalen-2-yl)-4-phenylbutyl)benzenesulfonamide (1.16)** was prepared according to Method D. The following amounts of reagents were used: **1.15** (498 mg, 1.16 mmol, 1.00 equiv), NaH (36 mg, 1.5 mmol, 1.3 equiv) MeI (80.  $\mu\text{L}$ , 1.3 mmol, 1.1 equiv), THF (23 mL, 50. mM in substrate). The compound was purified by flash chromatography (0–20 % EtOAc) to afford the title compound as a white solid (420 mg, 0.95 mmol, 82%). **TLC**  $R_f = 0.34$  (20% EtOAc); **m.p.** 99–101°C;  $^1\text{H}$  NMR (500MHz,  $\text{CDCl}_3$ )  $\delta$  7.80–7.73 (m, 1H), 7.71 (d,  $J = 8.5$  Hz, 1H), 7.69–7.61 (m, 2H), 7.51–7.39 (m, 3H), 7.34 (t,  $J = 7.5$  Hz, 1H), 7.25 (q,  $J = 6.9$  Hz, 3H), 7.17 (t,  $J = 9.1$  Hz, 3H), 7.11 (d,  $J = 7.4$  Hz, 2H), 5.26 (t,  $J = 7.7$  Hz, 1H), 2.64 (t,  $J = 7.3$  Hz, 2H), 2.60 (s, 3H), 2.34 (s, 3H), 2.03 (dt,  $J = 13.8$  Hz, 7.7 Hz, 1H), 1.80 (dt,  $J = 15.1$  Hz, 7.6 Hz, 1H), 1.69–1.54 (m, 2H);  $^{13}\text{C}$  NMR (125.4 MHz,  $\text{CDCl}_3$ )  $\delta$  143.1, 141.9, 137.5, 135.9, 133.1, 132.9, 129.6 (2C), 128.6 (2C), 128.5 (2C), 128.3, 128.1, 127.7, 127.3 (2C), 126.8, 126.5, 126.3 (2C), 126.0, 60.0, 35.6, 30.0, 28.9, 28.3, 21.6; **HRMS** (TOF MS ES+)  $m/z$  calcd for  $\text{C}_{28}\text{H}_{29}\text{NO}_2\text{SNa}$  ( $\text{M} + \text{Na}$ ) $^+$  466.1817, found 466.1816.

## 1.5 References

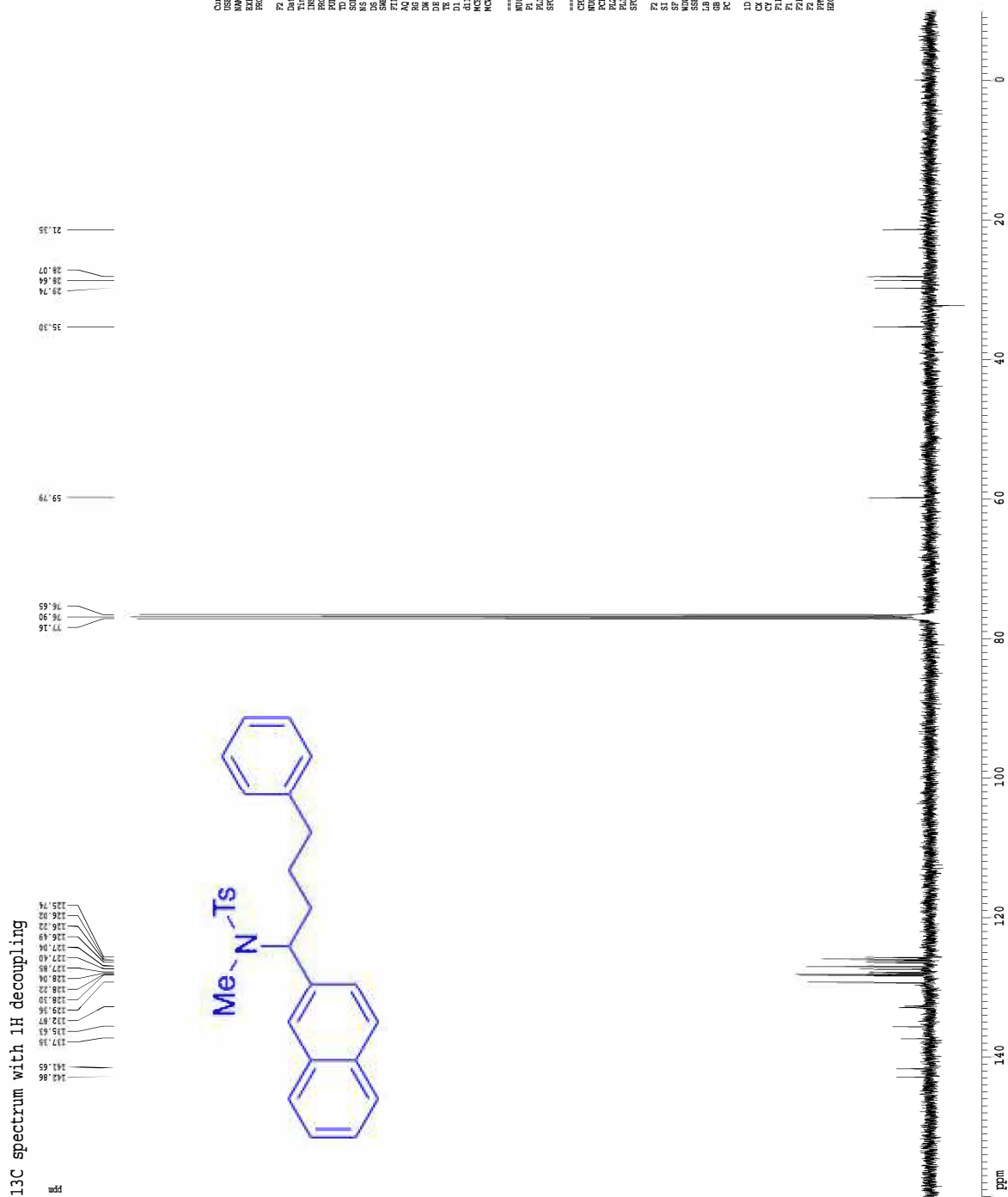
1. Bolm, C., Cross-Coupling Reactions. *The Journal of Organic Chemistry* **2012**, (77), 5221–5223.
2. Hartwig, J. F.; Collman, J. P., *Organotransition metal chemistry: from bonding to catalysis*. University Science Books Sausalito, CA: 2010; Vol. 1.
3. Jana, R.; Pathak, T. P.; Sigman, M. S., Advances in Transition Metal (Pd,Ni,Fe)-Catalyzed Cross-Coupling Reactions Using Alkyl-organometallics as Reaction Partners. *Chemical Reviews* **2011**, *111* (3), 1417-1492.
4. Diccianni, J. B.; Diao, T., Mechanisms of Nickel-Catalyzed Cross-Coupling Reactions. *Trends in Chemistry* **2019**, *1* (9), 830-844.
5. Tasker, S. Z.; Standley, E. A.; Jamison, T. F., Recent advances in homogeneous nickel catalysis. *Nature* **2014**, *509* (7500), 299-309.
6. Ting, S. I.; Williams, W. L.; Doyle, A. G., Oxidative Addition of Aryl Halides to a Ni(I)-Bipyridine Complex. *Journal of the American Chemical Society* **2022**, *144* (12), 5575-5582.
7. Tsou, T. T.; Kochi, J. K., Mechanism of oxidative addition. Reaction of nickel(0) complexes with aromatic halides. *Journal of the American Chemical Society* **1979**, *101* (21), 6319-6332.
8. Tang, T.; Hazra, A.; Min, D. S.; Williams, W. L.; Jones, E.; Doyle, A. G.; Sigman, M. S., Interrogating the Mechanistic Features of Ni(I)-Mediated Aryl Iodide Oxidative Addition Using Electroanalytical and Statistical Modeling Techniques. *Journal of the American Chemical Society* **2023**.
9. *Modern Organonickel Chemistry*. XIX ed.; Wiley-VCH: 2005.
10. Lucas, E. L.; Jarvo, E. R., Stereospecific and stereoconvergent cross-couplings between alkyl electrophiles. *Nature Reviews Chemistry* **2017**, *1* (9), 0065.

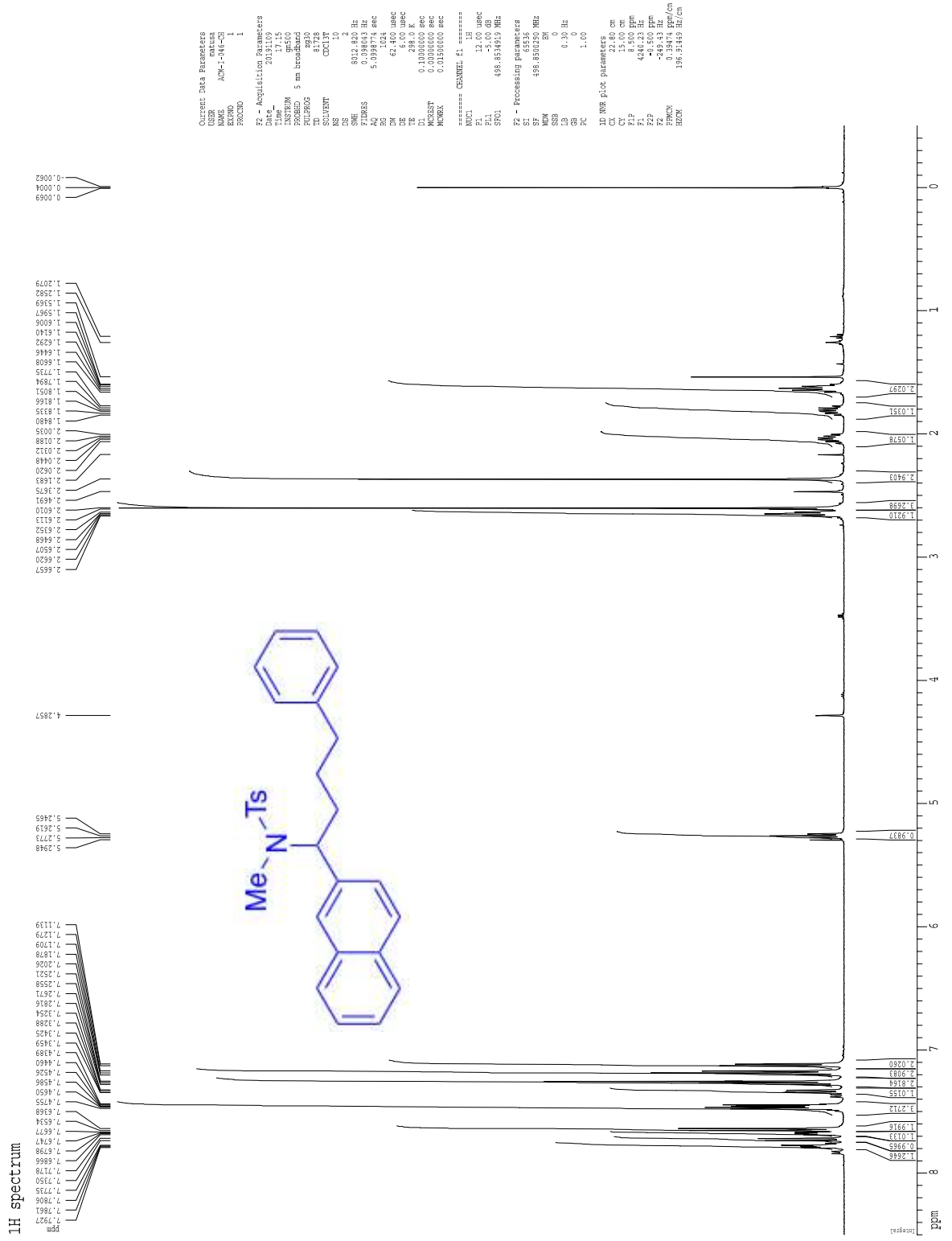


11. Ouyang, K.; Hao, W.; Zhang, W.-X.; Xi, Z., Transition-Metal-Catalyzed Cleavage of C–N Single Bonds. *Chemical Reviews* **2015**, *115* (21), 12045-12090.
12. Dongbang, S.; Doyle, A. G., Ni/Photoredox-Catalyzed C(sp<sup>3</sup>)–C(sp<sup>3</sup>) Coupling between Aziridines and Acetals as Alcohol-Derived Alkyl Radical Precursors. *Journal of the American Chemical Society* **2022**, *144* (43), 20067-20077.
13. Cherney, A. H.; Kadunce, N. T.; Reisman, S. E., Enantioselective and Enantiospecific Transition-Metal-Catalyzed Cross-Coupling Reactions of Organometallic Reagents To Construct C–C Bonds. *Chemical Reviews* **2015**, *115* (17), 9587-9652.
14. Huang, C.-Y.; Doyle, A. G., Nickel-Catalyzed Negishi Alkylations of Styrenyl Aziridines. *Journal of the American Chemical Society* **2012**, *134* (23), 9541-9544.
15. Basch, C. H.; Liao, J.; Xu, J.; Piane, J. J.; Watson, M. P., Harnessing Alkyl Amines as Electrophiles for Nickel-Catalyzed Cross Couplings via C–N Bond Activation. *Journal of the American Chemical Society* **2017**, *139* (15), 5313-5316.
16. Lucas, E. L.; Hewitt, K. A.; Chen, P.-P.; Castro, A. J.; Hong, X.; Jarvo, E. R., Engaging Sulfonamides: Intramolecular Cross-Electrophile Coupling Reaction of Sulfonamides with Alkyl Chlorides. *The Journal of Organic Chemistry* **2020**, *85* (4), 1775-1793.
17. Chen, P.-P.; Lucas, E. L.; Greene, M. A.; Zhang, S.-Q.; Tollefson, E. J.; Erickson, L. W.; Taylor, B. L. H.; Jarvo, E. R.; Hong, X., A Unified Explanation for Chemoselectivity and Stereospecificity of Ni-Catalyzed Kumada and Cross-Electrophile Coupling Reactions of Benzylic Ethers: A Combined Computational and Experimental Study. *Journal of the American Chemical Society* **2019**, *141* (14), 5835-5855.
18. Hewitt, K. A.; Herbert, C. A.; Matus, A. C.; Jarvo, E. R., Nickel-Catalyzed Kumada Cross-Coupling Reactions of Benzylic Sulfonamides. *Molecules* **2021**, *26* (19), 5947.

19. Pangborn, A. B.; Giardello, M. A.; Grubbs, R. H.; Rosen, R. K.; Timmers, F. J., Safe and Convenient Procedure for Solvent Purification. *Organometallics* **1996**, *15* (5), 1518-1520.
20. Davis, F. A.; Zhang, Y.; Andemichael, Y.; Fang, T.; Fanelli, D. L.; Zhang, H., Improved Synthesis of Enantiopure Sulfinimines (Thiooxime S-Oxides) from p-Toluenesulfinamide and Aldehydes and Ketones. *The Journal of Organic Chemistry* **1999**, *64* (4), 1403-1406.
21. Krasovskiy, A.; Knochel, P., Convenient Titration Method for Organometallic Zinc, Magnesium, and Lanthanide- Reagents. *Synthesis* **2006**, *2006* (05), 0890-0891.
22. Taylor, B. L. H.; Swift, E. C.; Waetzig, J. D.; Jarvo, E. R., Stereospecific Nickel-Catalyzed Cross-Coupling Reactions of Alkyl Ethers: Enantioselective Synthesis of Diarylethanes. *Journal of the American Chemical Society* **2011**, *133* (3), 389-391.
23. Standley, E. A.; Smith, S. J.; Müller, P.; Jamison, T. F., A Broadly Applicable Strategy for Entry into Homogeneous Nickel(0) Catalysts from Air-Stable Nickel(II) Complexes. *Organometallics* **2014**, *33* (8), 2012-2018.

# 1.6 1H and 13C NMR Spectra





Z-restored spin-echo 13C spectrum with 1H decoupling



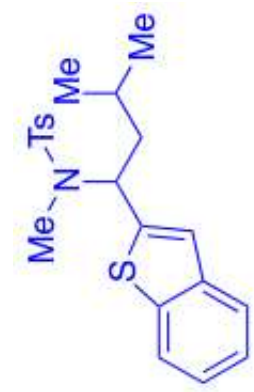
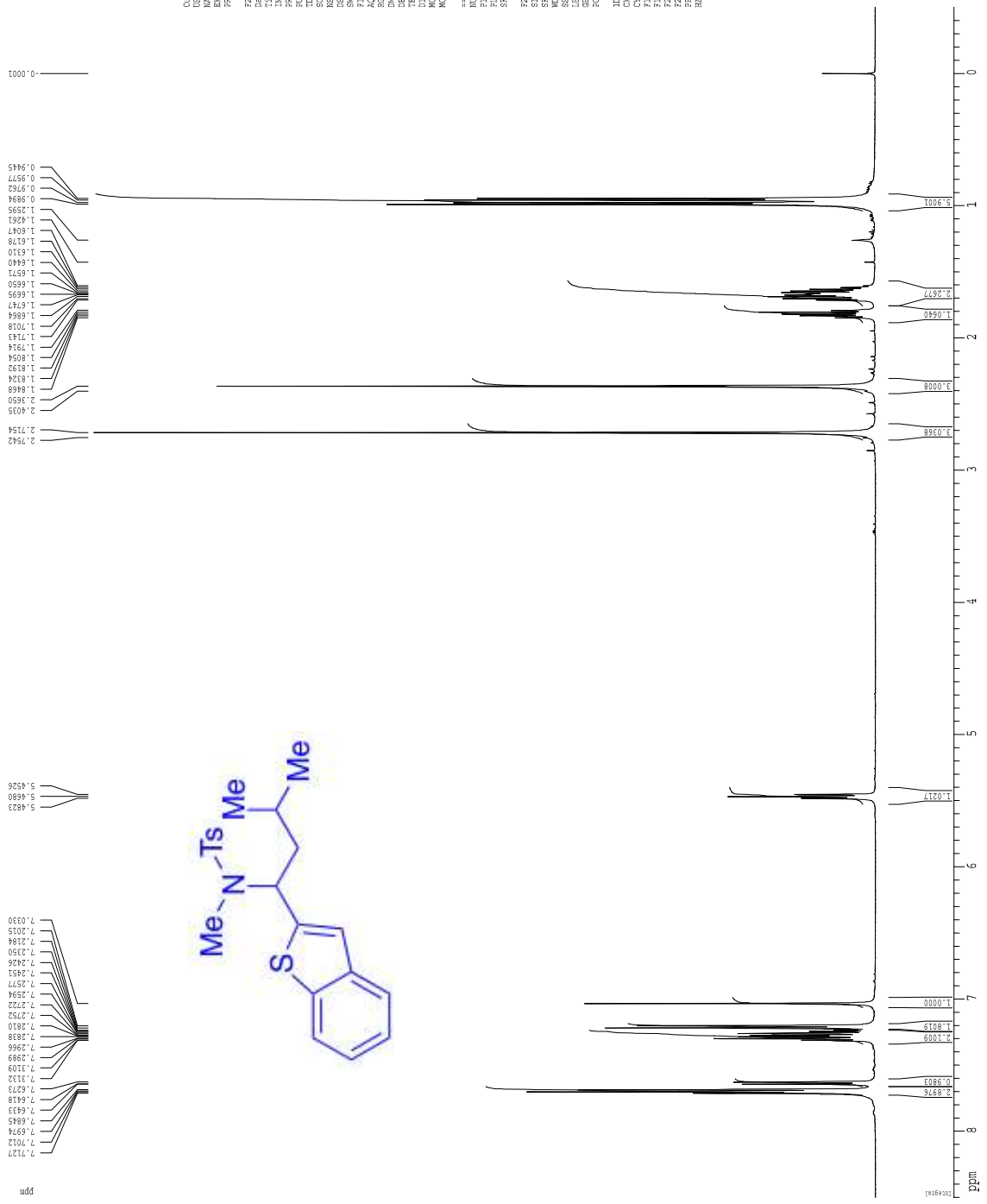
```

Current Data Parameters
USER          satuba
INSTRUM      ADR-450
PROCNO       22
PROCDS       1
F2 - Acquisition Parameters
Date_         20190923
Time          11:57
PROBHD       5 mm CPTX1-H
PULPROG      zgpg30
PCYCLPGM     3dzbpg30
AQ          0.10000000 sec
RG          722
SOLVENT      CDCl3
NS          722
DSM          3300.001 Hz
FIDRES      0.462288 Hz
AQ          0.0031997 sec
DE          15.500 umsec
ED          6.00 umsec
EI          0.2500000 sec
SI          0.0000000 sec
SF          100.6261200 MHz
WDW          EM
SSB          0.0000000 sec
RG          3276.800
AQ          0.0031997 sec
DE          6.00 umsec
EI          0.2500000 sec
SI          0.0000000 sec
WDW          EM
SSB          0.0000000 sec
RG          3276.800
F2 - Processing parameters
SI          100.6261200 MHz
SF          100.6261200 MHz
WDW          EM
SSB          0
RG          1.00
AQ          0.10000000 sec
DE          6.00000000 sec
EI          2.00
SI          100.6261200 MHz
F2 - Acquisition Parameters
USER          satuba
INSTRUM      ADR-450
PROCNO       22
PROCDS       1
F2 - Acquisition Parameters
Date_         20190923
Time          11:57
PROBHD       5 mm CPTX1-H
PULPROG      zgpg30
PCYCLPGM     3dzbpg30
AQ          0.10000000 sec
RG          722
SOLVENT      CDCl3
NS          722
DSM          3300.001 Hz
FIDRES      0.462288 Hz
AQ          0.0031997 sec
DE          15.500 umsec
ED          6.00 umsec
EI          0.2500000 sec
SI          0.0000000 sec
SF          100.6261200 MHz
WDW          EM
SSB          0.0000000 sec
RG          3276.800
AQ          0.0031997 sec
DE          6.00 umsec
EI          0.2500000 sec
SI          0.0000000 sec
WDW          EM
SSB          0.0000000 sec
RG          3276.800
F2 - Processing parameters
SI          100.6261200 MHz
SF          100.6261200 MHz
WDW          EM
SSB          0
RG          1.00
AQ          0.10000000 sec
DE          6.00000000 sec
EI          2.00
SI          100.6261200 MHz
F2 - Acquisition Parameters
USER          satuba
INSTRUM      ADR-450
PROCNO       22
PROCDS       1
F2 - Acquisition Parameters
Date_         20190923
Time          11:57
PROBHD       5 mm CPTX1-H
PULPROG      zgpg30
PCYCLPGM     3dzbpg30
AQ          0.10000000 sec
RG          722
SOLVENT      CDCl3
NS          722
DSM          3300.001 Hz
FIDRES      0.462288 Hz
AQ          0.0031997 sec
DE          15.500 umsec
ED          6.00 umsec
EI          0.2500000 sec
SI          0.0000000 sec
SF          100.6261200 MHz
WDW          EM
SSB          0.0000000 sec
RG          3276.800
AQ          0.0031997 sec
DE          6.00 umsec
EI          0.2500000 sec
SI          0.0000000 sec
WDW          EM
SSB          0.0000000 sec
RG          3276.800
F2 - Processing parameters
SI          100.6261200 MHz
SF          100.6261200 MHz
WDW          EM
SSB          0
RG          1.00
AQ          0.10000000 sec
DE          6.00000000 sec
EI          2.00
SI          100.6261200 MHz

```



1H spectrum



Current Data Parameters  
 NAME: ANV6-181821  
 EXPER: 21  
 PROCNO: 1

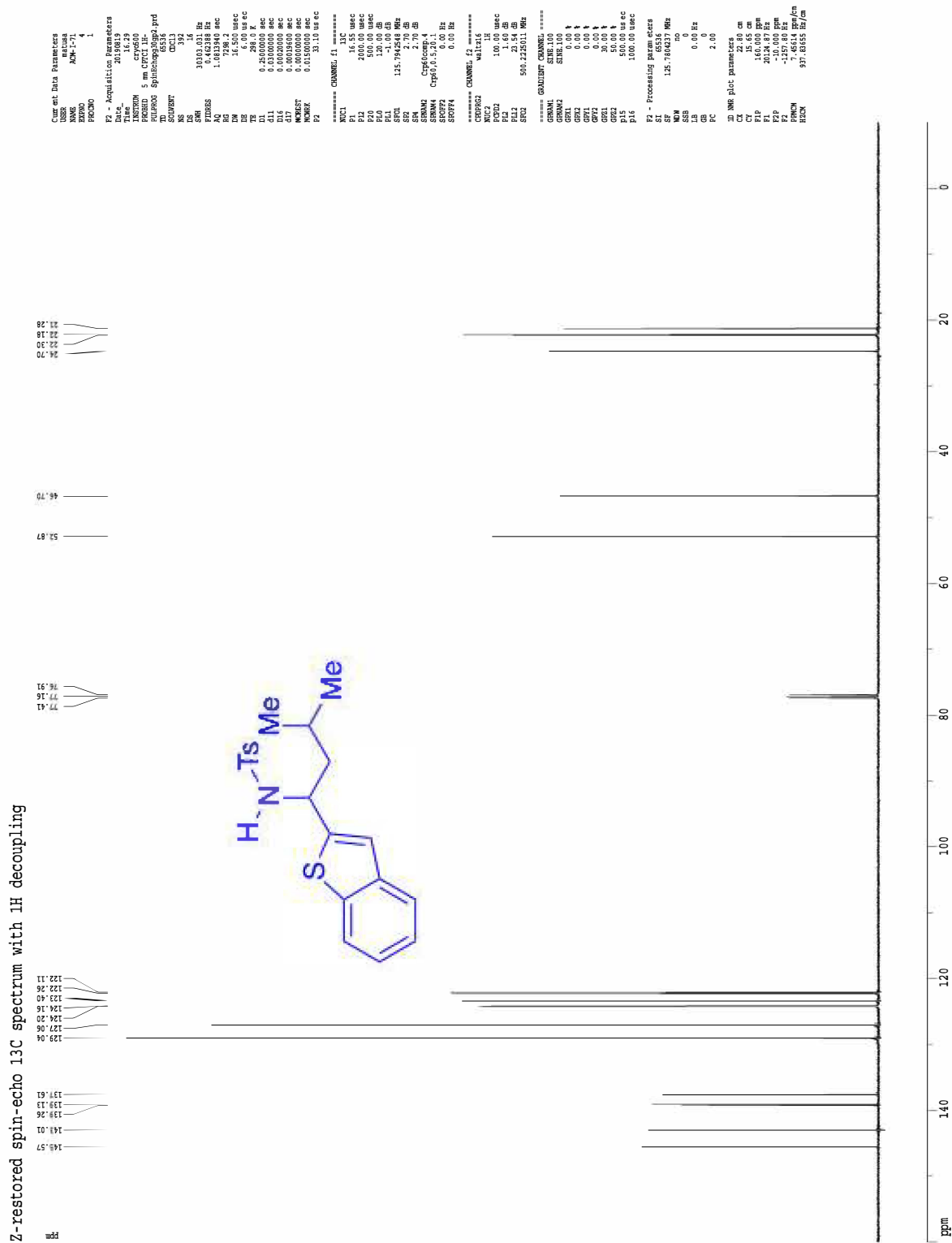
F2 - Acquisition Parameters  
 Date\_: 20180725  
 Time: 11:36  
 INSTRUM: spect  
 PROBNM: 5 mm CPCLP1H  
 PULPROG: zgpg30  
 F1F2: 177.8  
 CHANNEL: CPCLP1H  
 NS: 8  
 DS: 2  
 AS: 64.00 Hz  
 SF: 500.136000 MHz  
 AQ: 5.0348774 sec  
 RG: 5  
 SR: 64.00 usec  
 SE: 0.1000000  
 TE: 298.0 K  
 D1: 0.10000000 sec  
 DELT: 0.00000000 sec  
 ACQOFF: 0.00000000 sec  
 MWAVE: 0.01500000 sec

\*\*\*\*\* CHANNEL F1 \*\*\*\*\*  
 NU1: 7.50 MHz  
 PC1: 1.60 dB  
 PL1: 500.2215015 MHz  
 SF01: 500.2215015 MHz

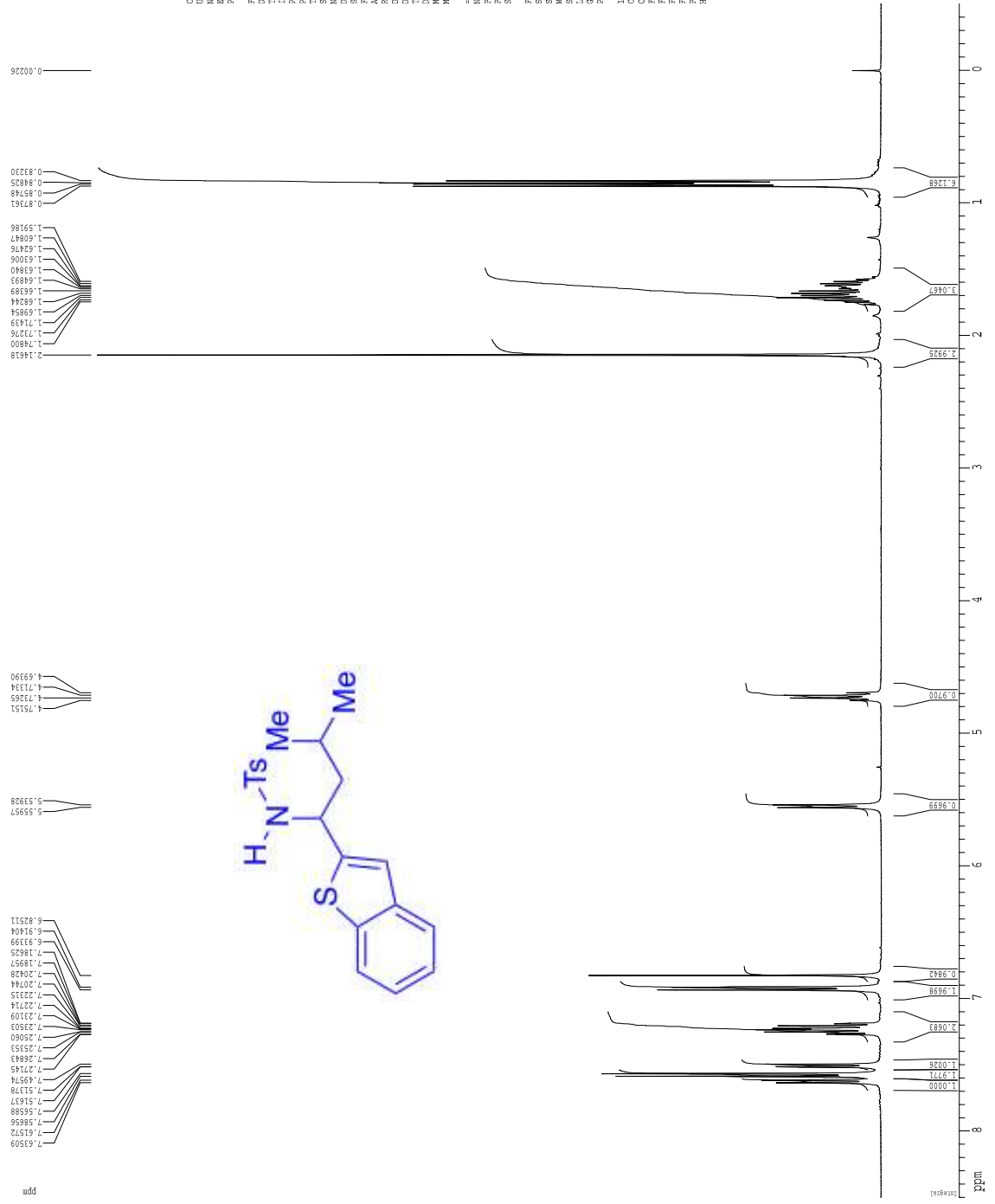
F2 - Processing parameters  
 S1: 645.56 MHz  
 SF: 500.2200435 MHz  
 W: 0  
 SSF: 0.00 Hz  
 GB: 0  
 PC: 1.00

ID NAME plot parameters  
 CC: 22.00 cm  
 C1: 1.00  
 F1P: 6.500 ppm  
 F1: 4251.87 Hz  
 F2: 21.500 ppm  
 F2P: 0.39474 ppm/cm  
 HZCN: 197.45528 Hz/cm

# 1.6 1H and 13C NMR Spectra



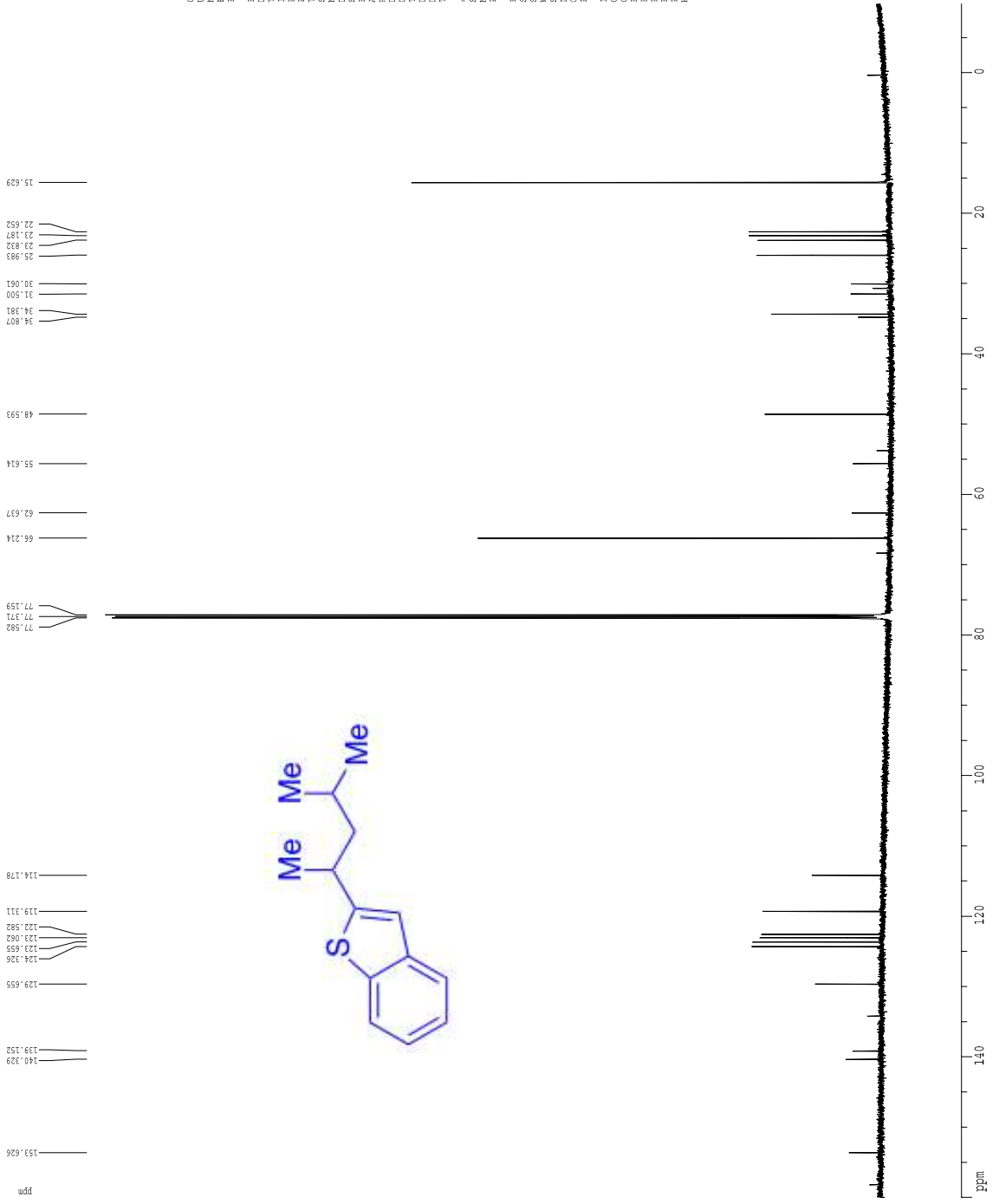
1H spectrum



Current Data Parameters  
Date\_ 2018119  
Time 15.08  
PROBHD 5 mm QNP 1H/13  
PULPROG zgpg30  
AQ 6.5538  
RG 641.345  
WDW EM  
SSB 0  
LB 12.00  
GB 0  
PC 2.00  
F2 - Acquisition Parameters  
Date\_ 2018119  
Time 15.08  
PROBHD 5 mm QNP 1H/13  
PULPROG zgpg30  
AQ 6.5538  
RG 641.345  
WDW EM  
SSB 0  
LB 12.00  
GB 0  
PC 2.00  
F2 - Processing parameters  
SI 65536  
SF 400.1300367 MHz  
WDW EM  
SSB 0  
LB 12.00 Hz  
GB 0  
PC 2.00  
ID NAME plot parameters  
CT 12.00 cm  
CT 1.00  
F2P 8.500 ppm  
F1 340.111 Hz  
F1P 1.500 ppm  
ZG 20.000 ppm  
FREQM 0.339474 ppm/cm  
HLOCK 157.84608 Hz/cm

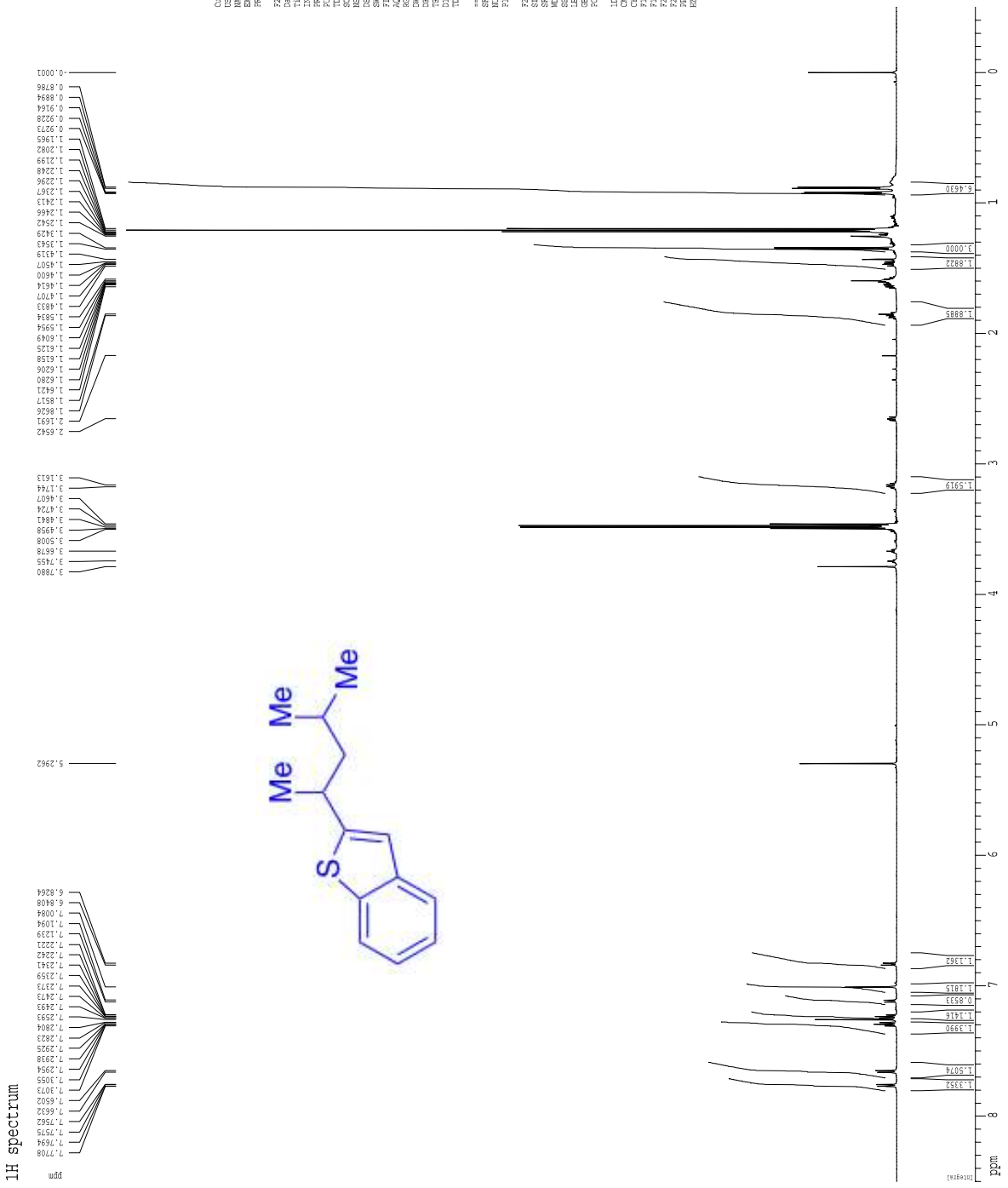


C



Current Data Parameters  
NAME AC6-077c and h  
EXPERO 2  
PROCNO 1  
F2 - Acquisition Parameters  
Date\_ 2013113  
Time\_ 0.00  
INSTRUM spect  
PROBHD 5 mm CPBBO BB-  
PULPROG zgpg30  
SFOC10 450.131  
SOLVENT CDCl3  
NS 384  
DS 4  
SWH 16211.884 Hz  
FIDRES 0.552855 Hz  
AQ 0.994466 sec  
RG 655.6  
GB 13.800 usec  
PC 15.64 usec  
T2 0.422863 K  
T2\* 298.2 K  
D11 0.0300000 sec  
TD0 1  
----- CHANNEL f1 -----  
SFO1 150.9154080 MHz  
NUC1 13C  
P1 10.10 usec  
F2 - Processing parameters  
SI 655.6  
SF 150.9154080 MHz  
WDW EM  
SSB 0  
GB 1.00 Hz  
PC 1.00  
F2 - MEG plot parameters  
CX 82.60 cm  
CY 15.00 cm  
ZP 160.000 ppm  
PC 2.000000 usec  
F2P -10.000000 ppm  
F2 -1500.00 Hz  
PPMCH 4.6511 ppm/cm  
PUSH 1125.1544 Hz/cm

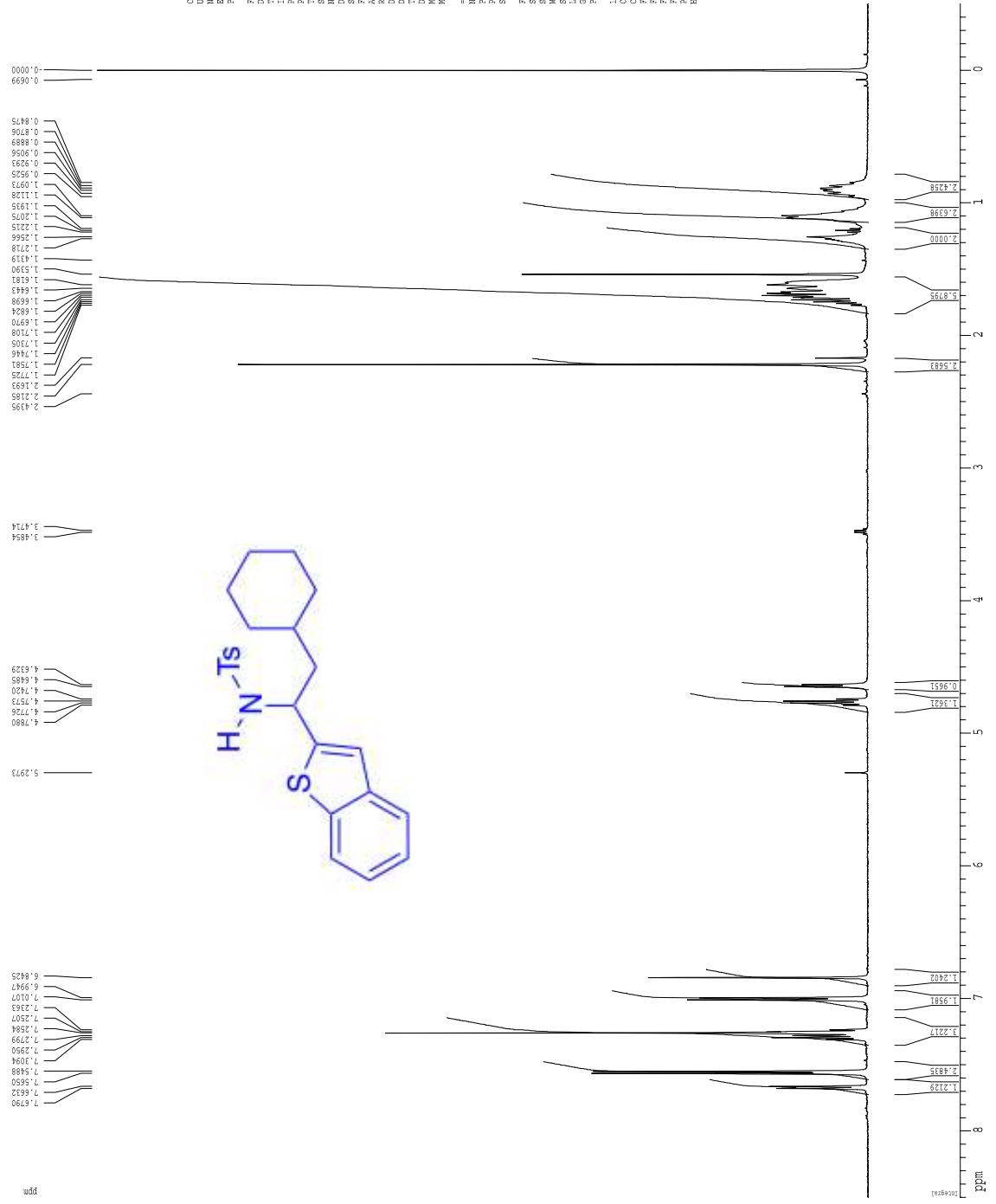
1H spectrum



Current Data Parameters  
NAME AC6-107c and h  
EXPTNO 1  
PROCNO 1  
Date\_ 2012113  
Time\_ 16:05:00  
INSTRUM spect  
PROBHD 5 mm CBBQ BB-  
PULPROG zg30  
SOLVENT CDCl3T  
NS 8  
DS 2  
SWH 9615.382 Hz  
FIDRES 0.098044 Hz  
AQ 5.0998977 sec  
RG 327.500  
SM 52.000 usec  
DS 11.70 usec  
TE 298.2 K  
TD 0.1000000 sec  
F2 - Acquisition Parameters  
Date\_ 2012113  
Time\_ 16:05:00  
INSTRUM spect  
PROBHD 5 mm CBBQ BB-  
PULPROG zg30  
SOLVENT CDCl3T  
NS 8  
DS 2  
SWH 9615.382 Hz  
FIDRES 0.098044 Hz  
AQ 5.0998977 sec  
RG 327.500  
SM 52.000 usec  
DS 11.70 usec  
TE 298.2 K  
TD 0.1000000 sec  
F2 - Processing parameters  
SI 65536  
SF 600.130051 MHz  
WDW EM  
SSB 0  
LB 0.33 Hz  
GB 0  
PC 1.00  
JD IMG plot parameters  
Z 25.00 mm  
CT 15.00 mm  
F1-P 8.500 ppm  
F2 50.011 Hz  
F3 100.626 Hz  
F4 -100.626 Hz  
F5 0.33474 ppm/cm  
BPCN 236.8916 Hz/cm

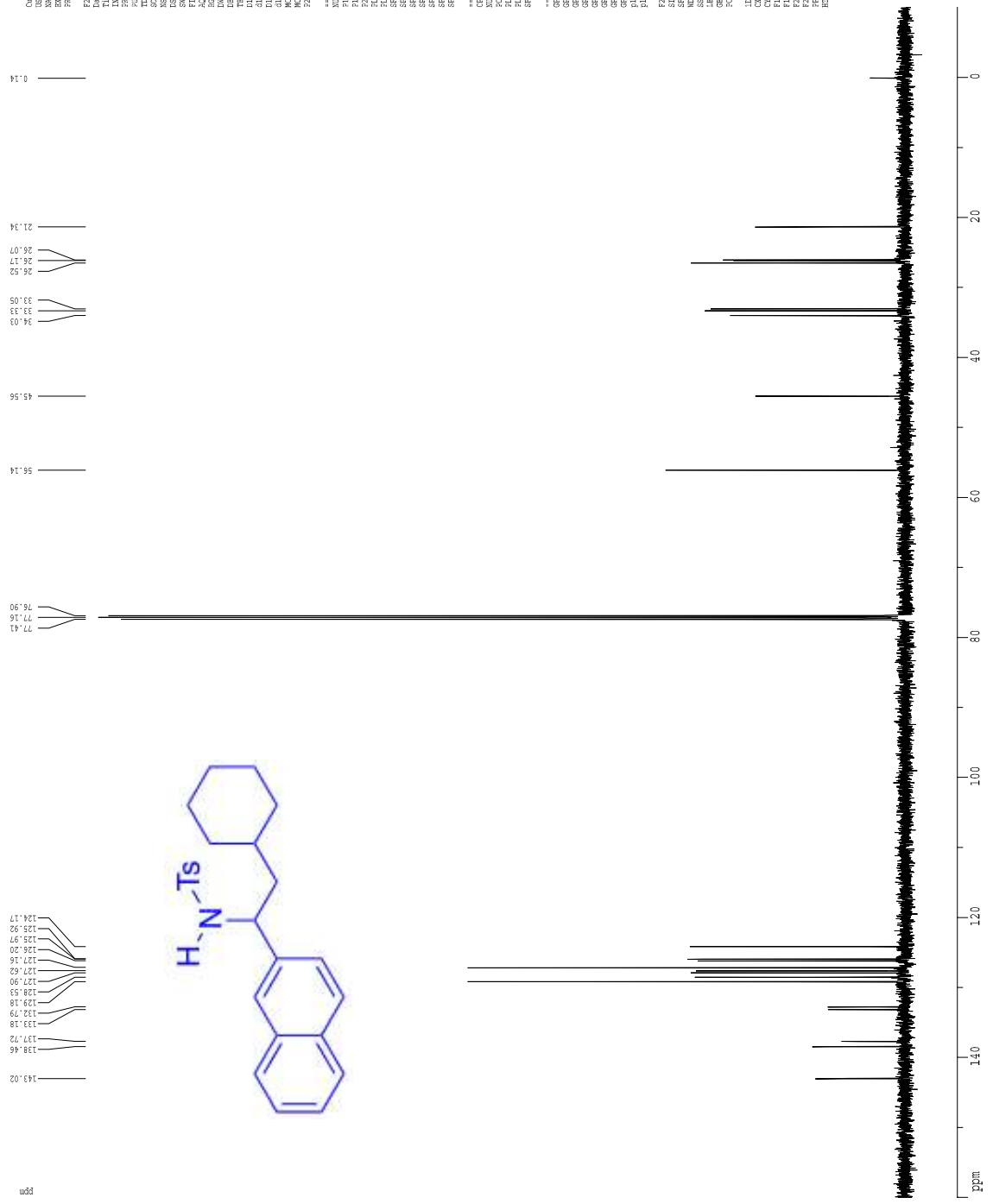


1H spectrum



Current Data Parameters  
 NAME ACW-5-18-Beta-Hc  
 EXPNO 1  
 PROCNO 1  
 F2 - Acquisition Parameters  
 Date\_ 2012108  
 Time 12.50  
 INSTRUM spect  
 PROBRD 5 mm CPCL1H-  
 PULPROG zgpg30  
 SOLVENT CDCl3  
 NS 10  
 DS 4  
 SWH 6032.823 Hz  
 FIDRES 0.098043 Hz  
 AQ 5.0998774 sec  
 RM 0.00000000  
 EQ 62.400 usec  
 DE 9.00000000  
 TE 300.2 K  
 TD 65536  
 MWDWST 0.00000000 sec  
 MORKS 0.01500000 sec  
 ===== CHANNEL f1 =====  
 NUC1 1H  
 P1 7.50 usec  
 PL1 0.00 dB  
 SFO1 500.2234513 MHz  
 F2 - Processing parameters  
 SI 32768  
 SF 500.223226 MHz  
 EM EN  
 SS 0.30 Hz  
 DS 4  
 RB 0  
 FC 1.00  
 F0 0.00000000 MHz  
 F1 F2 plot Parameters  
 CX 22.80 cm  
 CY 15.00 cm  
 CZ 15.00 cm  
 FX 4251.88 Hz  
 FY 4251.88 Hz  
 FZ -0.500 ppm  
 TX 0.00000000 Hz  
 TY 0.00000000 Hz  
 TZ 197.45528 Hz/cm

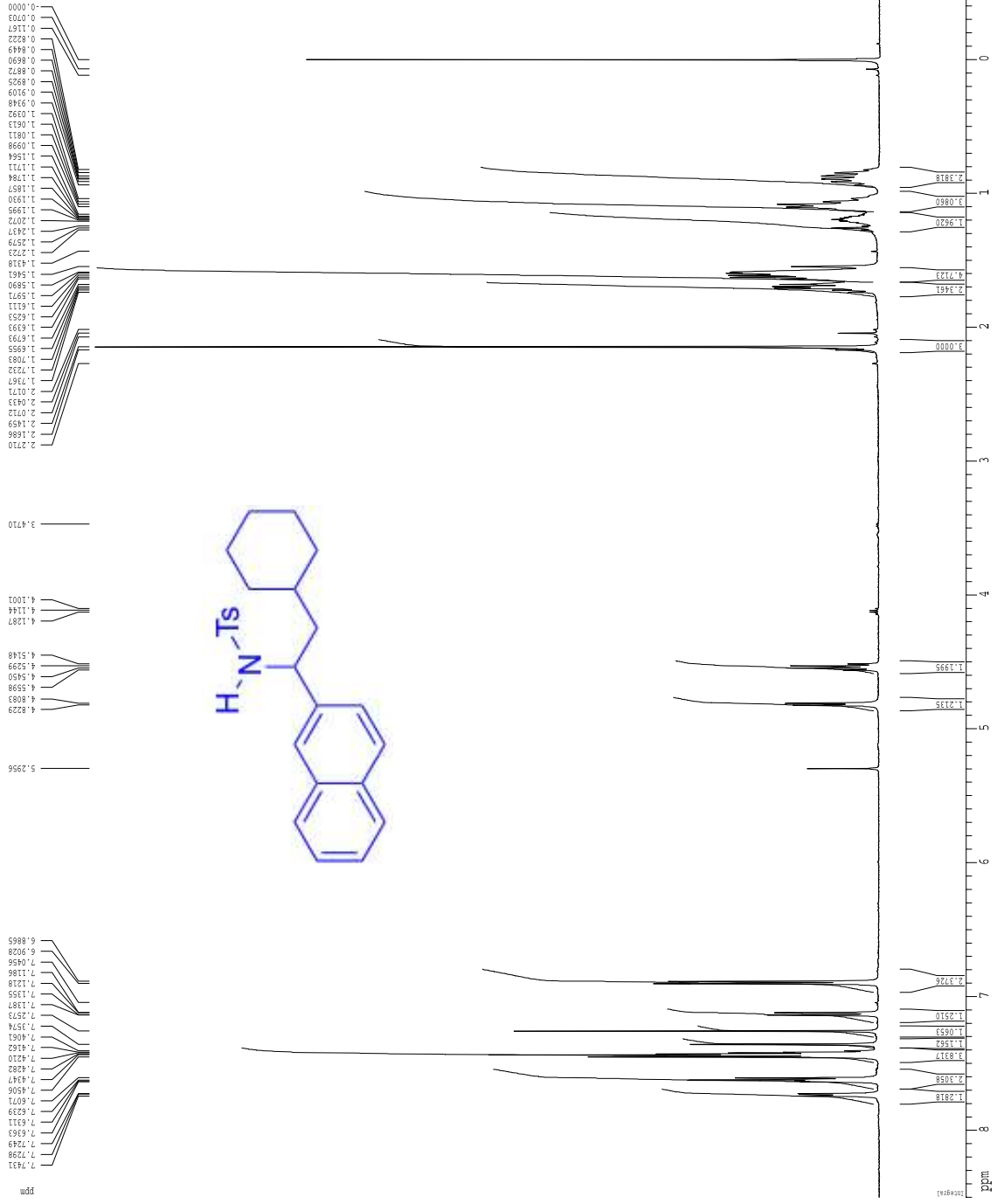
Z-restored spin-echo 13C spectrum with 1H decoupling



```

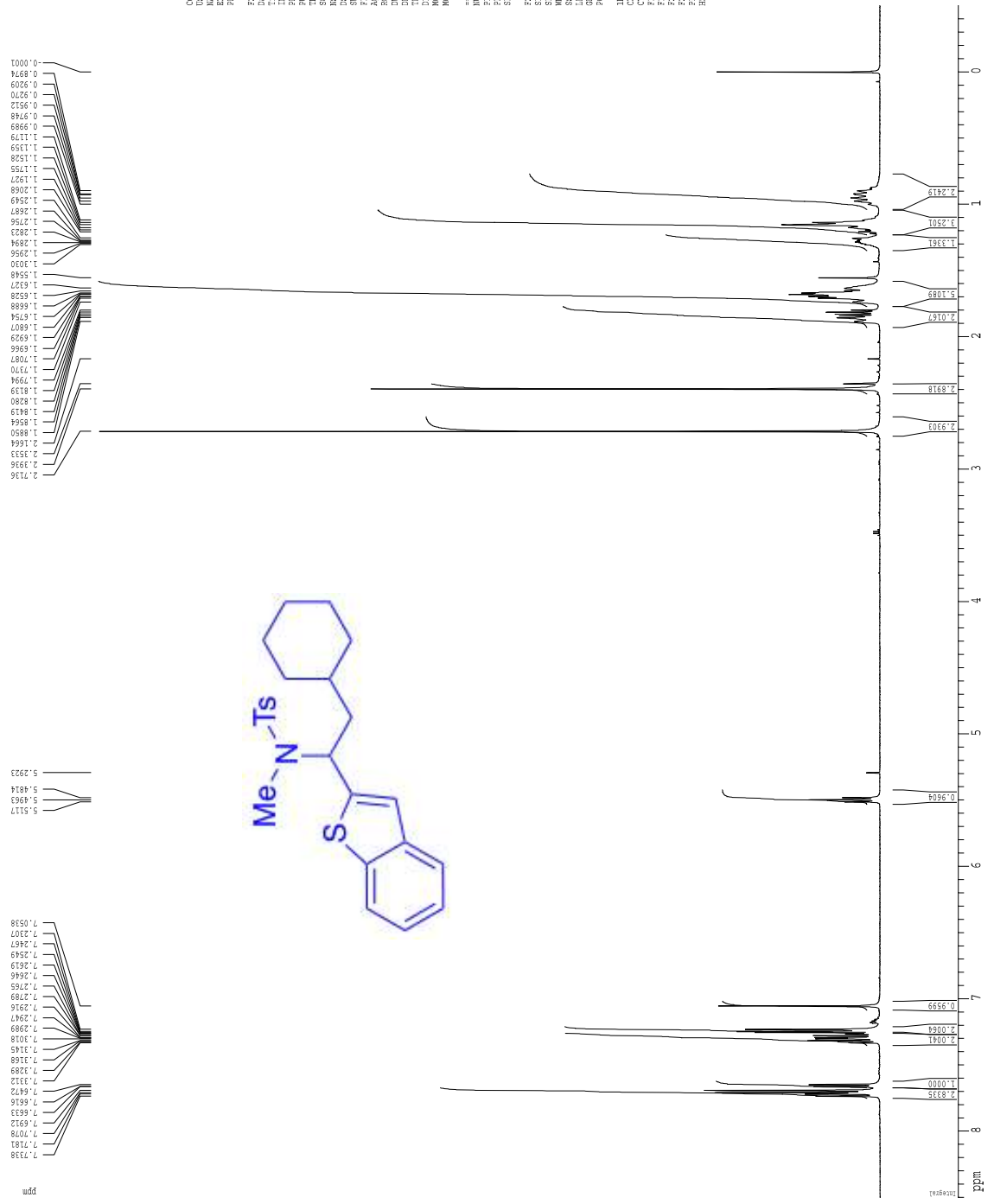
Current Data Parameters
USER          ANK-11-13-08
EXPNO        1
PROCNO       1
F2 - Acquisition Parameters
Date_         20191018
Time         17.20
INSTRUM      spect
PROBHD       5 mm CPXI 1H-
PULPROG      zgpg30
PCPDPRG2     spmzgpg30v.prd
AQ           0.09500000 sec
RG           327.50
SFOFFA       0.00 Hz
SI           512
SM          32768
FIDRES       0.462388 Hz
AQ           1.0319900 sec
SFOFFA       0.00 Hz
RG           15.500
SI           64.00
SFOFFA       0.00 Hz
RG           0.22000000 sec
SI           64.00
SFOFFA       0.00 Hz
RG           0.00000000 sec
SI           64.00
SFOFFA       0.00 Hz
RG           0.00000000 sec
SI           64.00
SFOFFA       0.00 Hz
RG           0.00000000 sec
SI           64.00
SFOFFA       0.00 Hz
RG           31.00
SFOFFA       0.00 Hz
***** CHANNEL f1 *****
NUC1         13
P1           16.55 usec
PL           0.00 dB
RG           32768
SFOFFA       0.00 Hz
RG           15.500
SI           64.00
SFOFFA       0.00 Hz
RG           0.22000000 sec
SI           64.00
SFOFFA       0.00 Hz
RG           0.00000000 sec
SI           64.00
SFOFFA       0.00 Hz
RG           0.00000000 sec
SI           64.00
SFOFFA       0.00 Hz
RG           31.00
SFOFFA       0.00 Hz
***** CHANNEL f2 *****
CPDPRG2      waltz16
NUC2         13
P2           100.00 usec
PL           1.60 dB
RG           32768
SFOFFA       0.00 Hz
RG           15.500
SI           64.00
SFOFFA       0.00 Hz
RG           0.22000000 sec
SI           64.00
SFOFFA       0.00 Hz
*****
GRANAME      SPMZG30
SINSE        100
SI           512
SFOFFA       0.00 Hz
GRANAME      SPMZG30
SINSE        100
SI           512
SFOFFA       0.00 Hz
*****
F2 - Processing parameters
SI           135.85594
SF           125.76184 MHz
RG           1.00
AQ           1.00 sec
SI           0
SFOFFA       0.00 Hz
RG           15.500
SI           64.00
SFOFFA       0.00 Hz
*****
ID: NMR file parameters
CX           22.80 cm
CY           16.00 cm
ETP         2624.87 Hz
F1           2624.87 Hz
F2           2624.87 Hz
FRAC1N      7.45814 ppm/cm
FRAC1R      937.8594 Hz/cm
    
```

1H spectrum



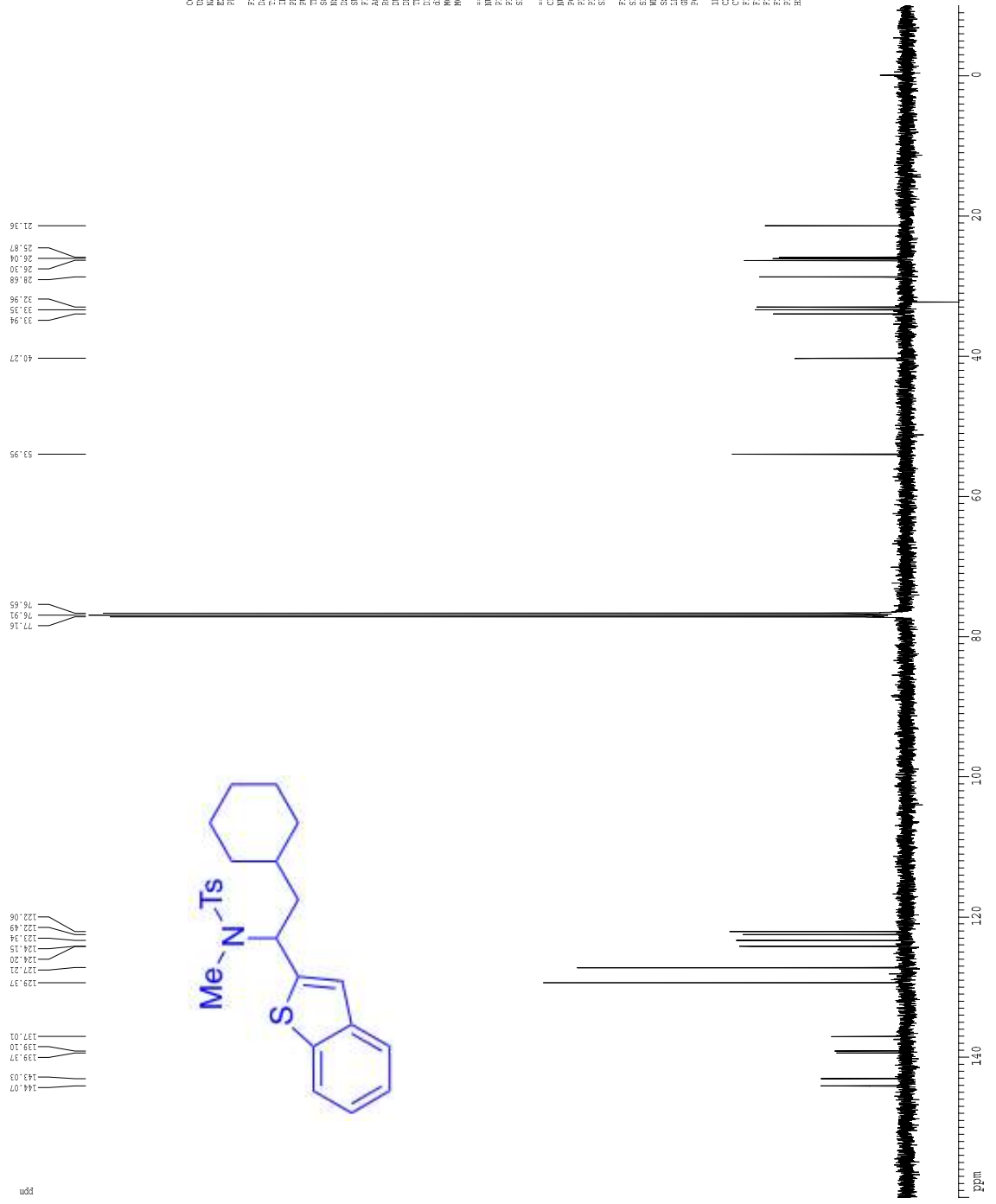
Current Data Parameters  
NAME: ACW-118-449-01  
EXTNO: 1  
PROCNO: 1  
F2 - Acquisition Parameters  
Date\_: 20131109  
Time: 17.05  
PROBHD: 5 mm QNP1H  
PULPROG: zgpg30  
PCYCLE: 1778  
SOLVENT: CDCl3  
NS: 1.0  
DS: 2  
AQ: 5.013600 Hz  
SFO1: 500.131515 MHz  
AQ: 5.0348774 sec  
RG: 6.3  
SF: 62.500 MHz  
AQ: 0.1000000 sec  
RG: 298.2 K  
TE: 300.2 K  
D1: 0.1000000 sec  
DELTA: 0.1000000 sec  
NUC1: 13C  
NUC2: 1H  
===== CHANNEL f1 =====  
PC1: 7.50 MHz  
PC2: 1.60 MHz  
SFO1: 500.131515 MHz  
F2 - Processing parameters  
SI: 65536  
SF: 500.131327 MHz  
WDW: EM  
SSB: 0  
GB: 0  
PC: 0.30 Hz  
SC: 1.00  
ID: NONE plot parameters  
CT: 32.00 cm  
CT2: 32.00 cm  
F1P: 61500 ppm  
F1: 4251.87 Hz  
F2P: 101500 ppm  
F2: 2512.87 Hz  
FREQN1: 0.39474 ppm/cm  
FREQN2: 197.45528 Hz/cm

<sup>1</sup>H spectrum



Current Data Parameters  
 Date\_ 20131112  
 Time 9:06  
 NAME ACM-121-082031  
 EXPNO 1  
 PROCNO 1  
 F2 - Acquisition Parameters  
 Date\_ 20131112  
 Time 9:06  
 NAME ACM-121-082031  
 PROCNO 1  
 PULPROG zgpg30  
 TD 65536  
 SFO1 498.813419 MHz  
 AQ 5.0388774 sec  
 RG 181  
 IN 64.000 usec  
 DE 298.0 K  
 TE 0.1000000 sec  
 D1 0.1000000 sec  
 DELT 0.1000000 sec  
 WDELT 0.1000000 sec  
 ===== CHANNEL f1 =====  
 NU1 12.00 MHz  
 F1 12.00 MHz  
 SF01 498.813419 MHz  
 F2 - Processing parameters  
 SI 65536  
 SF 498.813419 MHz  
 DS 0  
 SSF 0  
 GB 0  
 BR 0.30 Hz  
 B0 1.00  
 ID NAME plot parameters  
 CT 12.00 cm  
 C2 12.00 cm  
 F1P 0.500 ppm  
 F2 4240.23 Hz  
 F2P -24.500 ppm  
 ZF 0.300 ppm  
 ZFP 0.300 ppm/cm  
 HZCN 196.31449 Hz/cm

<sup>13</sup>C spectrum with <sup>1</sup>H decoupling



```

Current Data Parameters
NAME      A06-112-beach1
EXPERNO  2
PROCNO   1

F2 - Acquisition Parameters
Date_    20191112
Time     9:37
DateAcq  20191112
INSTRUM  spect
PROBHD   5 mm broadband
PULPROG  zgpg30
TD        65536
SFO1     125.497300 MHz
AQ        0.49400000 sec
RG        655.36
SR        299.0 K
SI        0.45000000 sec
SF        0.45000000 sec
WDW       EM
SSB       0
HYPERBK  0.01500000 sec

===== CHANNEL f1 =====
NUC1      13C
P1        10.00 usec
PL1       -6.00 dB
SFO1     125.497300 MHz

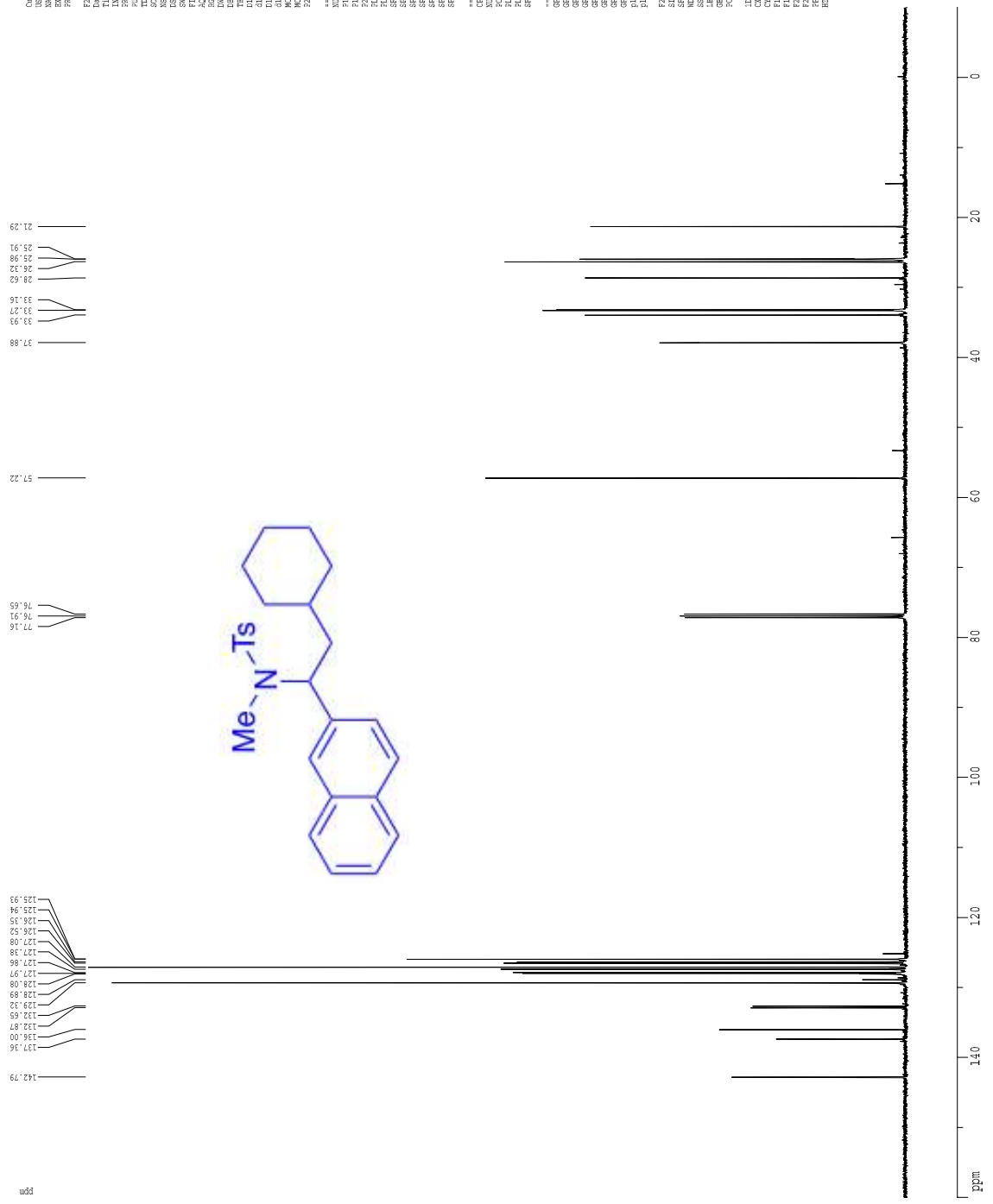
===== CHANNEL f2 =====
CPDPRG22 waltz16
NUC2      1H
P2        80.00 usec
PL2       -5.00 dB
SFO2     499.485943 MHz

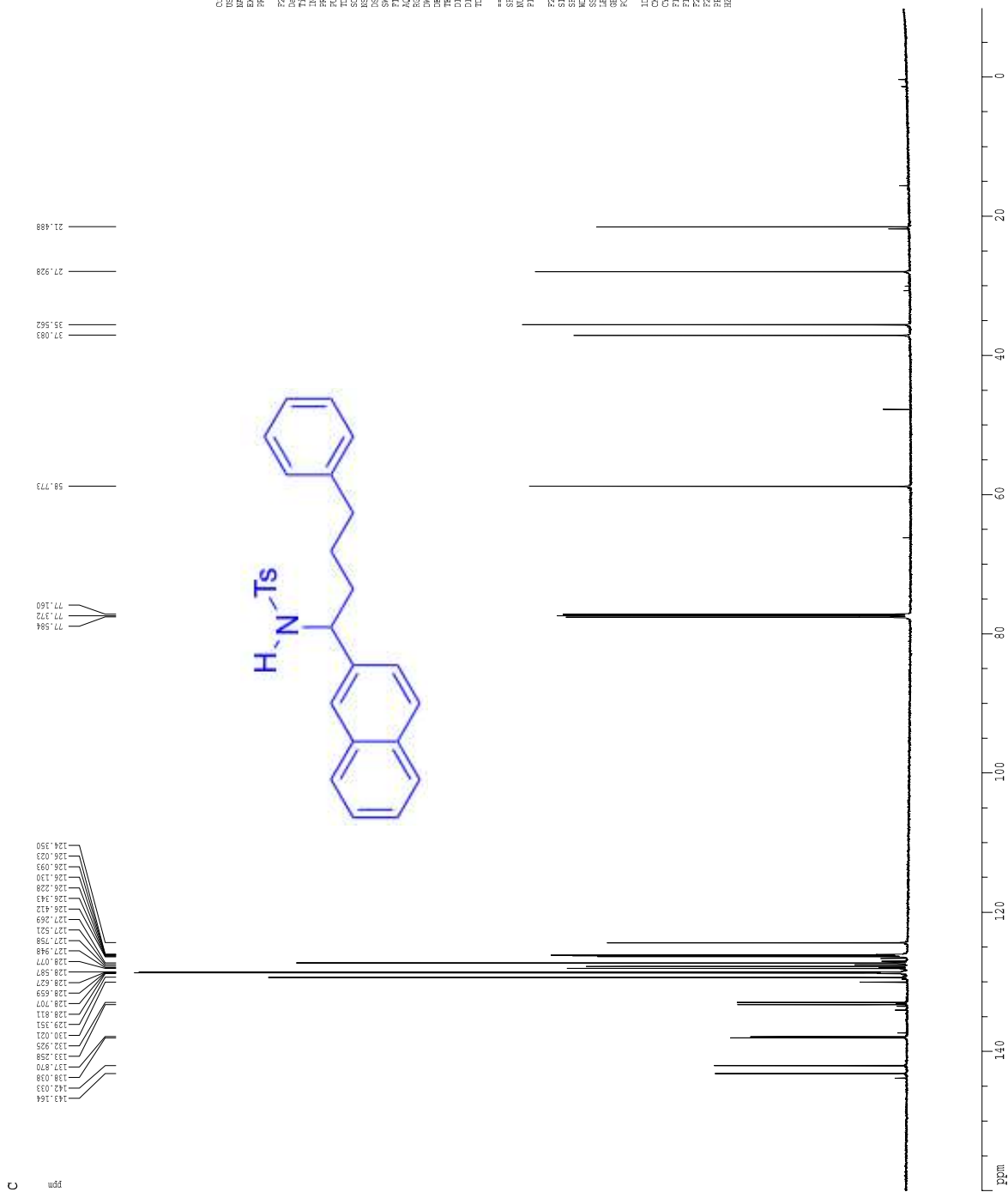
F2 - Processing parameters
SI        65536
SF        125.497300 MHz
WDW       EM
SSB       0
HYPERBK  0.01500000 sec
SI        65536
SF        125.497300 MHz
WDW       EM
SSB       0
HYPERBK  0.01500000 sec

2D NMR plot parameters
SI        65536
SF        125.497300 MHz
AQ        0.49400000 sec
RG        655.36
SR        299.0 K
SI        0.45000000 sec
SF        0.45000000 sec
WDW       EM
SSB       0
HYPERBK  0.01500000 sec
=====
  
```

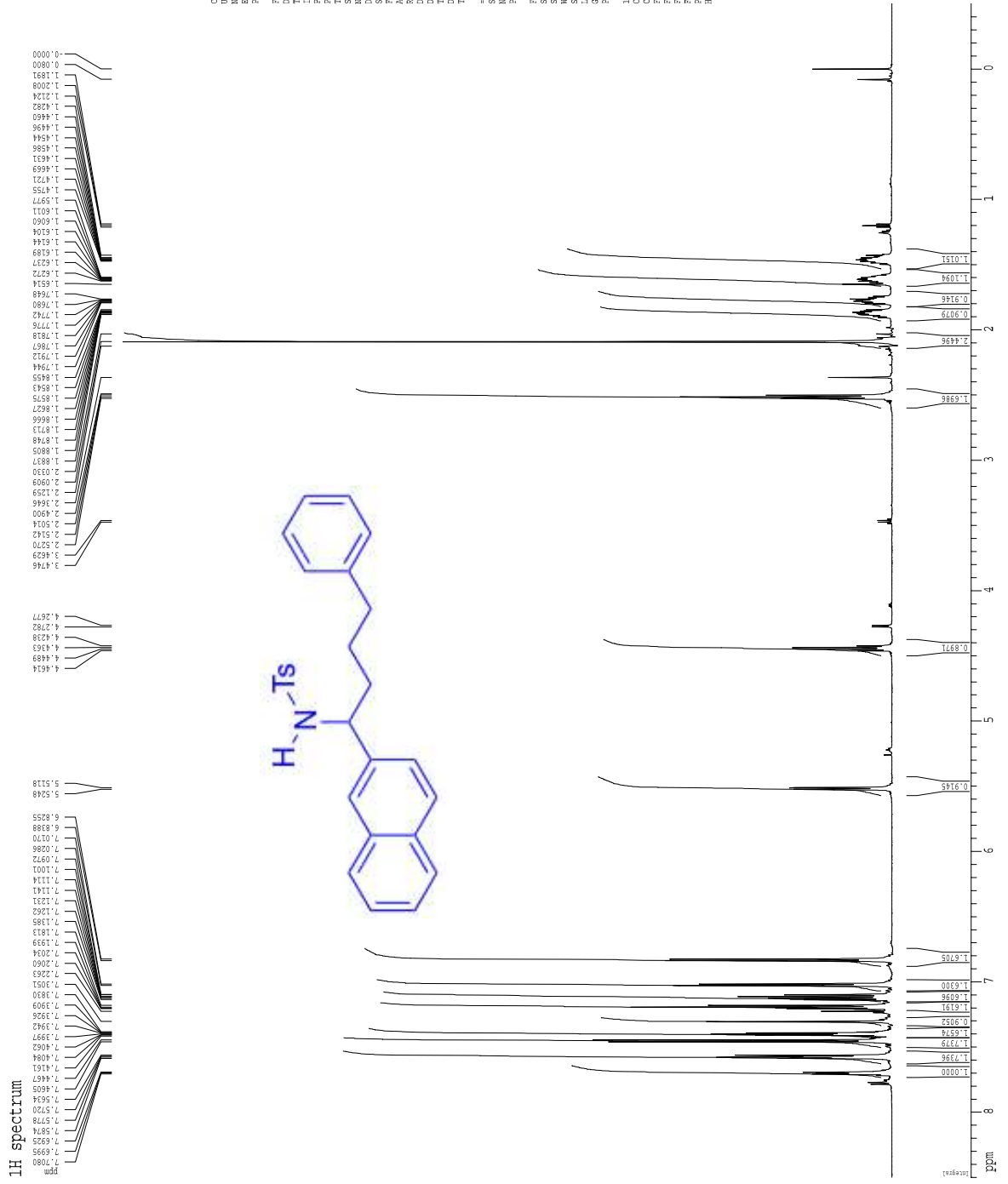


Z-restored spin-echo 13C spectrum with 1H decoupling

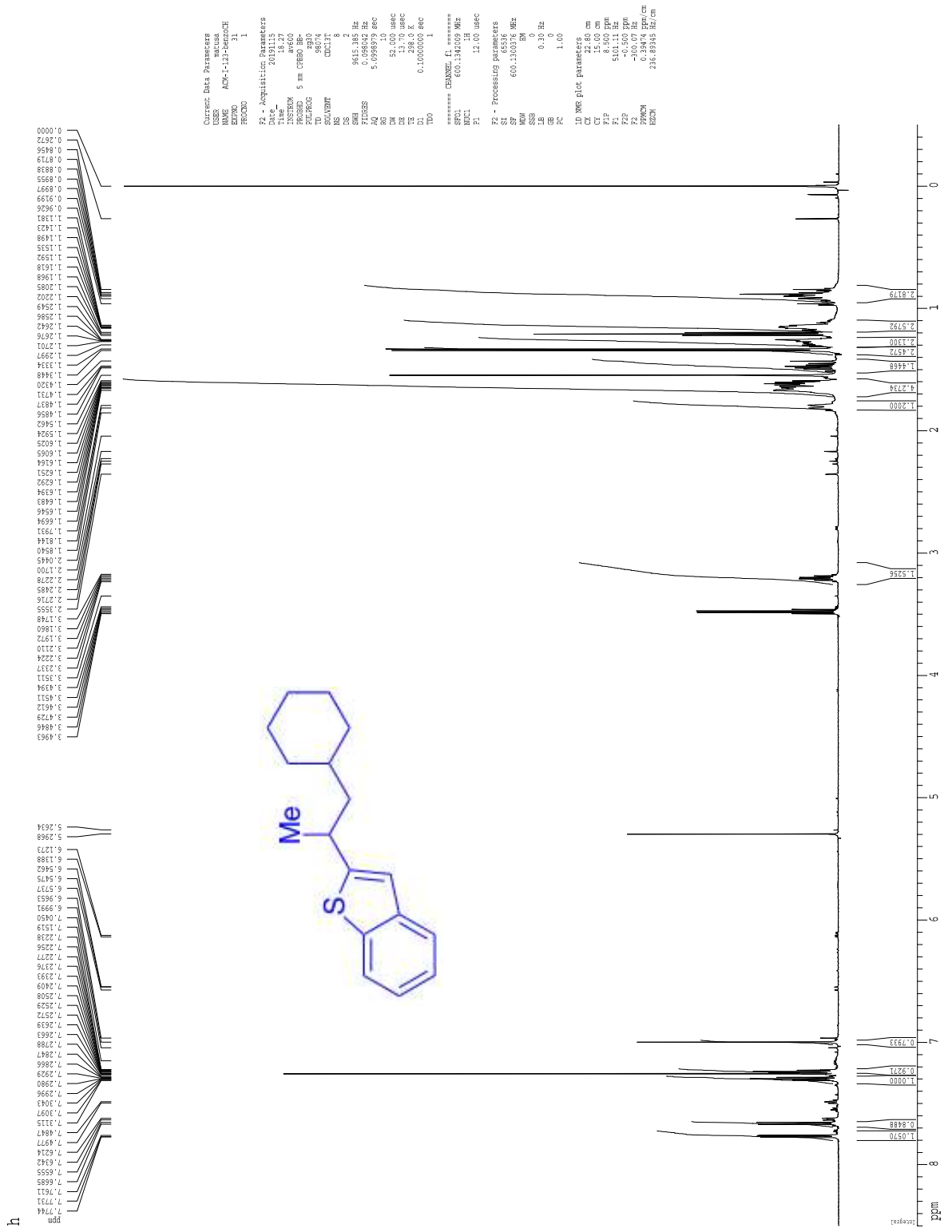


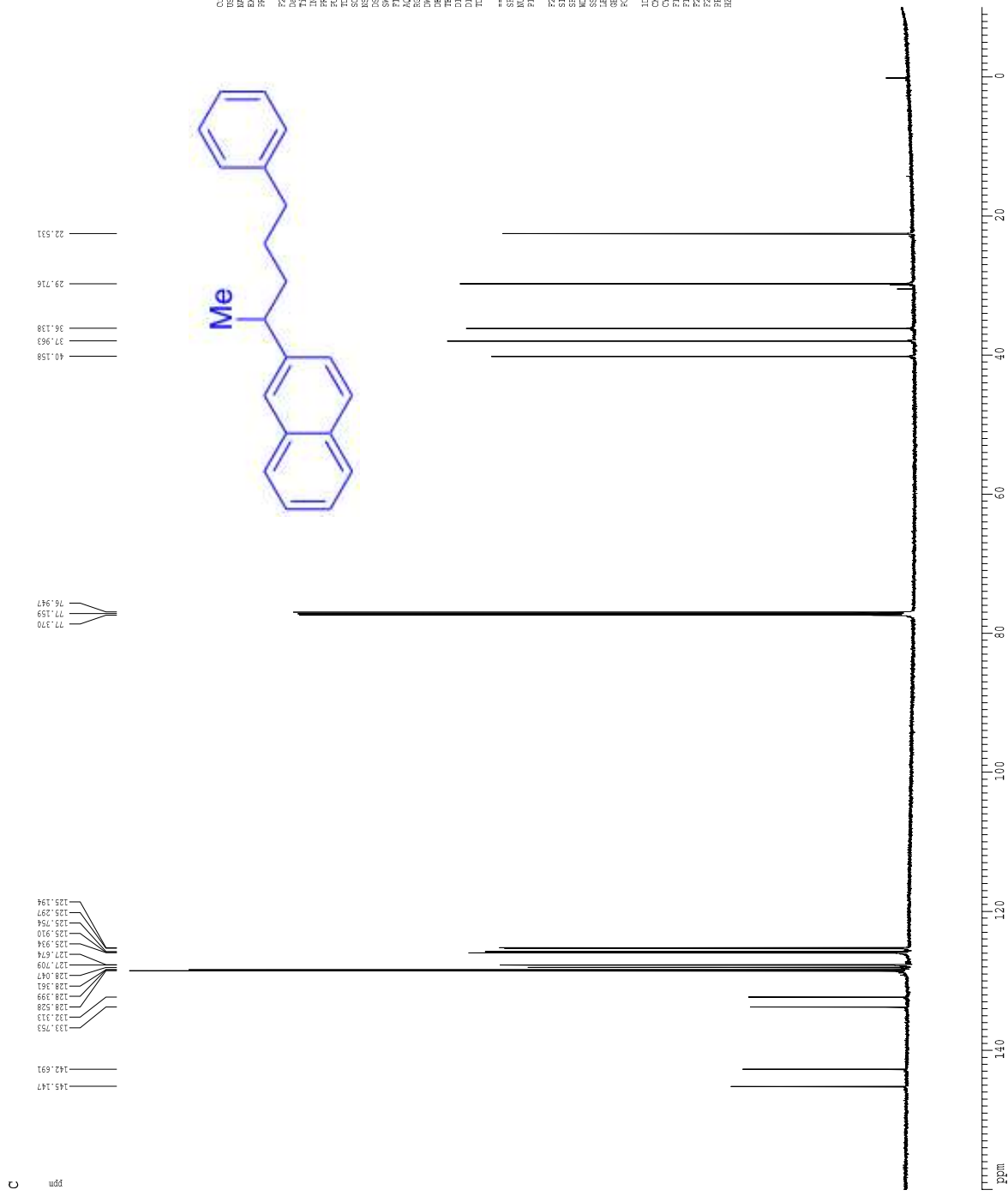


<sup>1</sup>H spectrum



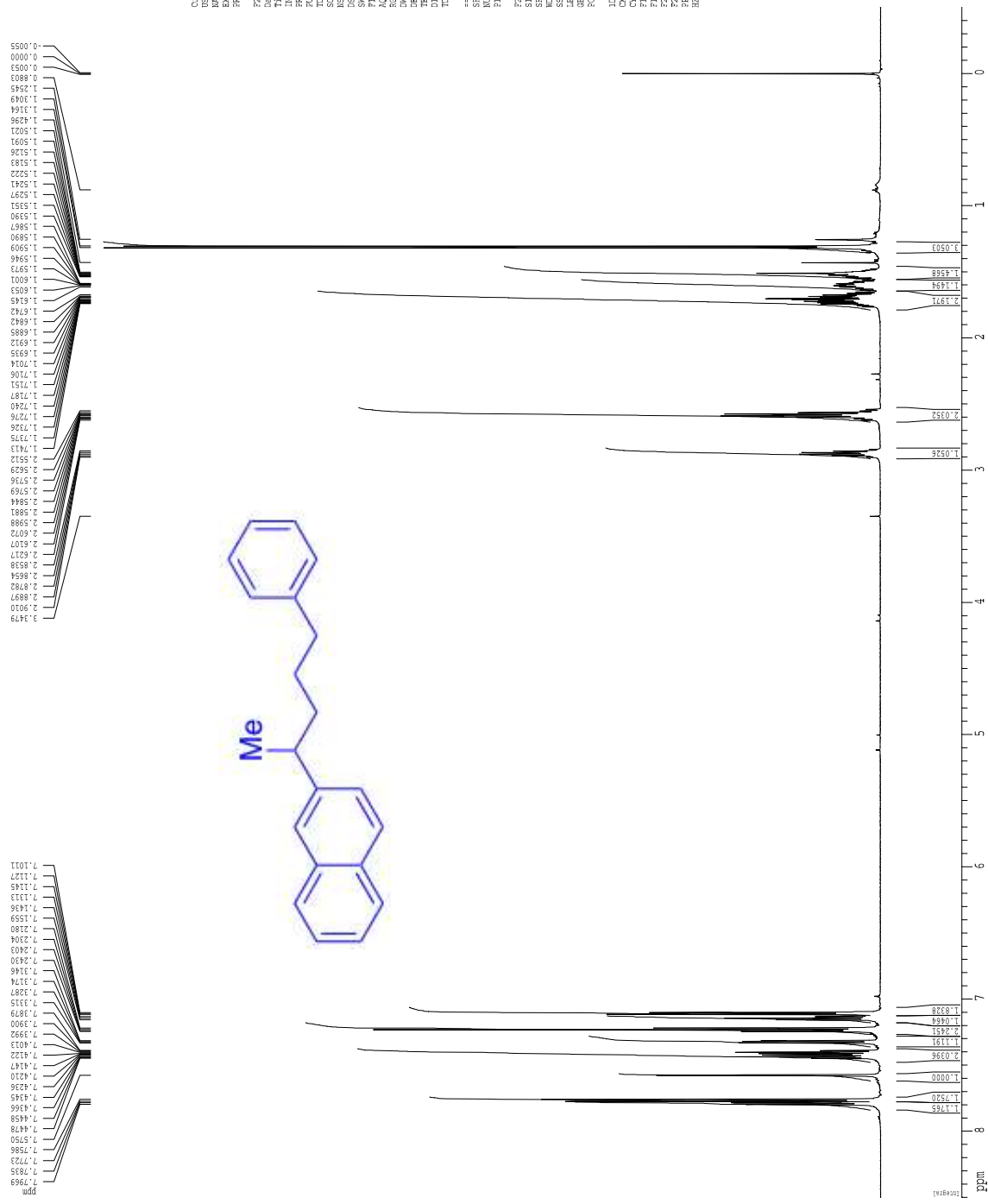
Current Data Parameters  
 Name: 20191112  
 Date: 20191112  
 User: ACN-1-212-00  
 Time: 5.18  
 Experiment: 1  
 PREPRO: 1  
 F2 - Acquisition Parameters  
 Date: 20191112  
 Time: 5.18  
 User: ACN-1-212-00  
 Program: 5 mm CPMAS 2D  
 PULPROG: zgpg30  
 TD: 65536  
 SFO1: 600.1342059 MHz  
 F1: 12.00 usec  
 SFO2: 600.1300557 MHz  
 F2: Processing parameters  
 SF: 600.1300557 MHz  
 D: 0.0000000 sec  
 SSF: 0.0000000 sec  
 LB: 0.30 Hz  
 GB: 0.0000000 sec  
 PC: 1.00  
 ID NMR plot parameters  
 CF: 22.80 cm  
 CR: 0.0000000 cm  
 F1P: 6.5000000 MHz  
 F1: 5101.11 Hz  
 F2P: -0.5000000 MHz  
 F2: -5101.11 Hz  
 FREQM: 0.0000000 MHz/cm  
 HZCM: 216.89345 Hz/cm





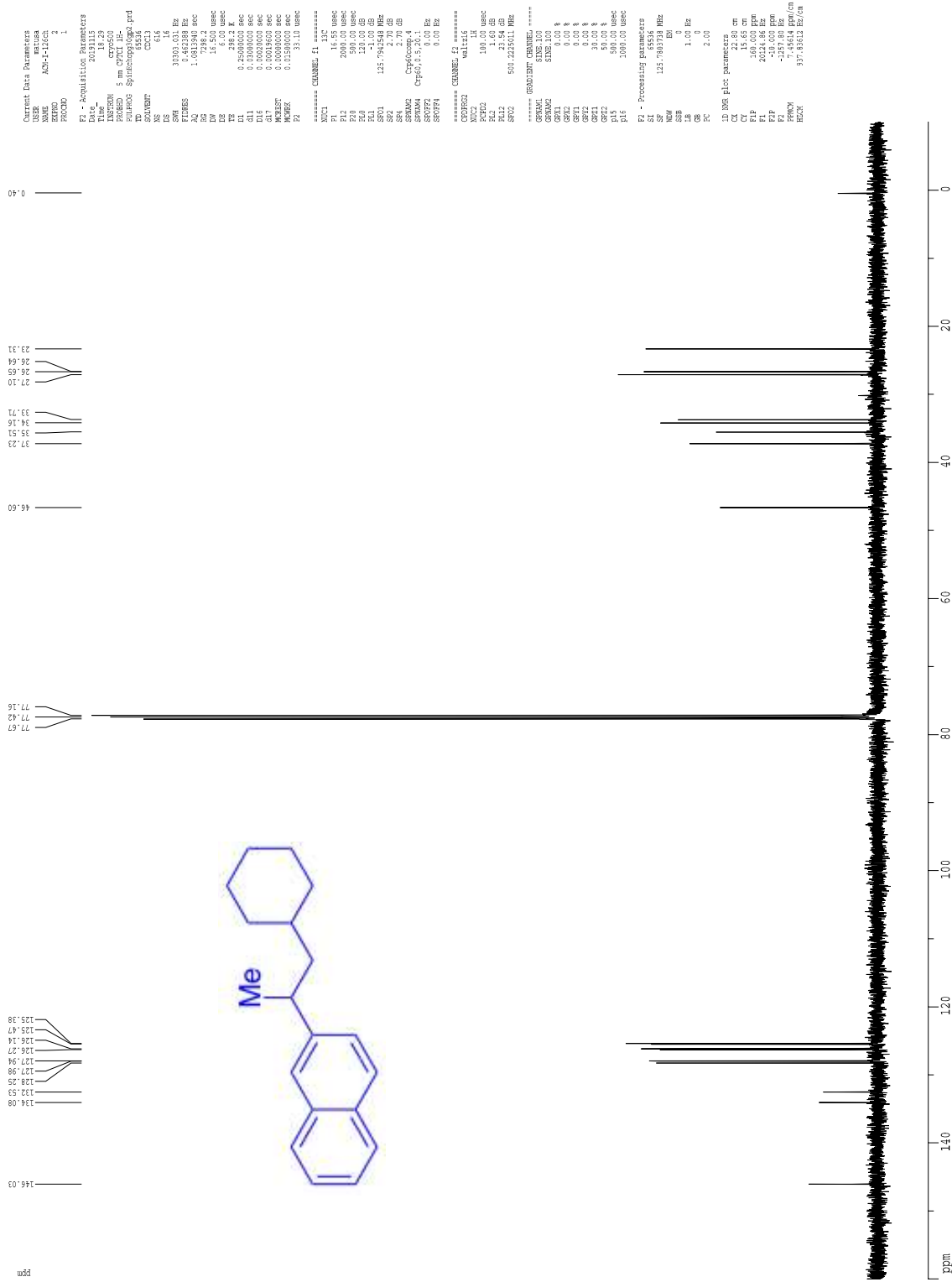
Current Data Parameters  
 Name: 200-112-0002  
 EXPNO: 2  
 PROCNO: 1  
 F2 - Acquisition Parameters  
 Date\_: 20131115  
 Time: 13.49  
 Operator: JG  
 PROGRAM: 5 mm CPMAS 2D  
 PULPROG: zgpg30  
 TD: 65536  
 SFO: 125.761 MHz  
 SOLVENT: CDCl3  
 NS: 314  
 DS: 4  
 SFE: 36231.883 Hz  
 FIDRES: 0.552855 Hz  
 AQ: 0.99100000 sec  
 RG: 2250  
 IN: 13.800 uSec  
 DE: 15.63 uSec  
 TE: 300.2 K  
 D1: 0.40000001 sec  
 D11: 0.03000000 sec  
 D10: 1  
 \*\*\*\*\* CHANNEL f1 \*\*\*\*\*  
 SFO1: 150.914080 MHz  
 P1: 1.00  
 PL1: 0.00 dB  
 PR1: 10.10 uSec  
 F2 - Processing parameters  
 SI: 65536  
 SF: 150.902798 MHz  
 RG: 2250  
 NS: 0  
 SSB: 0  
 LB: 1.00 Hz  
 GB: 0  
 PC: 1.00  
 ID MS plot parameters  
 X: 1.00 cm  
 Y: 15.00 cm  
 FID: 166.000 FPM  
 FI: 24144.45 Hz  
 FD: 0.00 Hz  
 FZ: 4590.03 Hz  
 FRCM: 7.45614 FPM/cm  
 HZCM: 1125.15247 Hz/cm

4

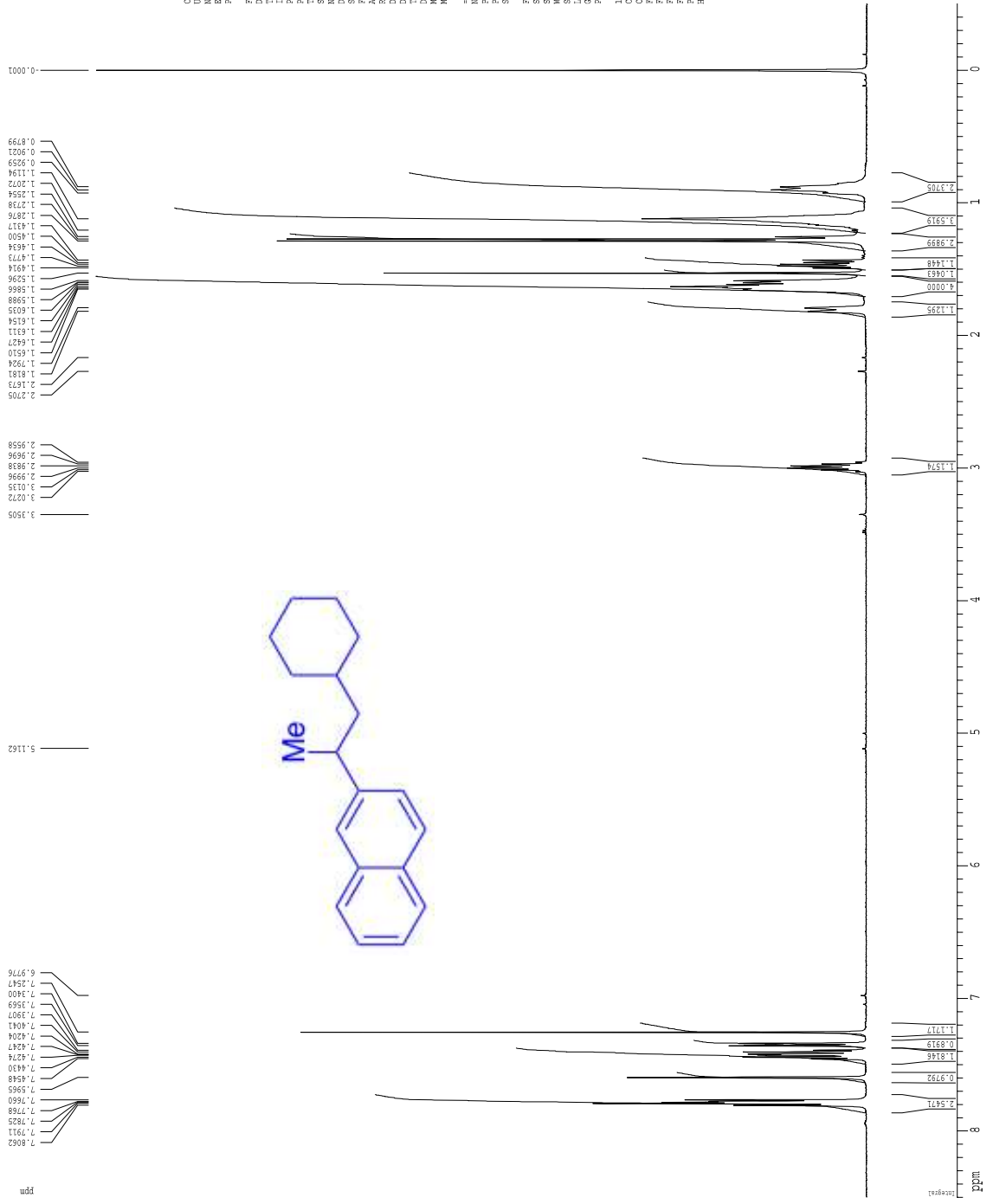


Current Data Parameters  
Date\_ 20131115  
Time\_ 13:46  
EXPNO\_ 1  
PROCNO\_ 1  
F2 - Acquisition Parameters  
Date\_ 20131115  
Time\_ 13:46  
PROBHD\_ 5 mm CPBBO P0  
PULPROG\_ zgpg30  
TD\_ 65536  
AQ\_ 0.10000000  
RG\_ 327.68000000  
WDW\_ EM  
SSB\_ 0  
LB\_ 0.30 Hz  
GB\_ 0  
PC\_ 1.00  
SFO1\_ 400.1342019 MHz  
NUC1\_ 1H  
P1\_ 12.00 usec  
F2 - Processing parameters  
SF\_ 400.1340536 MHz  
WDW\_ EM  
SSB\_ 0  
LB\_ 0.30 Hz  
GB\_ 0  
PC\_ 1.00  
ID MRB plot parameters  
CF\_ 22.80 cm  
C1P\_ 6.500 ppm  
F1P\_ 5101.11 Hz  
F2P\_ -0.500 ppm  
SFO1\_ 400.1340536 MHz/cm  
HZCM\_ 216.89345 Hz/cm

Z-restored spin-echo 13C spectrum with 1H decoupling



1H spectrum



Current Data Parameters  
 Name: 20111115  
 Name: ACQ5-1265h  
 EXPNO: 1  
 PROCNO: 1

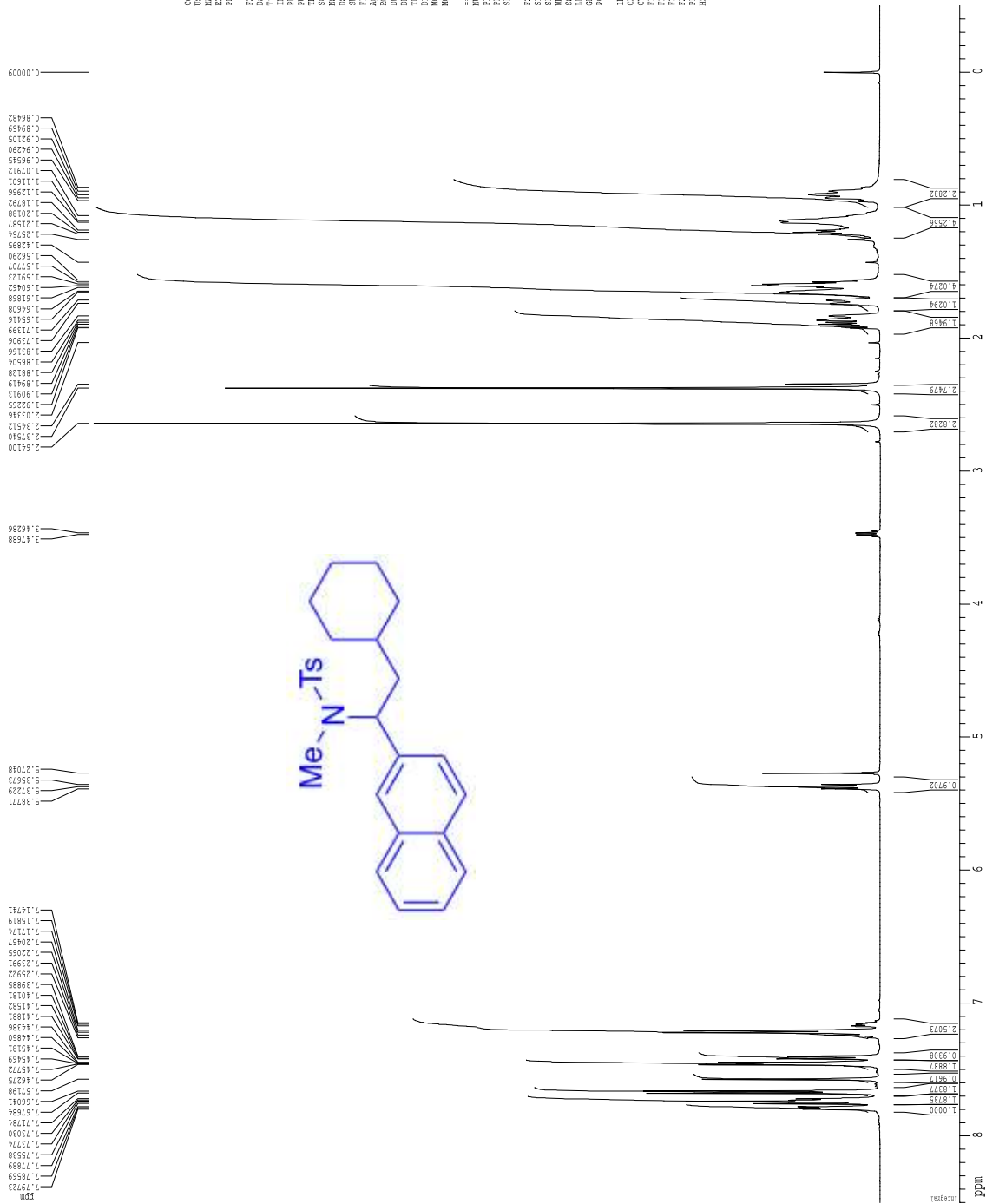
F2 - Acquisition Parameters  
 Date\_: 20111115  
 Time: 18.14  
 INSTRUM: spect  
 PROBHD: 5 mm CPDQZ 1H  
 PULPROG: zgpg30  
 F1: 499.999  
 F2: 125.761  
 CHANNEL: cpd1  
 NS: 1.0  
 DS: 2  
 SS: 6032.620 Hz  
 SF: 500.136050 MHz  
 AQ: 5.0348774 sec  
 RG: 4.5  
 RE: 64.000 usec  
 DE: 298.2 K  
 TE: 298.2 K  
 DI: 0.1000000 sec  
 DECI: 0.0000000 sec  
 ACQRES: 0.13150000 usec  
 SFO1: 500.136050 MHz  
 SFO2: 125.761000 MHz  
 SF01: 500.136050 MHz  
 SF02: 125.761000 MHz

F2 - Processing parameters  
 SI: 65536  
 SF: 500.136050 MHz  
 DS: 0  
 SS: 0  
 SSB: 0.30 Hz  
 GB: 0  
 PC: 1.00

ID: NMR plot parameters  
 CT: 22.00 cm  
 CX: 1.00 cm  
 FIDP: 0.500 ppm  
 F1: 4231.87 Hz  
 F2: 103.500 ppm  
 FWD: 2.00000000  
 FWHM: 0.339474 ppm/cm  
 HZCM: 137.44528 Hz/cm



1H spectrum



```

Current Data Parameters
=====
NAME      ACM4-120403-24
EXPNO    1
PROCNO   1

F2 - Acquisition Parameters
Date_    20141112
Time     9:24
INSTRUM  cpdpr
PROBHD   5 mm CPDCL 1H-
PULPROG zgpg30
AQ       0.17748
RG       327.5
SFO1     500.131515 MHz
SF       500.131515 MHz
WDW       EM
SSB       0
GB       0
PC       1.00

ID Name Parameters
-----
C1      7.40 ppm
P1      1.60 dB
SF01    500.131515 MHz

F2 - Processing parameters
=====
SI      65536
SF      500.131515 MHz
WDW     EM
SSB     0
GB     0
PC     1.00

ID Name Parameters
-----
C1      7.40 ppm
P1      1.60 dB
SF01    500.131515 MHz

===== CHANNEL f1 =====
PC1     7.40 ppm
P1      1.60 dB
SF01    500.131515 MHz
=====

===== CHANNEL f2 =====
PC2     7.40 ppm
P2      1.60 dB
SF02    500.131515 MHz
=====
  
```



# Chapter 2: Domino Cross-Electrophile Coupling of Propargylic Tosylpiperidines

Portions of this chapter have been published:

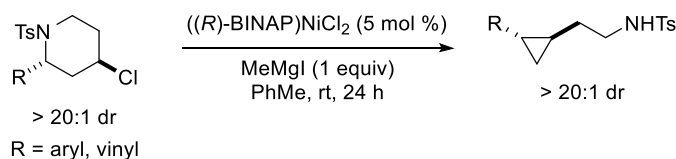
Hewitt, K.A.; Xie, P.-P.; Thane, T.A.; Hirbawi, N.; Zhang, S.-Q., **Matus, A. C.**; Lucas, E. L.; Hong, X.; Jarvo, E. R. *ACS Catalysis* **2021**, *23*, 14369.

## 2.1 Introduction

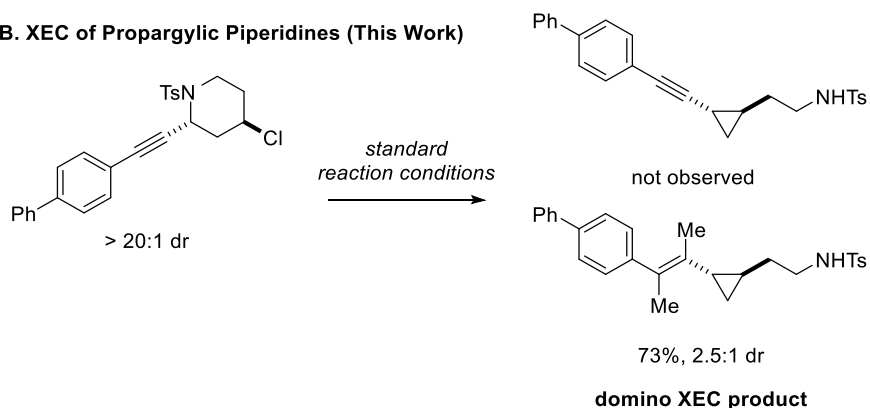
The development of cross-electrophile coupling (XEC) reactions has made great strides in generating valuable C–C bonds.<sup>1-3</sup> Typical cross-coupling reactions rely on the use of nucleophilic coupling partners, whereas XEC reactions can avoid the use of these reactive reagents.<sup>4,5</sup> Product selectivity is usually controlled by using electrophiles with differing electronics, which has led to the use of non-traditional electrophiles. In an effort to engage stronger bonds for XEC, Ni has been widely utilized due to its ability to undergo facile oxidative addition and engage in one- or two-electron chemistry.<sup>4,6-10</sup> This variety of reactivity, characteristic of Ni, makes it ideal for engaging sluggish electrophiles.

**Scheme 2.1: Cross-Electrophile Coupling (XEC) of Chlorotosylpiperidines**

**A. Established XEC Reaction (Jarvo, 2019)**



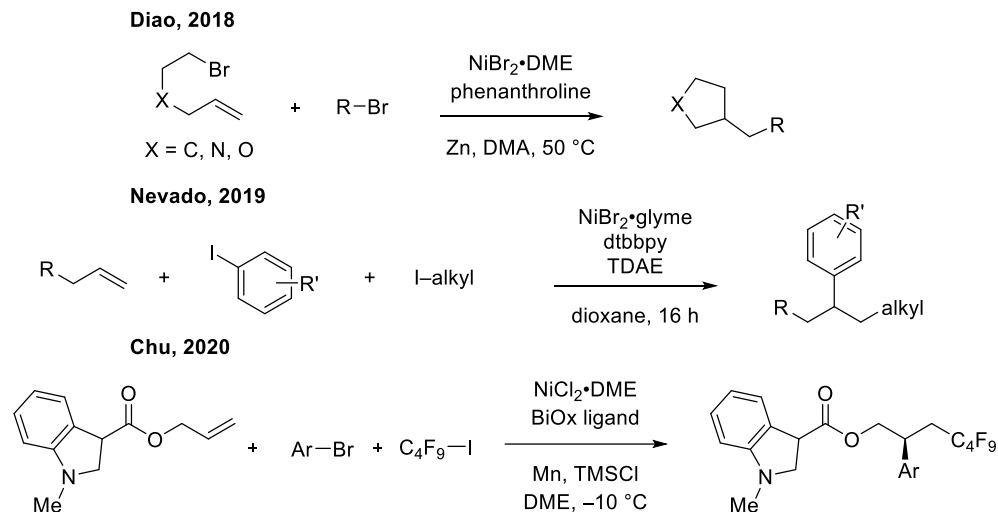
**B. XEC of Propargylic Piperidines (This Work)**



A recent example of C–N electrophiles being used in XEC reactions include the use of chlorotosylpiperidines (Scheme 2.1A).<sup>2</sup> This XEC reaction in particular exploits the different electronics of C–Cl and C–N bonds to afford an intramolecular transformation, affording cyclopropane products with high functional group tolerance. Despite the need for stoichiometric amounts of Grignard reagent to act as a reductant, the power of this transformation can be applied

with a variety of substrates. Interestingly, when a propargyl substrate was utilized in this reaction, instead of affording the expected propargyl cyclopropane, the alkyne participated in a domino XEC reaction to afford a vinyl cyclopropane product (Scheme 2.1B).

**Scheme 2.2: Selected Examples of Domino Reactions Involving XEC**



Examples of domino XEC reactions which include the formation of multiple new C–C bond are uncommon (Scheme 2.2) but do commonly rely on Ni catalysts.<sup>11-13</sup> Domino reactions are particularly advantageous because they can act as a pathway to rapidly introduce molecular complexity. With the discovery of this new reactivity and taking inspiration from the limited variety of reported domino-XEC reactions, I sought to expand the scope of the domino XEC dicarbofunctionalization reaction of tosylpiperidines to generate highly functionalized vinyl cyclopropanes.

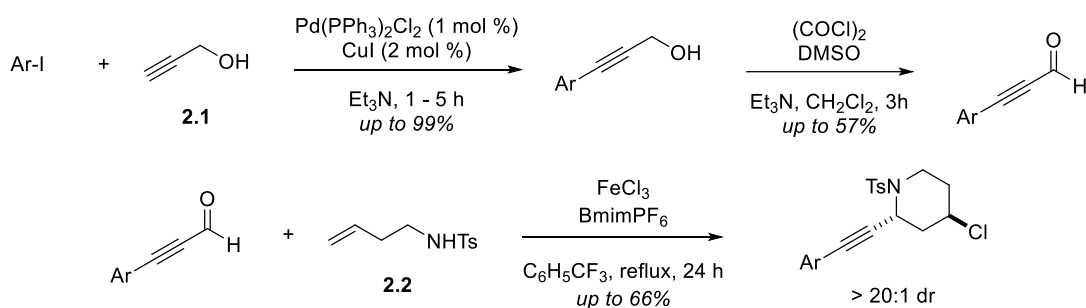
## 2.2 Results and Discussion

### 2.2.1 Synthesis of Piperidine Substrates

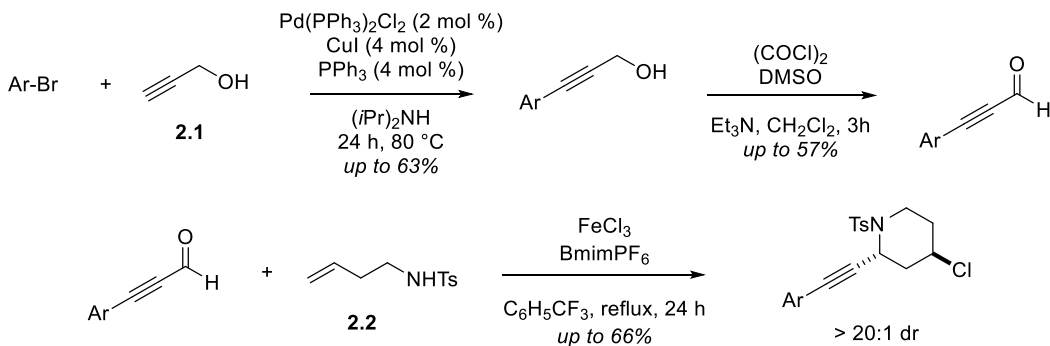
The need to utilize appropriate propargyl substrates for use in the domino reaction led to the development of two synthetic routes, starting with commercially available aryl iodides (Scheme 2.3) and aryl bromides (Scheme 2.4). This differentiation in route arose mainly from

access to materials, however the aryl bromide substrates were more challenging to use with the initial Sonogashira cross-coupling conditions used (Method B, *vide infra*). The addition of PPh<sub>3</sub>, increase in concentrations of Pd catalyst and CuI, and heating were effective in pushing the cross-coupling reaction forward, and the resulting propargylic alcohol substrates were converted to the corresponding aldehydes via Swern oxidation. Along with a linear, homoallylic amine (Method C, *vide infra*), the propargyl aldehydes were subjected to an aza-Prins cyclization to afford chlorotosylpiperidines in good yields with excellent dr.

**Scheme 2.3: Substrate Synthesis from Aryl Iodides**



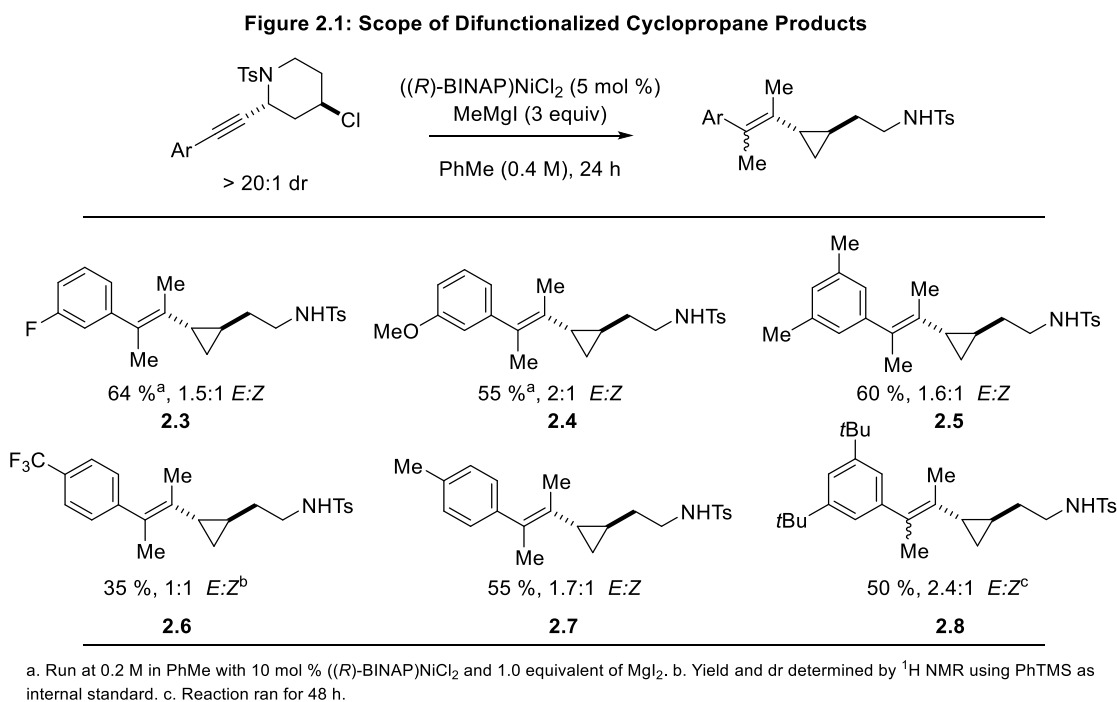
**Scheme 2.4: Substrate Synthesis from Aryl Bromides**



## 2.2.2 Cross-Electrophile Coupling Methods and Dicarbofunctionalization Scope

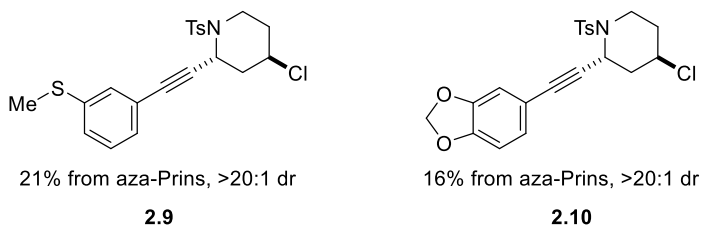
Previously established XEC conditions were utilized to generate carbodifunctionalized products. The use of MgI<sub>2</sub> was explored as an additive to increase yield, as it had previously impacted the results of XEC with vinyl substrates, however the desired increase in yield was not observed using propargylic substrates. The corresponding piperidines were subjected to the XEC

conditions, and resulted in the formation of six unique cyclopropane products (Figure 2.1). Of these results, only one cyclopropane product was identified to contain an (*E*)-alkene, and interestingly this product was generated using the most sterically bulky substrate (piperidine **2.21** reacting to form cyclopropane **2.8**). All other isolated products showed a small favoring of the trans-alkene products, apart from cyclopropane **2.6**, which showed no evidence of stereoselectivity for the (*E*)- or (*Z*)-alkene isomer (1:1 *E:Z*). The stereospecificity observed during formation of the cyclopropane moiety was later confirmed by a combination of theoretical and experimental data.<sup>14</sup>



After continued scope expansion by my coworkers, it was discovered that a smaller, alkyl substrate proceeded through the domino XEC reaction with complete retention of stereochemistry at the cyclopropane (>20:1 dr, favoring trans).<sup>14</sup> Before completion of the scope, two additional heteroatom-containing

**Figure 2.2: Other Piperidines Synthesized for XEC**



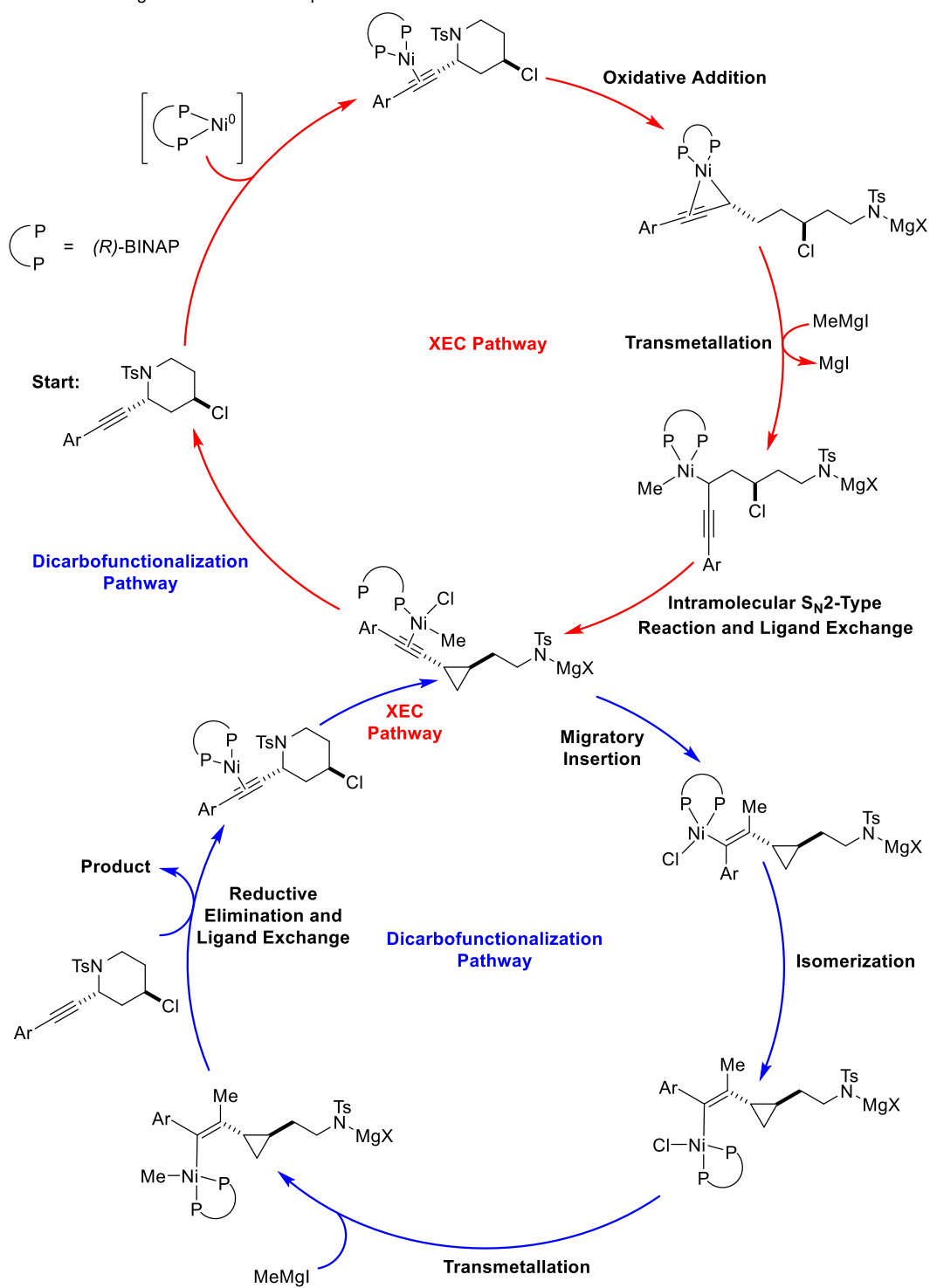
tosylpiperidines were synthesized for eventual use in the domino XEC reaction (Figure 2.2).

### 2.2.3 Mechanistic Investigation

The initial mechanism proposed for the domino XEC-dicarbofunctionalization is shown in Scheme 2.5. Starting with the *trans*-piperidine, Ni coordinates to the alkene as Ni<sup>0</sup>, then undergoes oxidative addition to open the piperidine, while nitrogen attaches to any Mg species in solution that acts as a Lewis acid. The Grignard reagent MeMgI then transmetalates with Ni, and an intramolecular S<sub>N</sub>2-type reaction affords the *trans*-cyclopropane, while a ligand exchange with one of (*R*)-BINAP's phosphines allows Ni to remain coordinated to the alkyne. From the XEC pathway, the Ni<sup>II</sup> species can deliver a methyl group to the alkyne through a migratory insertion. Then, to explain the *trans*-alkene results observed, the olefin can undergo an isomerization event. After final transmetalation event with another equivalent of MeMgI, reductive elimination will liberate the product and a ligand exchange with more starting material allows the cycle to begin with XEC again. This mechanism combines known reactivity elucidated from work previously described by the Jarvo lab, while the dicarbofunctionalization pathway may explain the stereochemical outcome of the vinyl products.<sup>2</sup>

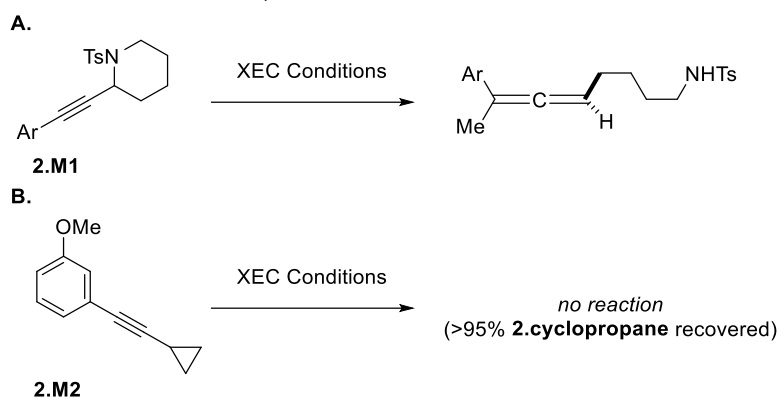
Density-functional theory (DFT) calculations revealed several key mechanistic details; the stereochemistry of the vinyl cyclopropane products is determined by the initial oxidative addition into the piperidine C–N bond and the intramolecular S<sub>N</sub>2-type reaction. The first oxidative addition step results in the inversion of stereochemistry, while the S<sub>N</sub>2-type reaction is also stereoinvertive. This net-retention of stereochemistry at the cyclopropane shows by all cyclopropanes isolated from the domino reaction display *trans*-stereochemistry. Enantioenriched propargyl piperidines were also synthesized and subjected to the domino XEC conditions, and exclusively afforded *trans*-cyclopropanes with retention of stereochemistry.

**Scheme 2.5.** Original Mechanism Proposed for Domino XEC Reaction





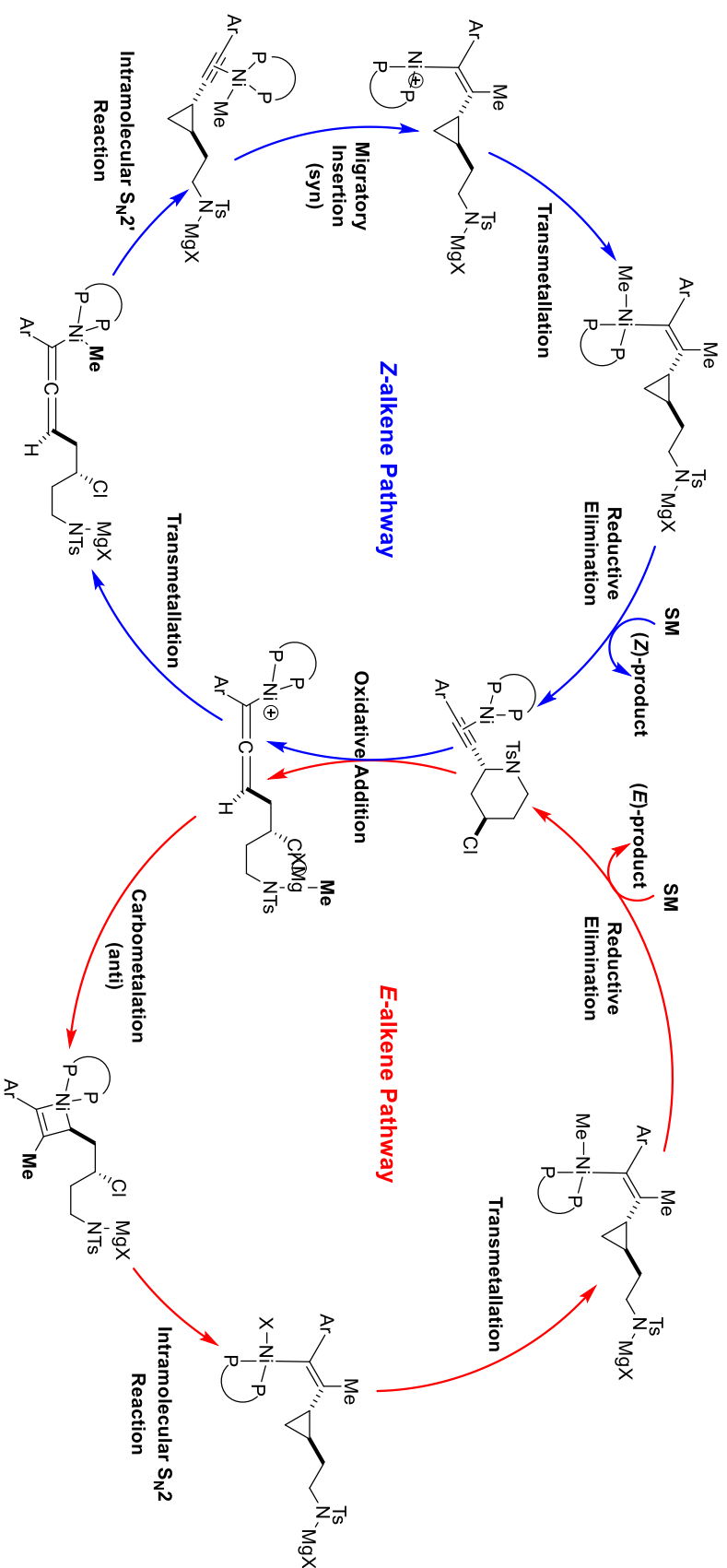
**Scheme 2.6:** Mechanistic Experiments



The final mechanistic aspect of the domino reaction, the dicarbofunctionalization pathway, was probed through a series of creative synthetic experiments. Two key substrates were synthesized, a propargyl piperidine with no Cl leaving group (**2.M1**), and an alkynyl cyclopropane (**2.M2**) (Scheme 2.6). The substrate **2.M1** was subjected to the XEC conditions and produced an allene product resulting from ring opening of the piperidine and single functionalization of the original alkyne. Conversely, **2.M2** was subjected to the XEC conditions and produced no product, providing evidence that the alkyne alone does not engage Ni for catalysis, and that the allenyl intermediate precedes cyclopropane formation. In combination with the DFT studies performed, a new mechanism was proposed based on experimental and theoretical data elucidated (Scheme 2.7).

This mechanism starts in the same way (Scheme 2.7), with coordination of Ni<sup>0</sup> to the alkyne, oxidative addition, and coordination of nitrogen to a Mg Lewis acid. This forms an allenyl Ni<sup>II</sup> intermediate, and the cycle can continue down two pathways. To form the Z-alkene product, transmetalation with the coordinated Grignard reagent followed by an intramolecular S<sub>N</sub>2' reaction affords the cyclopropane and regenerates the alkyne with Ni coordinating. Migratory insertion from Ni produces the singularly functionalized alkene, which then undergoes transmetalation once more. Product is generated after a final reductive elimination.

**Scheme 2.7:** Revised Domino XEC Mechanism



The *E*-alkene product starts with the same oxidative addition and coordination step to generate the allenyl Ni<sup>II</sup> intermediate. Carbometalation produces a 4-membered Ni metallocycle, which then goes through the intramolecular S<sub>n</sub>2 reaction to afford a vinyl cyclopropane. The Ni is liberated through transmetalation with another equivalent of Grignard reagent and produces the *E*-alkene after reductive elimination. This pathway dictates the stereochemistry of the cyclopropane and alkene, whereas the *Z*-alkene pathway has stereochemistry for each moiety determined across two separate steps (S<sub>n</sub>2' and migratory insertion). The DFT free-energy profiles for each pathway were compared and showed that the *Z*-alkene pathway has a slightly lower (<1 kcal/mol) barrier height than that of the *E*-alkene pathway, which mirrors the observed low selectivity between *Z*- and *E*-alkene products.

### 2.3 Conclusion

The scope of the domino XEC carbodifunctionalization reaction of tosylpiperidines was expanded, and routes for accessing starting materials were established. Cyclopropanes containing tetrasubstituted alkenes and primary sulfonamides were generated in good yields and high stereoselectivity for *trans*-cyclopropane formation, though stereoselectivity about the functionalized alkene was elusive. Further development of this reaction by my coworkers allowed for the rapid synthesis of structural analogues to known histone demethylase inhibitors. At the time of reporting, this was not only the first example of a reaction involving distinct XEC and dicarbofunctionalization events, but was also the first report of propargyl aldehydes undergoing an aza-Prins reaction to generate propargylic piperidines. The key allenyl Ni intermediates were also confirmed experimentally and theoretically, allowing for better mechanistic understanding of the domino transformation. Expansions of this work will focus on the replacement of MeMgI as

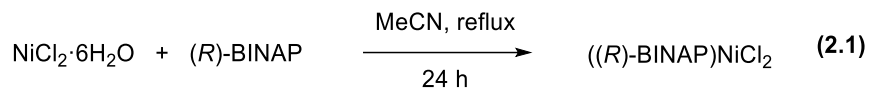
a coupling partner with other Grignard reagents, to investigate the boundaries of alkene functionalization using this established work.

## 2.4 Experimental Details

All reactions were carried out under a N<sub>2</sub> atmosphere, unless otherwise noted. All glassware was oven- or flame-dried prior to use. Tetrahydrofuran (THF), diethyl ether (Et<sub>2</sub>O), dichloromethane (CH<sub>2</sub>Cl<sub>2</sub>), and toluene (PhMe) were degassed with Ar and then passed through two 4 x 36 inch columns of anhydrous neutral A-2 alumina (8 x 14 mesh; LaRoche Chemicals; activated under a flow of argon at 350 °C for 12 h) to remove H<sub>2</sub>O.<sup>15</sup> Other solvents were purchased anhydrous commercially, or purified as described. <sup>1</sup>H NMR spectra were recorded on Bruker DRX-400 (400 MHz <sup>1</sup>H), GN-500 (500 MHz <sup>1</sup>H, 125.4 MHz <sup>13</sup>C), CRYO-500 (500 MHz <sup>1</sup>H, 125.8 MHz <sup>13</sup>C), or AVANCE-600 (600 MHz <sup>1</sup>H, 150.9 MHz <sup>13</sup>C, 564.7 MHz <sup>19</sup>F) spectrometers. Proton chemical shifts are reported in ppm (δ) relative to internal tetramethylsilane (TMS, δ 0.0). Data are reported as follows: chemical shift (multiplicity [singlet (s), broad singlet (br s), doublet (d), doublet of doublets (dd), triplet (t), doublet of triplets (dt), doublet of doublet of triplets (ddt), quartet (q) quintet (quin), sextet (sextet), apparent doublet (ad), multiplet (m)], coupling constants [Hz], integration). Carbon chemical shifts are reported in ppm (δ) relative to TMS with the respective solvent resonance as the internal standard (CDCl<sub>3</sub>, δ 77.16 ppm). NMR data were collected at 25 °C. Analytical thin-layer chromatography (TLC) was performed using Silica Gel 60 F254 precoated plates (0.25 mm thickness). Visualization was accomplished by irradiation with a UV lamp and stains were used as needed. Flash chromatography was performed using SiliaFlash F60 (40-63 μm, 60 Å) from SiliCycle. Automated chromatography was carried out on a Teledyne Isco CombiFlash Rf Plus. Melting points (m.p.) were obtained using a MelTemp melting point

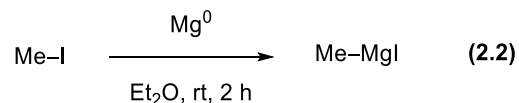
apparatus and are uncorrected. High resolution mass spectrometry was performed by the University of California, Irvine Mass Spectrometry Center.

#### 2.4.1 Preparation of ((*R*)-BINAP)NiCl<sub>2</sub>



This method is based on a procedure reported by Jamison.<sup>16</sup> To a flame-dried flask equipped with a stir bar was added NiCl<sub>2</sub>·6H<sub>2</sub>O (1.0 equiv). The flask was placed under vacuum and flame-dried until most of the nickel compound had turned from emerald green to yellow-orange. Some of the green hydrate complex is necessary for the reaction to proceed. The flask was allowed to cool to room temperature, and the solid was dissolved in MeCN (50. mM). The chiral (*R*)-BINAP (1.0 equiv) was added to the reaction flask, which was then fitted with a reflux condenser. The reaction mixture was heated to reflux and allowed to stir for 24 h. The reaction was cooled to room temperature and the black crystalline product was vacuum filtered. The precipitate was washed with excess MeCN and dried en vacuo.

#### 2.4.2 Preparation of MeMgI

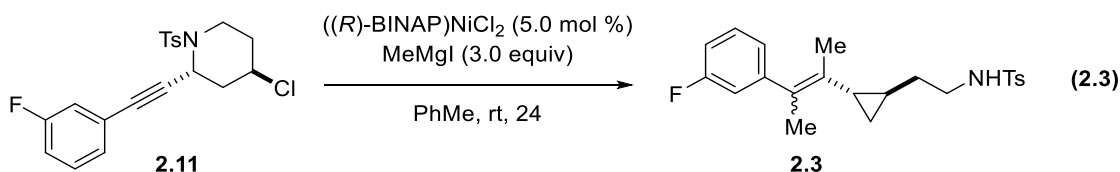


Under a N<sub>2</sub> atmosphere, a three-necked flask equipped with a stir bar, reflux condenser, and Schlenk filtration apparatus was charged with magnesium turnings (2.80 g, 115 mmol). The flask and magnesium turnings were then flame-dried under vacuum and the flask was backfilled with N<sub>2</sub>. Anhydrous Et<sub>2</sub>O (25 mL) and a crystal of iodine (ca. 2 mg) were added to the flask. The reaction mixture was brought to 0 °C and freshly distilled iodomethane (5.0 mL, 80. mmol) was slowly added over 30 min to maintain a gentle reflux. The reaction mixture was brought to room

temperature and allowed to stir for 2 h, then filtered through the fritted Schlenk filter into a pear-shaped flask under N<sub>2</sub> atmosphere. The pear-shaped flask was capped with a septum, sealed with parafilm, and stored in the glovebox under a N<sub>2</sub> atmosphere for up to eight weeks without detrimental effects. The resulting Grignard reagent was titrated by Knochel's method to 2.4 M to 3.0 M.<sup>17</sup>

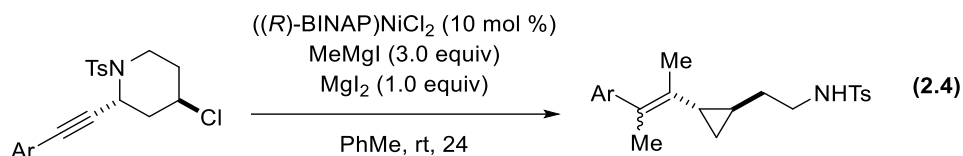
### 2.4.2.1 Method A: Domino Cross-Electrophile Coupling Reaction of Propargylic Tosylpiperidines

#### 2.4.2.1.1 Cross-Electrophile Coupling without MgI<sub>2</sub>



In a glovebox, an oven-dried 7 mL vial equipped with a stir bar was charged with piperidine substrate (1.0 equiv), ((*R*)-BINAP)NiCl<sub>2</sub> (5.0 mol %), and PhMe (0.20 M in substrate). MeMgI (3.0 equiv) was added dropwise, the vial was capped, and the reaction was allowed to stir. The reaction vial was removed from the glovebox after 24 h, quenched with methanol, filtered through a silica gel plug eluting with 100% Et<sub>2</sub>O, and concentrated in vacuo. Phenyltrimethylsilane (PhTMS; 8.6 μL, 50. μmol) was added and the yield was determined by <sup>1</sup>H NMR based on comparison to PhTMS as internal standard before further purification.

#### 2.4.2.1.2 Cross-Electrophile Coupling with MgI<sub>2</sub>



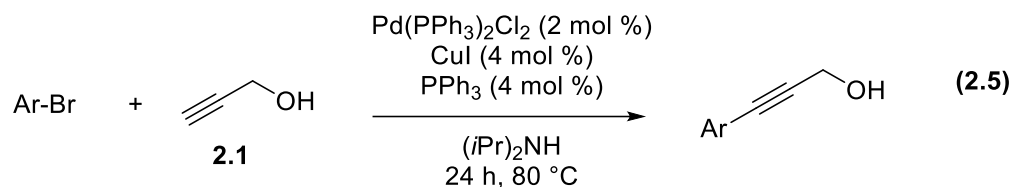
In a glovebox, an oven-dried 7 mL vial equipped with a stir bar was charged with piperidine substrate (1.0 equiv), ((*R*)-BINAP)NiCl<sub>2</sub> (10. mol %), MgI<sub>2</sub> (1.0 equiv), and PhMe (0.20 M in

substrate). The reagent MeMgI (3.0 equiv) was added dropwise, the vial was capped, and the reaction was allowed to stir. The reaction vial was removed from the glovebox after 24 h, quenched with methanol, filtered through a silica gel plug eluting with 100% Et<sub>2</sub>O, and concentrated in vacuo. Phenyltrimethylsilane (PhTMS; 8.6 μL, 50. μmol) was added and the yield was determined by <sup>1</sup>H NMR based on comparison to PhTMS as internal standard before further purification.

### 2.4.3 General Procedures for Substrate Synthesis

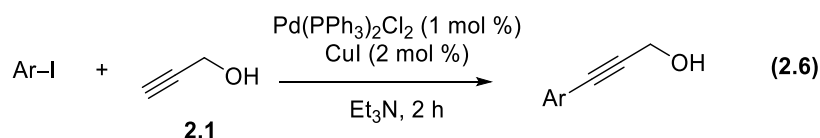
#### 2.4.3.1 Method B: Sonogashira Cross-Coupling of Aryl Halides with Propargyl Alcohol

##### 2.4.3.1.1 Sonogashira Cross-Coupling with Aryl Bromides



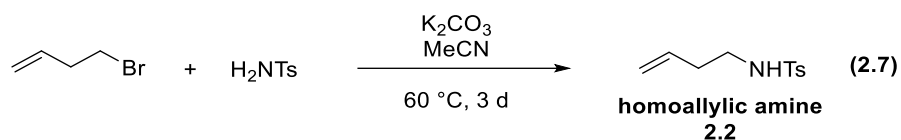
This procedure was adapted from a procedure reported by Nagumo.<sup>18</sup> To a flame-dried round bottom flask charged with a stir bar was added Pd(PPh<sub>3</sub>)<sub>2</sub>Cl<sub>2</sub> (2 mol %) and CuI (4 mol %). Diisopropylamine (0.01 M in CuI) was added to the flask, and the suspension was allowed to stir for five minutes. Aryl bromide (1.0 equiv) and propargyl alcohol (**2.1**, 1.1 equiv) were brought up in diisopropylamine (1.0 M in aryl bromide), and the solution was added dropwise to the reaction mixture. The reaction vessel was equipped with a reflux condenser, heated to 80 °C, and allowed to stir for 24 h. After cooling to room temperature, the crude reaction mixture was filtered through a pad of Celite. The filter cake was washed with EtOAc (x 3) and the combined solution was concentrated in vacuo.

##### 2.4.3.1.2 Sonogashira Cross-Coupling with Aryl Iodides



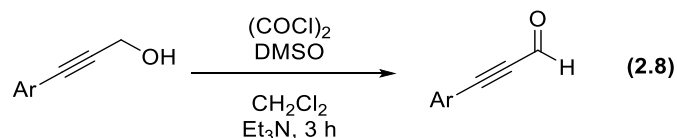
This procedure was adapted from a procedure reported by Tambar.<sup>19</sup> To a flame-dried round bottom flask charged with a stir bar was added Pd(PPh<sub>3</sub>)<sub>2</sub>Cl<sub>2</sub> (1 mol %) and CuI (2 mol %). Et<sub>3</sub>N (0.01 M in CuI) was added to the flask, and the suspension was allowed to stir for five minutes. Aryl iodide (1.0 equiv) and propargyl alcohol (1.1 equiv) were brought up in Et<sub>3</sub>N (1.0 M in aryl iodide), and the solution was added dropwise to the reaction mixture. The reaction was monitored by thin layer chromatography and typically went to completion after 2 h. The crude reaction mixture was filtered through a pad of Celite. The filter cake was washed with EtOAc (x 3) and the combined solution was concentrated in vacuo.

#### 2.4.3.2 Method C: Synthesis of Homoallylic Tosylamine



This procedure was adapted from a procedure reported by Jiang.<sup>20</sup> To a flame-dried two-neck flask equipped with a stir bar was added 4-bromo-1-butene (1.0 equiv), *p*-toluenesulfonamide (1.0 equiv), and K<sub>2</sub>CO<sub>3</sub> (1.2 equiv). The flask was fitted with an air condenser and MeCN (0.25 M in bromide) was added via cannula transfer. The reaction was heated to 60 °C and allowed to stir for 3 d. The reaction mixture was quenched with saturated aqueous NH<sub>4</sub>Cl and extracted with EtOAc (x 3). The combined organic layers were washed with brine, dried over Na<sub>2</sub>SO<sub>4</sub>, filtered, and concentrated in vacuo.

#### 2.4.3.3 Method D: Swern Oxidation of Propargylic Alcohols to Aldehydes

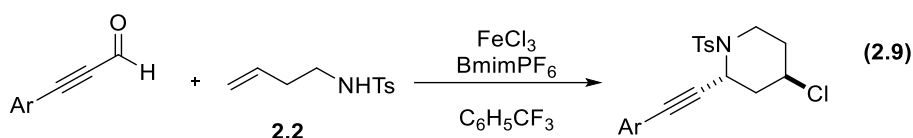


To a flame-dried round bottom flask under N<sub>2</sub> atmosphere charged with a stir bar was added oxalyl chloride (1.3 equiv). CH<sub>2</sub>Cl<sub>2</sub> (0.37 M in oxalyl chloride) was added to the reaction flask and



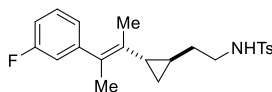
the reaction mixture was cooled to  $-78^{\circ}\text{C}$ . Dimethyl sulfoxide (1.2 equiv) was added dropwise to the reaction flask, and a vent was created to allow CO and CO<sub>2</sub> gasses to escape. After stirring for 15 min, alcohol substrate (1.0 equiv) as a solution in CH<sub>2</sub>Cl<sub>2</sub> (0.40 M in substrate) was added dropwise, and the vent was removed. The reaction mixture was allowed to stir at  $-78^{\circ}\text{C}$  for 1 h. Et<sub>3</sub>N (3.0 equiv) was added to the flask along with a vent, and the reaction mixture was allowed to warm to room temperature and stir for an additional 3 h. The reaction mixture was quenched with saturated aqueous NH<sub>4</sub>Cl and extracted with CH<sub>2</sub>Cl<sub>2</sub> (x 3). The combined organic layers were washed with brine, dried over Na<sub>2</sub>SO<sub>4</sub>, filtered, and concentrated in vacuo.

#### 2.4.3.4 Method E: Iron (III) Chloride/BmimPF<sub>6</sub>-Promoted Aza-Prins Reaction



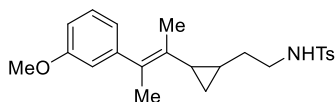
This procedure was adapted from a procedure reported by Hasegawa.<sup>21</sup> To a flame-dried round-bottom flask equipped with a stir bar was added FeCl<sub>3</sub> (1.5 equiv) and C<sub>6</sub>H<sub>5</sub>CF<sub>3</sub> (0.10 M in homoallylic amine). In a separate flask, a solution of aldehyde substrate (1.5 equiv) and homoallylic amine (1.0 equiv) in C<sub>6</sub>H<sub>5</sub>CF<sub>3</sub> (0.10 M in aldehyde) was prepared. The solution was added to the reaction flask via syringe. The flask was fitted with a reflux condenser and N<sub>2</sub> inlet, and the reaction mixture was heated to reflux. After stirring for 24 h the reaction mixture was quenched with H<sub>2</sub>O and extracted with Et<sub>2</sub>O (x 3). The combined organic layers were washed sequentially with Na<sub>2</sub>S<sub>2</sub>O<sub>3</sub>, saturated aqueous NaHCO<sub>3</sub>, and brine. The organic layers were dried over Na<sub>2</sub>SO<sub>4</sub>, filtered, and concentrated in vacuo.

#### 2.4.4 Characterization Data of Cyclopropane Products



**(E)-N-(2-(2-(3-(3-fluorophenyl)but-2-en-2-yl)cyclopropyl)ethyl)-4-**

**methylbenzenesulfonamide (2.3)** The following amounts of reagents were used: **2.11** (78 mg, 0.20 mmol, 1.0 equiv), ((*R*)-BINAP)NiCl<sub>2</sub> (8 mg, 10 μmol, 5 mol %), methylmagnesium iodide (0.21 mL, 2.8 M, 0.60 mmol, 3.0 equiv), PhMe (1.0 mL, 0.20 M in substrate). The compound was purified by flash column chromatography (0–20% EtOAc/hexanes) to afford the title compound as a clear yellow oil (39 mg, 98 μmol, 49%). The product is assigned to be a 1.5:1.0 mixture of diastereomers based on <sup>1</sup>H NMR. **TLC** R<sub>f</sub> = 0.41 (20%EtOAc/hexanes); **<sup>1</sup>H NMR** (500 MHz, CDCl<sub>3</sub>) δ 7.84 (d, *J* = 7.6 Hz, 2H, one diastereomer), 7.78 (m, 2H, other diastereomer), 7.40–7.33 (m, 4H, both diastereomers), 7.30 (m, 1H, other diastereomer), 7.23 (m, 1H, one diastereomer), 7.09–7.02 (m, 2H, both diastereomers), 7.02–6.90 (m, 4H, both diastereomers), 4.85 (m, 1H, one diastereomer), 4.67 (m, 1H, other diastereomer), 3.13 (m, 2H, one diastereomer), 2.97 (m, 2H, other diastereomer), 2.48 (s, 6H, both diastereomers), 2.39 (s, 3H, one diastereomer), 2.38 (s, 3H, other diastereomer), 2.08 (d, *J* = 1.4 Hz, 3H, one diastereomer), 2.00 (d, *J* = 5.8 Hz, 2H, one diastereomer), 1.52 (m, 2H, both diastereomers), 1.47 (d, *J* = 4.9 Hz, 2H, other diastereomer), 1.31 (d, *J* = 1.4 Hz, 3H, other diastereomer), 0.88 (m, 1H, one diastereomer) 0.78 (m, 1H, one diastereomer), 0.64 (m, 1H, other diastereomer), 0.54 (m, 1H, other diastereomer), 0.24 (m, 2H, both diastereomers); **<sup>13</sup>C NMR** (125.8 MHz, CDCl<sub>3</sub>) δ 162.8 (d, *J* = 245.2 Hz), 144.6 (d, *J* = 264.6 Hz), 137.34 (d, *J* = 68.0 Hz), 137.3 (d, *J* = 62.6 Hz), 132.1, 130.6, 129.8 (2C), 129.79, 129.78, 129.1, 128.0, 127.3 (2C), 127.2 (2C), 126.7, 125.9, 125.5, 124.6 (d, *J* = 2.9), 115.7 (d, *J* = 20.5), 112.8 (d, *J* = 20.9), 43.44, 43.40, 43.21, 43.18, 33.8, 33.7, 23.0, 22.9, 22.2, 21.6, 21.5, 21.5, 20.9, 16.2, 15.8, 15.7, 15.6, 14.0, 13.8, 11.82, 11.79, 11.6; **<sup>19</sup>F NMR** (564.6 MHz, CDCl<sub>3</sub>) δ –113.79 (1F, one diastereomer), –114.17 (1F, other diastereomer); **HRMS** (TOF MS ES<sup>+</sup>) *m/z* calcd for C<sub>22</sub>H<sub>26</sub>FNO<sub>2</sub>SNa (M + Na)<sup>+</sup> 410.1566, found 410.1556.

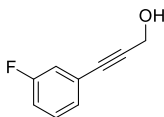


**(E)-N-(2-(2-(3-(3-methoxyphenyl)but-2-en-2-yl)cyclopropyl)ethyl)-4-**

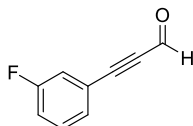
**methylbenzenesulfonamide (2.4)** The following amounts of reagents were used: **2.16** (81 mg, 0.20 mmol, 1.0 equiv), ((*R*)-BINAP)NiCl<sub>2</sub> (15 mg, 20. μmol, 10. mol %), methylmagnesium iodide (0.21 mL, 2.8 M, 0.60 mmol, 3.0 equiv), PhMe (1.0 mL, 0.20 M in substrate), MgI<sub>2</sub> (56 mg, 0.20 mmol, 1.0 equiv). The compound was purified by flash column chromatography (0–30% EtOAc/hexanes) to afford the title compound as a clear yellow oil (42 mg, 0.11 mmol, 55%). The product is assigned to be a 2.0:1.0 mixture of diastereomers based on <sup>1</sup>H NMR. **TLC** R<sub>f</sub> = 0.36 (20% EtOAc/hexanes); **<sup>1</sup>H NMR** (600 MHz, CDCl<sub>3</sub>) δ 7.77 (d, *J* = 8.2 Hz, 2H, diastereomer 1), 7.70 (d, *J* = 8.2 Hz, 2H, diastereomer 2), 7.30 (m, 3H, diastereomer 1), 7.20 (m, 3H, diastereomer 2), 6.73 (m, 2H, both diastereomers), 6.68 (d, *J* = 7.6, 1H, diastereomer 1), 6.64 (m, 1H, diastereomer 2), 4.61 (t, *J* = 6.1 Hz, 1H, diastereomer 1), 4.43 (t, *J* = 6.0 Hz, 1H diastereomer 2), 3.80 (s, 6H, both diastereomers), 3.07 (m, 2H, diastereomer 1), 2.91 (m, 2H, diastereomer 2), 2.42 (s, 6H, both), 2.02 (s, 3H, diastereomer 1), 1.95 (s, 3H, 2 diastereomer), 1.63 (m, 2H, both), 1.45 (m, 2H, diastereomer 1), 1.41 (s, 3H, diastereomer 2), 1.25 (s, 3H, diastereomer 1), 1.19 (m, 2H, both), 0.81 (m, 1H, diastereomer 1), 0.72 (m, 1H, diastereomer 1), 0.68 (m, 1H, diastereomer 2), 0.59 (m, 1H, diastereomer 2), 0.48 (m, 1H, diastereomer 1), 0.18 (dt, *J* = 9.0 Hz, 4.8 Hz, 1H, diastereomer 2); **<sup>13</sup>C NMR** (150.9 MHz, CDCl<sub>3</sub>) δ 159.5, 159.4, 147.2, 146.7, 143.5, 143.4, 137.2, 137.1, 132.0, 131.2, 129.9 (2C), 129.8 (2C), 129.7, 129.6, 129.2 (2C), 129.1 (2C), 127.3 (2C), 127.2 (2C), 121.3, 120.9, 114.5, 114.1, 111.5, 111.4, 55.2 (2C), 43.5, 43.2, 34.3, 33.7, 23.0, 22.2, 21.7, 20.8, 16.1, 15.7, 15.6, 13.8, 11.8, 11.6; **HRMS** (TOF MS ES<sup>+</sup>) *m/z* calcd for C<sub>23</sub>H<sub>29</sub>NO<sub>3</sub>SNa (M + Na)<sup>+</sup> 422.1766, found 422.1758.

Further characterization of cyclopropane products was performed by Hewitt, *et al.*<sup>14</sup>

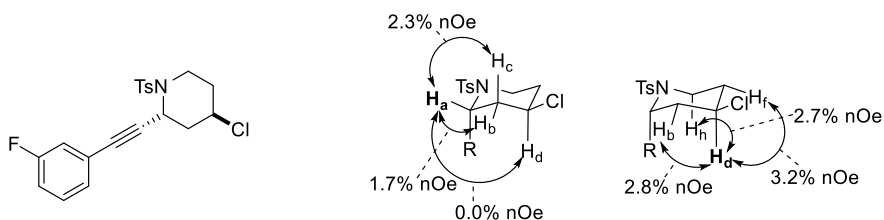
#### 2.4.5 Characterization Data of Starting Materials



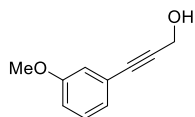
**3-(3-fluorophenyl)prop-2-yn-1-ol (2.12)** was prepared according to Method B. The following amounts of reagents were used: 1-fluoro-3-iodobenzene (1.08 mL, 10.0 mmol, 1.00 equiv), **2.1** (0.64 mL, 11 mmol, 1.1 equiv) CuI (38 mg, 0.20 mmol, 2.0 mol %), Pd(PPh<sub>3</sub>)<sub>2</sub>Cl<sub>2</sub> (70. mg, 0.10 mmol, 1.0 mol %), Et<sub>3</sub>N (20. mL, 0.50 M in aryl iodide). The compound was purified by flash column chromatography (20% EtOAc) to afford the title compound as a clear orange oil (1.25 g, 8.32 mmol, 83%). **TLC** *R<sub>f</sub>* = 0.15 (20% EtOAc/hexanes); **<sup>1</sup>H NMR** (400 MHz, CDCl<sub>3</sub>) δ 7.28–7.17 (m, 2H), 7.14–7.09 (m, 1H), 7.05–6.97 (m, 1H), 4.49 (s, 2H), 2.63 (br s, 1H). Analytical data are consistent with literature values.<sup>22</sup>



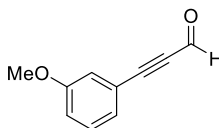
**3-(3-fluorophenyl)propionaldehyde (2.13)** was prepared according to Method D. The following amounts of reagents were used: **2.12** (4.1 mL, 0.40 M in CH<sub>2</sub>Cl<sub>2</sub>, 1.7 mmol, 1.0 equiv), oxalyl chloride (0.18 mL, 2.2 mmol, 1.3 equiv), dimethyl sulfoxide (0.14 mL, 2.0 mmol, 1.2 equiv), CH<sub>2</sub>Cl<sub>2</sub> (5.8 mL, 0.37 M in oxalyl chloride), Et<sub>3</sub>N (0.69 mL, 5.0 mmol, 2.9 equiv). The compound was isolated using flash column chromatography (0–20% EtOAc/hexanes, KMnO<sub>4</sub> stain) to afford the title compound as an orange oil (140 mg, 0.95 mmol, 56%). **TLC** *R<sub>f</sub>* = 0.71 (20% EtOAc/hexanes); **<sup>1</sup>H NMR** (400 MHz, CDCl<sub>3</sub>) δ 9.42 (s, 1H), 7.42–7.34 (m, 2H) 7.30–7.23 (m, 1H), 7.24–7.15 (m, 1H); Analytical data are consistent with literature values.<sup>23</sup>



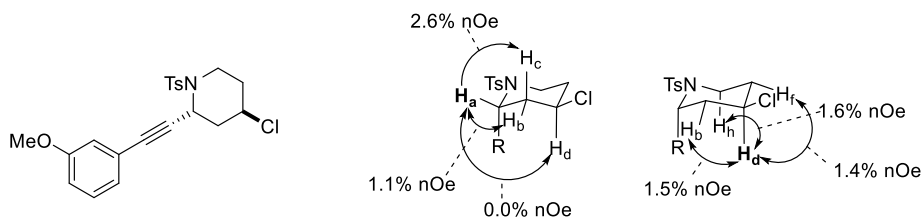
**4-chloro-2-((3-fluorophenyl)ethynyl)-1-tosylpiperidine (2.11)** was prepared according to Method E. The following amounts of reagents were used: **2.13** (280 mg, 1.9 mmol, 1.5 equiv), **2.2 (amine)** (0.63 mL, 2.0 M in  $C_6H_5CF_3$ , 1.3 mmol, 1.0 equiv),  $FeCl_3$  (306 mg, 1.89 mmol, 1.50 equiv),  $BmimPF_6$  (0.29 mL, 1.4 mmol, 1.5 equiv),  $C_6H_5CF_3$  (14 mL, 0.10 M in **2.13**). The compound was purified using column chromatography (10–20% EtOAc/hexanes) to afford the title compound as an orange solid (190 mg, 0.48 mmol, 37%, >20:1 dr trans:cis). The dr was determined based on the integration of resonances attributed to  $H_d$  in the  $^1H$  NMR. **TLC**  $R_f$  = 0.50 (20% EtOAc/hexanes); **m.p.** 126–128 °C;  **$^1H$  NMR** (400 MHz,  $CDCl_3$ )  $\delta$  7.71 (d,  $J$  = 8.3 Hz, 2H), 7.23 (d,  $J$  = 8.2 Hz, 2H), 7.20 (m, 3H), 6.99 (tdd,  $J$  = 8.5 Hz, 2.6 Hz, 0.8 Hz, 1H), 6.81 (d,  $J$  = 7.7 Hz, 1H), 6.56 (ddd  $J$  = 9.5 Hz, 2.6 Hz, 1.5 Hz, 1H), 5.12 (br s, 1H), 4.16 (tt,  $J$  = 12.0 Hz, 4.3 Hz, 1H), 3.86 (dq,  $J$  = 12.3 Hz, 2.3 Hz, 1H), 2.95 (td,  $J$  = 12.5 Hz, 2.6 Hz, 1H), 2.36 (ddt,  $J$  = 12.6 Hz, 5.5 Hz, 2.5 Hz, 1H), 2.31 (s, 3H), 2.27–2.21 (m, 1H), 2.16 (td,  $J$  = 12.4 Hz, 4.8 Hz, 1H), 1.96 (qd,  $J$  = 16.6 Hz, 4.8 Hz, 1H);  **$^{13}C$  NMR** (125.4 MHz,  $CDCl_3$ )  $\delta$  162.1 (d,  $J$  = 246.7 Hz), 144.0, 134.7, 129.9 (d,  $J$  = 8.7 Hz), 129.6 (2C), 128.1 (2C), 127.4 (d,  $J$  = 3.2 Hz), 123.5, 123.4, 118.4 (d,  $J$  = 23.0 Hz), 85.5 (d,  $J$  = 3.3 Hz), 83.8, 52.8, 47.2, 42.1, 41.3, 35.9, 21.4;  **$^{19}F$  NMR** (564.7 MHz,  $CDCl_3$ )  $\delta$  -112.7 (1F); **HRMS** (TOF MS ES+)  $m/z$  calcd for  $C_{20}H_{19}ClFNO_2SNa$  ( $M + Na$ )<sup>+</sup> 414.0707, found 414.0716.



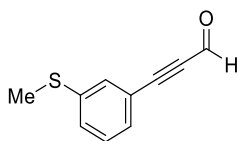
**3-(3-methoxyphenyl)prop-2-yn-1-ol (2.14)** was prepared according to Method B. The following amounts of reagents were used: 1-iodo-3-methoxybenzene (0.60 mL, 5.0 mmol, 1.0 equiv), propargyl alcohol (0.32 mL, 5.5 mmol, 1.1 equiv), Pd(PPh<sub>3</sub>)<sub>2</sub>Cl<sub>2</sub> (35 mg, 50. μmol, 1.0 mol %), CuI (19 mg, 0.10 mmol, 2.0 mol %), Et<sub>3</sub>N (10. mL, 0.01 M in CuI). The compound was purified using flash column chromatography (20% EtOAc/hexanes) to afford the title compound as a yellow oil (757 mg, 4.67 mmol, 93%). **TLC** R<sub>f</sub> = 0.14 (20% EtOAc/hexanes, KMNO<sub>4</sub> stain) **<sup>1</sup>H NMR** (500 MHz, CDCl<sub>3</sub>) δ 7.24–7.21 (m, 1H), 7.03 (d, *J* = 7.6 Hz, 1H), 6.97 (s, 1H), 6.88 (dd, *J* = 8.3 Hz, 1.8 Hz, 1H), 4.52 (s, 2H), 3.80 (s, 3H), 1.72 (br s, 1H). Analytical data consistent with literature values.<sup>24</sup>



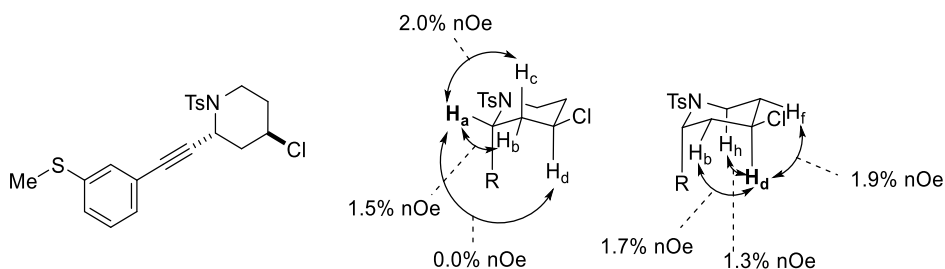
**3-(3-methoxyphenyl)propionaldehyde (2.15)** was prepared according to Method D. The following amounts of reagents were used: **2.14** (249 mg, 1.53 mmol, 1.00 equiv), oxalyl chloride (0.17 mL, 2.0 mmol, 1.3 equiv), dimethylsulfoxide (0.13 mL, 1.8 mmol, 1.2 equiv), Et<sub>3</sub>N (0.64 mL, 4.6 mmol, 3.0 equiv), CH<sub>2</sub>Cl<sub>2</sub> (5.4 mL, 0.37 M in oxalyl chloride). The compound was purified using flash column chromatography (0–20%) to afford the title compound as a yellow oil (144 mg, 0.899 mmol, 59%). **TLC** R<sub>f</sub> = 0.51 (20% EtOAc, KMNO<sub>4</sub> stain) **<sup>1</sup>H NMR** (400 MHz, CDCl<sub>3</sub>) δ 9.40 (s, 1H), 7.29 (t, *J* = 8.4 Hz, 1H), 7.18 (dt, *J* = 7.6 Hz, 1.2 Hz, 1H), 7.09 (dd, *J* = 2.6 Hz, 1.4 Hz, 1H), 7.02 (dd, *J* = 8.3 Hz, 2.6 Hz, 1H), 3.79 (s, 3H). Analytical data are consistent with literature values.<sup>25</sup>



**4-chloro-2-((3-methoxyphenyl)ethynyl)-1-tosylpiperidine (2.16)** was prepared according to Method E. The following amounts of reagents were used: **2.15** (290 mg, 1.8 mmol, 1.5 equiv), **2.2** (0.60 mL, 2.0 M in C<sub>6</sub>H<sub>5</sub>CF<sub>3</sub>, 1.2 mmol, 1.0 equiv), FeCl<sub>3</sub> (292 mg, 1.80 mmol, 1.50 equiv), BmimPF<sub>6</sub> (0.37 mL, 1.8 mmol, 1.5 equiv), C<sub>6</sub>H<sub>5</sub>CF<sub>3</sub> (18 mL, 0.10 M in **XX**). The compound was purified using flash column chromatography (0–20% EtOAc/hexanes) to afford the title compound as a yellow, crystalline solid (156 mg, 0.386 mmol, 32%, >20:1 dr trans:cis). The dr was determined based on the integration of resonances attributed to H<sub>d</sub> in the <sup>1</sup>H NMR. **TLC R<sub>f</sub>** = 0.50 (20% EtOAc/hexanes); **m.p.** 115–117 °C; **<sup>1</sup>H NMR** (600 MHz, CDCl<sub>3</sub>) δ 7.71 (d, *J* = 8.3 Hz, 2H), 7.22 (d, *J* = 8.0 Hz, 2H), 7.14 (t, *J* = 7.8 Hz, 1H), 6.83 (ddd, *J* = 8.4 Hz, 2.6 Hz, 0.8 Hz, 1H), 6.56 (d, *J* = 7.6 Hz, 1H), 6.50 (dd, *J* = 2.5 Hz, 1.4 Hz, 1H), 5.12 (br s, 1H), 4.19 (tt, *J* = 12.0 Hz, 4.2 Hz, 1H), 3.84 (dq, *J* = 12.5 Hz, 2.1 Hz, 1H), 3.77 (s, 3H), 2.97 (td, *J* = 12.5 Hz, 2.6 Hz, 1H), 2.38 (ddt, *J* = 12.7 Hz, 4.6 Hz, 2.5 Hz, 1H), 2.30 (s, 3H), 2.23 (m, 1H), 2.16 (td, *J* = 12.4 Hz, 4.8 Hz, 1H), 1.97 (qd, *J* = 12.6 Hz, 4.8 Hz, 1H); **<sup>13</sup>C NMR** (150.9 MHz, CDCl<sub>3</sub>) δ 159.3, 144.0, 134.8, 129.6 (2C), 129.3, 129.1 (2C), 124.1, 122.8, 117.1, 114.1, 87.5, 82.6, 55.2, 52.9, 47.3, 41.9, 41.4, 35.8, 21.3; **HRMS** (TOF MS ES<sup>+</sup>) *m/z* calcd for C<sub>21</sub>H<sub>22</sub>ClFNO<sub>3</sub>SNa (M + Na)<sup>+</sup> 426.0907, found 426.0903.



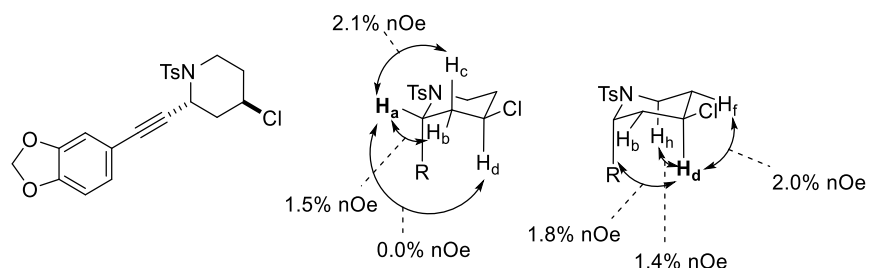
**3-(3-(methylthio)phenyl)propionaldehyde (2.17)** was prepared according to Method D on a 1.68 mmol scale in quadruplicate. The following amounts of reagents were used: 3-(3-(methylthio)phenyl)prop-2-yn-1-ol (synthesized from the corresponding aryl bromide following Method B, 299 mg, 1.68 mmol, 1.00 equiv), oxalyl chloride (0.19 mL, 2.2 mmol, 1.3 equiv), dimethylsulfoxide (0.14 mL, 2.0 mmol, 1.2 equiv), Et<sub>3</sub>N (0.71 mL, 5.0 mmol, 3.0 equiv), CH<sub>2</sub>Cl<sub>2</sub> (5.5 mL, 0.40 M in oxalyl chloride). The compound was purified using flash column chromatography (0–65% CH<sub>2</sub>Cl<sub>2</sub>/hexanes) to afford the title compound as an orange oil (649 mg, 3.68 mmol, 55%). **TLC** *R<sub>f</sub>* = 0.42 (65% CH<sub>2</sub>Cl<sub>2</sub>/hexanes, KMNO<sub>4</sub> stain); **<sup>1</sup>H NMR** (400 MHz, CDCl<sub>3</sub>) δ 9.43 (s, 1H), 7.45 (br s, 1H), 7.40–7.28 (m, 3H), 2.51 (s, 3H); **<sup>13</sup>C NMR** (125.4 MHz, CDCl<sub>3</sub>) δ 176.7, 140.0, 130.1, 129.6, 129.3, 129.0, 120.2, 94.5, 88.5, 15.5.



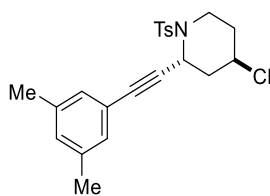
**4-chloro-2-((3-(methylthio)phenyl)ethynyl)-1-tosylpiperidine (2.18)** was prepared according to Method E. The following amounts of reagents were used: **2.17** (625 mg, 3.55 mmol, 1.50 equiv), homoallylic amine (533 mg, 2.37 mmol, 1.00 equiv), FeCl<sub>3</sub> (578 mg, 3.55 mmol, 1.50 equiv), BmimPF<sub>6</sub> (0.73 mL, 3.55 mmol, 1.50 equiv), C<sub>6</sub>H<sub>5</sub>CF<sub>3</sub> (23 mL, 0.10 M in aldehyde). The compound was purified using flash chromatography (0–20% EtOAc/hexanes) to afford the title compound as a yellow oil (313 mg, 0.745 mmol, 21%, >20:1 dr trans:cis). **TLC** *R<sub>f</sub>* = 0.61 (20% EtOAc/hexanes, KMNO<sub>4</sub> stain); **<sup>1</sup>H NMR** (500 MHz, CDCl<sub>3</sub>) δ 7.71 (d, *J* = 8.2 Hz, 2H), 7.23 (d, *J* = 8.1 Hz, 2H), 7.19–7.11 (m, 2H), 6.85 (s, 1H), 6.76 (m, 1H), 5.13 (br s, 1H), 4.18 (tt, *J* = 12.0,



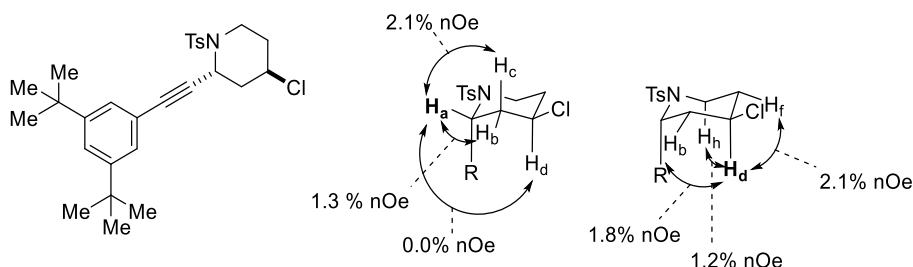
4.2 Hz, 1H), 3.88–3.82 (m, 1H), 2.96 (td,  $J = 12.5, 2.5$  Hz, 1H), 2.46 (s, 3H), 2.42–2.34 (m, 1H), 2.32 (s, 3H), 2.24 (ddd,  $J = 12.9, 4.1, 1.9$  Hz, 1H), 2.17 (td,  $J = 12.5, 4.7$  Hz, 1H), 1.98 (ddd,  $J = 25.1, 12.6, 4.8$  Hz, 1H);  $^{13}\text{C}$  NMR (125.8 MHz,  $\text{CDCl}_3$ )  $\delta$  144.0, 139.0, 134.8, 129.6 (2C), 129.5, 128.7, 128.2 (3C), 126.7, 122.4, 87.3, 83.3, 53.0, 47.4, 42.1, 41.5, 36.0, 21.6, 15.8.



**2-(benzo[*d*][1,3]dioxol-5-ylethynyl)-4-chloro-1-tosylpiperidine (2.19)** was prepared according to Method E. The following amounts of reagents were used: 3-(benzo[*d*][1,3]dioxol-5-yl)propionaldehyde (synthesized from the corresponding aryl bromide, following Methods B and D, 453 mg, 2.60 mmol, 1.50 equiv), homoallylic amine (389 mg, 1.73 mmol, 1.00 equiv),  $\text{FeCl}_3$  (422 mg, 2.60 mmol, 1.50 equiv),  $\text{BmimPF}_6$  (0.54 mL, 2.60 mmol, 1.50 equiv),  $\text{C}_6\text{H}_5\text{CF}_3$  (26 mL, 0.10 M in aldehyde). The compound was purified using flash chromatography (0–20% EtOAc/hexanes) to afford the title compound as a white solid (119 mg, 0.285 mmol, 16%, >20:1 dr trans:cis). **TLC**  $R_f = 0.45$  (20 % EtOAc/hexanes,  $\text{KMnO}_4$  stain); **m.p.** 134–136 °C;  $^1\text{H}$  NMR (500 MHz,  $\text{CDCl}_3$ )  $\delta$  7.71 (d,  $J = 8.2$  Hz, 2H), 7.24 (d,  $J = 8.1$  Hz, 2H), 6.66 (d,  $J = 8.0$  Hz, 1H), 6.53 (dd,  $J = 8.0, 1.3$  Hz, 1H), 6.33 (s, 1H), 5.96 (s, 2H), 5.10 (br s, 1H), 4.18 (tt,  $J = 12.0, 4.2, 1$  Hz), 3.88–3.81 (m, 1H), 2.95 (td,  $J = 12.5, 2.4$  Hz, 1H), 2.39–2.33 (m, 4H), 2.26–2.19 (m, 1H), 2.15 (td,  $J = 12.4, 4.7$  Hz, 1H), 1.97 (ddd,  $J = 25.1, 12.6, 4.8$  Hz, 1H);  $^{13}\text{C}$  NMR (125.8 MHz,  $\text{CDCl}_3$ )  $\delta$  148.2, 147.4, 143.9, 135.0, 129.6 (2C), 128.2 (2C), 126.3, 114.9, 111.6, 108.4, 101.5, 87.7, 81.2, 53.1, 47.4, 42.1, 41.6, 36.0, 21.5.

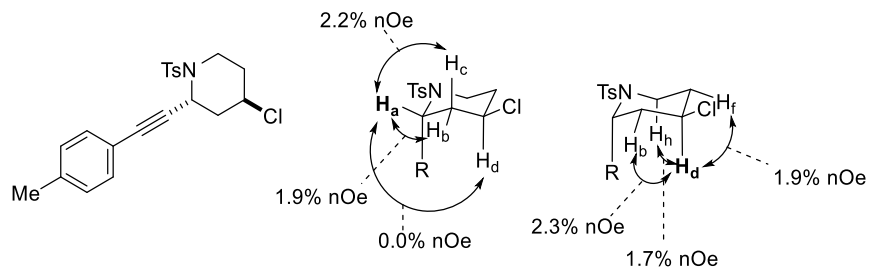


**4-chloro-2-((3,5-dimethylphenyl)ethynyl)-1-tosylpiperidine (2.20)** was prepared according to Method E. The following amounts of reagents were used: 3-(3,5-dimethylphenyl)propionaldehyde (synthesized from the corresponding aryl bromide, following Methods B and D, 400 mg, 2.53 mmol, 1.50 equiv), homoallylic amine (380 mg, 1.69 mmol, 1.00 equiv), FeCl<sub>3</sub> (410 mg, 2.53 mmol, 1.50 equiv), BmimPF<sub>6</sub> (0.52 mL, 2.5 mmol, 1.5 equiv), C<sub>6</sub>H<sub>5</sub>CF<sub>3</sub> (25 mL, 0.10 M in aldehyde). The compound was purified using flash chromatography (0–20% EtOAc/hexanes) to afford the title compound as a white solid (147 mg, 0.366 mmol, 22%, >20:1 dr trans:cis). **TLC**  $R_f$  = 0.65 (20% EtOAc/hexanes, KMNO<sub>4</sub> stain); **m.p.** 123–125 °C; **<sup>1</sup>H NMR** (400 MHz, CDCl<sub>3</sub>)  $\delta$  7.73 (d,  $J$  = 8.3 Hz, 2H), 7.25 (d,  $J$  = 8.0 Hz, 2H), 6.93 (s, 1H), 6.62 (s, 2H), 5.15–5.11 (m, 1H), 4.21 (tt,  $J$  = 12.0, 4.3 Hz, 1H), 3.88–3.80 (m, 1H), 2.98 (td,  $J$  = 12.5, 2.6 Hz, 1H), 2.42–2.35 (m, 1H), 2.33 (s, 3H), 2.28–2.21 (m, 7H), 2.17 (td,  $J$  = 12.8, 4.8 Hz, 1H), 1.98 (qd,  $J$  = 12.7, 4.8 Hz, 1H).



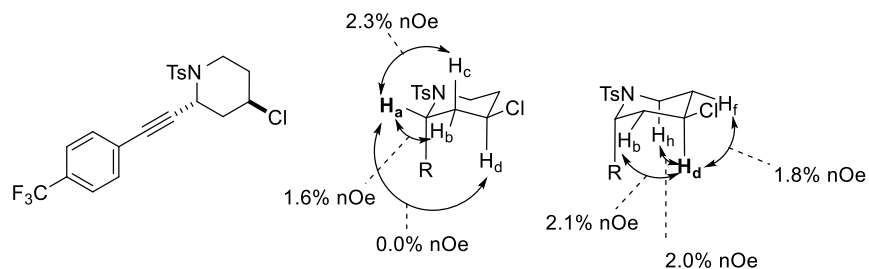
**4-chloro-2-((3,5-di-tert-butylphenyl)ethynyl)-1-tosylpiperidine (2.21)** was prepared according to Method E. The following amounts of reagents were used: 3-(3,5-di-tert-butylphenyl)propionaldehyde (synthesized from the corresponding aryl bromide, following

Methods B and D, 688 mg, 3.03 mmol, 1.50 equiv), homoallylic amine (455 mg, 2.02 mmol, 1.00 equiv), FeCl<sub>3</sub> (492 mg, 3.03 mmol, 1.50 equiv), BmimPF<sub>6</sub> (0.62 mL, 3.0 mmol, 1.5 equiv), C<sub>6</sub>H<sub>5</sub>CF<sub>3</sub> (30. mL, 0.10 M in aldehyde). The compound was purified using flash chromatography (0–20% EtOAc/hexanes) to afford the title compound as a white solid (354 mg, 0.728 mmol, 36%, >20:1 dr trans:cis). **TLC** R<sub>f</sub> = 0.68 (20% EtOAc/hexanes, KMNO<sub>4</sub> stain); **m.p.** 117–120 °C; **<sup>1</sup>H NMR** (500 MHz, CDCl<sub>3</sub>) δ 7.75 (d, *J* = 8.2 Hz, 2H), 7.36 (s, 1H), 7.21 (d, *J* = 8.0 Hz, 2H), 6.93 (s, *J* = 1.6 Hz, 2H), 5.19 (br s, 1H), 4.26 (tt, *J* = 12.0, 4.2 Hz, 1H), 3.86–3.78 (m, 1H), 3.02 (td, *J* = 12.2, 1.7 Hz, 1H), 2.45–2.38 (m, *J* = 1H), 2.28–2.21 (m, 4H), 2.17 (td, *J* = 12.4, 4.7 Hz, 1H), 1.97 (ddd, *J* = 25.1, 12.6, 4.9 Hz, 1H), 1.30 (s, 18H); **<sup>13</sup>C NMR** (125.8 MHz, CDCl<sub>3</sub>) δ 151.0 (2C), 143.7, 135.2, 129.5 (2C), 128.2 (2C), 125.7 (2C), 123.2, 121.0, 88.8, 81.6, 53.2, 47.5, 42.0, 41.8, 36.1, 34.9, 31.5 (7C), 21.6.



**4-chloro-2-(p-tolylethynyl)-1-tosylpiperidine (2.22)** was prepared according to Method E. The following amounts of reagents were used: 3-(p-tolyl)propionaldehyde (prepared from the corresponding aryl halide following Methods B and F, 518 mg, 3.59 mmol, 1.50 equiv), homoallylic amine (538 mg, 2.39 mmol, 1.00 equiv), FeCl<sub>3</sub> (582 mg, 3.59 mmol, 1.50 equiv), BmimPF<sub>6</sub> (0.74 mL, 3.59 mmol, 1.50 equiv), C<sub>6</sub>H<sub>5</sub>CF<sub>3</sub> (36 mL, 0.10 M in aldehyde). The compound was purified using flash chromatography (0–20% EtOAc/hexanes) to afford the title compound as a yellow solid (600. mg, 1.57 mmol, 66%, >20:1 dr trans:cis). **TLC** R<sub>f</sub> = 0.68 (EtOAc/hexanes, KMNO<sub>4</sub> stain); **m.p.** 109–111 °C; **<sup>1</sup>H NMR** (600 MHz, CDCl<sub>3</sub>) δ 7.70 (d, *J* =

8.3 Hz, 2H), 7.21 (d,  $J = 8.0$  Hz, 2H), 7.03 (d,  $J = 7.8$  Hz, 2H), 6.86 (d,  $J = 8.1$  Hz, 2H), 5.13–5.10 (m, 1H), 4.20 (tt,  $J = 12.0, 4.3$  Hz, 1H), 3.90–3.77 (m, 1H), 2.96 (td,  $J = 12.5, 2.6$  Hz, 1H), 2.40–2.34 (m, 1H), 2.32 (s, 3H), 2.29 (s, 3H), 2.26–2.20 (m, 1H), 2.15 (td,  $J = 12.4, 4.8$  Hz, 1H), 1.96 (ddd,  $J = 25.1, 12.7, 4.8$  Hz, 1H);  $^{13}\text{C}$  NMR (125.8 MHz,  $\text{CDCl}_3$ )  $\delta$  143.8, 138.9, 134.9, 131.5 (2C), 129.6 (2C), 129.0 (2C), 128.1 (2C), 118.7, 87.9, 82.1, 53.1, 47.4, 42.0, 41.6, 36.0, 21.6, 21.5.



**4-chloro-1-tosyl-2-((4-(trifluoromethyl)phenyl)ethynyl)piperidine (2.23)** was prepared according to Method E. The following amounts of reagents were used: 3-(4-(trifluoromethyl)phenyl)propiolaldehyde (synthesized from the corresponding aryl halide following Methods B and D, 522 mg, 2.63 mmol, 1.50 equiv), homoallylic amine (394 mg, 1.75 mmol, 1.00 equiv),  $\text{FeCl}_3$  (427 mg, 2.63 mmol, 1.50 equiv),  $\text{BmimPF}_6$  (0.54 mL, 2.62 mmol, 1.50 equiv),  $\text{C}_6\text{H}_5\text{CF}_3$  (26 mL, 0.10 M in aldehyde). The compound was purified using flash chromatography (0–20% EtOAc/hexanes) to afford the title compound as an orange solid (310 mg, 0.702 mmol, 40%, >20:1 dr trans:cis). **TLC**  $R_f = 0.46$  (EtOAc/hexanes,  $\text{KMnO}_4$  stain); **m.p.** 73–75 °C;  $^1\text{H}$  NMR (600 MHz,  $\text{CDCl}_3$ )  $\delta$  7.71 (d,  $J = 8.3$  Hz, 2H), 7.49 (d,  $J = 8.1$  Hz, 2H), 7.21 (d,  $J = 8.0$  Hz, 2H), 7.08 (d,  $J = 8.0$  Hz, 2H), 5.15 (br s, 1H), 4.16 (tt,  $J = 12.0, 4.2$  Hz, 1H), 3.90–3.85 (m, 1H), 2.96 (td,  $J = 12.5, 2.6$  Hz, 1H), 2.41–2.36 (m, 1H), 2.30–2.22 (m, 4H), 2.18 (td,  $J = 12.5, 4.8$  Hz, 1H), 1.98 (ddd,  $J = 25.1, 12.7, 4.8$  Hz, 1H);  $^{13}\text{C}$  NMR (125.8 MHz,  $\text{CDCl}_3$ )  $\delta$  143.9, 134.9, 131.9 (2C), 129.6 (4C), 128.2 (4C), 125.2 (q,  $J = 3.7$  Hz), 86.3, 85.6, 52.8, 47.3, 42.2, 41.3, 35.9, 21.5;  $^{19}\text{F}$  NMR (564.7 MHz,  $\text{CDCl}_3$ )  $\delta$  –62.9 (3F).

## 2.5 References

- (1) Everson, D. A.; Weix, D. J. Cross-Electrophile Coupling: Principles of Reactivity and Selectivity. *The Journal of Organic Chemistry* **2014**, *79* (11), 4793-4798. DOI: 10.1021/jo500507s.
- (2) Chen, P.-P.; Lucas, E. L.; Greene, M. A.; Zhang, S.-Q.; Tollefson, E. J.; Erickson, L. W.; Taylor, B. L. H.; Jarvo, E. R.; Hong, X. A Unified Explanation for Chemoselectivity and Stereospecificity of Ni-Catalyzed Kumada and Cross-Electrophile Coupling Reactions of Benzylic Ethers: A Combined Computational and Experimental Study. *Journal of the American Chemical Society* **2019**, *141* (14), 5835-5855. DOI: 10.1021/jacs.9b00097.
- (3) Cherney, A. H.; Kadunce, N. T.; Reisman, S. E. Enantioselective and Enantiospecific Transition-Metal-Catalyzed Cross-Coupling Reactions of Organometallic Reagents To Construct C–C Bonds. *Chemical Reviews* **2015**, *115* (17), 9587-9652. DOI: 10.1021/acs.chemrev.5b00162.
- (4) Diccianni, J. B.; Diao, T. Mechanisms of Nickel-Catalyzed Cross-Coupling Reactions. *Trends in Chemistry* **2019**, *1* (9), 830-844. DOI: <https://doi.org/10.1016/j.trechm.2019.08.004>.
- (5) Lucas, E. L.; Jarvo, E. R. Stereospecific and stereoconvergent cross-couplings between alkyl electrophiles. *Nature Reviews Chemistry* **2017**, *1* (9), 0065. DOI: 10.1038/s41570-017-0065.
- (6) *Modern Organonickel Chemistry*; Wiley-VCH, 2005.
- (7) DeLano, T. J.; Reisman, S. E. Enantioselective Electroreductive Coupling of Alkenyl and Benzyl Halides via Nickel Catalysis. *ACS Catalysis* **2019**, *9* (8), 6751-6754. DOI: 10.1021/acscatal.9b01785.
- (8) Rosen, B. M.; Quasdorf, K. W.; Wilson, D. A.; Zhang, N.; Resmerita, A.-M.; Garg, N. K.; Percec, V. Nickel-Catalyzed Cross-Couplings Involving Carbon–Oxygen Bonds. *Chemical Reviews* **2011**, *111* (3), 1346-1416. DOI: 10.1021/cr100259t.

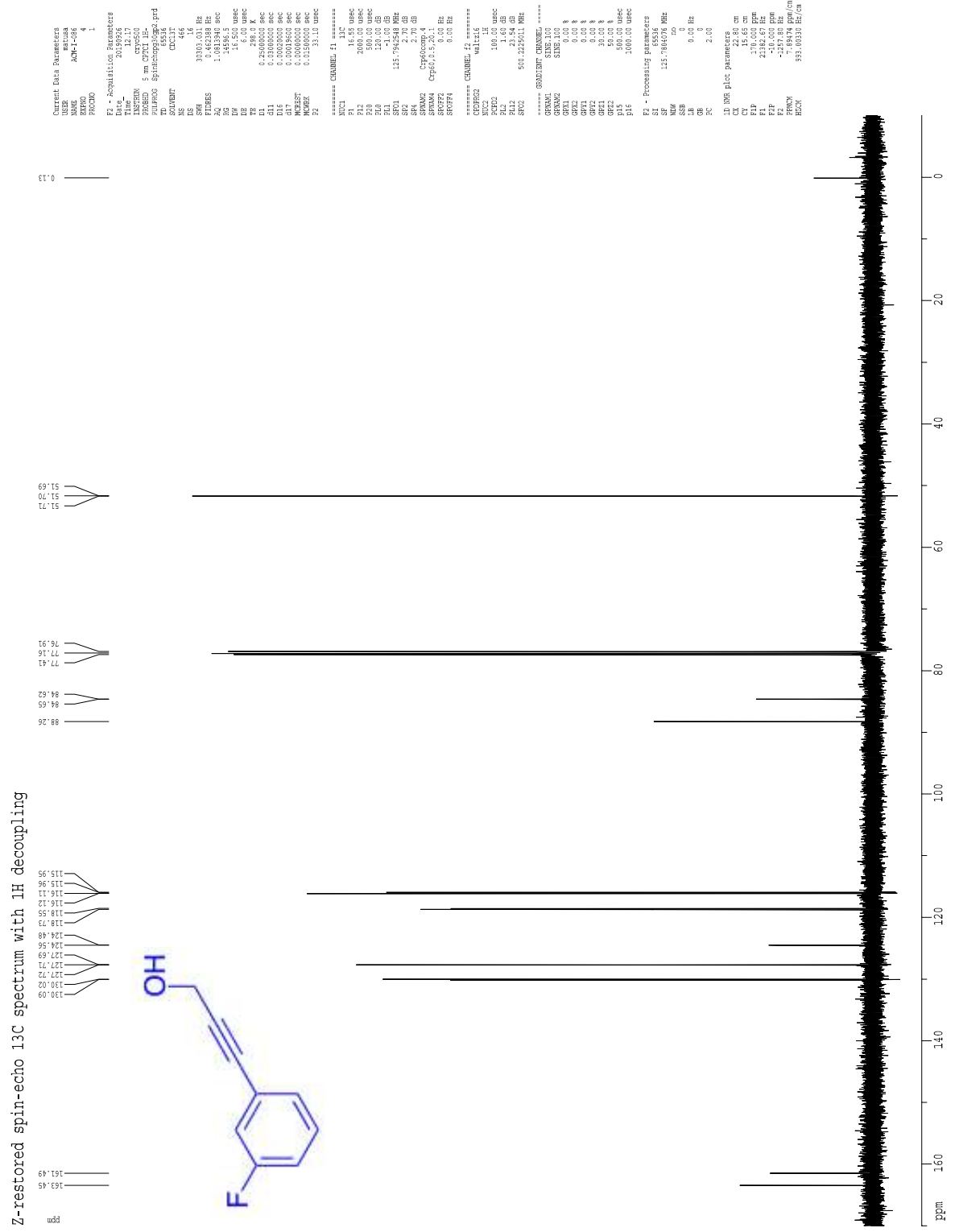
- (9) Baker, K. M.; Lucas Baca, D.; Plunkett, S.; Daneker, M. E.; Watson, M. P. Engaging Alkenes and Alkynes in Deaminative Alkyl–Alkyl and Alkyl–Vinyl Cross-Couplings of Alkylpyridinium Salts. *Organic Letters* **2019**, *21* (23), 9738-9741. DOI: 10.1021/acs.orglett.9b03899.
- (10) Ni, S.; Li, C.-X.; Mao, Y.; Han, J.; Wang, Y.; Yan, H.; Pan, Y. Ni-catalyzed deaminative cross-electrophile coupling of Katritzky salts with halides via C–N bond activation. *Science Advances* **2019**, *5* (6), eaaw9516. DOI: doi:10.1126/sciadv.aaw9516.
- (11) Kuang, Y.; Wang, X.; Anthony, D.; Diao, T. Ni-catalyzed two-component reductive dicarbofunctionalization of alkenes via radical cyclization. *Chemical Communications* **2018**, *54* (20), 2558-2561, 10.1039/C8CC00358K. DOI: 10.1039/C8CC00358K.
- (12) Shu, W.; García-Domínguez, A.; Quirós, M. T.; Mondal, R.; Cárdenas, D. J.; Nevado, C. Ni-Catalyzed Reductive Dicarbofunctionalization of Nonactivated Alkenes: Scope and Mechanistic Insights. *Journal of the American Chemical Society* **2019**, *141* (35), 13812-13821. DOI: 10.1021/jacs.9b02973.
- (13) Tu, H.-Y.; Wang, F.; Huo, L.; Li, Y.; Zhu, S.; Zhao, X.; Li, H.; Qing, F.-L.; Chu, L. Enantioselective Three-Component Fluoroalkylarylation of Unactivated Olefins through Nickel-Catalyzed Cross-Electrophile Coupling. *Journal of the American Chemical Society* **2020**, *142* (21), 9604-9611. DOI: 10.1021/jacs.0c03708.
- (14) Hewitt, K. A.; Xie, P.-P.; Thane, T. A.; Hirbawi, N.; Zhang, S.-Q.; Matus, A. C.; Lucas, E. L.; Hong, X.; Jarvo, E. R. Nickel-Catalyzed Domino Cross-Electrophile Coupling Dicarbofunctionalization Reaction To Afford Vinylcyclopropanes. *ACS Catalysis* **2021**, *11* (23), 14369-14380. DOI: 10.1021/acscatal.1c04235.

- (15) Pangborn, A. B.; Giardello, M. A.; Grubbs, R. H.; Rosen, R. K.; Timmers, F. J. Safe and Convenient Procedure for Solvent Purification. *Organometallics* **1996**, *15* (5), 1518-1520. DOI: 10.1021/om9503712.
- (16) Standley, E. A.; Smith, S. J.; Müller, P.; Jamison, T. F. A Broadly Applicable Strategy for Entry into Homogeneous Nickel(0) Catalysts from Air-Stable Nickel(II) Complexes. *Organometallics* **2014**, *33* (8), 2012-2018. DOI: 10.1021/om500156q.
- (17) Krasovskiy, A.; Knochel, P. Convenient Titration Method for Organometallic Zinc, Magnesium, and Lanthanide- Reagents. *Synthesis* **2006**, *2006* (05), 0890-0891. DOI: 10.1055/s-2006-926345.
- (18) Sakata, Y.; Yasui, E.; Mizukami, M.; Nagumo, S. Cascade reaction including a formal [5 + 2] cycloaddition by use of alkyne-Co<sub>2</sub>(CO)<sub>6</sub> complex. *Tetrahedron Letters* **2019**, *60* (11), 755-759. DOI: <https://doi.org/10.1016/j.tetlet.2019.01.045>.
- (19) Xu, B.; Gartman, J. A.; Tambar, U. K. Copper-catalyzed [1,2]-rearrangements of allylic iodides and aryl  $\alpha$ -diazoacetates. *Tetrahedron* **2017**, *73* (29), 4150-4159. DOI: <https://doi.org/10.1016/j.tet.2017.01.048>.
- (20) Huang, J.; Zheng, J.; Wu, W.; Li, J.; Ma, Z.; Ren, Y.; Jiang, H. Palladium-Catalyzed Intermolecular Oxidative Cyclization of Allyltosylamides with AcOH: Assembly of 3-Pyrrolin-2-ones. *The Journal of Organic Chemistry* **2017**, *82* (15), 8191-8198. DOI: 10.1021/acs.joc.7b00804.
- (21) Osawa, C. T., M.; Miura, K.; Tayama, E.; Iwamoto, H.; Hasegawa, E. An Effective Procedure to Promote Aza-Prins Cyclization Reactions Employing a Combination of Ferric Chloride and an Imidazolium Salt in Benzotrifluoride. *Heterocycles* **2012**, *86* (2), 1211. DOI: 10.3987/COM-12-S(N)78.

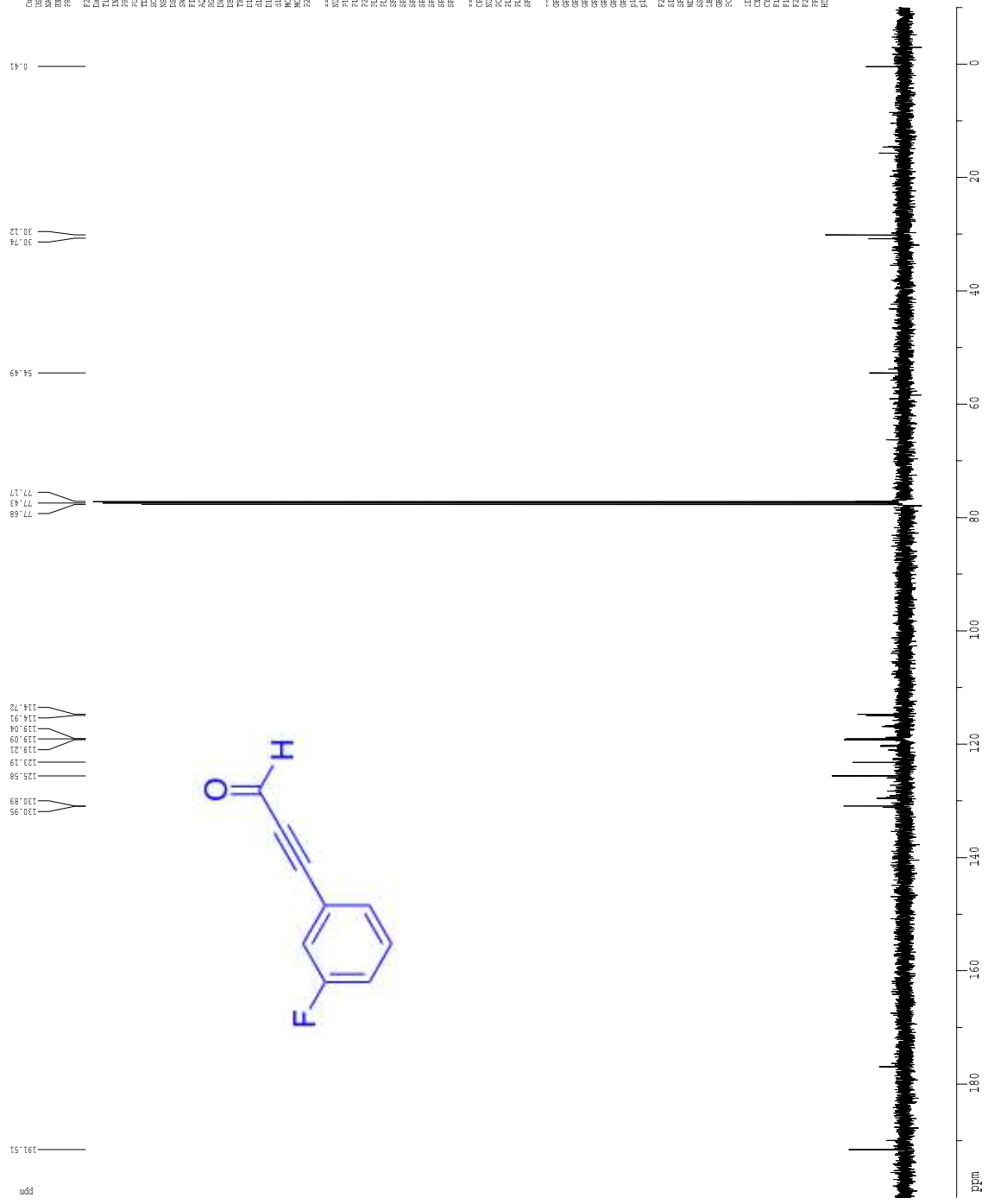
- (22) Dell'Isola, A.; McLachlan, M. M. W.; Neuman, B. W.; Al-Mullah, H. M. N.; Binks, A. W. D.; Elvidge, W.; Shankland, K.; Cobb, A. J. A. Synthesis and Antiviral Properties of Spirocyclic [1,2,3]-Triazolooxazine Nucleosides. *Chemistry – A European Journal* **2014**, *20* (37), 11685-11689. DOI: <https://doi.org/10.1002/chem.201403560>.
- (23) Gambouz, K.; Driowya, M.; Loubidi, M.; Tber, Z.; Allouchi, H.; El Kazzouli, S.; Akssira, M.; Guillaumet, G. Unusual rearrangement of imidazo[1,5-a]imidazoles and imidazo[1,2-b]pyrazoles into imidazo[1,5-a]pyrimidines and pyrazolo[1,5-a]pyrimidines. *RSC Advances* **2019**, *9* (50), 29051-29055, 10.1039/C9RA04609G. DOI: 10.1039/C9RA04609G.
- (24) Chen, C.; Huang, Y.; Zhang, Z.; Dong, X.-Q.; Zhang, X. Cobalt-catalyzed (Z)-selective semihydrogenation of alkynes with molecular hydrogen. *Chemical Communications* **2017**, *53* (33), 4612-4615, 10.1039/C7CC01228D. DOI: 10.1039/C7CC01228D.
- (25) Xu, Y.; Wang, Q.; Wu, Y.; Zeng, Z.; Rudolph, M.; Hashmi, A. S. K. Gold-Catalyzed Synthesis of 2,5-Disubstituted Oxazoles from Carboxamides and Propynals. *Advanced Synthesis & Catalysis* **2019**, *361* (10), 2309-2314. DOI: <https://doi.org/10.1002/adsc.201801386>.



## 2.6 <sup>1</sup>H, <sup>13</sup>C, <sup>19</sup>F, and COSY NMR Spectra



Z-restored spin-echo 13C spectrum with 1H decoupling

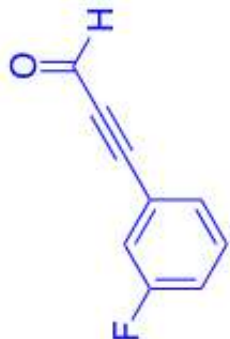
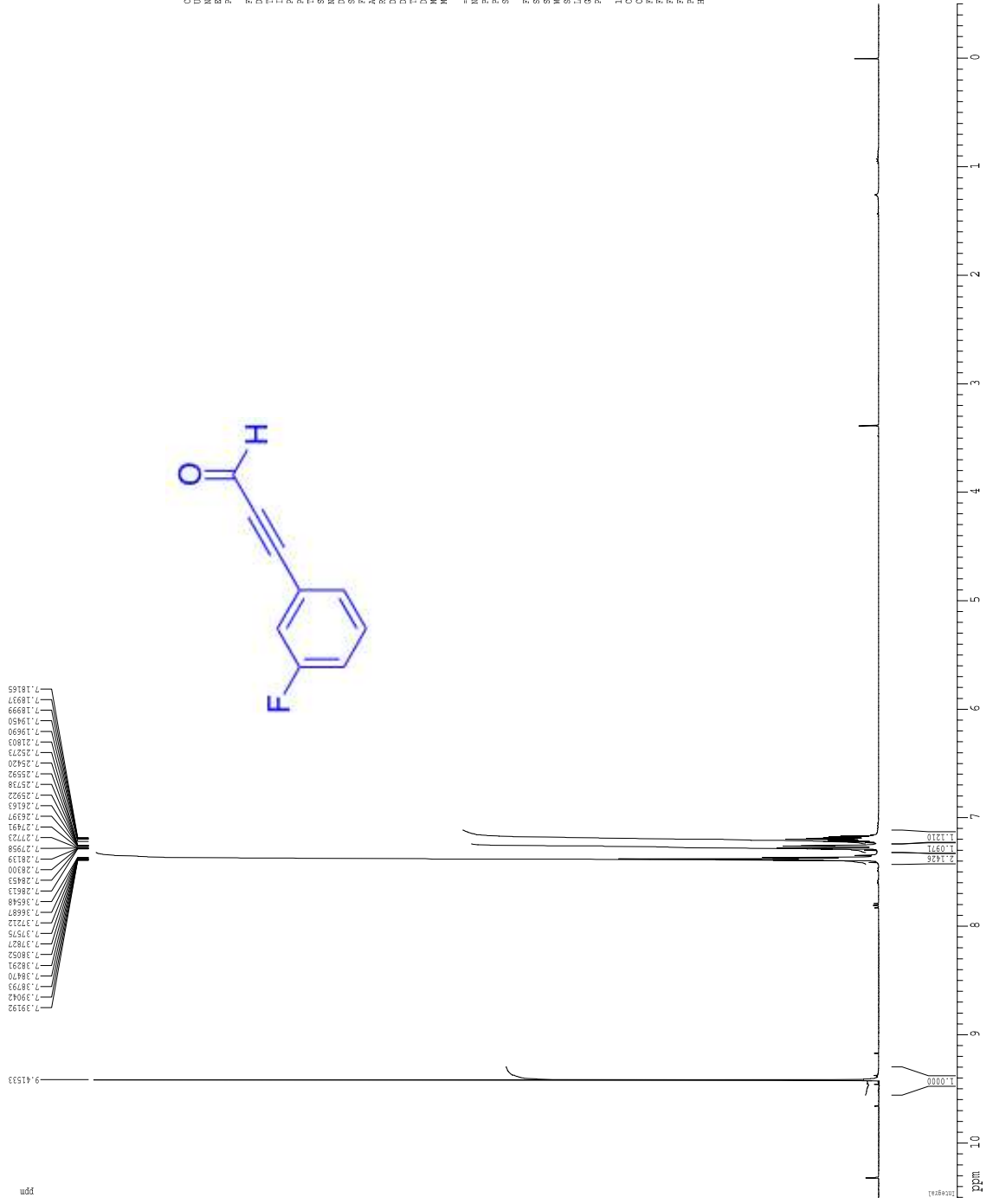


1H spectrum



Current Data Parameters  
 Date\_ 20131002  
 Time 5.16  
 NAME AHC-4-088  
 EXTEN 1  
 PROCNO 1  
 F2 - Acquisition Parameters  
 Date\_ 20131002  
 Time 5.16  
 INSTRUM 4ht  
 PROGNO 5 mm QNP H1/F1P  
 PULPROG zgpg30  
 ACQPROG zgpg30  
 CHANNEL1 C13H138  
 NS 8  
 DS 2  
 SS 6413.656 Hz  
 SFREQ 125.761 MHz  
 AQ FIDRESS 5.11148719 sec  
 RG 11.4  
 SE 78.000 usec  
 TE 298.0 K  
 D1 0.10000000 sec  
 DELTAD 0.00000000 sec  
 WALTZ16 0.13500000 sec  
 WALTZ17 0.13500000 sec  
 ===== CHANNEL F1 =====  
 P1 12.00 usec  
 PL1 -1.10 dB  
 SF01 400.1328009 MHz  
 F2 - Processing parameters  
 S1 645136  
 SF 400.1301199 MHz  
 DS 0  
 SS 0  
 TE 0.00 Hz  
 SE 0  
 SF 2.00  
 ID NMR plot parameters  
 CC 12.00 cm  
 CT 12.00 cm  
 F1P 8.500 ppm  
 F1 340.110 Hz  
 F2P 20.500 ppm  
 F2 -20.500 ppm  
 FREQCN 0.339474 ppm/cm  
 HZCN 157.84606 Hz/cm

1H spectrum



Current Data Parameters  
 NAME: 4FC-10193Y  
 EXTEN: 1  
 PROCNO: 1

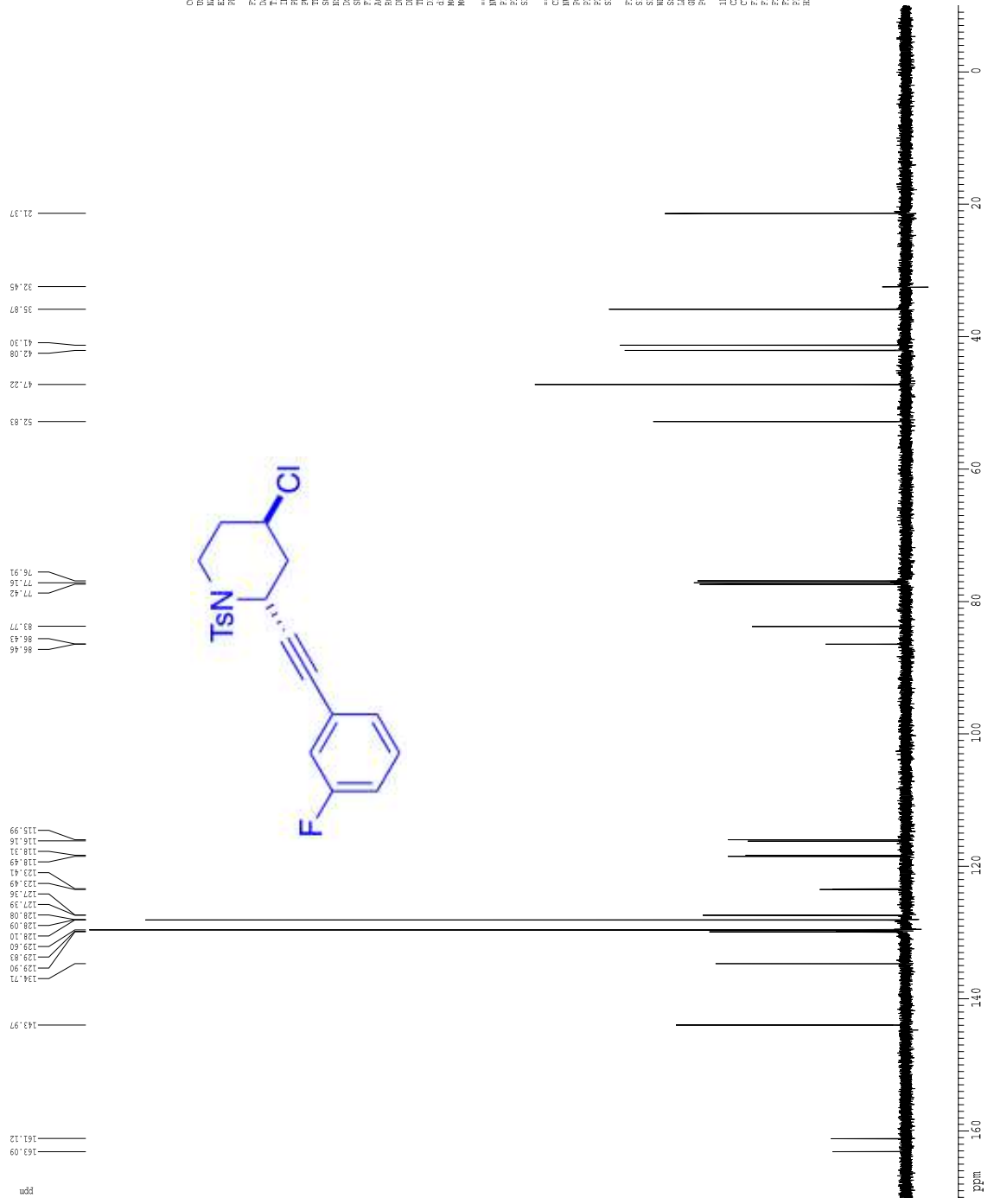
F2 - Acquisition Parameters  
 Date\_: 20131007  
 Time: 8.47  
 OPER: dm  
 PROBN: 5 mm QNP H1/P  
 PULPROG: zgpg30  
 F2 - Processing parameters  
 SF: 400.130055 MHz  
 SI: 65536  
 DS: 2  
 AS: 8  
 SS: 0  
 IS: 0  
 OS: 0  
 PS: 0  
 PC: 0

===== CHANNEL f1 =====  
 NU1: 12.00 MHz  
 F1: 400.130055 MHz  
 SF01: 400.130009 MHz

F2 - Processing parameters  
 SF: 400.130055 MHz  
 SI: 65536  
 DS: 2  
 AS: 8  
 SS: 0  
 IS: 0  
 OS: 0  
 PS: 0  
 PC: 0

ID: NMR plot parameters  
 CT: 12.00 cm  
 FID: 1  
 F2P: 10.500 PPM  
 F1: 420.137 Hz  
 F2: 10.500 PPM  
 F2: 420.137 Hz  
 FREQC: 0.482416 PPM/cm  
 HZCM: 193.84518 Hz/cm

13C spectrum with 1H decoupling



Current Data Parameters  
 Name: 2005-1-18-2-13C  
 NAME: 2005-1-18-2-13C  
 EXPNO: 1  
 PROCNO: 1

F2 - Acquisition Parameters  
 Date\_: 20131012  
 Time: 13.28  
 CONTC: 0  
 PROCNO: 1  
 PULPROG: zgpg30  
 5 mm broad  
 TD: 65536  
 SFO1: 125.760343 MHz  
 CQ1: 13.2000000  
 DS: 4  
 SFO2: 30300.031 Hz  
 SFO3: 0.482388 Hz  
 FIDRES: 1.07922880  
 SF: 5792.5  
 IN: 16.500 uSsec  
 DE: 4.750 uSsec  
 BE: 0.25000000 sec  
 DT: 0.03000000 sec  
 d11: 0.03000000 sec  
 ACQRES: 0.03000000 sec  
 FWHM: 0.03000000 sec

\*\*\*\*\* CHANNEL f1 \*\*\*\*\*  
 NUCL1: 13C  
 P1: 12.00 uSsec  
 PL1: -6.00 dB  
 SFO1: 125.760343 MHz

\*\*\*\*\* CHANNEL f2 \*\*\*\*\*  
 CEPRP2: wa1z15  
 NUCL2: 1H  
 P2P2: 80.00 uSsec  
 PL2: 19.00 dB  
 PL12: 13.20 dB  
 SFO2: 498.852443 MHz

F2 - Processing parameters  
 SI: 32768  
 SF: 125.4335256 MHz  
 FIDRES: 0.00 Hz  
 SFO: 0.00 Hz  
 DS: 0  
 DE: 2.00

1D NMR plot parameters  
 CX: 22.80 cm  
 CT: 15.65 cm  
 C1: 233.00 ppm  
 C2: 150.00 ppm  
 F2P: -16.000 ppm  
 F2: -1284.36 Hz  
 FWHM: 89474 ppm/cm  
 RESOL: 930.26972 Hz/cm



gcoosy60

```

Current Data Parameters
USER          natasa
NAME         ADM-1-095-01
EXPNO        2
PROCNO       1

F2 - Acquisition Parameters
Date_        20191015
Time         18.04
INSTRUM     CPY6500
PROBHD     5 mm QNP1H/1
PULPROG     zgpg30
TD          65536
SOLVENT     CDCl3
NS          1
DS          16
SFO1        446.400 Hz
F2          446.400 Hz
RG          0.2277876 sec
AQ          35.9
DM          111.200 usec
DE          6.00 usec
TE          298.3 K
D1          0.0000300 sec
d11         0.0000300 sec
d12         0.0000300 sec
d13         0.0000300 sec
d14         0.0002000 sec
d15         0.0002000 sec
d16         0.0002244 sec
IN0         0.0002244 sec

***** CHANNEL f1 *****
NUC1        13C
P1          1.50 usec
PL1         1.60 dB
SFO1        500.222009 MHz

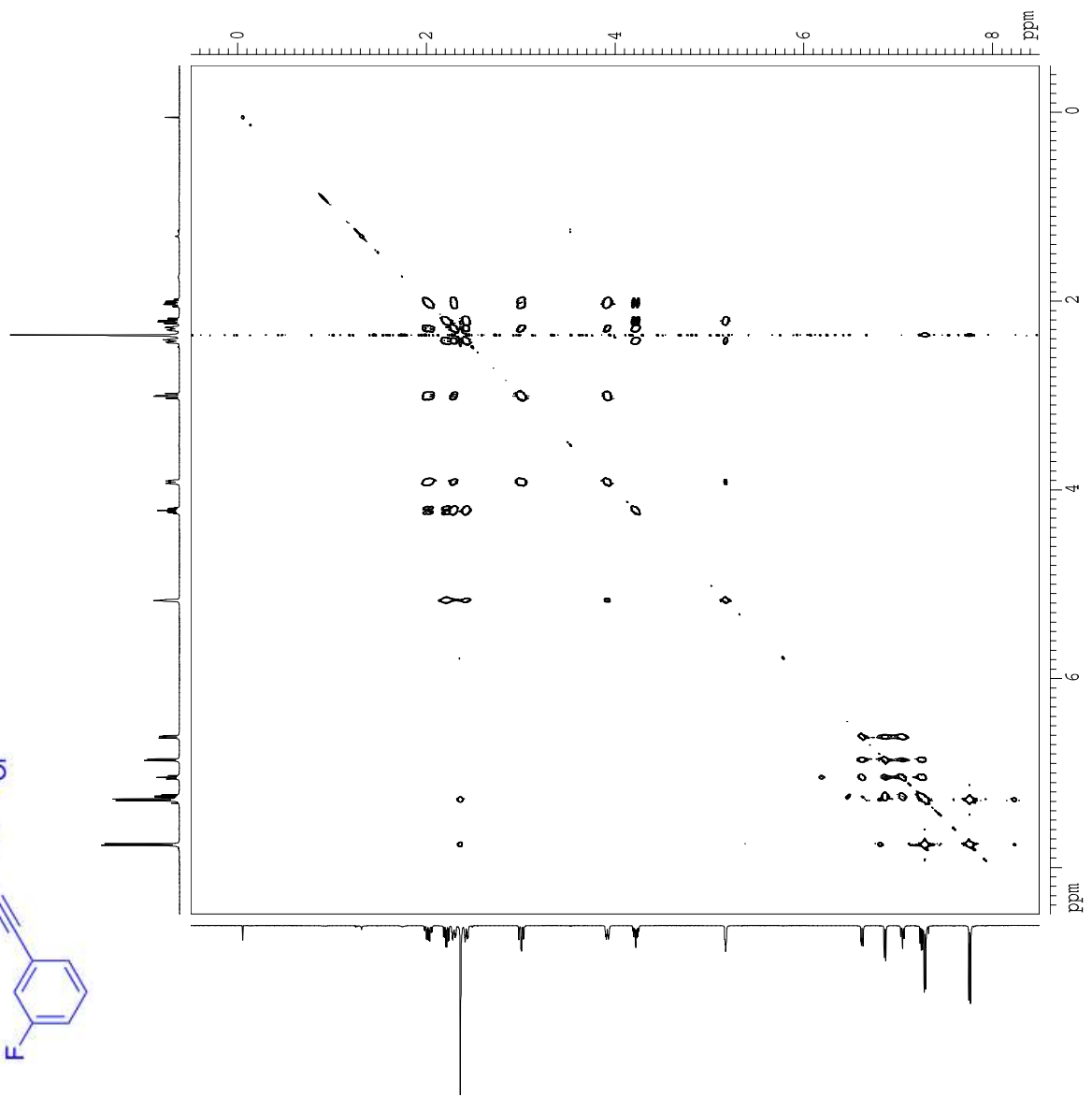
***** GRADIENT CHANNEL *****
GPM1        sine-100
GPM2        sine-100
GAX1        0.00 %
GAX2        0.00 %
GXY1        0.00 %
GXY2        0.00 %
GZL1        17.00 %
GZL2        17.00 %
P16         1000.00 usec

F1 - Acquisition parameters
ND0         1
TD          512
SFO1        500.222 MHz
FIDRES     8.784037 Hz
SI          32768
SOLVENT    CDCl3
PROCNO     01

F2 - Processing parameters
SI          1024
SF          500.220000 MHz
SFO1        500.220000 MHz
SOLVENT    CDCl3
LB          0.00 Hz
GB          0
PC          1.00

F1 - Processing parameters
SI          1024
SF          500.220000 MHz
SFO1        500.220000 MHz
SOLVENT    CDCl3
LB          0.00 Hz
GB          0

2D NMR plot parameters
CX1         15.00 cm
CX2         15.00 cm
F2F1O      8.494 ppm
F2F1LO     4245.08 Hz
F2F1HI     -0.494 ppm
F2F1LO     -447.32 Hz
F2F1HI     4245.08 Hz
F1F1O      -0.494 ppm
F1F1LO     -247.32 Hz
F1F1HI     4245.08 Hz
F2F1PCON  0.58826 ppm/cm
F2F1LOCON 299.76019 Hz/cm
F2F1HICON 0.58826 ppm/cm
F1F1PCON  299.76019 Hz/cm
F1F1LOCON 0.58826 ppm/cm
F1F1HICON 299.76019 Hz/cm
  
```



19F spectrum with inverse gated 1H decoupling



Current Data Parameters  
NAME: 6195.0  
EXTRO: ACQ-F-6195.0 2  
PROCNO: 1

F2 - Acquisition Parameters  
Date\_: 20131029  
Time: 11:24  
INSTRUM: spect  
PROBHD: 5 mm CPBBO BB-  
PULPROG: zgpg30p10.2  
PCYCL1: 131072  
CQ1VENT: 0  
NS: 16  
DS: 4  
SFO: 176.671622 Hz  
SF: 176.671622 Hz  
AQ: 0.38795116 sec  
RG: 456  
SWH: 7.800 MHz  
FIDRES: 2.9916 Hz  
TE: 300.2 K  
D1: 3.00000000 sec  
D11: 0.05000000 sec  
D12: 0.05000000 sec  
D13: 0.05000000 sec  
TD0: 1

\*\*\*\*\* CHANNEL f1 \*\*\*\*\*  
SFO1: 554.61481915 MHz  
NUC1: 19F  
P1: 17.50 usec

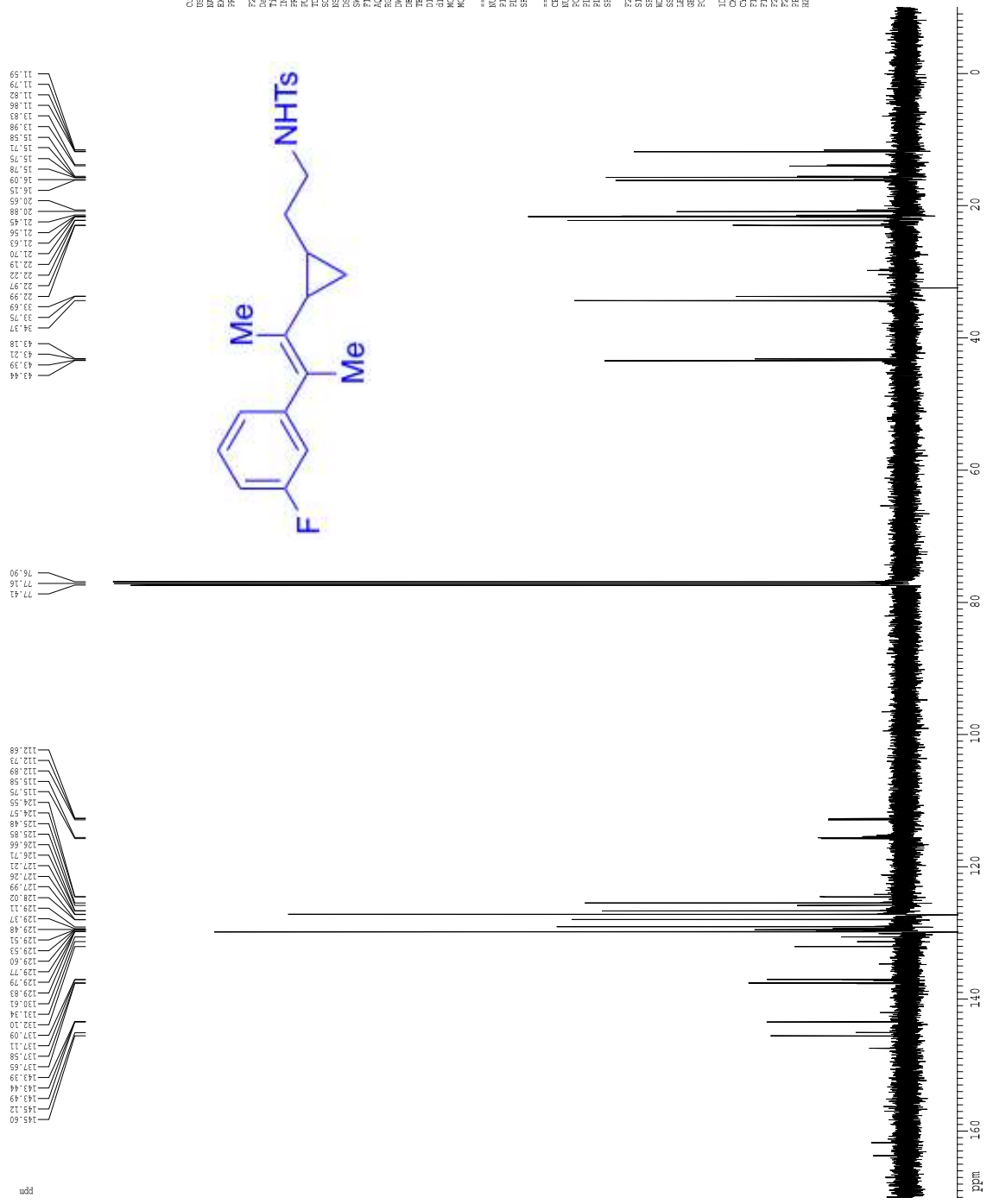
F2 - Processing parameters  
SI: 131072  
SF: 554.61481915 MHz  
WDW: 0  
SSB: 0  
GB: 0  
PC: 1.00

ID: NMR plot parameters  
CT: 12.00 cm  
SI: 1  
F1P: -110.000 PPM  
F1: -62115.50 Hz  
F2P: -4431.00 PPM  
F2: -22155.00 Hz  
FREQC: 0.221930 PPM/cm  
HZCM: 123.63474 Hz/cm



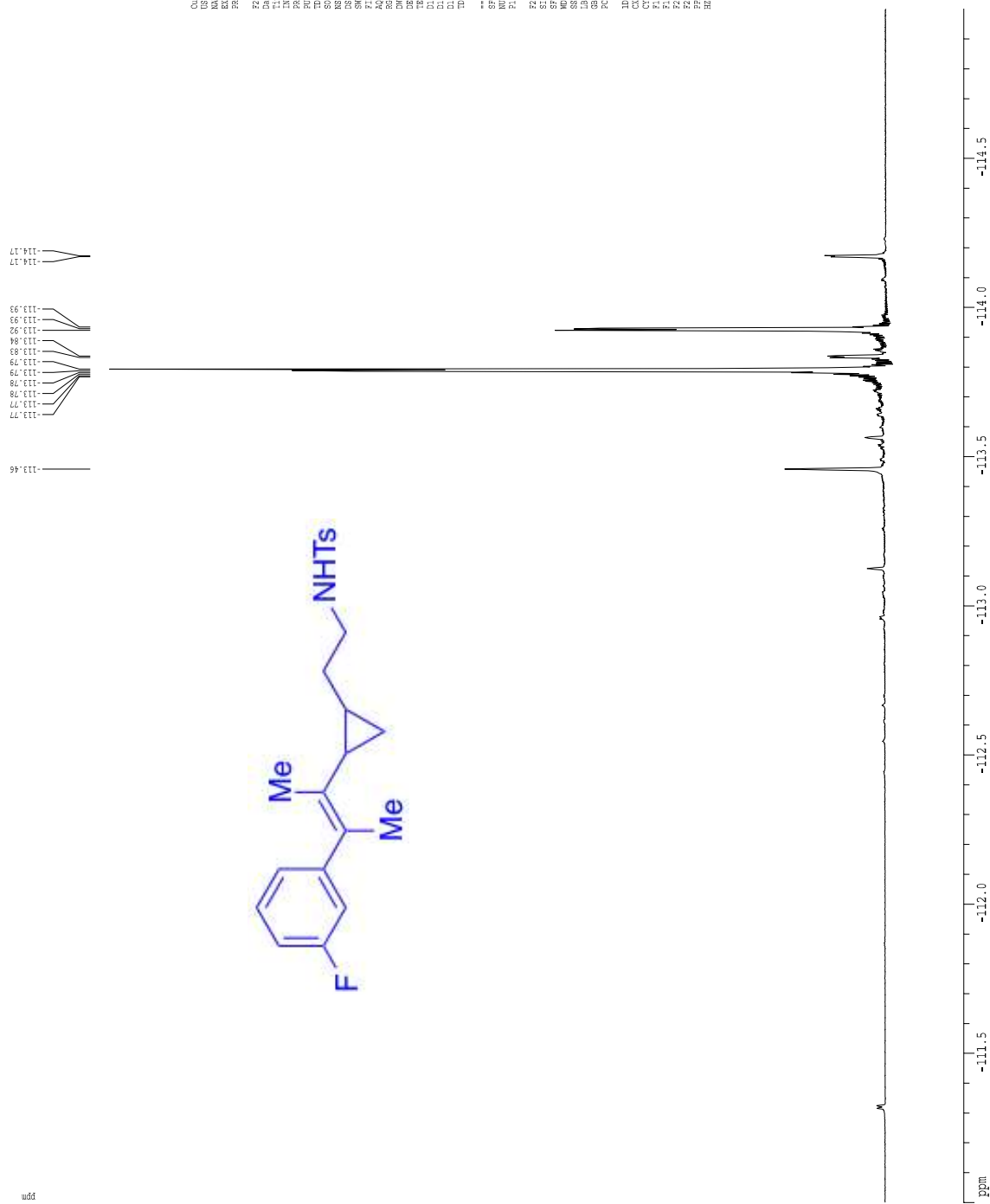


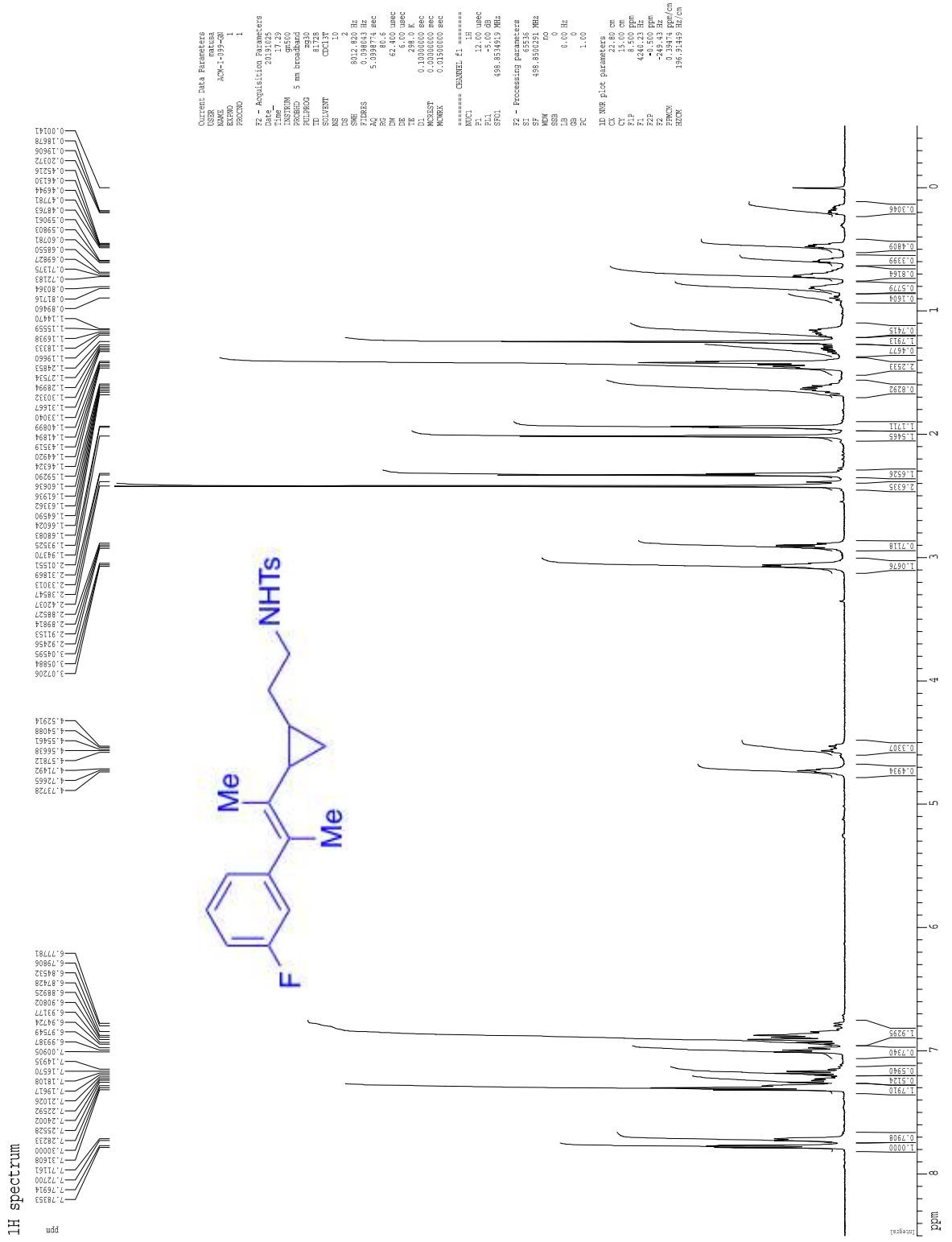
13C spectrum with 1H decoupling



Current Data Parameters  
 INSTRUM spect  
 NAME ACN-1-01P-201  
 EXPRNO 2  
 PROCNO 1  
 F2 - Acquisition Parameters  
 Date\_ 20191005  
 Time 17:45  
 CONV 90.00  
 PULPROG zgpg30  
 PRGNAME 5 mm broad  
 TD 65536  
 ID 65536  
 SOLVENT ACN-D3  
 NS 4  
 DS 4  
 SFR 30300.031 Hz  
 L1 0.42388 Hz  
 FIDRES 1.79225 Hz  
 IN 16.500 MHz  
 DE 4.500 MHz  
 BE 0.25000000 sec  
 DT 0.1  
 GC 0.03000000 sec  
 ACQST 0.03000000 sec  
 PCMR 0.03000000 sec  
 \*\*\*\*\* CHANNEL f1 \*\*\*\*\*  
 NUCL 13C  
 P1 13.00 Hz  
 PL 16.00 dB  
 SFO1 125.447100 MHz  
 \*\*\*\*\* CHANNEL f0 \*\*\*\*\*  
 CEPRP22 waltz16  
 NUCL2 1H  
 P2P22 80.00 MHz  
 PL2 19.00 dB  
 PL12 13.20 dB  
 SFO2 498.8524943 MHz  
 F2 - Processing parameters  
 SI 65536  
 SF 125.4335240 MHz  
 RG 65536  
 DE 0.00 Hz  
 AS 0  
 BS 0  
 FC 2.00  
 D0 NMR plot parameters  
 CX 22.80 cm  
 CT 15.65 cm  
 C1 13.00 Hz  
 C2 13.00 Hz  
 F2 16.000 ppm  
 F4 -1254.36 Hz  
 FREQ 89474.8771/cm  
 WVA 930.26970 Hz/cm

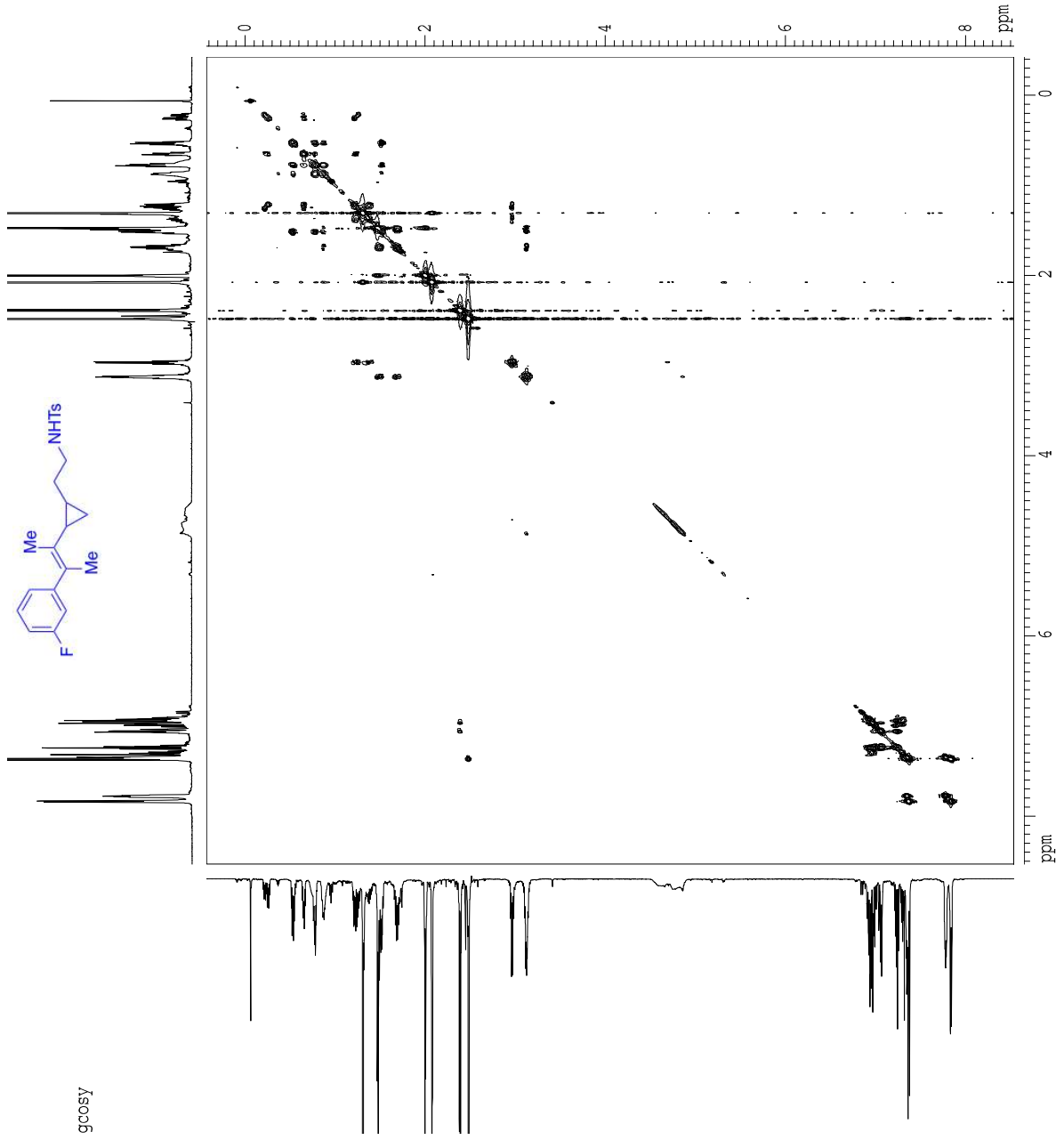
<sup>19</sup>F spectrum with inverse gated <sup>1</sup>H decoupling







gc05y



Current Data Parameters  
 USHR matusa  
 NAME ACM-I-019-coey  
 EXPRNO 4  
 PROCNO 1

F2 - Acquisition Parameters

Date\_ 20191104  
 Time 18.53  
 INSTRUM av600  
 PROBHD 5 mm CPBBO BB-  
 PULPROG cosyzgpgf  
 TD 2048  
 SOLVENT CDCl3T  
 NS 1  
 DS 16  
 SWH 5376.344 Hz  
 FIDRES 2.625168 Hz  
 AQ 0.1951140 sec  
 RG 114  
 SR 93.000 usec  
 DR 8.000 usec  
 DE 208.000 usec  
 TE 303.2 K  
 TD 0.0000000 sec  
 D1 1.48869198 sec  
 D13 0.0000000 sec  
 D16 0.0002000 sec  
 INO 0.00018600 sec

\*\*\*\*\* CHANNEL f1 \*\*\*\*\*

SFO1 600.1324335 MHz  
 NUC1 1H  
 P0 12.00 usec  
 PL 12.00 usec

F1 - Acquisition parameters

ND0 1  
 TD 256  
 SFO1 600.1324 MHz  
 FIDRES 21.001345 Hz  
 SW 8.959 ppm  
 FWHMDE QF

F2 - Processing parameters

SI 1024  
 SF 600.1300000 MHz  
 WDW SINE  
 SSB 0  
 LB 0.00 Hz  
 GB 0  
 PC 1.40

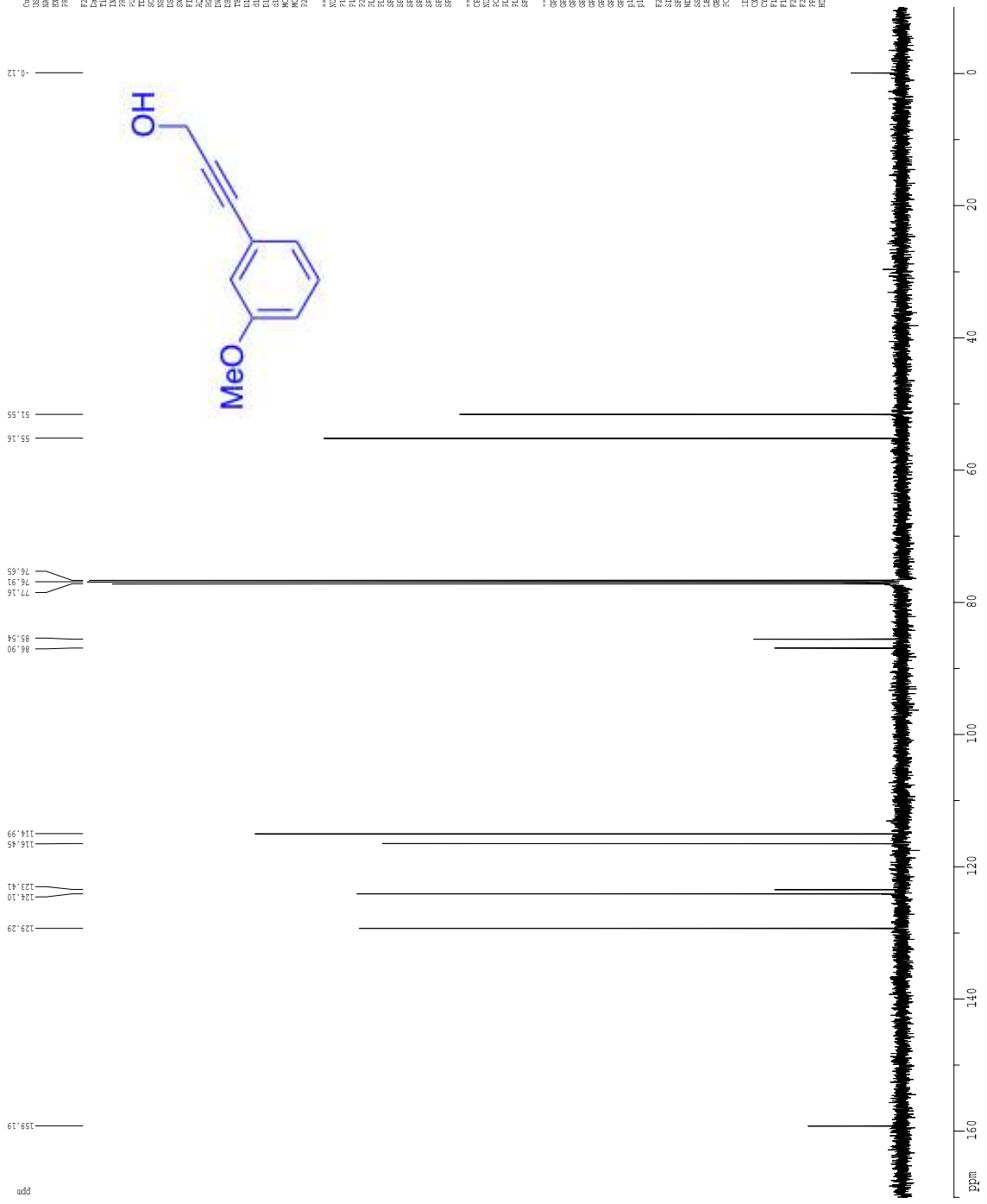
F1 - Processing parameters

SI 1024  
 SF 600.1300000 MHz  
 WDW SINE  
 SSB 0  
 LB 0.00 Hz  
 GB 0

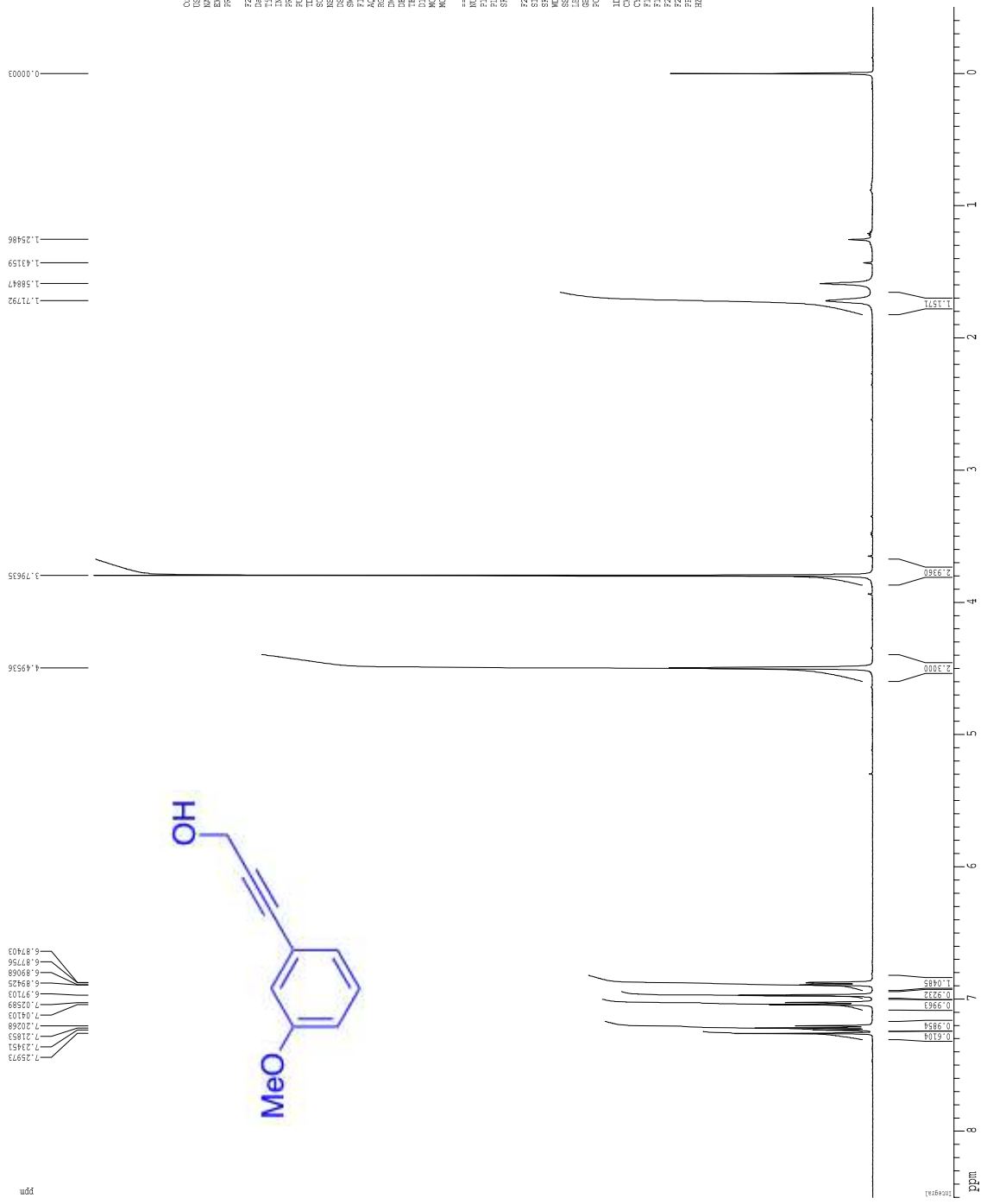
2D NMR plot parameters

CX2 15.00 cm  
 CX1 15.00 cm  
 F2FLO 8.534 ppm  
 F2LO 5121.70 Hz  
 F2FHI -0.424 ppm  
 F2HI -254.65 Hz  
 F1FLO 8.534 ppm  
 F1LO 5121.70 Hz  
 F1FHI -0.424 ppm  
 F1HI -254.65 Hz  
 F2FPMCM 0.559724 ppm/cm  
 F2HCM 358.442294 Hz/cm  
 F1FPMCM 0.559724 ppm/cm  
 F1HCM 358.442294 Hz/cm

Z-restored spin-echo 13C spectrum with 1H decoupling



1H spectrum



Current Data Parameters  
 NAME: NMF-111-CH-2  
 EXTEN: 1  
 PROCNO: 1

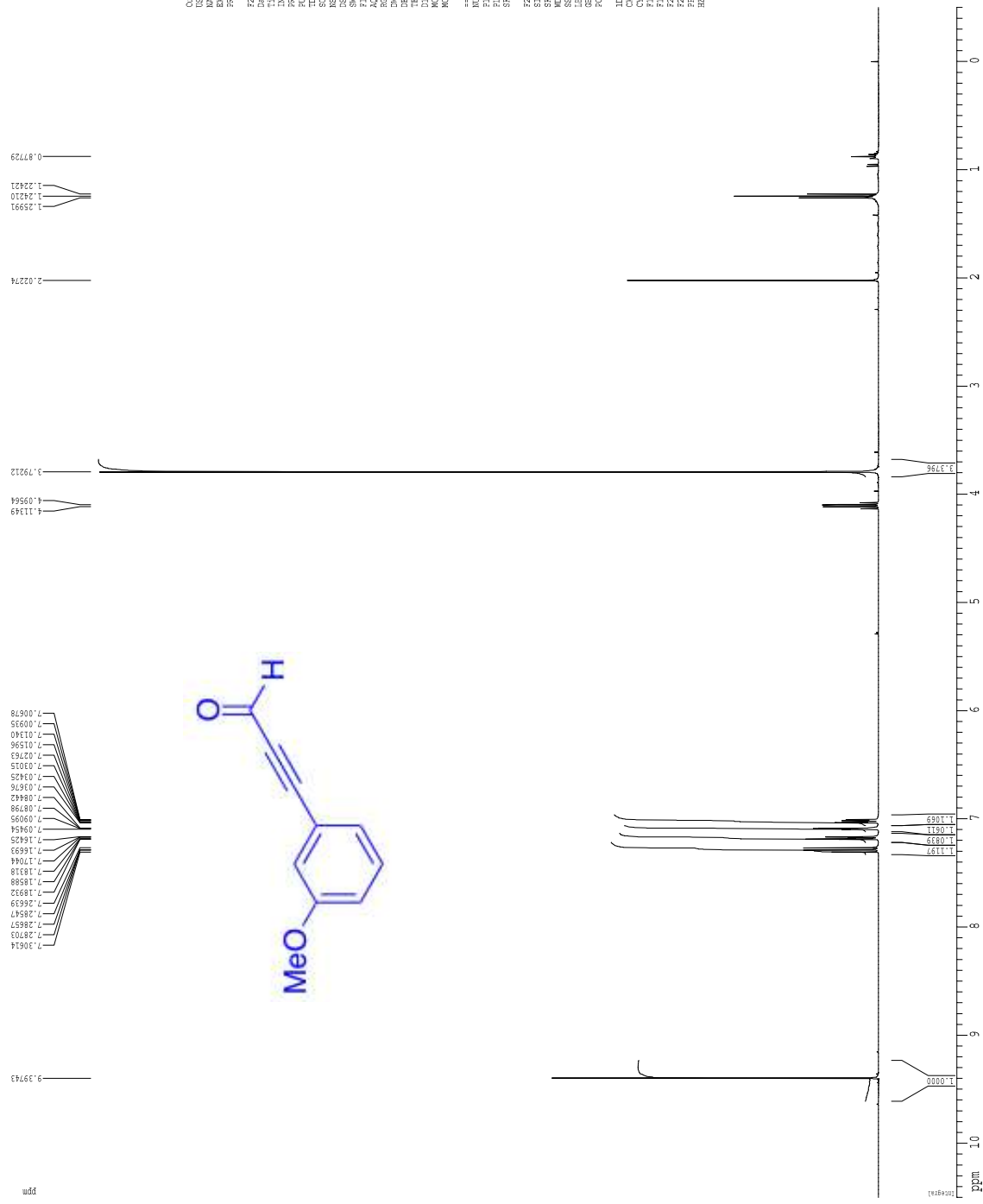
F2 - Acquisition Parameters  
 Date\_: 2014121  
 Time: 17.00  
 PROBNM: 1  
 PULPROG: zgpg30  
 ACQPROG: 5 mm CPIC1.1F  
 PROCNO: 2930  
 F1F2: 177.8  
 CHANNEL: CP113.8  
 NS: 8  
 DS: 2  
 SWH: 6153.600 Hz  
 FWHM: 0.191800 Hz  
 AQ: 5.0348774 sec  
 RG: 5.7  
 RB: 64.000 lines  
 RE: 298.0 K  
 TE: 0.1000000 sec  
 DE: 0.0000000 sec  
 DELT: 0.0000000 sec  
 WDELT: 0.1350000 sec

\*\*\*\*\* CHANNEL F1 \*\*\*\*\*  
 NUCL1: 13C  
 P1: 7.500000 sec  
 PL1: 1.60 dB  
 SFO1: 500.2215015 MHz

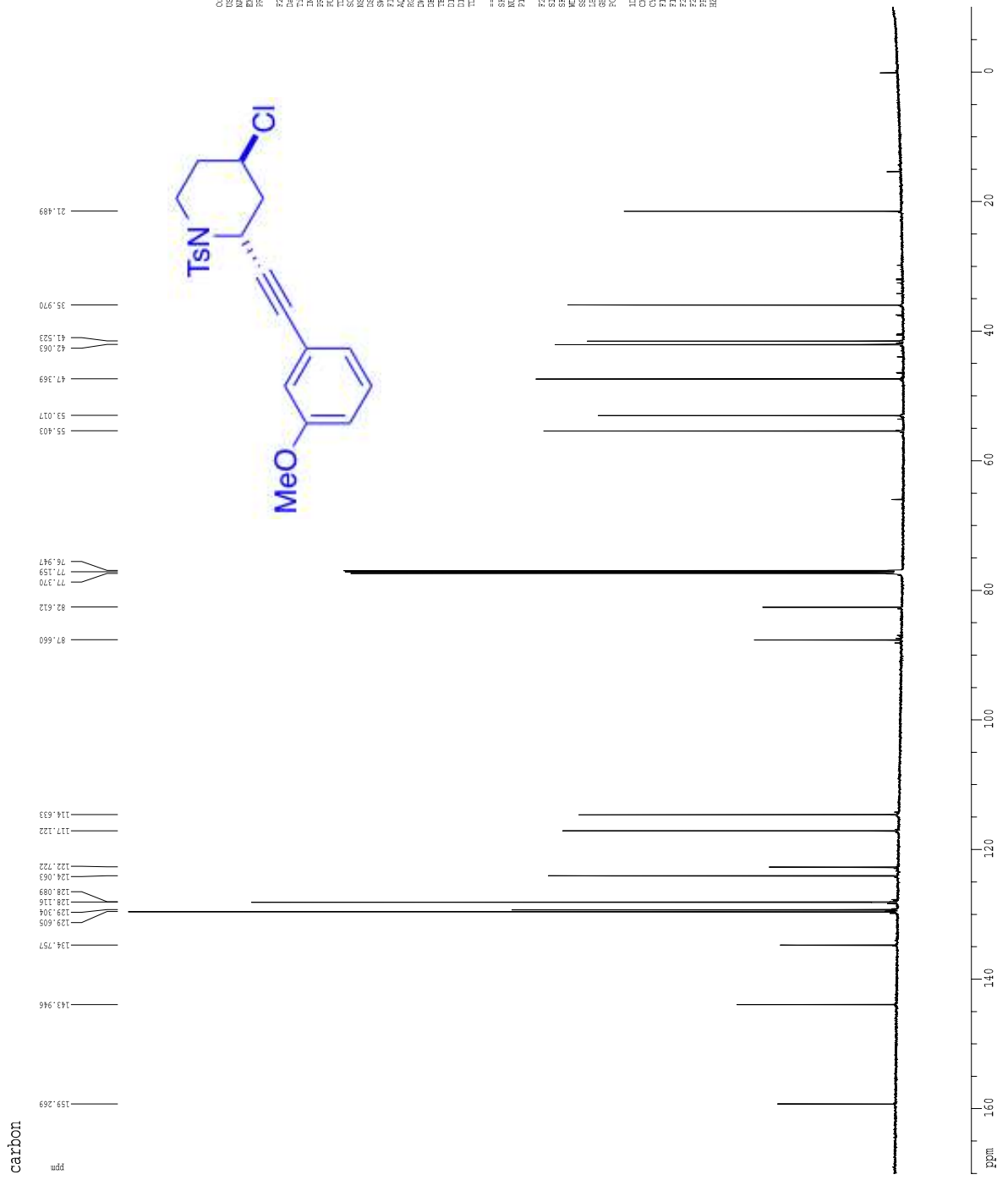
F2 - Processing parameters  
 SI: 645136  
 SF: 500.2215015 MHz  
 WID: 0  
 SSB: 0  
 LB: 0.30 Hz  
 GB: 0  
 PC: 1.00

ID: ME plot parameters  
 CT: 12.00 cm  
 CD: 5.00 mm  
 F1P: 6.500000 MHz  
 F1: 4251.87 Hz  
 F2P: 251.500000 MHz  
 F2: 251.500000 MHz  
 FREQC: 0.39474 ppm/cm  
 HZCM: 137.45528 Hz/cm

1H spectrum

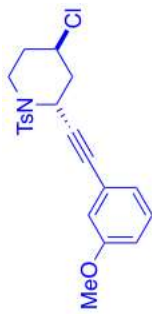


Current Data Parameters  
 NAME: NCM-111-CL-847  
 EXTNO: 1  
 PROCNO: 1  
 F2 - Acquisition Parameters  
 Date\_: 2011101  
 Time: 13.02  
 PROBNM: 41  
 PROCNO: 5 mm QNP H1/P1  
 PULPROG: zgpg30  
 ACQPROG: zgpg30  
 CHANNEL: 1H  
 NS: 2  
 DS: 4  
 SFO1: 400.13636 MHz  
 SF02: 400.13636 MHz  
 AQ1: 5.1114519 sec  
 RG: 32  
 IN: 74.00 umsec  
 DE: 4.00 umsec  
 TE: 297.5 K  
 D1: 0.10000000 sec  
 DELT: 0.00000000 sec  
 DELT2: 0.00000000 sec  
 DELT3: 0.00000000 sec  
 DELT4: 0.00000000 sec  
 \*\*\*\*\* CHANNEL f1 \*\*\*\*\*  
 NU1: 12.00 umsec  
 SF01: 400.1363609 MHz  
 F2 - Processing parameters  
 SI: 65536  
 SF: 400.1363609 MHz  
 DS: 4  
 SSF: 0  
 SSB: 0.00 Hz  
 GB: 0  
 GPC: 0.00  
 ID: NONE plot parameters  
 CT: 12.00 cm  
 FID: 1  
 F1: 10.500 PPM  
 F2: 420.137 Hz  
 F3: 10.500 PPM  
 F4: 20.000 PPM  
 F5: 10.500 PPM  
 F6: 10.500 PPM  
 FREQC1: 0.482416 PPM/cm  
 HZC1: 193.84518 Hz/cm





COSY



Current Data Parameters  
USHR matsusa  
NAME ACM-1-14-charac  
EXTNO 4  
PROCNO 1

F2 - Acquisition Parameters  
Date\_ 20191107  
Time 19.03  
INSTRUM av600  
PROBHD 5 mm CPBBO BE-  
PULPROG cosyzgaf  
TD 2048  
SOLVENT CDCl3T  
NS 1  
DS 16  
SHE 5411.255 Hz  
FIDRES 2.642215 Hz  
AQ 0.1892852 sec  
RG 114  
RG2 92.400 usec  
DE 0.0000000 Hz  
TE 298.00 usec  
TD 2  
DO 0.00000000 K  
D1 1.48868198 sec  
D13 0.00000400 sec  
D14 0.00020000 sec  
IN0 0.00018480 sec

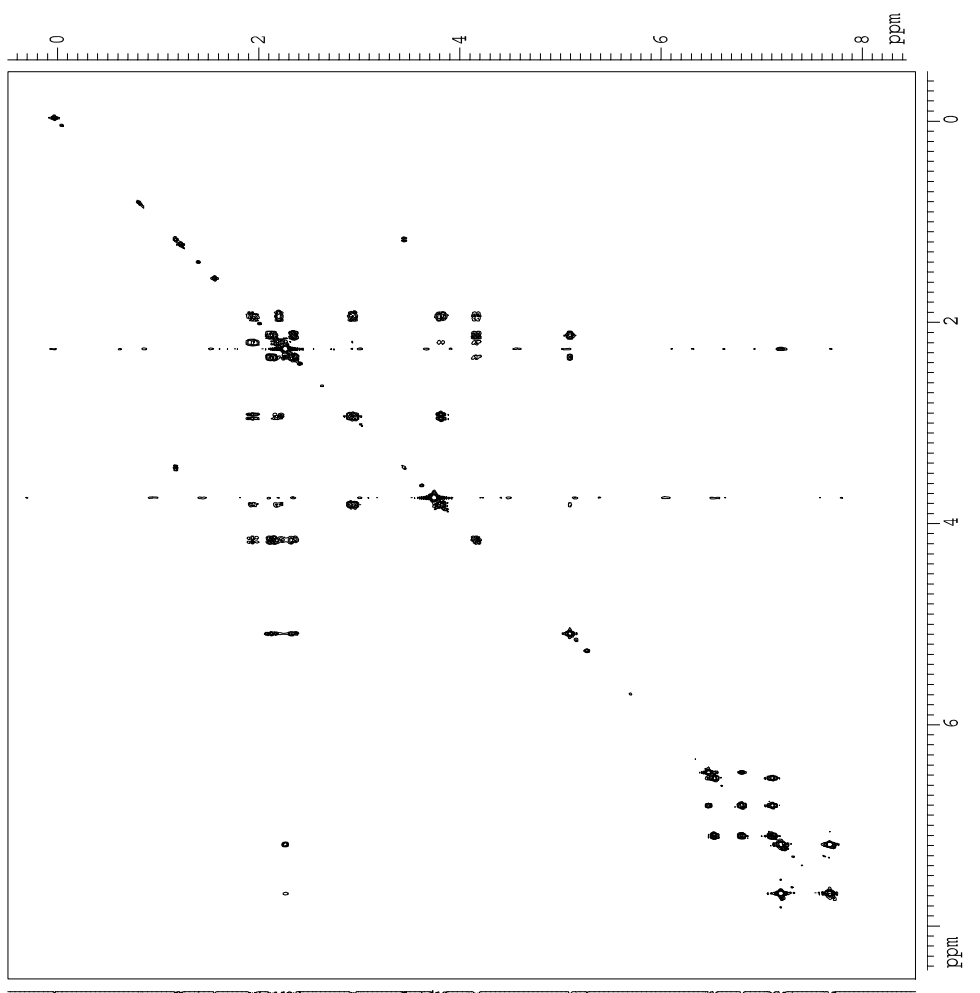
\*\*\*\*\* CHANNEL f1 \*\*\*\*\*  
SFO1 600.1324113 MHz  
NUC1 1H  
P0 12.00 usec  
PL 12.00 usec

F1 - Acquisition Parameters  
ND0 1  
TD 256  
SFO1 600.1324 MHz  
FIDRES 21.137716 Hz  
SW 9.017 ppm  
FHM0DE QF

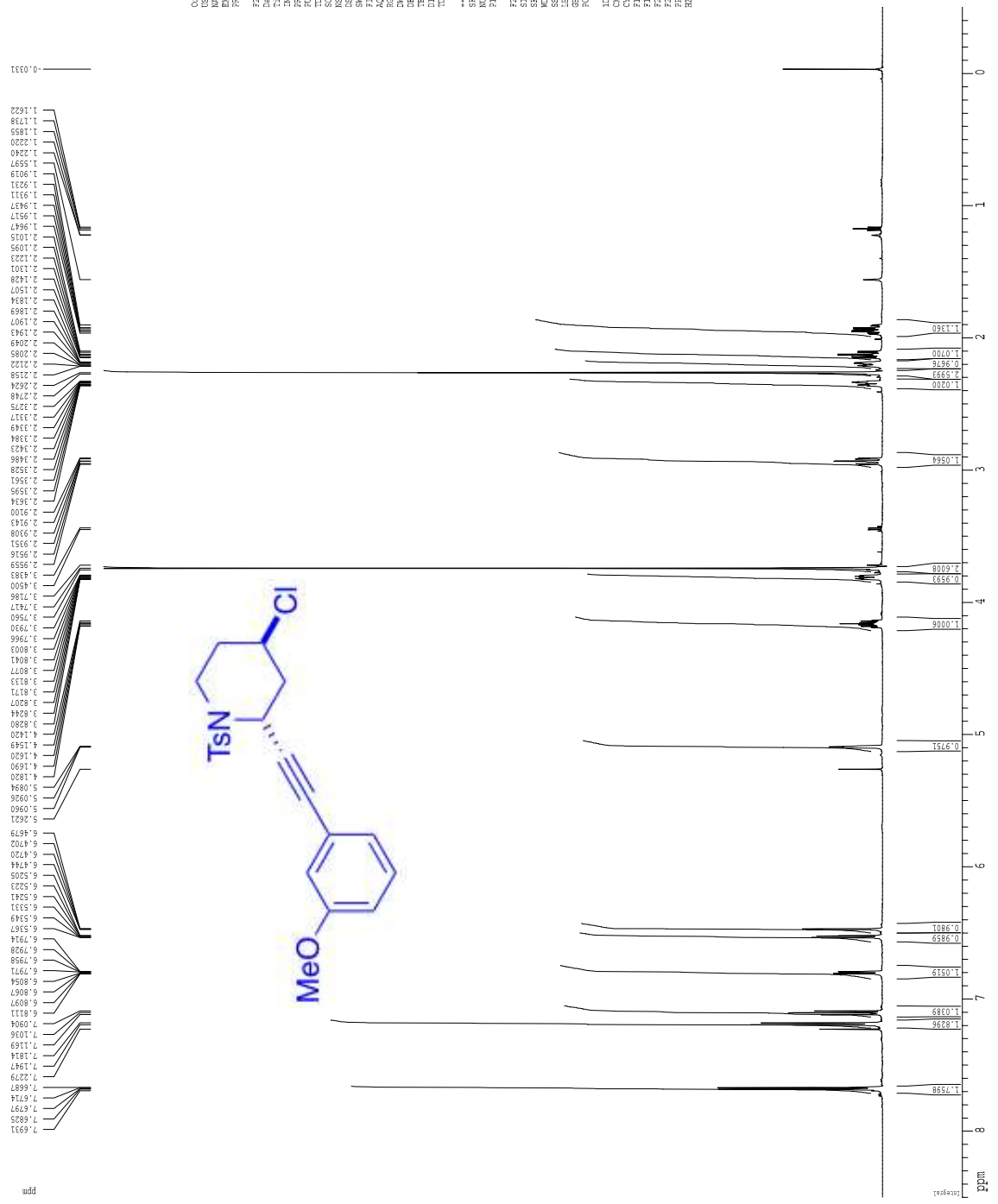
F2 - Processing parameters  
SI 1024  
SF 600.1300549 MHz  
WDW SINE  
SSB 0  
LB 0.00 Hz  
GB 0  
PC 1.40

F1 - Processing parameters  
SI 1024  
SF 600.1300546 MHz  
WDW SINE  
SSB 0  
LB 0.00 Hz  
GB 0

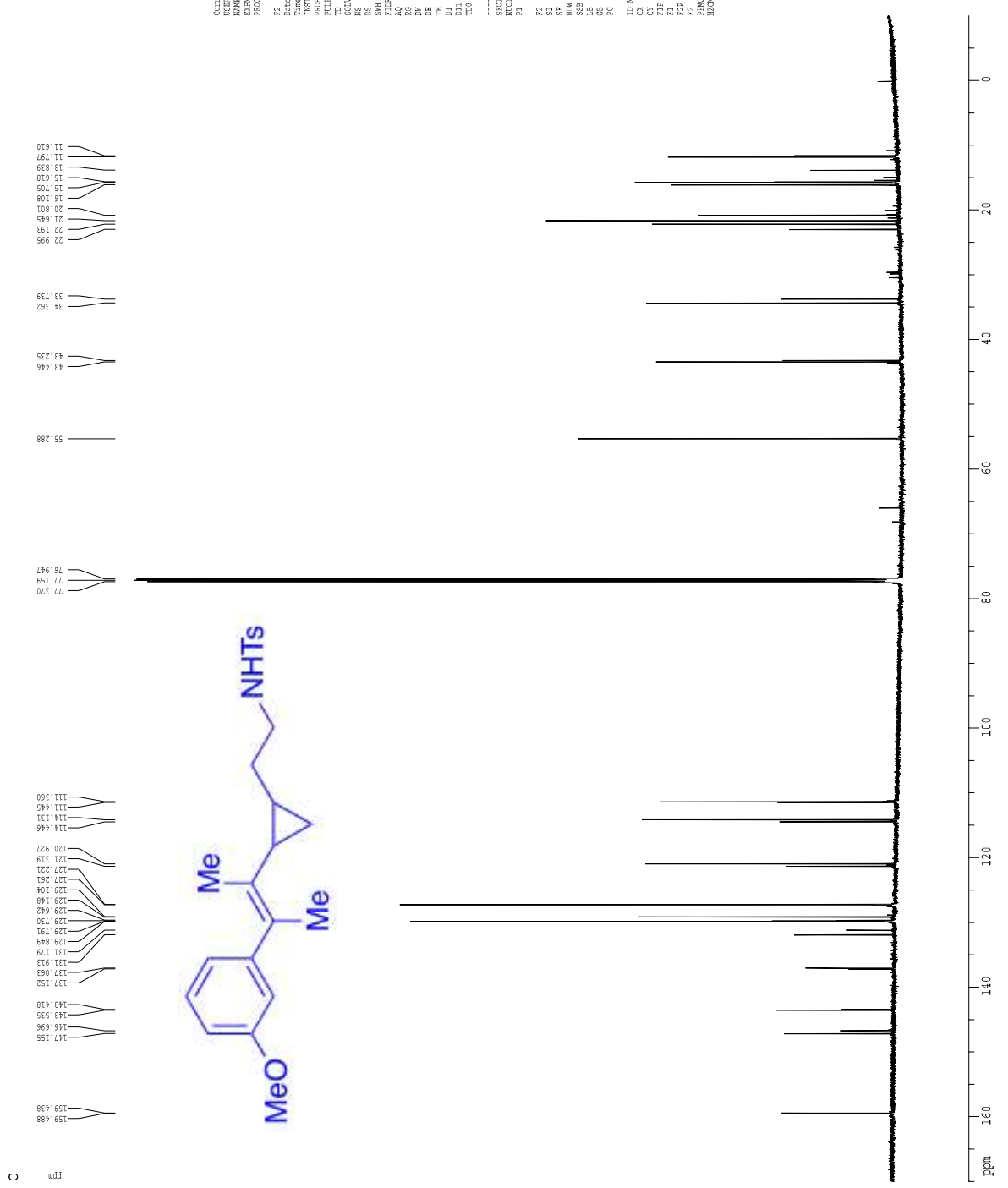
2D NMR plot parameters  
CX2 15.00 cm  
CX1 15.00 cm  
F2FLO 8.526 ppm  
F2FID 5116.95 Hz  
F2FHI -0.490 ppm  
F2FLO -294.31 Hz  
F2FLO 8.526 ppm  
F2FID 5116.95 Hz  
F2FHI -0.490 ppm  
F2FPCMC 0.60112 ppm/cm  
F2FZCM 360.75040 Hz/cm  
F1FPCMC 0.60112 ppm/cm  
F1FZCM 360.75040 Hz/cm



Current Data Parameters  
 Name: 20191107  
 NAME: ACM-114-01424  
 EXERO: 1  
 PRACNO: 1  
 Date\_: 20191107  
 Time: 13.37  
 Operator:   
 PROBMF: 5 mm CBBBO BB-  
 PULPROG: zgpg30  
 TD: 2874  
 SOLVENT: CDCl3  
 NS: 8  
 DS: 2  
 SFRF: 9815.385 Hz  
 AQ: 5.0989779 sec  
 RG: 10  
 DM: 52.000 usec  
 DE: 2.0000000 sec  
 TE: 298.0 K  
 D1: 0.1000000 sec  
 D2: 1  
 \*\*\*\*\* CHANGED FL \*\*\*\*\*  
 SFO1: 600.1314209 MHz  
 F1: 14  
 F2: 12.00 usec  
 SFO2: 600.1314209 MHz  
 F3: 14  
 F4: 12.00 usec  
 F2 - Processing parameters  
 SI: 32768  
 SF: 600.1314209 MHz  
 KW: 60  
 EN: EN  
 SSF: 0.0 Hz  
 SS: 0.0 Hz  
 RB: 1.00  
 GC: 1.00  
 US ME p/oc parameters  
 CU: 32.80 cm  
 CT: 15.00 cm  
 F1P: 8.500 Hz  
 F2P: 10.500 Hz  
 F3P: -10.500 Hz  
 F4: -100.07 Hz  
 FPMON: 0.38474 Hz/cm  
 FOCN: 235.8345 Hz/cm



C



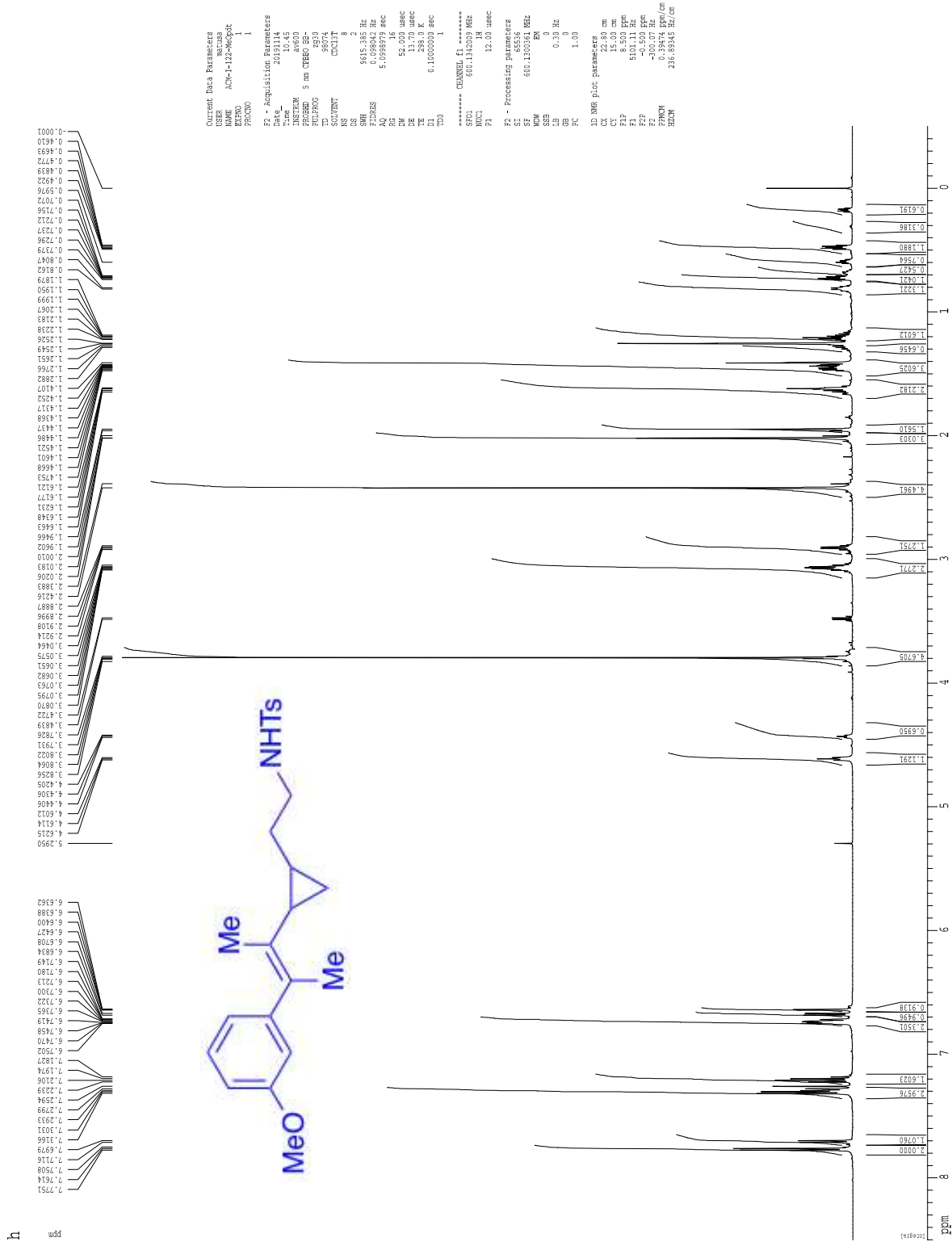
Current Data Parameters  
NAME AC6-112-860ct  
EXPER 3  
PROCNO 1

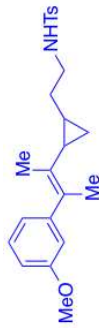
F2 - Acquisition Parameters  
Date\_ 2019114  
Time 11.03  
Operator  
PROBHD 5 mm CBBO1 BBI-  
PULPROG zgpg30  
TD 65536  
SOLVENT CDCl3  
NS 315  
DS 4  
SHE 3021.883 Hz  
FIDRESS 0.5044468 sec  
AQ 2050  
RG 11.800 usec  
DE 2.000 usec  
TE 298.0 K  
D1 0.4000001 sec  
D11 0.0300000 sec  
D12 1

\*\*\*\*\* CHANNEL f1 \*\*\*\*\*  
NUC1 13C  
P1 10.10 usec

F2 - Processing parameters  
SI 65536  
SF 150.9027969 MHz  
WDW EM  
SS 0  
SB 1.00 Hz  
GB 0  
PC 1.00

1D NMR file parameters  
CX 22.80 cm  
CT 15.00 cm  
CP 15.00 cm  
F1 25653.468 Hz  
F2 -10.000 ppm  
F3 -1509.03 Hz  
GAMMA 13C  
NUC2 13C  
HZNW 1181.31749 Hz/cm





cosy

Current Data Parameters  
 USHR matusa  
 NAME ACM-1-122-MeOcdt  
 EXNO 2  
 PROCNO 1

F2 - Acquisition Parameters  
 Date\_ 20191114  
 Time 10.50  
 INSTRUM av600  
 PROBED 5 mm CPBEO BE-  
 PULPROG cosyzgpgf  
 TD 2048  
 SOLVENT CDCl3T  
 NS 1  
 DS 16  
 SFE 5411.255 Hz  
 FIDRES 2.642215 Hz  
 AQ 0.1892852 sec  
 RG 114  
 DE 92.400 usec  
 TE 298.00 usec  
 TD 0.0000700 K  
 D0 1.48889198 sec  
 D1 0.00009400 sec  
 D13 0.00009400 sec  
 D16 0.00020000 sec  
 INO 0.00018480 sec

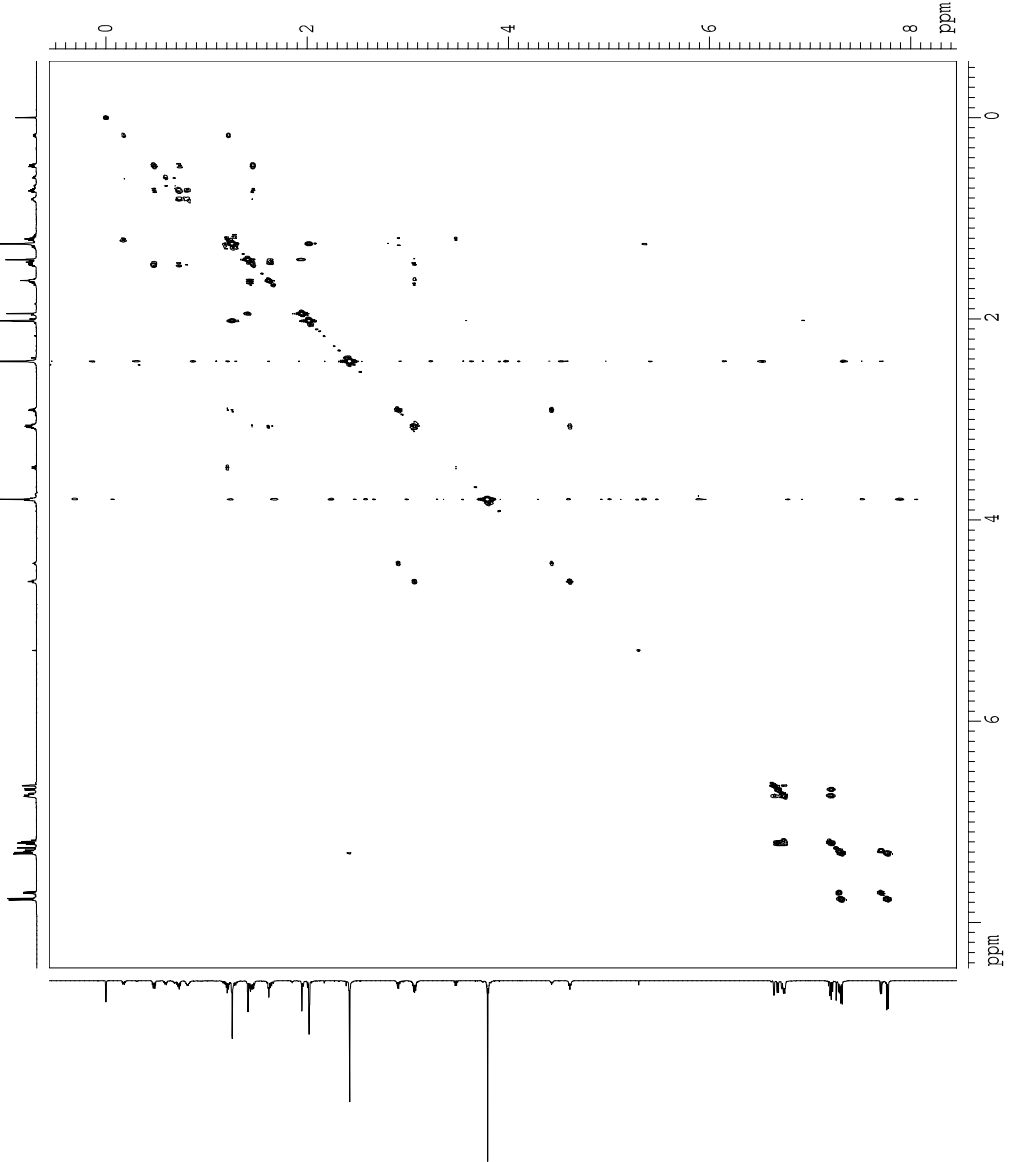
\*\*\*\*\* CHANNEL f1 \*\*\*\*\*  
 SF01 600.1324041 MHz  
 NUC1 1H  
 P0 12.00 usec  
 PL 12.00 usec

F1 - Acquisition Parameters  
 ND0 1  
 TD 256  
 SF01 600.1324 MHz  
 FIDRES 21.137716 Hz  
 SW 9.017 ppm  
 FMODE QF

F2 - Processing parameters  
 SI 1024  
 SF 600.1300361 MHz  
 WDW SINE  
 SSB 0  
 LB 0.00 Hz  
 GB 0  
 PC 1.40

F1 - Processing parameters  
 SI 1024  
 SF 600.1300361 MHz  
 WDW SINE  
 SSB 0  
 LB 0.00 Hz  
 GB 0

2D NMR plot parameters  
 CX2 15.00 cm  
 CX1 15.00 cm  
 F2FLO 8.454 ppm  
 F2LO 5073.61 Hz  
 F2FHI -0.563 ppm  
 F2HI -337.65 Hz  
 F1FLO 8.454 ppm  
 F1LO 5073.61 Hz  
 F1FHI -0.563 ppm  
 F1HI -337.65 Hz  
 F2PRMCM 0.60112 ppm/cm  
 F2HZCM 360.75037 Hz/cm  
 F1PRMCM 0.60112 ppm/cm  
 F1HZCM 360.75037 Hz/cm



**Chapter 3: Examining Structure and Reactivity  
of Isolated Ru-MACHO® Dihydrides for  
Reduction of CO<sub>2</sub> and Carbamates**

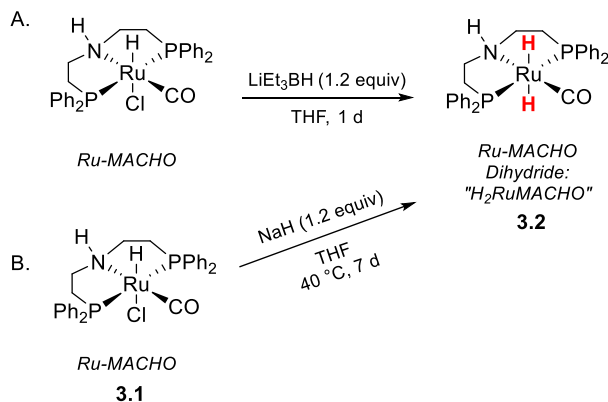
### 3.1 Introduction

Designing complex transformations of CO<sub>2</sub>, enabled by transition metal catalysts, is a key strategy for valorization of CO<sub>2</sub> to produce fuel and C1 building blocks.<sup>1-3</sup> Research efforts focused on decreasing the impact of CO<sub>2</sub> emissions must work to design processes that generate high-value products without requiring a high input of energy.<sup>4</sup> One method that addresses this concern is combined CO<sub>2</sub> capture and CO<sub>2</sub> conversion. Current hydrogenation technology for this approach requires harsh conditions and costly solvents.<sup>5</sup> The Prakash group and others have reported efficient methods for capturing and converting CO<sub>2</sub> using amines.<sup>6,7</sup> Superbases such as DABCO and TMG have been the most effective, and linear polyamines have also demonstrated the ability to capture CO<sub>2</sub> in the form of carbamates.<sup>5,8,9</sup> To hydrogenate these carbamates, homogenous Ru pincer complexes are used as catalysts with molecular hydrogen to generate methanol.<sup>7</sup> However, these methods typically require high temperatures (60–145 °C) and pressures (40–110 bar). If these conversions can be performed using captured CO<sub>2</sub> in the form of carbamates and a Ru complex as an electrocatalyst, the goal of an artificial photosynthetic approach to CO<sub>2</sub> capture and conversion using amines becomes more feasible.

The powerhouse hydrogenation catalyst Ru-MACHO® (**3.1**) has been widely utilized in hydrogenation of CO<sub>2</sub>-captured products, including carbamates and hydroxide-captured CO<sub>2</sub>.<sup>1,5,10</sup> Ru-MACHO-type catalysts ('MACHO' describes PNP-pincer ligands with various alkyl or aryl phosphines) have been utilized to perform catalytic hydrogenation of CO<sub>2</sub>, carbamates, and alkyl carbonate salts to methanol.<sup>3</sup> These hydrogenations using carbamates and alkyl carbonate salts demonstrate the strength of these catalysts, as substrates that are formed from CO<sub>2</sub> capture are typically more challenging to transform.<sup>5,11</sup> Despite these advances in hydrogenation, little is known about the reactive species responsible for hydrogenation with Ru-MACHO®. Many

proposed mechanisms of hydrogenation feature *trans*-dihydride complexes, which align well with previously reported Ru dihydride complexes.<sup>12, 13</sup> Yet, despite widespread usage of Ru-MACHO® and its analogues for hydrogenation, little has been reported regarding the active dihydride species responsible for the reduction of substrates. The proposed structure most commonly featured in hydrogenation literature is a *trans*-dihydride (**3.2**, Scheme 3.1), retaining the overall structure of Ru-MACHO® by swapping the chloride ligand for a hydride, presumed to be from heterolysis of H<sub>2</sub>. However, experimental and modeling data only assume the presence of this dihydride.<sup>1, 10</sup> The goal of this work is to gain a more complete understanding of the reactivity of Ru-MACHO® and CO<sub>2</sub>, for the purpose of utilizing Ru-MACHO® as an electrocatalyst for CO<sub>2</sub> reduction.

Scheme 3.1. Methods of Reducing of Ru-MACHO in this Chapter



## 3.2 Results and Discussion

### 3.2.1 Synthesis and Characterization of H<sub>2</sub>Ru-MACHO Dihydrides

To access the proposed Ru-MACHO® dihydride, H<sub>2</sub>Ru-MACHO (**3.2**), two chemical reduction methods were explored (*vide infra*). Initially, Super-Hydride® was utilized to produce the proposed *trans*-dihydride **3.2** (Scheme 3.1A). This produced a single product observed by NMR (Figure 3.1) but involved a challenging isolation from unreacted **3.1**. The <sup>1</sup>H NMR spectrum features broad peaks in the hydride region, which may be a result of the hydride atoms coordinating



to Li atoms left behind following reduction with Super-Hydride® (Figure 3.1A), which would be consistent with the isolated complex showing coordinating Li (*vide infra*).

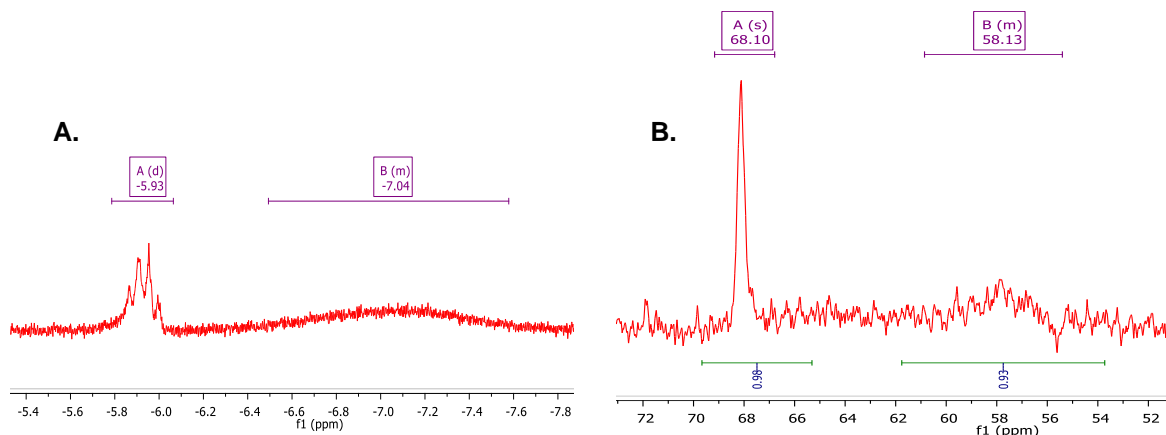


**Figure 3.1.** NMR spectra of product isolated from Super-Hydride® reduction of Ru-MACHO® in THF-*d*<sub>8</sub>. **A:** <sup>1</sup>H NMR spectrum **B:** <sup>31</sup>P NMR spectrum.

Alternative pathways of reduction of **3.1** were explored to allow for easier isolation of dihydride. NaBH<sub>4</sub> could not be utilized, as reacting **3.1** with NaBH<sub>4</sub> is the synthetic route for generating Ru-MACHO-BH.<sup>14</sup> Instead, NaH was used to reduce **3.1** at 40 °C for 7 days. Complete conversion to the reduced dihydride could be observed by NMR after cooling to room temperature (Figure 3.2).

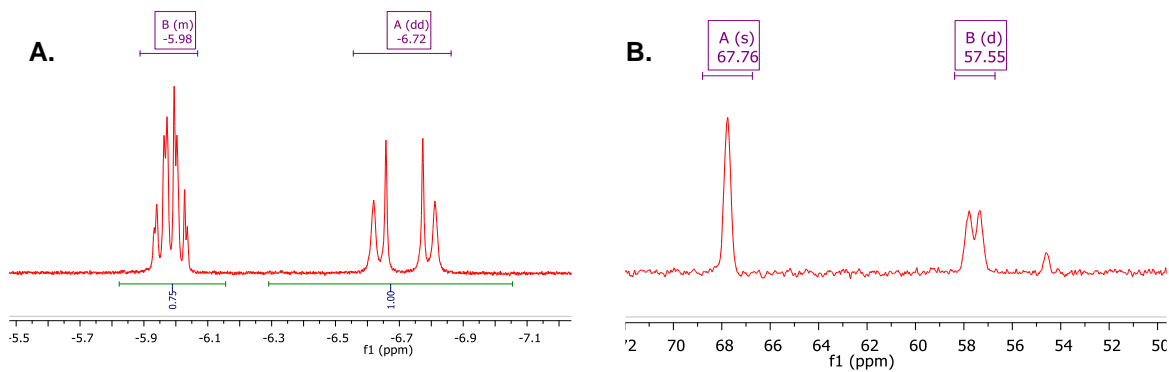


**Figure 3.2.** NMR spectra of product isolated from NaH reduction of Ru-MACHO® in THF-*d*<sub>8</sub>. **A:** <sup>1</sup>H NMR spectrum **B:** <sup>31</sup>P NMR spectrum.

NaH reduction of **3.1** was repeated at a slightly elevated temperature (50 °C versus 40 °C). The isolated product showed a singular peak in the hydride region by  $^1\text{H}$  NMR and one doublet in the  $^{31}\text{P}$  NMR spectrum (Figure 3.3). The hydride peak integration increased to two, corresponding to a dihydride with equivalent hydride atoms.

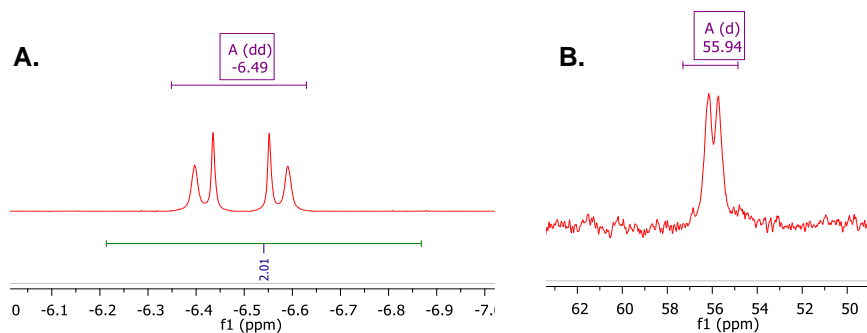


**Figure 3.3.** NMR spectra of product isolated from NaH reduction of Ru-MACHO® in THF- $d_8$  at 50 °C. **A:**  $^1\text{H}$  NMR spectrum **B:**  $^{31}\text{P}$  NMR spectrum.

### 3.2.1.1 Comparing NMR Data Across Methods

The NMR spectra of the products isolated from Super-Hydride® reduction versus NaH reduction bare striking similarities (Table 3.1, entries 1–4). In contrast, the product isolated following NaH reduction at 50 °C shows a singular doublet present in the  $^{31}\text{P}$  NMR spectrum with a coupling constant that clearly matches the observed coupling present in the hydride region of the  $^1\text{H}$  NMR spectrum (Table 3.1, entry 6), further supporting the formation of a dihydride product. As NaH is commonly used as a base, the unknown dihydride may have resulted from deprotonation of the amine in the pincer ligand. Another plausible explanation could be that the PNP ligand detached and reattached, causing some type of isomerization to occur.

Entry	Reductant	NMR Nucleus	Distinct Peaks	$\delta$ Shift (ppm)	Multiplicities	J-coupling (Hz)	Integration
1	LiEt <sub>3</sub> BH	<sup>1</sup> H	2	-5.93, -7.04	Broad multiplet, broad multiplet	-	1H, 1H
2	LiEt <sub>3</sub> BH	<sup>31</sup> P	2	68.1, 58.1	Broad singlet, broad multiplet	-	1P, 1P
3	NaH	<sup>1</sup> H	2	-5.98, -6.72	Multiplet, doublet of doublets	dd = 92.1, 22.8	1H, 1H
4	NaH	<sup>31</sup> P	2	67.8, 57.8	Broad singlet, doublet	d = 92.5	1P, 1P
5 <sup>a</sup>	NaH	<sup>1</sup> H	1	-6.49	Doublet of doublets	dd = 92.9, 22.8	2H
6 <sup>a</sup>	NaH	<sup>31</sup> P	1	55.9	Doublet	d = 90.9	2P

**Table 3.1.** Summary of NMR data collected from Ru-MACHO® reductions in THF-d<sub>8</sub>. A: Reduction run at 50 °C.

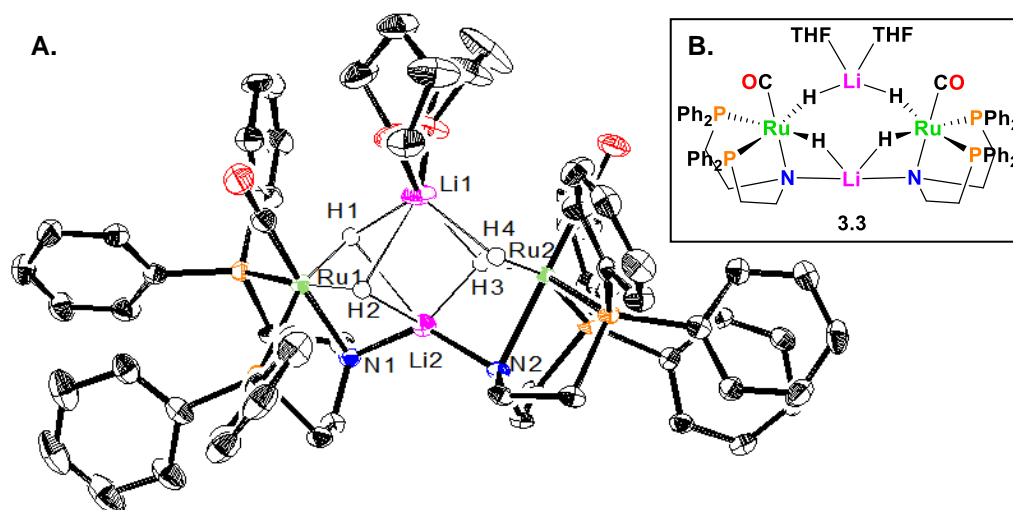
### 3.2.1.2 Crystal Structures

Two crystals suitable for x-ray diffraction were isolated using the product isolated from Super-Hydride® reduction. The recrystallization techniques explored are listed in Table 3.2, with entry 11 representing the conditions used to isolate the following crystal structures. However, the complexes isolated for x-ray diffraction showed two distinct cis-dihydride complexes, **3.3** and **3.4**.

Entry	Solvent	°C	Co-solvent	Well Size <sup>a</sup>	Result
1	toluene	25	pentane	large	powder
2	toluene	-40	pentane	large	powder
3	toluene	25	pentane	small	small specks
4	toluene	-40	pentane	small	needles
5	toluene	-40	pentane	small	powder
6	THF	25	pentane	large	powder
7	THF	25	pentane	small	powder
8	THF	-40	none	small	none
9	THF	-40	none	medium	none
10	THF	-40	none	large	none
11	THF	-40	pentane	large	<b>crystals</b>

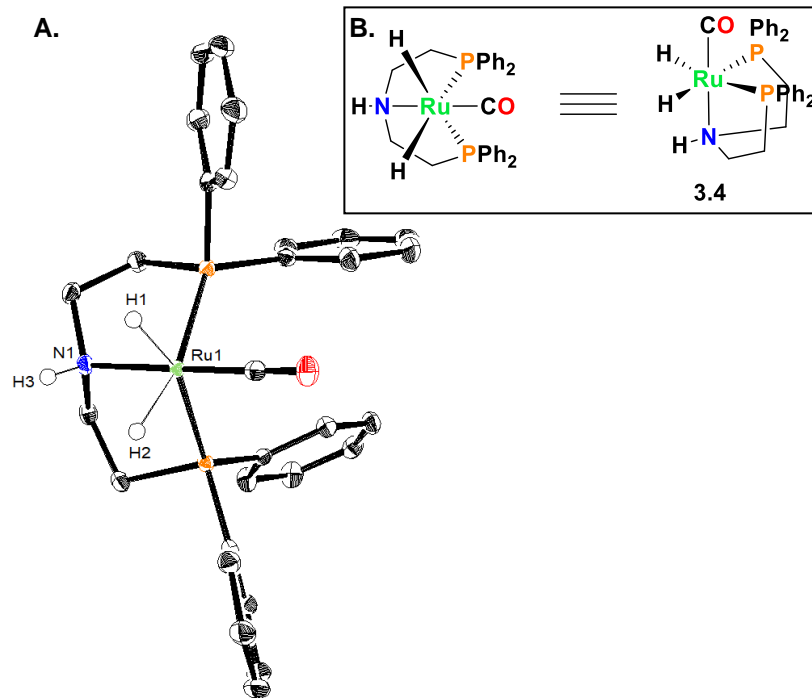
**Table 3.2** Selected recrystallization trials. <sup>a</sup>Recrystallization trials were setup in 20 mL scintillation vials with internal glass wells of varying sizes: Large well = 1 dram shell vial, flat bottom; medium well = 0.5 dram shell vial, flat bottom; small well = 5 mm glass tube.

Figure 3.4 shows the first structure elucidated (**3.3**), including two cis-dihydride complexes bridged by a coordinating Li atom, likely leftover from Super-hydride® use. The N atom in the ligand backbone is deprotonated in both hydrides, and lithiated to Li atoms likely left behind following Super-Hydride® reduction.



**Figure 3.4. A:** Crystal structure of **3.3**. Thermal ellipsoids are drawn at 50% probability. Non-hydride hydrogen atoms and non-coordinating solvent molecules are omitted for clarity. **B:** ChemDraw showing 3D line structure.

A second single crystal was grown using conditions identical to those described above following Super-Hydride® reduction (Figure 3.5). The resulting structure (**3.4**) was markedly different than the first, with no coordinating Li atoms present and a protonated nitrogen atom. The hydride atoms are still cis to each other, and the crystal lattice (not depicted here) shows an unusual hydrogen bonding interaction between two dihydride complexes, where the amine proton in one molecule is donating to a hydride atom in another molecule. This indicates that the hydride atom is so electron dense, it is acting as a hydrogen bonding acceptor, which has been observed in other systems.<sup>15</sup> This interaction is unlikely to occur in solution but some complex <sup>1</sup>H NMR splitting may be observed between molecules in solution using a NMR spectrometer with a stronger field.



**Figure 3.5.** **A:** Crystal structure of **3.4**. Thermal ellipsoids are drawn at 50% probability. Non-hydride and N–H hydrogen atoms and solvent molecules are omitted for clarity. **B:** ChemDraw showing 3D line structure.

It is unclear why these recrystallization conditions produced two different crystal structures. The most likely explanation is that the lithiated, deprotonated dihydride complexes crystallized using Li atoms for stability. Failed crystallization conditions typically yielded small, needle-shaped crystals, which were generally of poor quality. However, the consistent positioning of the hydrides indicates that the preferred geometry (*cis*-dihydride) is being observed.

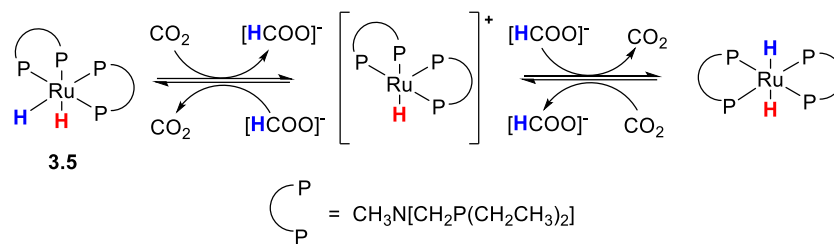
Bond <sup>a</sup>	Distance (Å) <sup>a</sup>	Bond <sup>b</sup>	Distance (Å) <sup>b</sup>
Ru1–H1	1.577	Ru1–H1	1.536
Ru1–H2	1.688	Ru1–H2	1.604
Ru2–H3	1.455	-	-
Ru2–H4	1.687	-	-

**Table 3.3.** Metal–hydride bond lengths determined experimentally via X-ray crystallography. <sup>a</sup>Structural information from **3.3**. <sup>b</sup>Structural information from **3.4**.

Structurally, observation of a *cis*-dihydride complex was not expected. It is also of note that the Ru–H bond lengths vary from **3.3** to **3.4** (Table 3.3). Ru<sup>II</sup> dihydrides are known, but

typically contain diphosphine ligands or require *cis-trans* isomerization before reactivity can be observed.<sup>16, 17</sup> In one example, a Ru-dihydride complex forms both *cis*- and *trans*-dihydride isomers, although only the *cis*-dihydride is consumed for the reduction of a carbonate substrate. However, both isomers were consumed in the reduction of CO<sub>2</sub> in solution.<sup>18</sup> The same *cis*-dihydride is presumed to isomerize to the *trans*-dihydride following reversible hydride transfer from formate (Scheme 3.2). In contrast, **3.4** reacts to completion with CO<sub>2</sub>, and the generated formate then coordinates to the Ru complex. No hydride transfer from formate to the Ru complex was observed, indicating **3.4** is a stronger hydride donor than formate.

Scheme 3.2. Mechanism of *cis-trans* isomerization (Heldebrant, 2016)



A few structural comparisons can be made between **3.4** and Heldebrant's *cis*-dihydride (**3.5**); while both complexes contain 6-coordinate octahedral Ru<sup>II</sup> and PNP ligands, **3.4**'s singular PNP ligand binds tridentate to Ru while **3.5** includes two bidentate PNP ligands. The greater degree of movement allowed by **3.5**'s bidentate ligands may explain the ease of isomerization. In an effort to observe any possible isomerization of **3.4** to another isomer, a sample of **3.4** in THF-*d*<sub>8</sub> was heated to 50 °C in an NMR tube for 30 minutes. No spectral changes could be observed via <sup>1</sup>H NMR and <sup>31</sup>P NMR (<sup>1</sup>H coupled and decoupled). This likely indicates that **3.4** is the strongly preferred isomer. While X-ray crystal structures have yet to be produced of the NaH-reduced compound, the dihydride structure **3.4** is presumed to be the product isolated following NaH reduction.

## 3.2.2 Reactivity of Isolated H<sub>2</sub>Ru-MACHO

### 3.2.2.1 Stoichiometric Reactivity of Isolated H<sub>2</sub>Ru-MACHO and CO<sub>2</sub>

Following NaH reduction of Ru-MACHO® (for experimental details, *vide infra*), the isolated dihydride product **3.4** was utilized in stoichiometric experiments with CO<sub>2</sub>. The parent complex **3.1** does not display reactivity with CO<sub>2</sub> at ambient conditions, so any present starting material present would not impact formate production.<sup>1, 10</sup> The reducing agents used to generate **3.4** are also known not to have CO<sub>2</sub> reduction activity.

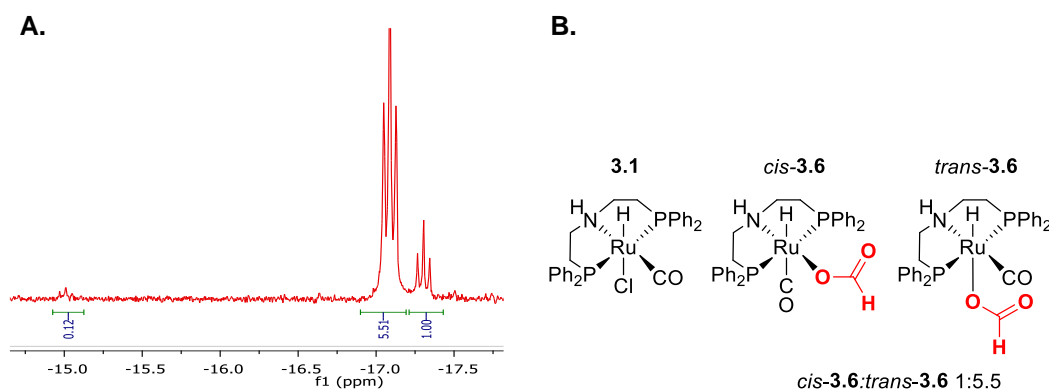


**Figure 3.6.** A: <sup>1</sup>H NMR of hydride region (−14 ppm to −18 ppm) after exposing Super-Hydride®-reduced Ru-MACHO® to 1 atm of CO<sub>2</sub> in THF-*d*<sub>8</sub>. B: Products formed after CO<sub>2</sub> reduction.

Starting with gaseous CO<sub>2</sub>, a solution of **3.4** in THF-*d*<sub>8</sub> was exposed to 1 atm of CO<sub>2</sub> for 30 minutes. After 30 minutes, complete conversion of dihydride to formylated Ru<sup>II</sup> complexes (*cis-3.6* and *trans-3.6* in Figure 3.6B) was observed by NMR (Figure 3.6A). The formation of the formyl complex *trans-3.6* at  $\delta$  −17.1 ppm has been reported previously by Prakash,<sup>10</sup> while the structure of the *cis*-dihydride complex at  $\delta$  −17.3 ppm (*cis-3.6*) is proposed here based on the identical proton coupling constants between both triplet peaks.<sup>10</sup> HSQC was also performed to support the production of formate (Figure 3.7). A correlation between formyl proton and carbon of Ru-bound-formate is visible between peaks at  $\delta$  8.01 ppm from the <sup>1</sup>H NMR spectrum and  $\delta$  179.6 ppm from the <sup>13</sup>C NMR spectrum (Figure 3.7). Excitingly, this observed reactivity shows

that **3.4** displays the same CO<sub>2</sub>-reduction capability of hydride complexes typically used for electrocatalytic CO<sub>2</sub> conversion.<sup>19</sup>

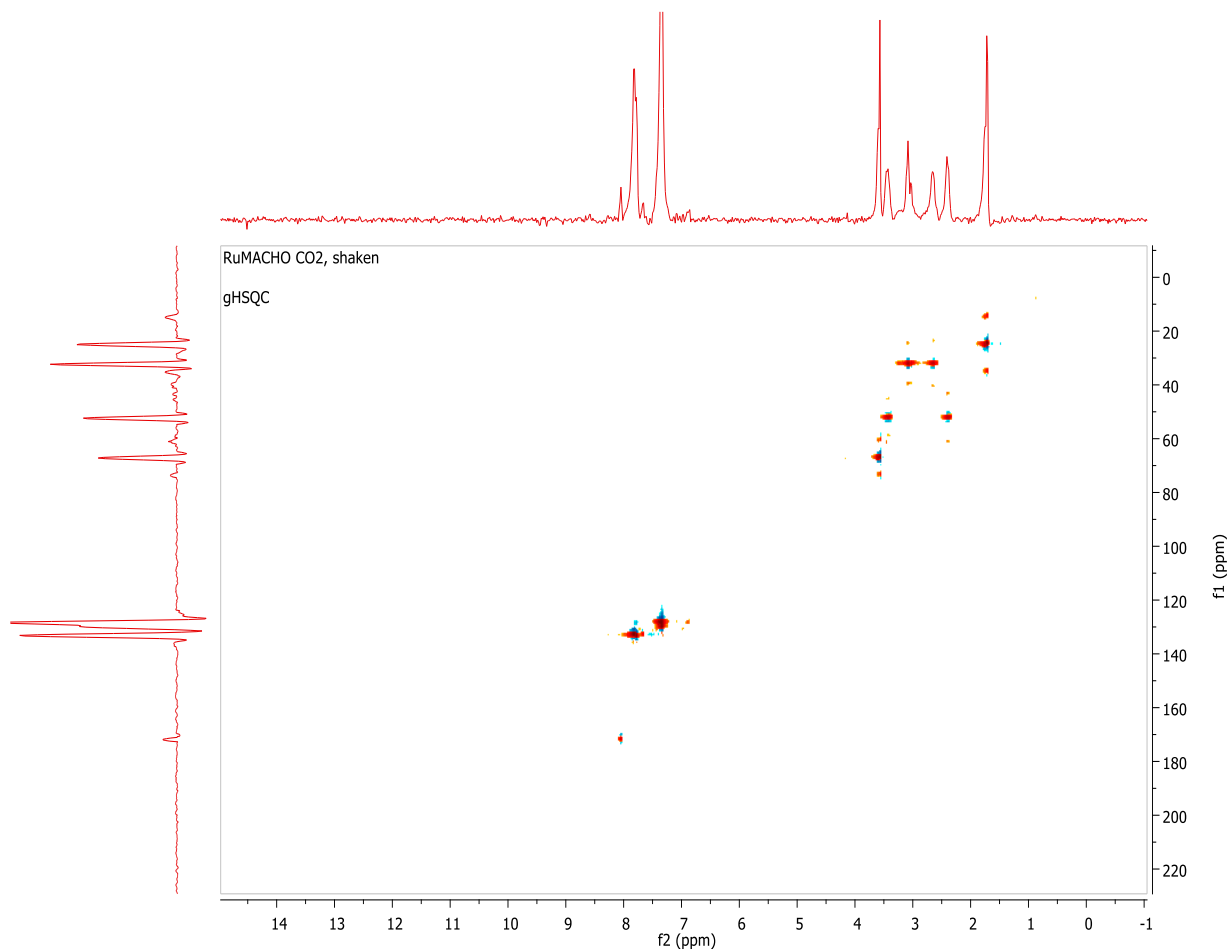


**Figure 3.7.** HSQC (x-axis: <sup>1</sup>H; y-axis: <sup>13</sup>C) of NMR-scale experiment with reduced Ru-MACHO® under 1 atm of CO<sub>2</sub> in THF-*d*<sub>8</sub>.

### 3.2.2.2 Stoichiometric Reactivity of H<sub>2</sub>Ru-MACHO with Dimethylammonium Dimethyl Carbamate

Hydrogenation with Ru-MACHO® may occur under high temperatures and pressure, however, in order to design a mild electrochemical alternative it would be ideal to see reducing activity from the Ru-MACHO-dihydride at room temperature. To this end, an NMR-scale experiment was performed, where NaH-reduced Ru-MACHO® was treated with excess (greater than 5 equiv) of dimethylammonium dimethyl carbamate, a commercially available and THF-



soluble carbamate that serves as a proxy for a captured-CO<sub>2</sub> substrate. It is also of note that the dihydride was exposed to air during the reaction, but no evidence of decomposition was observed by NMR. Spectra were obtained approximately 20 minutes following carbamate addition (Figure 3.8), and clearly show the formation of formate and some hydrogen by <sup>1</sup>H NMR. The major peak present in the <sup>31</sup>P NMR spectrum is a broad singlet, with some trace dihydride leftover. A single triplet is present in the hydride region at -17.3 ppm. These peaks are attributed to the formation of a Ru(II) complex that is not a dihydride, but is also not a formylated complex, or Ru-MACHO®. However, with the return of the splitting observed in the <sup>31</sup>P{<sup>1</sup>H} NMR spectrum of Ru-MACHO®, this new data indicates that the resulting complex has the same degree of symmetry as the parent Ru-MACHO®.

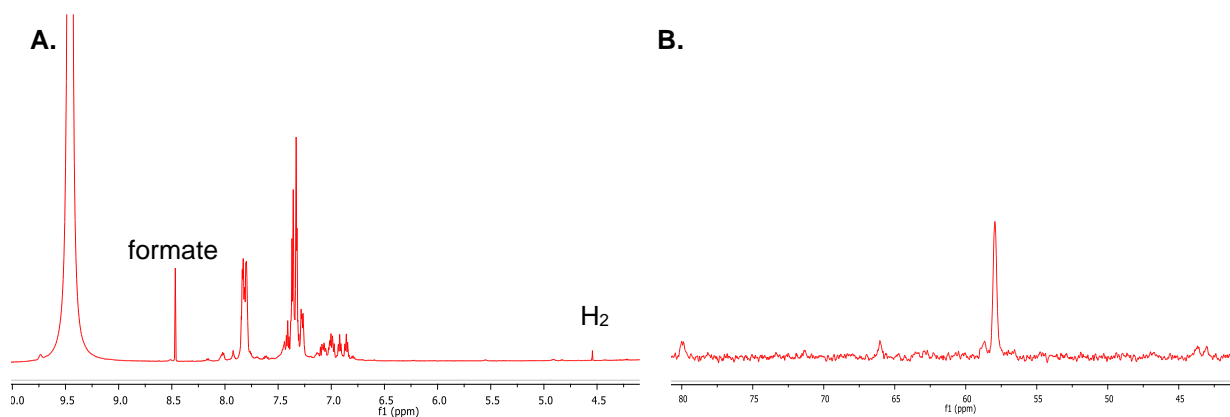


**Figure 3.8.** NMR spectra after adding excess dimethylammonium dimethyl carbamate to **3.4** in THF-*d*<sub>8</sub>. **A:** <sup>1</sup>H NMR spectrum, formyl proton and H<sub>2</sub> peaks are labeled. **B:** <sup>31</sup>P NMR spectrum.

### 3.3 Conclusion

A *cis*-Ru-MACHO-dihydride was isolated, characterized, and assessed for stoichiometric CO<sub>2</sub> and carbamate reduction activity. This study reports structural information regarding the proposed Ru-MACHO® dihydride responsible for many hydrogenation reactions involving captured-CO<sub>2</sub>. Future work will rely heavily on this established reactivity with the purpose of designing a mild electrochemical method utilizing Ru-MACHO® as an electrocatalyst.

### 3.4 Experimental Details

Solvents were degassed by sparging with argon gas and dried by passage through columns of activated alumina or molecular sieves. Deuterated solvents were purchased from Cambridge Isotopes Laboratories, Inc. and were degassed and stored over activated 3 Å molecular sieves prior to use.  $^1\text{H}$  NMR spectra were recorded on Bruker DRX-400 (400 MHz  $^1\text{H}$ ), GN-500 (500 MHz  $^1\text{H}$ , 125.4 MHz  $^{13}\text{C}$ ), CRYO-500 (500 MHz  $^1\text{H}$ , 125.8 MHz  $^{13}\text{C}$ ), or AVANCE-600 (600 MHz  $^1\text{H}$ , 150.9 MHz  $^{13}\text{C}$ , 564.7 MHz  $^{19}\text{F}$ ) spectrometers. NMR data were collected at 25 °C unless otherwise noted. NMR data are reported as follows: chemical shift (multiplicity [singlet (s), broad singlet (br s), doublet (d), doublet of doublets (dd), triplet (t), doublet of triplets (dt), doublet of doublet of triplets (ddt), quartet (q) quintet (quin), sextet (sextet), apparent doublet (ad), multiplet (m)], coupling constants [Hz], integration). Chemical shifts are reported in ppm ( $\delta$ ). X-ray diffraction data were obtained at the UCI Department of Chemistry X-ray Crystallography facility using a Bruker X8 Prospector APEX II diffractometer. X-ray data were collected at 92 K, and APEX3<sup>20</sup> program package was used to determine the unit-cell parameters and for data collection (10 sec/frame scan time). The raw frame data was processed using SAINT<sup>21</sup> and SADABS<sup>22</sup> to yield the reflection data file. Subsequent calculations were carried out using the SHELXTL<sup>23</sup> program package. Infrared (IR) absorption data were collected on a Thermo Scientific Nicolet iS5 FTIR spectrometer. Reagents were purchased from commercial vendors and used without further purification unless otherwise noted. Metal complex Ru-MACHO® was purchased from STREM Chemicals, Inc. and used without further purification. Impurities present in the  $^{31}\text{P}$  NMR spectrum of Ru-MACHO® in THF- $d_8$  are labeled below:

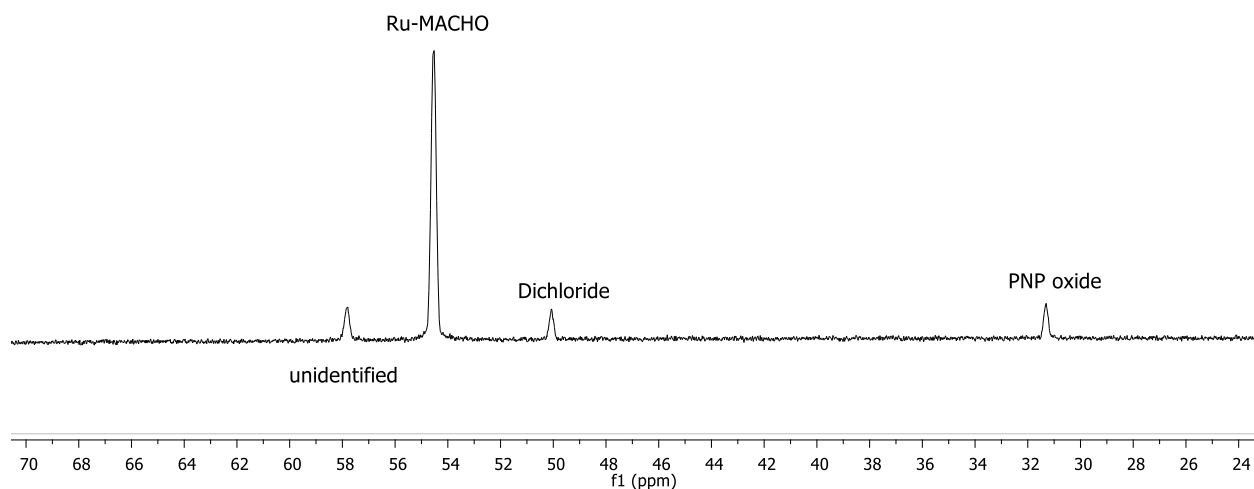


**Figure 3.9.**  $^1\text{H}$  NMR Spectra of Ru-MACHO® from STREAM Chemicals in  $\text{THF-}d_8$ . Impurities are labeled and were present following opening of the purchased bottle in a glovebox.

#### 3.4.1.1 Method A: Superhydride® Reduction

This procedure is adapted from a procedure reported by Milstein.<sup>24</sup> In a glovebox, an oven-dried 20 mL scintillation vial equipped with a stir bar was charged with Ru-MACHO®, and THF, and the resulting suspension was allowed to stir for 30 min. The reducing agent  $\text{LiEt}_3\text{BH}$  (Super-Hydride®) was added dropwise and the reaction mixture continued to stir for 3 h at room temperature. The resulting yellow solution was concentrated en vacuo and washed with pentane (x 3). After washing, the residual pale yellow solid was brought up in toluene, filtered, and concentrated en vacuo.

#### 3.4.1.2 Method B: NaH Reduction

In a glovebox, an oven-dried 20 mL scintillation vial equipped with a stir bar was charged with Ru-MACHO®, NaH, and THF. The suspension was allowed to stir at  $45^\circ\text{C}$  for 18 h. The resulting yellow solution was cooled to room temperature and filtered through celite. The filtrate was concentrated en vacuo and washed with pentane (x 3), producing a pale yellow powder.

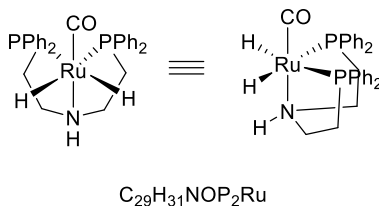
### 3.4.1.3 Method C: Stoichiometric CO<sub>2</sub> Reduction

In a glovebox, a J-Young NMR tube was charged with 0.75 mL of a solution of **3.4** (3 mg, 5 μmol) in THF-*d*<sub>8</sub>. The J-Young NMR tube was attached to a Schlenk line connected to a CO<sub>2</sub> gas cylinder, and was freeze-pump-thawed with CO<sub>2</sub> (x 3) to ensure proper incorporation of CO<sub>2</sub>. The J-Young tube was sonicated for 60 s and NMR spectra were obtained immediately.

### 3.4.1.4 Method D: Stoichiometric Carbamate Reduction

In a glovebox, a J-Young NMR tube was charged with 0.75 mL of a solution of **3.4** (3 mg, 5 μmol) in THF-*d*<sub>8</sub>. Dimethylammonium dimethyl carbamate (0.03 mL, 2 mmol) was added to the solution. The J-Young tube was agitated for 1 h and NMR spectra were obtained immediately after.

## 3.4.2 Characterization Data for Ru-MACHO Dihydride



### **Carbonyldihydrido bis[2-(diphenylphosphinomethyl)ethyl]aminoethylamino ruthenium**

**(II) (3.4)** Characterization data reported herein is from product isolated via Method B. The following amounts of reagents were used: Ru-MACHO® (45 mg, 0.07 mmol, 1.0 equiv), NaH (4 mg, 0.17 mmol, 2.4 equiv), THF (10 mL). Yield = 100% (based on complete conversion observed via crude NMR); <sup>1</sup>H NMR (600 MHz, THF-*d*<sub>8</sub>) δ 7.79 (dd, *J* = 11.4 Hz, 6.1 Hz, 2H), 7.86 (m, 4H), 7.72 (m, 8H), 7.07 (m, 2H), 7.02 (m, 2H), 6.88 (atd, *J* = 7.9 Hz, 1.4 Hz, 2H), 6.14 (br s, 1H), 5.51 (br t, *J* = 10.7 Hz, 1H), 3.23 (br t, *J* = 21.0 Hz, 1H), 2.81 (ad, *J* = 11.1 Hz, 1H), 2.34 (m, 4H), 2.15 (d, *J* = 5.2 Hz, 1H), 1.87 (m, 1H), -6.00 (m, 1H) -6.69 (dd, *J* = 92.0 Hz, 22.6 Hz, 1H); <sup>13</sup>C NMR (125.8 MHz, THF-*d*<sub>8</sub>) δ 188.9 (s), 135.6 (s), 134.1 (s), 131.1 (s), 129.6 (d, *J* = 56.1 Hz),

62.6 (s), 30.1 (s); **<sup>31</sup>P NMR** (242.9 MHz, THF-*d*<sub>8</sub>) δ 67.72 (br s, 1P), 57.70 (d, *J* = 90.2 Hz, 1P); **<sup>31</sup>P {<sup>1</sup>H} NMR** (242.9 MHz, THF-*d*<sub>8</sub>) δ 67.72 (br s, 1P), 57.49 (br s, 1P); **IR** (neat) 2849, 1894, 1856, 1829, 1541, 1481, 1453, 1432, 1403, 1352, 1096 cm<sup>-1</sup>; **HRMS** (TOF MS ES+) *m/z* calcd for C<sub>29</sub>H<sub>30</sub>NOP<sub>2</sub>Ru (M – H)<sup>+</sup> 566.0879, found 566.087; **X-ray Crystallography** (generated from crystals isolated following Method A):

Identification code	jyy267 (Alissa Matus)
Empirical formula	C <sub>29</sub> H <sub>31</sub> N O P <sub>2</sub> Ru •2(C <sub>4</sub> H <sub>8</sub> O)
Formula weight	716.76
Temperature	93(2) K
Wavelength	1.54178 Å
Crystal system	Triclinic
Space group	<i>P</i> $\bar{1}$
Unit cell dimensions	<i>a</i> = 10.3555(6) Å $\alpha$ = 75.125(2)°.
	<i>b</i> = 12.7396(7) Å $\beta$ = 73.399(2)°.
	<i>c</i> = 13.9772(8) Å $\gamma$ = 86.148(2)°.
Volume	1707.83(17) Å <sup>3</sup>
<i>Z</i>	2
Density (calculated)	1.394 Mg/m <sup>3</sup>
Absorption coefficient	4.884 mm <sup>-1</sup>
F(000)	748
Crystal color	colorless
Crystal size	0.195 x 0.151 x 0.137 mm <sup>3</sup>
Theta range for data collection	3.406 to 68.824°
Index ranges	-12 ≤ <i>h</i> ≤ 12, -15 ≤ <i>k</i> ≤ 15, -16 ≤ <i>l</i> ≤ 16
Reflections collected	47693
Independent reflections	6263 [R(int) = 0.0375]
Completeness to theta = 67.679°	99.8 %
Absorption correction	Semi-empirical from equivalents
Max. and min. transmission	0.5213 and 0.4143
Refinement method	Full-matrix least-squares on F <sup>2</sup>
Data / restraints / parameters	6263 / 0 / 454

Goodness-of-fit on F <sup>2</sup>	1.058
Final R indices [I > 2σ(I) = 6122 data]	R1 = 0.0213, wR2 = 0.0526
R indices (all data, 0.83 Å)	R1 = 0.0218, wR2 = 0.0528
Largest diff. peak and hole	0.478 and -0.366 e.Å <sup>-3</sup>

### 3.5 References

- (1) Kar, S.; Sen, R.; Kothandaraman, J.; Goepfert, A.; Chowdhury, R.; Munoz, S. B.; Haiges, R.; Prakash, G. K. S. Mechanistic Insights into Ruthenium-Pincer-Catalyzed Amine-Assisted Homogeneous Hydrogenation of CO<sub>2</sub> to Methanol. *Journal of the American Chemical Society* **2019**, *141* (7), 3160-3170. DOI: 10.1021/jacs.8b12763.
- (2) Olah, G. A.; Goepfert, A.; Prakash, G. K. S. Chemical Recycling of Carbon Dioxide to Methanol and Dimethyl Ether: From Greenhouse Gas to Renewable, Environmentally Carbon Neutral Fuels and Synthetic Hydrocarbons. *The Journal of Organic Chemistry* **2009**, *74* (2), 487-498. DOI: 10.1021/jo801260f.
- (3) Olah, G. A.; Prakash, G. K. S.; Goepfert, A. Anthropogenic Chemical Carbon Cycle for a Sustainable Future. *Journal of the American Chemical Society* **2011**, *133* (33), 12881-12898. DOI: 10.1021/ja202642y.
- (4) Cheon, J.; Yang, J. Y.; Koper, M.; Ishitani, O. From Pollutant to Chemical Feedstock: Valorizing Carbon Dioxide through Photo- and Electrochemical Processes. *Accounts of Chemical Research* **2022**, *55* (7), 931-932. DOI: 10.1021/acs.accounts.2c00129.
- (5) Kar, S.; Goepfert, A.; Prakash, G. K. S. Integrated CO<sub>2</sub> Capture and Conversion to Formate and Methanol: Connecting Two Threads. *Accounts of Chemical Research* **2019**, *52* (10), 2892-2903. DOI: 10.1021/acs.accounts.9b00324.

- (6) Kar, S.; Kothandaraman, J.; Goeppert, A.; Prakash, G. K. S. Advances in catalytic homogeneous hydrogenation of carbon dioxide to methanol. *Journal of CO<sub>2</sub> Utilization* **2018**, *23*, 212-218. DOI: <https://doi.org/10.1016/j.jcou.2017.10.023>.
- (7) Rezayee, N. M.; Huff, C. A.; Sanford, M. S. Tandem Amine and Ruthenium-Catalyzed Hydrogenation of CO<sub>2</sub> to Methanol. *Journal of the American Chemical Society* **2015**, *137* (3), 1028-1031. DOI: 10.1021/ja511329m.
- (8) Jakobsen, J. B.; Rønne, M. H.; Daasbjerg, K.; Skrydstrup, T. Are Amines the Holy Grail for Facilitating CO<sub>2</sub> Reduction? *Angewandte Chemie International Edition* **2021**, *60* (17), 9174-9179. DOI: <https://doi.org/10.1002/anie.202014255>.
- (9) Kar, S.; Goeppert, A.; Kothandaraman, J.; Prakash, G. K. S. Manganese-Catalyzed Sequential Hydrogenation of CO<sub>2</sub> to Methanol via Formamide. *ACS Catalysis* **2017**, *7* (9), 6347-6351. DOI: 10.1021/acscatal.7b02066.
- (10) Kothandaraman, J.; Goeppert, A.; Czaun, M.; Olah, G. A.; Prakash, G. K. S. Conversion of CO<sub>2</sub> from Air into Methanol Using a Polyamine and a Homogeneous Ruthenium Catalyst. *Journal of the American Chemical Society* **2016**, *138* (3), 778-781. DOI: 10.1021/jacs.5b12354.
- (11) Sen, R.; Goeppert, A.; Kar, S.; Prakash, G. K. S. Hydroxide Based Integrated CO<sub>2</sub> Capture from Air and Conversion to Methanol. *Journal of the American Chemical Society* **2020**, *142* (10), 4544-4549. DOI: 10.1021/jacs.9b12711.
- (12) Balaraman, E.; Gunanathan, C.; Zhang, J.; Shimon, L. J. W.; Milstein, D. Efficient hydrogenation of organic carbonates, carbamates and formates indicates alternative routes to methanol based on CO<sub>2</sub> and CO. *Nature Chemistry* **2011**, *3* (8), 609-614. DOI: 10.1038/nchem.1089.

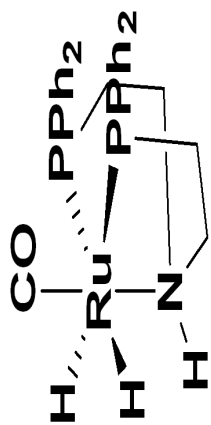
- (13) Alberico, E.; Lennox, A. J. J.; Vogt, L. K.; Jiao, H.; Baumann, W.; Drexler, H.-J.; Nielsen, M.; Spannenberg, A.; Checinski, M. P.; Junge, H.; et al. Unravelling the Mechanism of Basic Aqueous Methanol Dehydrogenation Catalyzed by Ru–PNP Pincer Complexes. *Journal of the American Chemical Society* **2016**, *138* (45), 14890-14904. DOI: 10.1021/jacs.6b05692.
- (14) Yao, Q. Ruthenium, carbonyl[2-(diphenylphosphino-κP)-N-[2-(diphenylphosphino-κP)ethyl]ethanamine-κN][tetrahydroborato(1-)-κH]-hydrido, (OC-6-13). In *Encyclopedia of Reagents for Organic Synthesis (EROS)*, pp 1-3.
- (15) Crabtree, R. H.; Siegbahn, P. E. M.; Eisenstein, O.; Rheingold, A. L.; Koetzle, T. F. A New Intermolecular Interaction: Unconventional Hydrogen Bonds with Element–Hydride Bonds as Proton Acceptor. *Accounts of Chemical Research* **1996**, *29* (7), 348-354. DOI: 10.1021/ar950150s.
- (16) Shen, J.; Stevens, E. D.; Nolan, S. P. Synthesis and Reactivity of the Ruthenium(II) Dihydride Ru(Ph<sub>2</sub>PNMeNMePPh<sub>2</sub>)<sub>2</sub>H<sub>2</sub>. *Organometallics* **1998**, *17* (18), 3875-3882. DOI: 10.1021/om9802212.
- (17) Zhang, P.; Ni, S.-F.; Dang, L. Steric and Electronic Effects of Bidentate Phosphine Ligands on Ruthenium(II)-Catalyzed Hydrogenation of Carbon Dioxide. *Chemistry – An Asian Journal* **2016**, *11* (18), 2528-2536. DOI: <https://doi.org/10.1002/asia.201600611>.
- (18) Lao, D. B.; Galan, B. R.; Linehan, J. C.; Heldebrant, D. J. The steps of activating a prospective CO<sub>2</sub> hydrogenation catalyst with combined CO<sub>2</sub> capture and reduction. *Green Chemistry* **2016**, *18* (18), 4871-4874, 10.1039/C6GC01800A. DOI: 10.1039/C6GC01800A.
- (19) DuBois, D. L.; Berning, D. E. Hydricity of transition-metal hydrides and its role in CO<sub>2</sub> reduction. *Applied Organometallic Chemistry* **2000**, *14* (12), 860-862. DOI: [https://doi.org/10.1002/1099-0739\(200012\)14:12<860::AID-AOC87>3.0.CO;2-A](https://doi.org/10.1002/1099-0739(200012)14:12<860::AID-AOC87>3.0.CO;2-A).
- (20) APEX3 Version 2018.1-0, Bruker AXS, Inc.; Madison, WI 2018.



- (21) SAINT Version 8.38a, Bruker AXS, Inc.; Madison, WI 2013.
- (22) Sheldrick, G. M. SADABS, Version 2014/5, Bruker AXS, Inc.; Madison, WI 2014.
- (23) Sheldrick, G. M. SHELXTL, Version 2014/7, Bruker AXS, Inc.; Madison, WI 2014.
- (24) Zhang, J.; Leitus, G.; Ben-David, Y.; Milstein, D. Efficient Homogeneous Catalytic Hydrogenation of Esters to Alcohols. *Angewandte Chemie International Edition* **2006**, *45* (7), 1113-1115. DOI: <https://doi.org/10.1002/anie.200503771>.

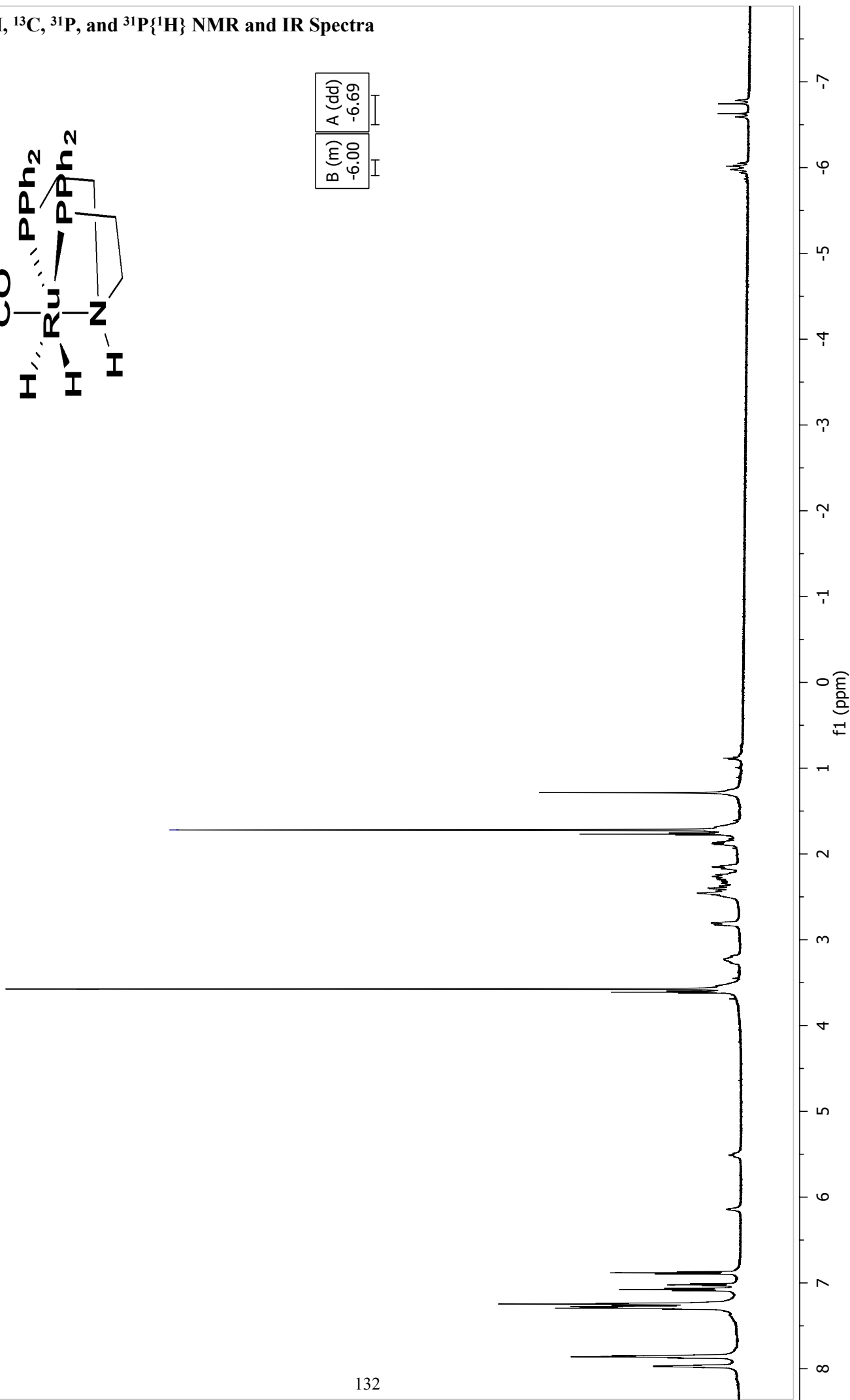
3.6  $^1\text{H}$ ,  $^{13}\text{C}$ ,  $^{31}\text{P}$ , and  $^{31}\text{P}\{^1\text{H}\}$  NMR and IR Spectra

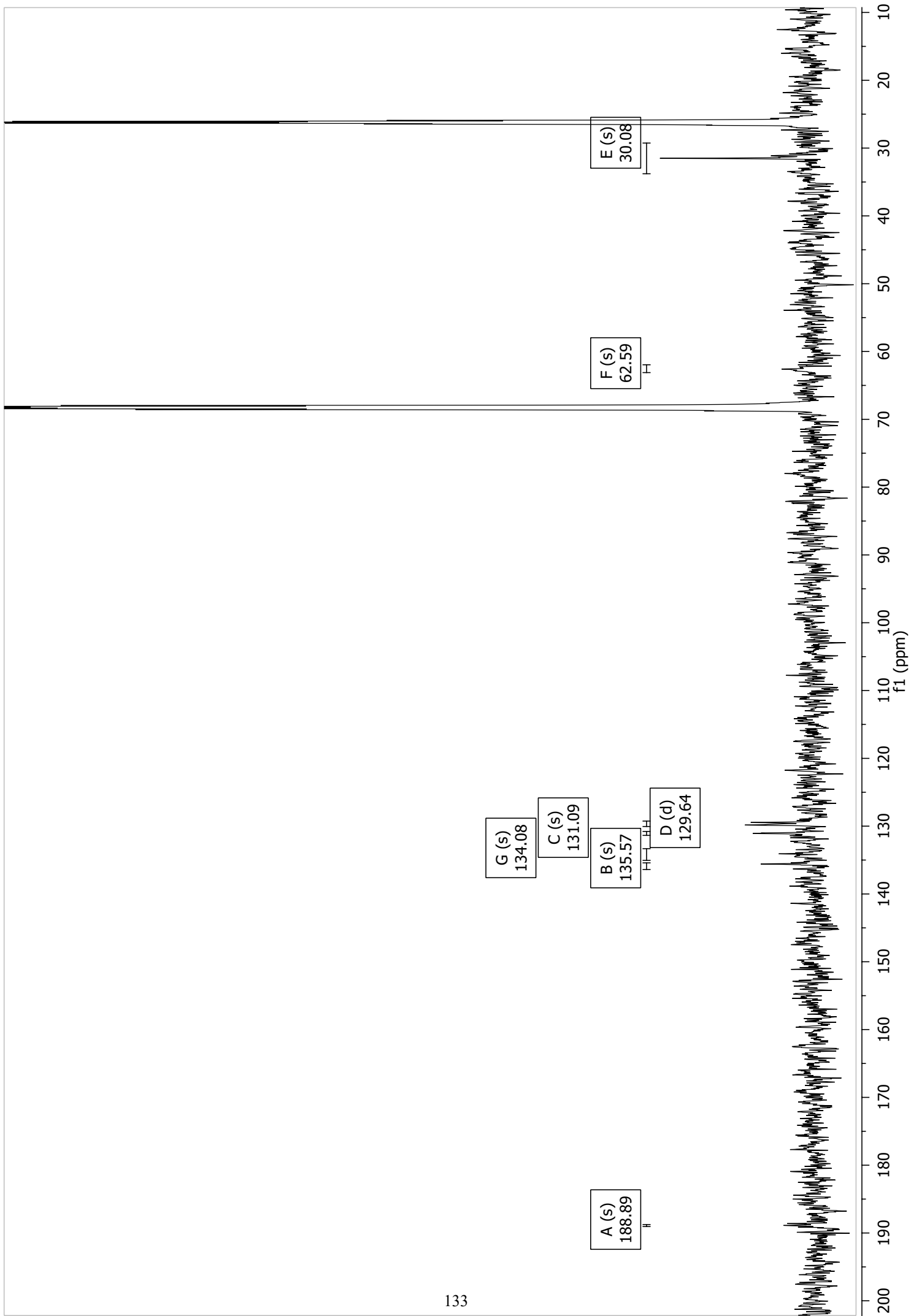
ACM-I-Y-129- NaHcrude-THFd8  
 $^1\text{H}$

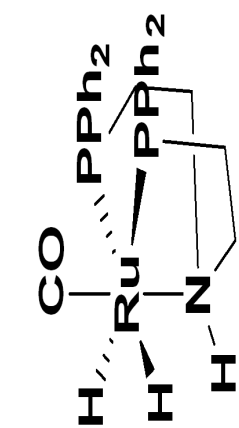


B (m)	A (dd)
-6.00	-6.69

—1.72 THF

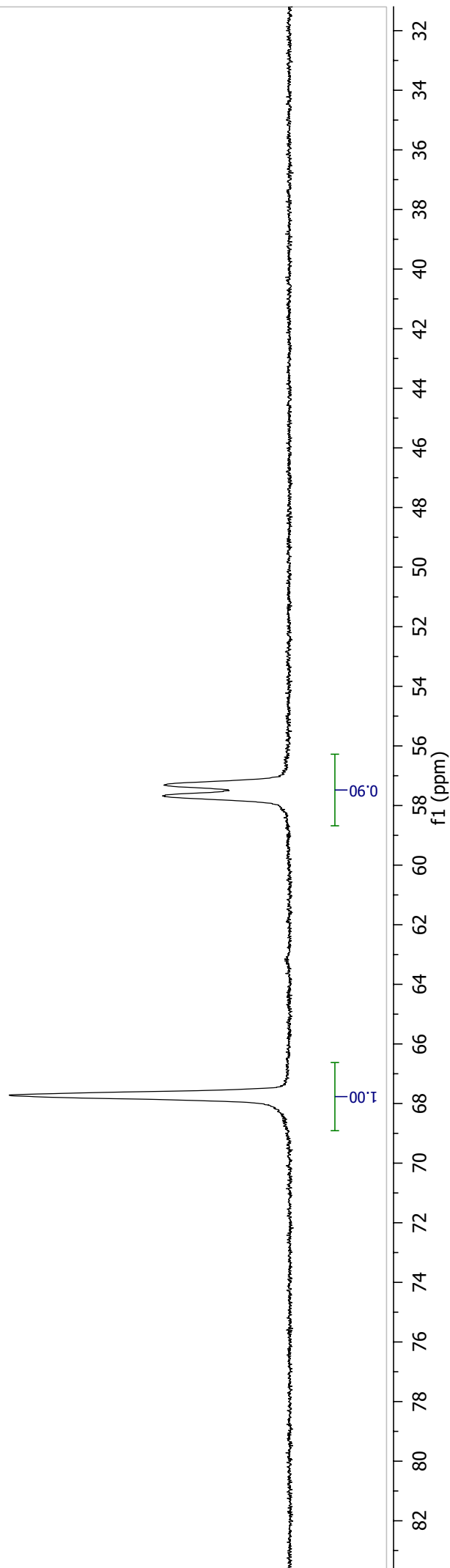


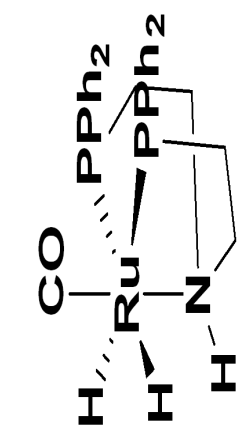




A (s)  
67.72

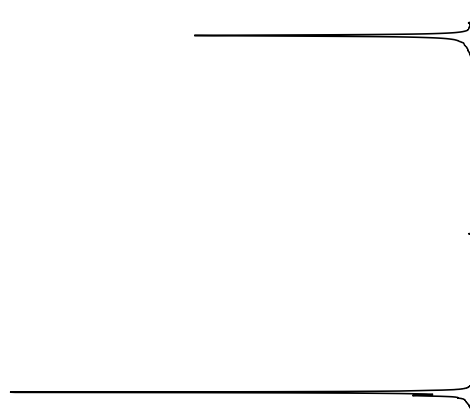
B (d)  
57.49





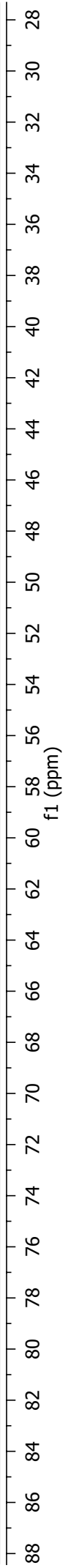
D (s)  
67.72

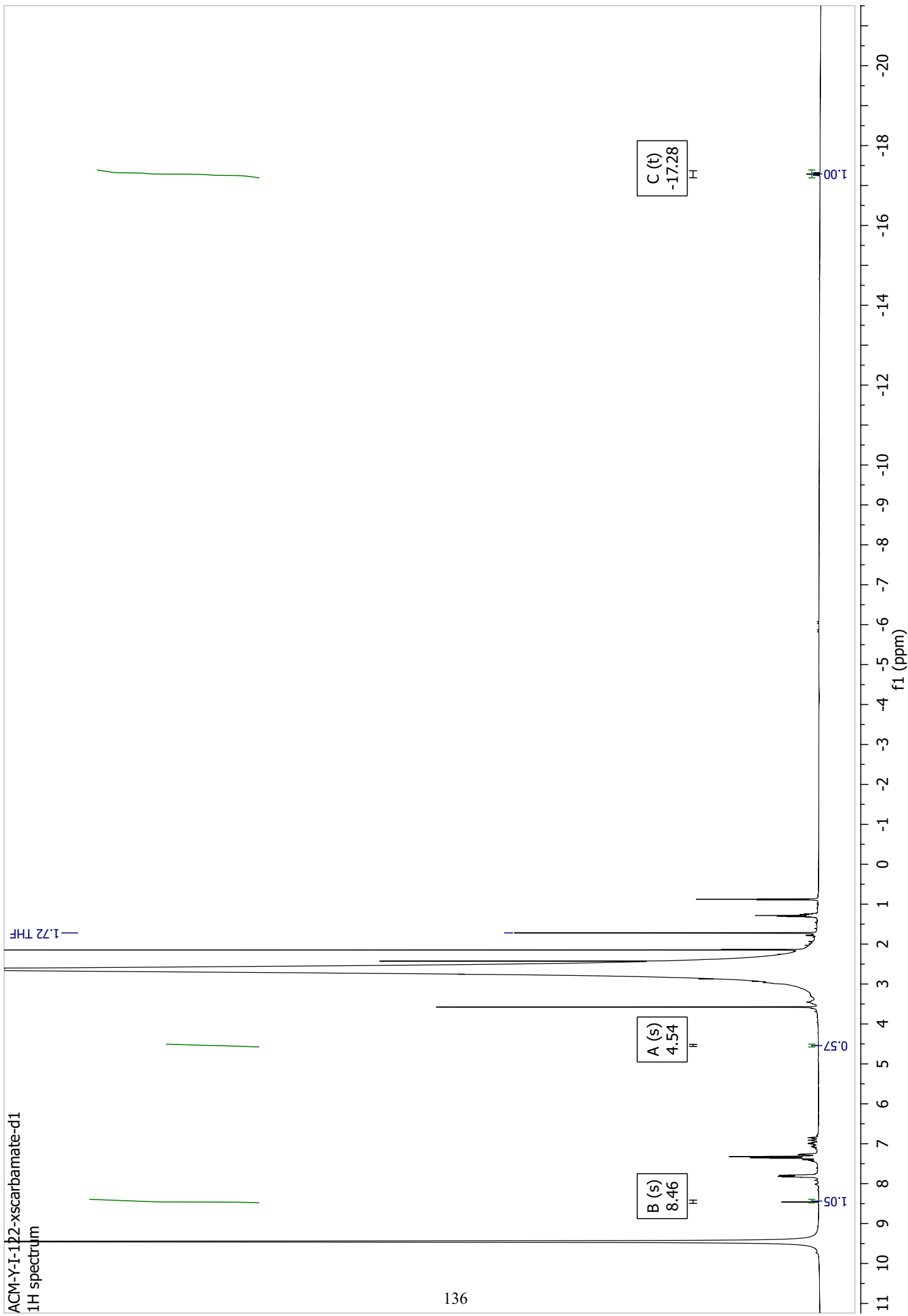
B (s)  
57.49

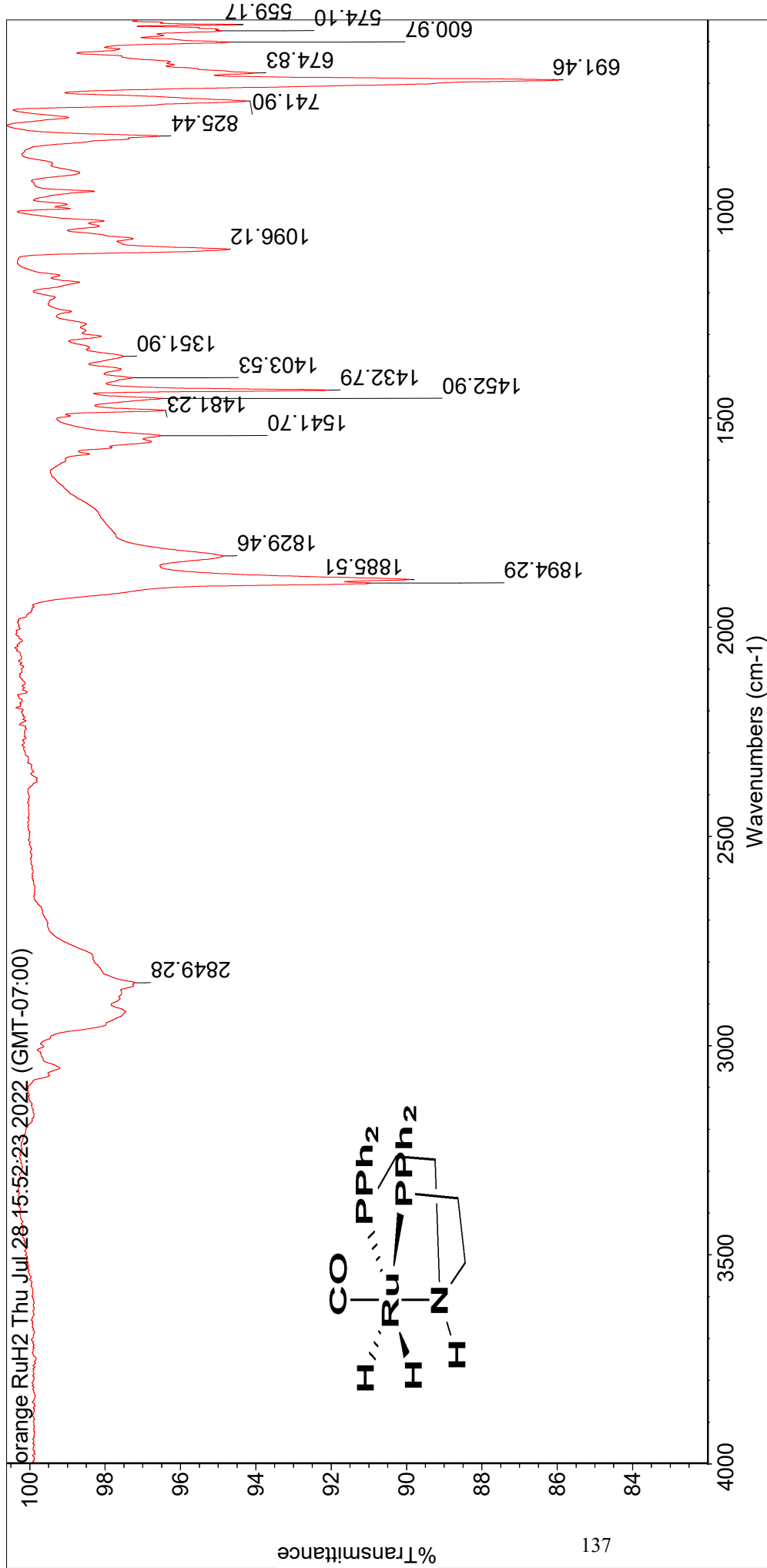


1.00

0.96







Sat Aug 06 15:22:07 2022 (GMT-07:00)

FIND PEAKS:

Spectrum: orange RuH2 Thu Jul 28 15:52:23 2022 (GMT-07:00)

Region: 4000.12 550.10

Absolute threshold: 97.965

Sensitivity: 50

Peak list:

Position:	559.17	Intensity:	94.526
Position:	574.10	Intensity:	94.900
Position:	600.97	Intensity:	94.715
Position:	674.83	Intensity:	94.063
Position:	691.46	Intensity:	85.949
Position:	741.90	Intensity:	94.253
Position:	825.44	Intensity:	96.537

Position:	1096.12	Intensity:	94.710
Position:	1351.90	Intensity:	97.523
Position:	1403.53	Intensity:	97.282
Position:	1432.79	Intensity:	92.069
Position:	1452.90	Intensity:	96.502
Position:	1481.23	Intensity:	96.456
Position:	1541.70	Intensity:	96.527
Position:	1829.46	Intensity:	94.881
Position:	1885.51	Intensity:	89.904
Position:	1894.29	Intensity:	90.957
Position:	2849.28	Intensity:	97.219



**APPENDIX A: Electrochemical Activity of Ru-  
MACHO® for CO<sub>2</sub> Reduction**

## A.1 Introduction

Metal hydride complexes with known reactivity for CO<sub>2</sub> hydrogenation make excellent candidates for use as CO<sub>2</sub> reduction electrocatalysts. Recently, the Yang group demonstrated the use of a Co hydrogenation catalyst as a selective CO<sub>2</sub>-to-formate electrocatalyst in water.<sup>1</sup> Not only is this activity exciting, as there are many hydrogenation catalysts that may be utilized in the same way, but this also demonstrates the potential for mild electrochemical methods to replace harsh hydrogenation conditions. One hydrogenation catalyst of particular interest is Ru-MACHO® (Figure A.1A). This catalyst converts amine-captured CO<sub>2</sub> to formate and methanol via hydrogenation, but has never been explored using electrochemistry.<sup>2-6</sup> The combination of the known reactivity of Ru-MACHO® to reduce carbamates and amides with the electrochemical reactions explored by the Yang group would lead to an ideal reactive carbon capture (RCC) strategy.<sup>7, 8</sup> Unlike other known electrocatalysts, the active reductant version of Ru-MACHO® is a dihydride, which may make electrocatalysis more challenging as the dihydride complex will need to be regenerated using electrochemistry. To this end, this appendix presents cyclic voltammetry (CV) experiments using Ru-MACHO® and the H<sub>2</sub>Ru-MACHO dihydride isolated and discussed in **Chapter 3**.

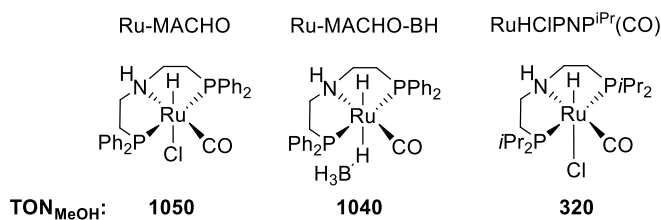


**Figure A.1.** Ru-MACHO®-type hydrogenation catalysts with turnover numbers for MeOH production.

## A.2 Results and Discussion

### A.2.1 Cyclic Voltammetry of Ru-MACHO® upon addition of Water as an Acid Source and 1 atm of CO<sub>2</sub>

Adventitious water is used frequently as an acid source in electrochemical reactions, so it could be useful to rely on water to facilitate electrocatalysis with H<sub>2</sub>Ru-MACHO.<sup>9, 10</sup> Initially, an excess of water was added to determine if a catalytic current for CO<sub>2</sub> reduction with Ru-MACHO® could be observed. The CVs of Ru-MACHO® with an excess of water and 1 atm of CO<sub>2</sub> are presented in Figure A.2. No significant changes were observed by CV, but 2 irreversible reduction events were observed at -2.43V and -2.20V. However, significant current enhancement resulting from direct proton reduction was also not observed, indicating that water is not acidic enough to generate hydrogen with Ru-MACHO®. After the traces pass -3.0 V some crossover was observed at 10 mV/s, which may indicate deposition of reduces products onto the electrode.

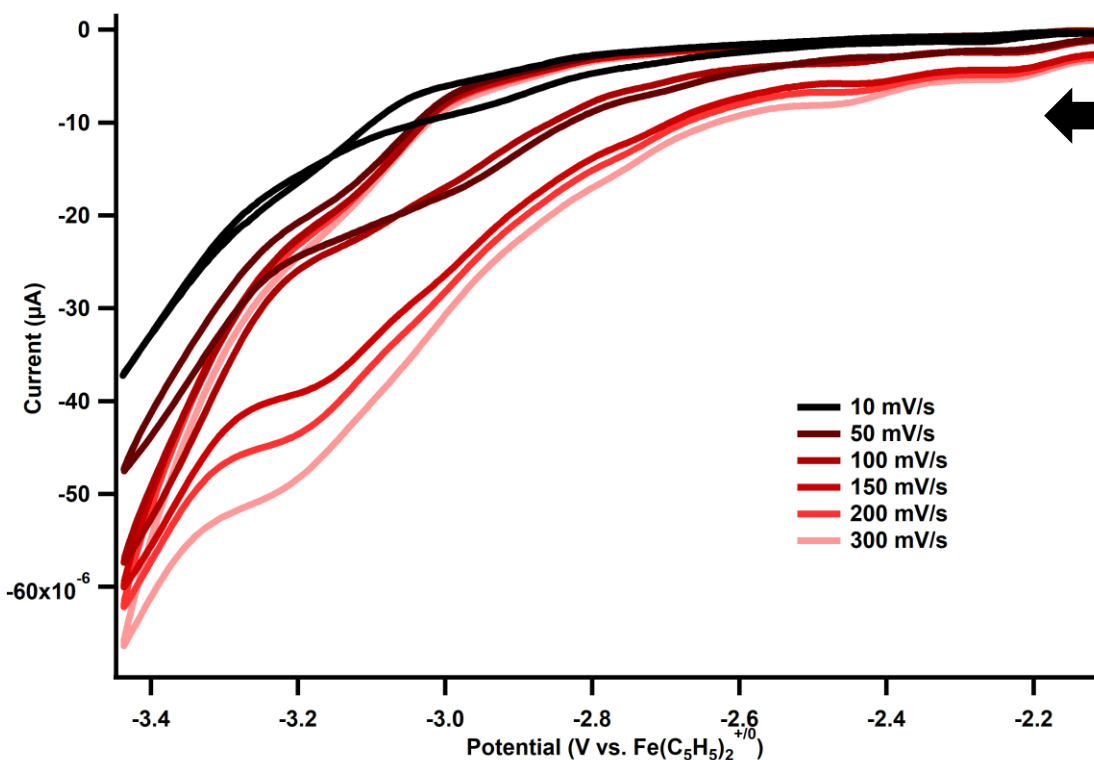


**Figure A.2.** Ru-MACHO® (1mM), CoCp\* (3mM, not pictured), TBAPF<sub>6</sub> (100mM), H<sub>2</sub>O (1.7 mM) under 1 atm CO<sub>2</sub> THF. Before scanning, iR compensation was performed.

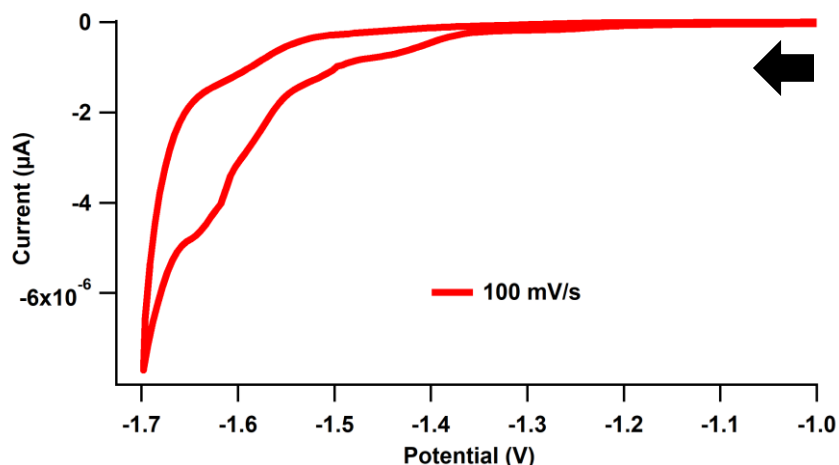


**Figure A.3.** Ru-MACHO® (1mM), TBAPF<sub>6</sub> (100mM), in PhCN. Not iR compensated.

Although the parent complex Ru-MACHO® is only sparingly soluble in MeCN, excitingly the RuMACHO® was easily solubilized in benzonitrile (PhCN), prompting a CV study to identify relevant reductive features (Figure A.3). Two irreversible reductive features were observed at –1.51V and –1.62V. This experiment was performed without internal reference CoCp\* to avoid any side reactivity.

### A.2.2 Cyclic Voltammetry of H<sub>2</sub>Ru-MACHO

Upon isolation of the dihydride H<sub>2</sub>RuMACHO, a series of CV experiments were utilized to examine its reactivity with CO<sub>2</sub>. In **Chapter 3**, the ability of H<sub>2</sub>Ru-MACHO to stoichiometrically convert CO<sub>2</sub> to formate was discussed. Given this reactivity, upon exposure to CO<sub>2</sub> the complex should be consumed entirely. Catalytic current enhancement indicative of CO<sub>2</sub> reduction was not observed by CV, but some degree of current enhancement did occur past –3.1V (Figure A.4).

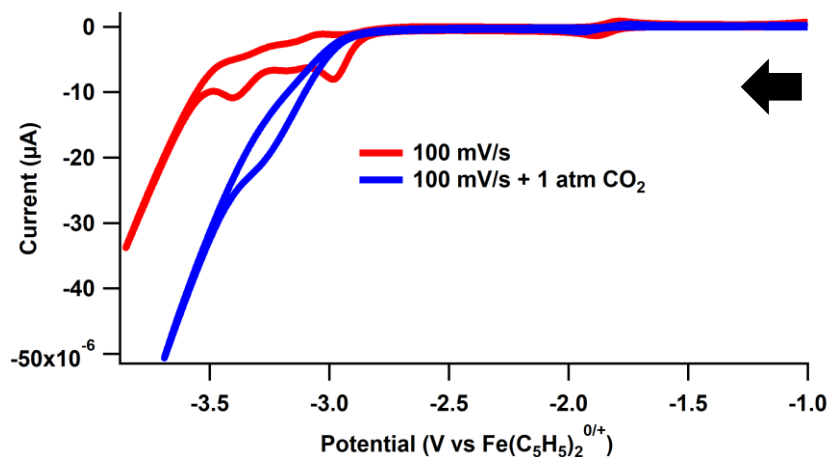


**Figure A.4.** CV of 3mM H<sub>2</sub>RuMACHO, 100 mM TBAPF<sub>6</sub>, 3 mM CoCp\* in THF, under 1 atm of N<sub>2</sub> (red trace), and under and 1 atm CO<sub>2</sub> in THF (blue trace). Not iR compensated.

After the complete consumption of H<sub>2</sub>Ru-MACHO from reaction of CO<sub>2</sub>, I anticipated observing reduction peaks similar to those of the parent Ru-MACHO®, which was not the case (Figure A.4). Increasing the scan rate also did not reveal any significant reductive peaks (Figure A.5). Some possible current enhancement began after -3.1 V, but no other significant reductive features were observed. These data indicate that the H<sub>2</sub>Ru-MACHO complex reacts completely with CO<sub>2</sub>. Addition of water, or a suitable acid, may regenerate the dihydride for further reduction of CO<sub>2</sub>, although the very negative window may facilitate the hydrogen evolution reaction (HER).

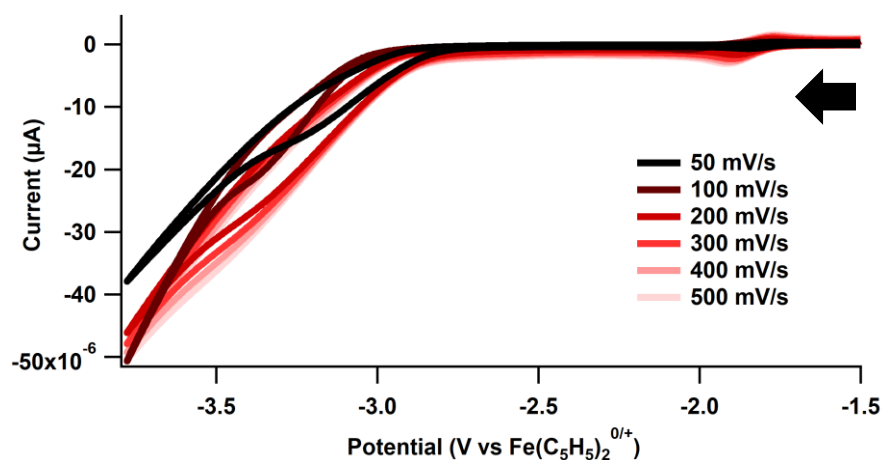


**Figure A.5.** H<sub>2</sub>-Ru-MACHO, TBAPF<sub>6</sub>, CoCp\* and CO<sub>2</sub> in THF. Not iR compensated.

### A.3 Conclusion

Much is still unknown about how Ru-MACHO® will participate in an electrochemical cycle, however a plausible route towards a Ru-MACHO®-based electrochemical system might involve the following: a 2-electron reduction of the parent complex followed by loss of the chloride ligand ( $\text{Ru}^{\text{II}0}$ ), then protonation of the reduced-Ru-MACHO to generate the dihydride ( $\text{Ru}^{\text{0II}}$ ). If from here, the dihydride would react with a substrate to form  $\text{Ru}^{\text{IV}}$ , it may then require 4 electrons to reduce it back to the  $\text{Ru}^{\text{0}}$ . While continued efforts to gauge Ru-MACHO®'s ability to act as an electrocatalyst are required, this preliminary work has identified potential conditions for future electrochemical studies.

### A.4 Experimental Details

All reactions were carried out under a  $\text{N}_2$  or Ar atmosphere, unless otherwise noted. All glassware was oven- or flame-dried prior to use. Solvents were degassed by sparging with argon gas and dried by passage through columns of activated alumina or molecular sieves. Electrochemical experiments were performed using a Pine Wavedriver 10 potentiostat. Electrochemical experiments were carried out in MeCN or PhCN. The working electrode was a glassy carbon disc with a 2mm diameter, the counter electrode was a glassy carbon rod, and a Ag/AgCl pseudoreference electrode was used. Phosphine ligands were purchased from Fisher or STREM Chemicals, and metal complex precursors were purchased from STREM Chemicals. Reagents were purchased from commercial vendors and used without further purification unless otherwise noted.

## A.5 References

- (1) Wang, X. S.; Yang, J. Y. Translating aqueous CO<sub>2</sub> hydrogenation activity to electrocatalytic reduction with a homogeneous cobalt catalyst. *Chemical Communications* **2023**, *59* (3), 338-341, 10.1039/D2CC05473F. DOI: 10.1039/D2CC05473F.
- (2) Kar, S.; Kothandaraman, J.; Goeppert, A.; Prakash, G. K. S. Advances in catalytic homogeneous hydrogenation of carbon dioxide to methanol. *Journal of CO<sub>2</sub> Utilization* **2018**, *23*, 212-218. DOI: <https://doi.org/10.1016/j.jcou.2017.10.023>.
- (3) Kothandaraman, J.; Goeppert, A.; Czaun, M.; Olah, G. A.; Prakash, G. K. S. Conversion of CO<sub>2</sub> from Air into Methanol Using a Polyamine and a Homogeneous Ruthenium Catalyst. *Journal of the American Chemical Society* **2016**, *138* (3), 778-781. DOI: 10.1021/jacs.5b12354.
- (4) Sen, R.; Goeppert, A.; Kar, S.; Prakash, G. K. S. Hydroxide Based Integrated CO<sub>2</sub> Capture from Air and Conversion to Methanol. *Journal of the American Chemical Society* **2020**, *142* (10), 4544-4549. DOI: 10.1021/jacs.9b12711.
- (5) Kar, S.; Goeppert, A.; Prakash, G. K. S. Integrated CO<sub>2</sub> Capture and Conversion to Formate and Methanol: Connecting Two Threads. *Accounts of Chemical Research* **2019**, *52* (10), 2892-2903. DOI: 10.1021/acs.accounts.9b00324.
- (6) Kar, S.; Sen, R.; Kothandaraman, J.; Goeppert, A.; Chowdhury, R.; Munoz, S. B.; Haiges, R.; Prakash, G. K. S. Mechanistic Insights into Ruthenium-Pincer-Catalyzed Amine-Assisted Homogeneous Hydrogenation of CO<sub>2</sub> to Methanol. *Journal of the American Chemical Society* **2019**, *141* (7), 3160-3170. DOI: 10.1021/jacs.8b12763.
- (7) Siegel, R. E.; Pattanayak, S.; Berben, L. A. Reactive Capture of CO<sub>2</sub>: Opportunities and Challenges. *ACS Catalysis* **2023**, *13* (1), 766-784. DOI: 10.1021/acscatal.2c05019.

- (8) Cunningham, D. W.; Barlow, J. M.; Velazquez, R. S.; Yang, J. Y. Reversible and Selective CO<sub>2</sub> to HCO<sub>2</sub><sup>-</sup> Electrocatalysis near the Thermodynamic Potential. *Angewandte Chemie International Edition* **2020**, *59* (11), 4443-4447. DOI: <https://doi.org/10.1002/anie.201913198>.
- (9) Bi, J.; Hou, P.; Liu, F.-W.; Kang, P. Electrocatalytic Reduction of CO<sub>2</sub> to Methanol by Iron Tetradentate Phosphine Complex Through Amidation Strategy. *ChemSusChem* **2019**, *12* (10), 2195-2201. DOI: <https://doi.org/10.1002/cssc.201802929>.
- (10) Zhao, S.-F.; Lu, J.-X.; Bond, A. M.; Zhang, J. Remarkable Sensitivity of the Electrochemical Reduction of Benzophenone to Proton Availability in Ionic Liquids. *Chemistry – A European Journal* **2012**, *18* (17), 5290-5301. DOI: <https://doi.org/10.1002/chem.201103365>.



**APPENDIX B: Stoichiometric Reduction of  
Carbamates with Known CO<sub>2</sub> Reduction  
Catalysts**

## B.1 Introduction

Reactive carbon capture (RCC) describes the combined capture and conversion of CO<sub>2</sub> utilizing capture agents that are capable of being regenerated for repeated use.<sup>1</sup> To accomplish this, suitable homogenous catalysts must be identified. The best candidates for RCC are complexes with known CO<sub>2</sub> reduction abilities, and hydrogenation catalysts that are used to generate methanol from captured CO<sub>2</sub>. Hydrogenation conditions exploit high temperature and pressure to afford the desired transformation, but the catalysts used may be capable of performing the same transformations under more mild, electrochemical conditions.<sup>2-4</sup>

Previous Yang group work demonstrated the selective reduction of CO<sub>2</sub> to formate using metal hydrides, and the successful repurposing of a hydrogenation catalyst for electrochemical CO<sub>2</sub> reduction.<sup>5-8</sup> This exciting work opens the door to other hydrogenation catalysts such as Ru-MACHO® (Figure B.1A) that may serve as suitable electrocatalysts, as discussed in Chapter 3. Combined capture-and-conversion (CCC) of CO<sub>2</sub> in hydrogenation literature can be accomplished using amines, which react with CO<sub>2</sub> to form carbamates.<sup>2, 3, 9-14</sup> These carbamates may perform well in RCC, however, the reactivity of these carbamates is expected to be lower than CO<sub>2</sub> in solution.<sup>1</sup> As such, powerful metal hydrides will have to be utilized to achieve electrochemical conversion of carbamates in RCC systems.<sup>2, 15, 16</sup>

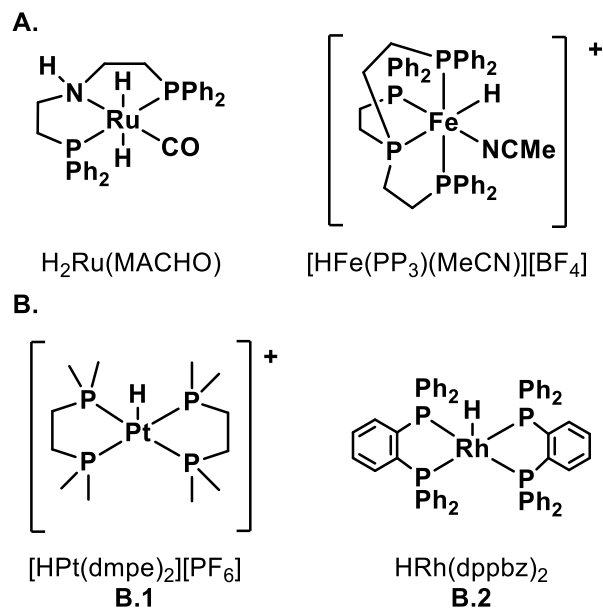
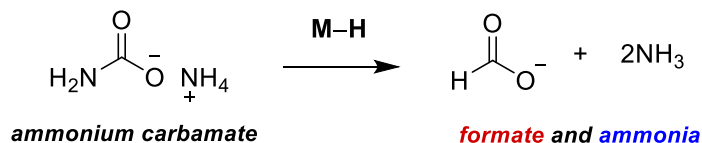


**Figure B.1.** Metal hydride complexes of interest in RCC with amine capture agents. **A:** Metal hydrides known to generate formate and methanol using amine-captured  $\text{CO}_2$ . **B:** Metal hydrides with known  $\text{CO}_2$  reduction activity.

Metal hydrides capable of converting  $\text{CO}_2$  should generate stoichiometric amounts of formate when exposed to  $\text{CO}_2$  in solution.<sup>17</sup> By extension, potential electrocatalysts for conversion of amine-captured  $\text{CO}_2$  should generate formate when mixed 1:1 with captured  $\text{CO}_2$  (Scheme B.1). To identify ideal catalysts for RCC, two known  $\text{CO}_2$ -reduction catalysts (Figure B.1B) were selected for proof-of-concept reductions of ammonium carbamate, a commercially available carbamate salt.

**Scheme B.1: Reduction of Ammonium Carbamate with a Metal Hydride.**



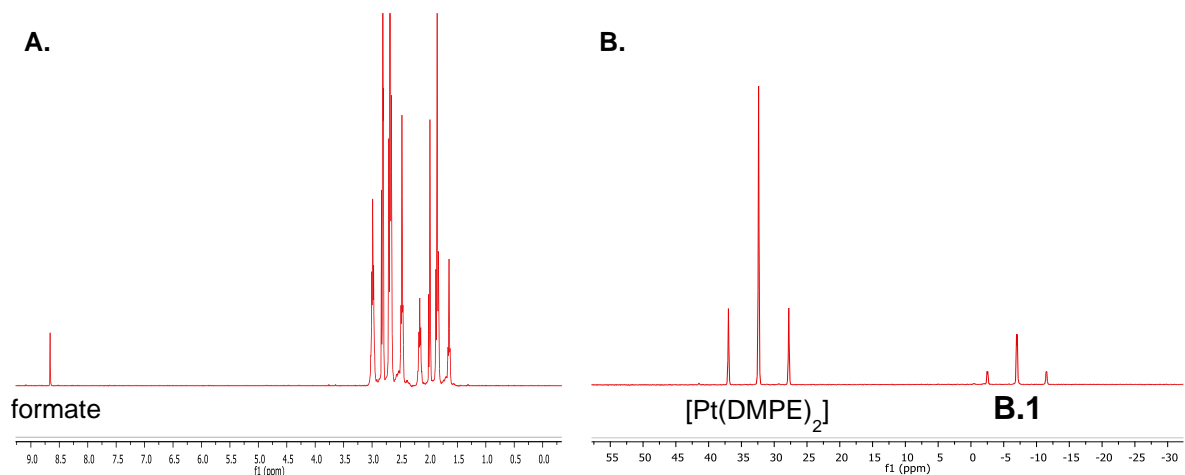
## B.2 Results and Discussion

Ammonium carbamate was determined to have poor solubility in several organic solvents, including MeCN, benzene, pentane, heptane, THF, diethyl ether, and DCM. DMSO is the only solvent examined that fully solubilized ammonium carbamate. These solvents were examined for

their ability to solubilize ammonium carbamate, but ultimately MeCN was selected for initial stoichiometric reduction because it would be the ideal solvent for any electrochemical experiments planned in the future.

### B.2.1 [HPt(DMPE)<sub>2</sub>] and Ammonium Carbamate

The complex [HPt(DMPE)<sub>2</sub>][PF<sub>6</sub>] (**B.1**) was synthesized according to reported procedures.<sup>18, 19</sup> A 1:1 amount of **B.1** and ammonium carbamate was brought up in MeCN-*d*<sub>3</sub> in an NMR tube. Immediately following the preparation of this solution, formate was detected by <sup>1</sup>H NMR (Figure B.2A). <sup>31</sup>P NMR also showed the conversion of the hydride to [Pt(DMPE)<sub>2</sub>][PF<sub>6</sub>]<sub>2</sub> (Figure B.2B), however, after 24 h no additional formate had been produced while the hydride had been consumed completely. It is unclear what the hydride reacted to form, as there was no H<sub>2</sub> detected by NMR. However, NMR cannot completely rule out HER as H<sub>2</sub> quantification using NMR is not reliable at room temperature.<sup>20</sup>



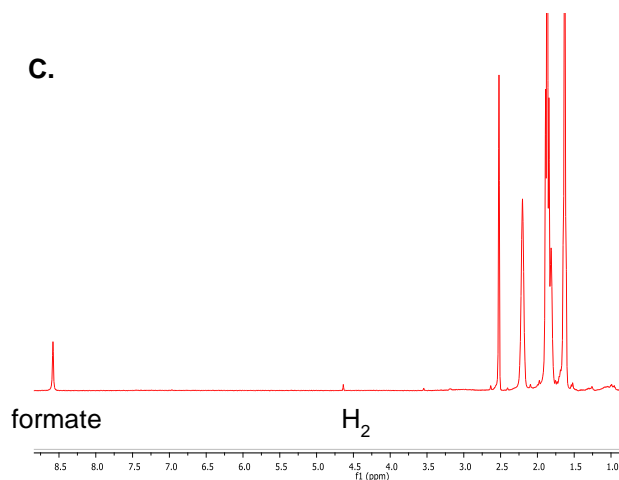


**Figure B.2.** NMR spectra of **B.1** and ammonium carbamate. **A:**  $^1\text{H}$  NMR spectrum taken in  $\text{MeCN-}d_3$ . **B:**  $^{31}\text{P}$  NMR spectrum taken in  $\text{MeCN-}d_3$ . **C:**  $^1\text{H}$  NMR spectrum taken in  $\text{DMSO-}d_6$ .

Further investigation with ammonium carbamate was performed in  $\text{DMSO-}d_6$ , with the purpose of increasing solubility of the substrate. A 1:1 mixture of **B.1** and ammonium carbamate in  $\text{DMSO-}d_6$  was prepared in an NMR tube, and  $^1\text{H}$  NMR showed formate production with some detected  $\text{H}_2$  (Figure B.2B). While  $\text{H}_2$  was detected for the first time, the reaction was monitored over the course of 27 hours to quantify the amount of formate produced over time. The initial yield of formate was less than 1 percent, and only increased to 7.2% after 27 hours (Table B.1). At this timepoint,  $^{31}\text{P}$  NMR showed the hydride had completely been consumed. As opposed to the trial in  $\text{MeCN-}d_3$ , this time it is likely that the additional hydride consumption resulted from HER.

**Table B.1: Formate Quantification in  $\text{DMSO-}d_6$**

Time (h)	Yield (%) <sup>a</sup>
0.17	0.1
1	4.4
24	6.1
27	7.2

<sup>a</sup>Yield determined by  $^1\text{H}$  NMR using benzene as an internal standard.

### B.2.2 $\text{HRh}(\text{DPPBz})_2$ and Ammonium Carbamate

The complex **B.1** demonstrated the ability of a  $\text{CO}_2$  conversion catalyst to convert a carbamate to formate, but the reaction appeared to be slow and low-yielding. The stronger hydride donor,  $\text{HRh}(\text{DPPBz})_2$  (**B.2**), could produce formate more quickly, although HER is more likely

with stronger metal hydrides.<sup>21,22</sup> DMSO-*d*<sub>6</sub> was selected for initial use with ammonium carbamate and **B.2** for solubility purposes. The complex **B.2** was synthesized following published procedures.<sup>21</sup> However, the decomposition of **B.2** in DMSO-*d*<sub>6</sub> was observed, generating significant amounts of water after only 15 minutes at room temperature (Figure B.3A). The decomposition of DMSO to water is known, and likely began after hydride transfer from **B.2**.<sup>23,24</sup> The disappearance of strong doublet peaks in the <sup>31</sup>P NMR was also rapid, and may indicate further reactivity with DMSO (Figure B.3B). No color change of the NMR sample solution was observed. To avoid decomposition of the hydride, MeCN-*d*<sub>3</sub> was used for carbamate reduction with **B.2** despite the limited solubility of ammonium carbamate.

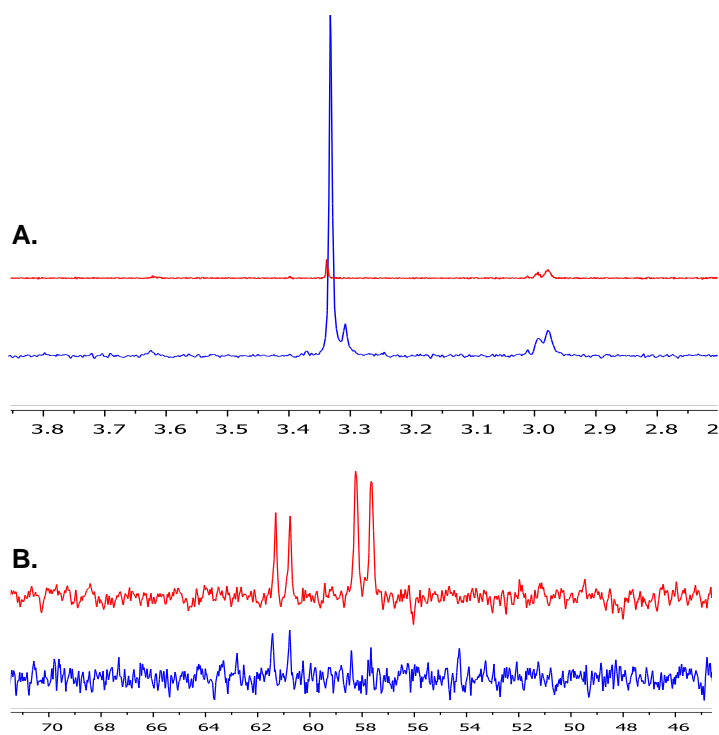


**Figure B.3.** NMR Spectra of **B.2** in DMSO-*d*<sub>6</sub>. **A:** <sup>1</sup>H NMR spectra at 5 minutes (red) and 15 minutes (blue). **B:** <sup>31</sup>P NMR spectra at 5 minutes (red) and 15 minutes (blue).

Upon addition of ammonium carbamate to an NMR sample of **B.2** in MeCN- $d_3$ , formate could quickly be detected without  $H_2$  detected (Figure B.4A). While the amount of formate generated was trace,  $^{31}P$  NMR quickly revealed that the hydride reacted to completion, generating the charged Rh(III) complex (Figure B.4B). No further formate was generated in this sample.

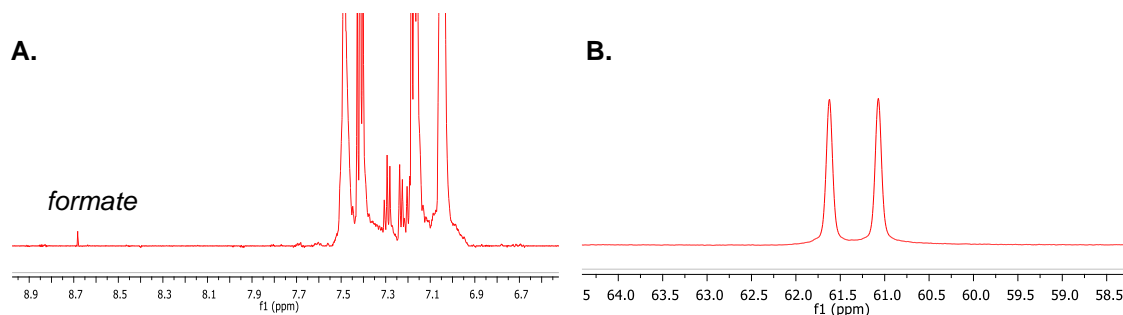


**Figure B.4.** NMR Spectra of **B.2** and ammonium carbamate in MeCN- $d_3$ . **A:**  $^1H$  NMR spectrum. **B:**  $^{31}P$  NMR spectrum.

### B.3 Conclusion

Ammonium carbamate, while stable in solution and commercially available, does not appear to be a suitable substrate to model the conversion of amine-captured  $CO_2$  to formate. While to some extent, it is encouraging to see the formation of formate from stoichiometric reactions of carbamate and **B.1** or **B.2**, the consistent solubility issues caused by the carbamate make this data limited for interpretation. An alternative carbamate could be dimethylammonium dimethylcarbamate, which has good solubility in some organic solvents, but will likely also lead to some observable HER and the ammonium ion is very acidic. However, these stoichiometric reductions will act as a foundation for the design of other attempts to quantify formate production from carbamates using  $CO_2$  reduction catalysts.

## B.4 Experimental Details

All reactions were carried out under a N<sub>2</sub> atmosphere, unless otherwise noted. All glassware was oven- or flame-dried prior to use. Solvents were degassed by sparging with argon gas and dried by passage through columns of activated alumina or molecular sieves. <sup>1</sup>H NMR spectra were recorded on Bruker DRX-400 (400 MHz <sup>1</sup>H), GN-500 (500 MHz <sup>1</sup>H, 125.4 MHz <sup>13</sup>C), CRYO-500 (500 MHz <sup>1</sup>H, 125.8 MHz <sup>13</sup>C), or AVANCE-600 (600 MHz <sup>1</sup>H, 150.9 MHz <sup>13</sup>C, 564.7 MHz <sup>19</sup>F) spectrometers. NMR data were collected at 25 °C unless otherwise noted. Deuterated solvents were purchased from Cambridge Isotopes Laboratories, Inc. and were degassed and stored over activated 3 Å molecular sieves prior to use. NMR spectra were analyzed and exported as figures using MestReNova software. Phosphine ligands were purchased from Fisher or STREM Chemicals, and metal complex precursors were purchased from STREM Chemicals. Reagents were purchased from commercial vendors and used without further purification unless otherwise noted.

## B.5 References

- (1) Siegel, R. E.; Pattanayak, S.; Berben, L. A. Reactive Capture of CO<sub>2</sub>: Opportunities and Challenges. *ACS Catalysis* **2023**, *13* (1), 766-784. DOI: 10.1021/acscatal.2c05019.
- (2) Kar, S.; Goeppert, A.; Prakash, G. K. S. Integrated CO<sub>2</sub> Capture and Conversion to Formate and Methanol: Connecting Two Threads. *Accounts of Chemical Research* **2019**, *52* (10), 2892-2903. DOI: 10.1021/acs.accounts.9b00324.
- (3) Kar, S.; Sen, R.; Kothandaraman, J.; Goeppert, A.; Chowdhury, R.; Munoz, S. B.; Haiges, R.; Prakash, G. K. S. Mechanistic Insights into Ruthenium-Pincer-Catalyzed Amine-Assisted Homogeneous Hydrogenation of CO<sub>2</sub> to Methanol. *Journal of the American Chemical Society* **2019**, *141* (7), 3160-3170. DOI: 10.1021/jacs.8b12763.



- (4) Jeletic, M. S.; Hulley, E. B.; Helm, M. L.; Mock, M. T.; Appel, A. M.; Wiedner, E. S.; Linehan, J. C. Understanding the Relationship Between Kinetics and Thermodynamics in CO<sub>2</sub> Hydrogenation Catalysis. *ACS Catalysis* **2017**, *7* (9), 6008-6017. DOI: 10.1021/acscatal.7b01673.
- (5) Ceballos, B. M.; Yang, J. Y. Directing the reactivity of metal hydrides for selective CO<sub>2</sub> reduction. *Proceedings of the National Academy of Sciences* **2018**, *115* (50), 12686-12691. DOI: doi:10.1073/pnas.1811396115.
- (6) Ceballos, B. M.; Yang, J. Y. Highly Selective Electrocatalytic CO<sub>2</sub> Reduction by [Pt(dmpc)<sub>2</sub>]<sup>2+</sup> through Kinetic and Thermodynamic Control. *Organometallics* **2020**, *39* (9), 1491-1496. DOI: 10.1021/acs.organomet.9b00720.
- (7) Cunningham, D. W.; Yang, J. Y. Kinetic and mechanistic analysis of a synthetic reversible CO<sub>2</sub>/HCO<sub>2</sub><sup>-</sup> electrocatalyst. *Chemical Communications* **2020**, *56* (85), 12965-12968, 10.1039/D0CC05556E. DOI: 10.1039/D0CC05556E.
- (8) Wang, X. S.; Yang, J. Y. Translating aqueous CO<sub>2</sub> hydrogenation activity to electrocatalytic reduction with a homogeneous cobalt catalyst. *Chemical Communications* **2023**, *59* (3), 338-341, 10.1039/D2CC05473F. DOI: 10.1039/D2CC05473F.
- (9) Jakobsen, J. B.; Rønne, M. H.; Daasbjerg, K.; Skrydstrup, T. Are Amines the Holy Grail for Facilitating CO<sub>2</sub> Reduction? *Angewandte Chemie International Edition* **2021**, *60* (17), 9174-9179. DOI: <https://doi.org/10.1002/anie.202014255>.
- (10) Kuß, D. A.; Hölscher, M.; Leitner, W. Combined Computational and Experimental Investigation on the Mechanism of CO<sub>2</sub> Hydrogenation to Methanol with Mn-PNP-Pincer Catalysts. *ACS Catalysis* **2022**, *12* (24), 15310-15322. DOI: 10.1021/acscatal.2c04806.
- (11) Balaraman, E.; Gunanathan, C.; Zhang, J.; Shimon, L. J. W.; Milstein, D. Efficient hydrogenation of organic carbonates, carbamates and formates indicates alternative routes to

methanol based on CO<sub>2</sub> and CO. *Nature Chemistry* **2011**, *3* (8), 609-614. DOI: 10.1038/nchem.1089.

(12) Erickson, J. D.; Preston, A. Z.; Linehan, J. C.; Wiedner, E. S. Enhanced Hydrogenation of Carbon Dioxide to Methanol by a Ruthenium Complex with a Charged Outer-Coordination Sphere. *ACS Catalysis* **2020**, *10* (13), 7419-7423. DOI: 10.1021/acscatal.0c02268.

(13) Kumar, N.; Camaioni, D. M.; Dupuis, M.; Raugei, S.; Appel, A. M. Mechanistic insights into hydride transfer for catalytic hydrogenation of CO<sub>2</sub> with cobalt complexes. *Dalton Transactions* **2014**, *43* (31), 11803-11806, 10.1039/C4DT01551G. DOI: 10.1039/C4DT01551G.

(14) Bai, S.-T.; Zhou, C.; Wu, X.; Sun, R.; Sels, B. Suppressing Dormant Ru States in the Presence of Conventional Metal Oxides Promotes the Ru-MACHO-BH-Catalyzed Integration of CO<sub>2</sub> Capture and Hydrogenation to Methanol. *ACS Catalysis* **2021**, *11* (20), 12682-12691. DOI: 10.1021/acscatal.1c02638.

(15) Sullivan, I.; Goryachev, A.; Digdaya, I. A.; Li, X.; Atwater, H. A.; Vermaas, D. A.; Xiang, C. Coupling electrochemical CO<sub>2</sub> conversion with CO<sub>2</sub> capture. *Nature Catalysis* **2021**, *4* (11), 952-958. DOI: 10.1038/s41929-021-00699-7.

(16) Bhattacharya, M.; Sebghati, S.; VanderLinden, R. T.; Saouma, C. T. Toward Combined Carbon Capture and Recycling: Addition of an Amine Alters Product Selectivity from CO to Formic Acid in Manganese Catalyzed Reduction of CO<sub>2</sub>. *Journal of the American Chemical Society* **2020**, *142* (41), 17589-17597. DOI: 10.1021/jacs.0c07763.

(17) DuBois, D. L.; Berning, D. E. Hydricity of transition-metal hydrides and its role in CO<sub>2</sub> reduction. *Applied Organometallic Chemistry* **2000**, *14* (12), 860-862. DOI: [https://doi.org/10.1002/1099-0739\(200012\)14:12<860::AID-AOC87>3.0.CO;2-A](https://doi.org/10.1002/1099-0739(200012)14:12<860::AID-AOC87>3.0.CO;2-A).

- (18) Berning, D. E.; Noll, B. C.; DuBois, D. L. Relative Hydride, Proton, and Hydrogen Atom Transfer Abilities of [HM(diphosphine)<sub>2</sub>]PF<sub>6</sub> Complexes (M = Pt, Ni). *Journal of the American Chemical Society* **1999**, *121* (49), 11432-11447. DOI: 10.1021/ja991888y.
- (19) Curtis, C. J.; Miedaner, A.; Ellis, W. W.; DuBois, D. L. Measurement of the Hydride Donor Abilities of [HM(diphosphine)<sub>2</sub>]<sup>+</sup> Complexes (M = Ni, Pt) by Heterolytic Activation of Hydrogen. *Journal of the American Chemical Society* **2002**, *124* (9), 1918-1925. DOI: 10.1021/ja0116829.
- (20) Buser, J. Y.; McFarland, A. D. Reaction characterization by flow NMR: quantitation and monitoring of dissolved H<sub>2</sub> via flow NMR at high pressure. *Chemical Communications* **2014**, *50* (32), 4234-4237, 10.1039/C4CC00055B. DOI: 10.1039/C4CC00055B.
- (21) Price, A. J.; Ciancanelli, R.; Noll, B. C.; Curtis, C. J.; DuBois, D. L.; DuBois, M. R. HRh(dppb)<sub>2</sub>, a Powerful Hydride Donor. *Organometallics* **2002**, *21* (22), 4833-4839. DOI: 10.1021/om020421k.
- (22) Wilson, A. D.; Miller, A. J. M.; DuBois, D. L.; Labinger, J. A.; Bercaw, J. E. Thermodynamic Studies of [H<sub>2</sub>Rh(diphosphine)<sub>2</sub>]<sup>+</sup> and [HRh(diphosphine)<sub>2</sub>(CH<sub>3</sub>CN)]<sub>2</sub><sup>+</sup> Complexes in Acetonitrile. *Inorganic Chemistry* **2010**, *49* (8), 3918-3926. DOI: 10.1021/ic100117y.
- (23) Jones-Mensah, E.; Karki, M.; Magolan, J. Dimethyl Sulfoxide as a Synthon in Organic Chemistry. *Synthesis* **2016**, *48* (10), 1421-1436. DOI: 10.1055/s-0035-1560429.
- (24) Traynelis, V. J.; Hergenrother, W. L. Decomposition of Dimethyl Sulfoxide Aided by Ethylene Glycol, Acetamide, and Related Compounds<sup>1</sup>. *The Journal of Organic Chemistry* **1964**, *29* (1), 221-222. DOI: 10.1021/jo01024a505.